ucc

Coláiste na hOllscoile Corcaigh, Éire
University College Cork, Ireland

Insulin-Like Growth Factor 1 Effects on Mitochondrial Dynamics and Mitophagy in Cancer

A thesis submitted to the National University of Ireland, Cork

in fulfilment of the requirements for the degree of

Doctor of Philosophy

by

Sarah Riis, MSc

April 2020

School of Biochemistry and Cell Biology

University College Cork, Ireland

Supervisor: Prof. Rosemary O'Connor

Head of Department.: Prof. Rosemary O'Connor

Table of Contents

Declaration

This is to certify that the work I am submitting is my own and has not been submitted for another degree, either at University College Cork or elsewhere. All external references and sources are clearly acknowledged and identified within the contents. I have read and understood the regulations of University College Cork concerning plagiarism. Digital signature of the candidate:

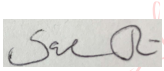
Digitally signed by
Sarah Riis
Date: 2020.06.23
15:35:16 +01'00'

Acknowledgements

My PhD journey has taught me much and taken me many places. The learning curve was steep with many ups and downs, but the rewards that presented themselves along the way made it all worthwhile.

First, I would like to thank my supervisor Prof. Rosemary O'Connor for her mentorship and advice and for granting me the opportunity to undertake this exciting but challenging project.

I would also like to extend my gratitude to the people who shared the journey with me. This includes past and present members of the ROC lab group (Mike, Joanna, Janina, Steph, Grant, Joss, Leonie and Orla) and the lunch group (Rachel, Sarah, Patrycja, Orlagh, Christina and Katie). Thank you for the support and encouragement. I will miss the chats, the laughs and the madness. If it weren't for you guys, I would never have known, what kind of potato I am.

Furthermore, I wish to thank Julia for the all the good times, pep-talks and failed gym-missions we have shared.

To my friends outside of academia and my family, thank you for the encouragement and for providing much appreciated distractions along the way.

Finally, I want to thank Philip, who was always there to listen, motivate and remind me of life outside academia. The PhD road was long and demanding, but you believed in me through it all.

List of Figures

List of Tables

Abstract

The evolutionarily conserved Insulin-Like Growth Factor 1 (IGF-1) signalling pathway is essential for growth and development and may facilitate cancer progression. While IGF-1 mediates mitochondria protection in some pathologies, whether it is essential for mitochondrial homeostasis in tumour cells remains mostly unknown. Mitochondria are key organelles for energy production, and, therefore, cancer cells rely on mitochondrial maintenance to support rapid cell proliferation. In this thesis, the effects of IGF-1 signalling on mitochondrial biogenesis, dynamics and turnover in cancer cells were investigated.

IGF-1 signalling was shown to promote mitochondrial biogenesis by inducing Peroxisome Proliferator-Activated Receptor-γ (PPAR-γ) Coactivator-1 β (PGC-1β) and PGC-1-Related Coactivator (PRC) to promote mitochondrial biogenesis, while also inducing the mitophagy receptor B-cell Lymphoma 2 (BCL-2)/Adenovirus E1B 19 kDa Protein-Interacting Protein 3 (BNIP3). IGF-1 also activated the transcriptional regulator Nuclear Factor, Erythroid 2 Like 2 (NFE2L2/Nrf2), likely through inactivation of Glycogen Synthase 3β (GSK-3β). Both Nrf2 and Hypoxia-Inducible Factor 1α (HIF-1α) were required for IGF-1-mediated induction of BNIP3.

While BNIP3 apparently inhibited cellular macro-autophagy, it facilitated mitophagy in cancer cells in response to a range of stimuli. A mitophagy reporter (pcDNA3.1-VLCAD(1-40)-mCherry-EGFP) was generated and tested to allow direct visualisation and quantification of cellular mitophagy. Unexpectedly, this reporter indicated that IGF-1 suppresses overall mitophagy in serum-deprived cell cultures. However, IGF-1 also induced colocalisation of BNIP3 with EGFP-LC3 in these cells, demonstrating that IGF-1 signalling selectively activates BNIP3-mediated mitophagy. The importance of IGF-1 signalling in mitochondrial turnover was further

demonstrated in IGF-1 receptor null mouse embryonic fibroblasts (R- cells) and these cells re-constituted with the IGF-1 receptor (R+ cells). Compared to R+ cells, R- cells exhibited impaired mitophagic clearance and reduced cell survival in response to mitochondrial stress.

Overall the findings of the thesis demonstrate that IGF-1 signalling enhances mitochondria health to support cellular robustness. This basal IGF-1 signal enhances mitophagy while also supressing macro autophagy, thus providing a critical mitochondrial protection signal. In cancer, this could be exploited therapeutically by co-targeting the IGF-1R with other therapies to generate mitochondrial vulnerabilities that would limit cancer progression.

List of Abbreviations

Abbreviation	Full name
ADP	Adenosine Diphosphate
AKT	AKT Serine/Threonine Kinase 1
AMBRA1	Activating Molecule in BECN1-Regulated Autophagy Protein 1
AMPK	AMP-Activated Protein Kinase
ARALAR	SCL25A12/Calcium-Binding Mitochondrial Carrier Protein Aralar1
ATP	Adenosine Triphosphate
BAX	BCL-2-Associated X Protein
BCL-2	B-Cell Lymphoma 2
BCL-x_L	B-Cell Lymphoma-Extra Large
β-TrCP	β-Transducin Repeat Containing E3 Ubiquitin Protein Ligase
BH	BCL-2 Homology
BNIP3	BCL-2/Adenovirus E1B 19 kDa Protein-Interacting Protein 3
BNIP3L	BCL-2/Adenovirus E1B 19 kDa Protein-Interacting Protein 3-Like
BSA	Bovine Serum Albumin
caMK	Ca^{2+}/Calmodulin-dependent protein Kinase
CCCP	Carbonyl Cyanide 3-Chlorophenylhydrazone
cDNA	Complementary DNA
C. elegans	Caenorhabditis elegans
CM	Complete Medium
CQ	Chloroquine
Cyt C	Cytochrome C
DDP1	DNA damage-binding protein 1
DFP	Deferiprone
DMEM	Dulbecco's Modified Eagles Medium
DMSO	Dimethyl Sulfoxide
DNA	Deoxyribonucleic Acid
DRP1	Dynamin-Related Protein 1
E. coli	Escherichia Coli
EGF	Epidermal Growth Factor
EGFP	Enhanced Green Fluorescent Protein
EMT	Epithelial-Mesenchymal Transition
Erk	Extracellular Signal-Regulated Kinases
ETC	Electron transport chain
EV	Empty Vector
FCCP	Carbonyl cyanide 4-(trifluoromethoxy)phenylhydrazone
FBS	Fetal bovine serum
FOX	Forkhead Box
FUNDC1	FUN14 Domain-Containing Protein 1
GABARAP	Gamma-Aminobutyric Acid (GABAA) Receptor-Associated Protein
GATE-16	GABAA-Receptor-Associated Protein 2/Golgi-associated ATPase enhancer of 16 kDa
GCLC	Glutamate-Cysteine Ligase Catalytic Subunit

GDP	Guanosine Diphosphate
GH	Growth Hormone
GHR	Growth Hormone Receptor
Gp78	Glycoprotein 78
GRB2	Growth Factor Receptor Bound Protein 2
GSK-3	Glycogen Synthase Kinase 3
GTP	Guanosine Triphosphate
HIF-1α	Hypoxia-Inducible Factor 1 subunit α
HO1	Heme oxygenase 1
HRD1	HMG-CoA Reductase Degradation 1 Homolog
IGF-1/2	Insulin-Like Growth Factor 1/2
IGF-1/2R	Insulin-Like Growth Factor 1/2 Receptor
IGFBP	Insulin-Like Growth Factor Binding Proteins
IMM	Inner Mitochondrial Membrane
IR	Insulin Receptor
IRS	Insulin Receptor Substrates
JNK	c-Jun N-terminal Kinases
KEAP1	Kelch Like ECH Associated Protein 1
LC3	Microtubule Associated Protein 1 Light Chain 3α
LIR	LC3-Interacting Region
MAPK	Mitogen-Activated Protein Kinase
MFN1/2	Mitofusin 1/2
mt	Mitochondrial
mRNA	Messenger Ribonucleic Acid
mTORC12	Mammalian Target of Rapamycin Complex 1/2
NADP	Nicotinamide Adenine Dinucleotide Phosphate
NDP52	Nuclear Dot Protein 52/Calcium Binding and Coiled-Coil Domain 2
Nrf2/NFE2L2	Nuclear Factor Erythroid 2-Related Factor 2
NRF1/NRF2	Nuclear Respiratory Factor 1/2
OMM	Outer Mitochondrial Membrane
OPA1	Optic Atrophy Protein 1
OXPHOS	Oxidative phosphorylation
Parkin/PRKN	Parkin RBR E3 Ubiquitin Protein Ligase
PBS	Phosphate-buffered Saline
PCR	Polymerase Chain Reaction
PDK1	Phosphoinositide-Dependent Kinase 1
PFA	Paraformaldehyde
PKA	Protein Kinase A
PGC-1α	Peroxisome Proliferator-Activated Receptor (PPAR)-γ Coactivator 1-α
PGC-1β	PPAR-γ Coactivator 1-β
PHB1/PHB2	Prohibitin 1/2
PI 3-K	Phosphoinositide 3-Kinase
PINK1	PTEN-Induced Kinase 1
PNC1	Pyrimidine Nucleotide Carrier 1/SLC25A33
POLRMT	Polymerase (RNA) Mitochondrial (DNA Directed)
PRC	PGC-1-Related Coactivator

PTPC	Permeability Transition Pore Complex
p62/SQSTM1	Sequestosome 1
p70 S6 kinase	Ribosomal protein S6 kinase, 70kDa, polypeptide 1
RACK1	Receptor for Activated C Kinase 1
RHEB	Ras Homolog Enriched in Brain
ROS	Reactive Oxygen Species
RPMI	Roswell Park Memorial Institute medium
rRNA	Ribosomal RNA
RTK	Receptor Tyrosine Kinase
RT-qPCR	Real-time Quantitative Polymerase Chain Reaction
SDS-PAGE	Sodium Dodecyl Sulphate-Polyacrylamide Gel Electrophoresis
SEM	Standard error of the mean
SHC	Src Homology Collagen
siRNA	Small interfering RNA
SOS	Son of Sevenless
Src	SRC Proto-Oncogene, Non-Receptor Tyrosine Kinase
SS	Serum-starvation
TBS	Tris-buffered Saline
TFAM	Transcription Factor A, Mitochondrial
TFB2M	Transcription Factor B2, Mitochondrial
TFEB	Transcription Factor EB
TMRM	Tetramethylrhodamine, methyl ester
TNF	Tumour Necrosis Factor
TOM20	Translocase of Outer Mitochondrial Membrane 20
tRNA	Transfer RNA
Ub	Ubiquitin
UCP	Uncoupling Protein
ULK1	Unc-51 Like Autophagy Activating Kinase 1
VDAC	Voltage Dependent Anion Channel
VLCAD	Very Long Chain Acyl-CoA Dehydrogenase
WDR23	WD Repeat-Containing Protein 23
WT	Wildtype

Units:

Abbreviation	**Full name**
kb	kilobases
kDa	kilodalton
ml	mililiter
mM	milimolar
M	molar
mM	milimolar
nM	nanomolar
RPM	Revolutions per minute
µg	microgram
µl	microliter
µm	micrometer
µM	micromolar

Chapter 1. General Introduction

1.1 Insulin/IGF-1 family

1.1.1 The conserved Insulin/IGF system regulates development, metabolism and longevity

The Insulin/Insulin-Like Growth Factor 1 (IGF-1) signalling pathway is highly conserved through evolution, emphasizing the importance of this endocrine system (van Heemst, 2010). IGF-1 is transcriptionally induced in response to Growth Hormone (GH) signalling from the pituitary gland and is mainly produced in the liver from where it is released into circulation to act on many tissues (Carter-Su et al., 1996, Sjögren et al., 1999). The IGF family consists of three ligands: Insulin, IGF-1 and IGF-2, four receptors: two Insulin Receptors (IR-A and IR-B), IGF-1 Receptor (IGF-1R) and IGF-2R (mannose 6 phosphate receptor) and IGF-Binding Proteins (IGFBPs) that bind IGFs in circulation (Guevara-Aguirre et al., 2018).

Insulin/IGFs are essential for normal embryonic and fetal development as evidenced in for example Drosophila (Fernandez et al., 1995), mice (Liu et al., 1993), and zebrafish (Schlueter et al., 2007). In humans, IGFs are also essential for proper fetal growth and development (Gluckman et al., 1983, Lassarre et al., 1991, Fowden, 2003).

IGF-1 deficiency has been linked to growth retardation in patients with Laron syndrome for example, which is characterized by mutations in the GH receptor and GH insensitivity causing a dramatic reduction in circulating IGF-1 levels (Laron and Kauli, 2016). These patients also present with severe obesity, reduced muscle and bone mass (Laron et al., 2006), smaller hearts (Feinberg et al., 2000) and some patient groups have impaired brain development associated with reduced intellectual capacity, which is thought to be caused by different mutations in the GH receptor (Shevah et al., 2005). Since GH, Insulin and IGF-1 signalling coordinate metabolic homeostasis

in humans (Møller and Jørgensen, 2009), IGF-1 deficiency has also been linked to metabolic syndrome, which is characterised by the manifestation of several symptoms including central obesity, elevated blood pressure and/or elevated fasting blood glucose levels (Eckel et al., 2005). Similarly, diabetes commonly presents with elevated levels of GH (Molnar et al., 1972) and reduced levels of serum IGF-1 (Tan and Baxter, 1986), emphasizing the importance of a balanced Insulin/IGF-1 system for maintenance of healthy metabolism.

Besides its role in developmental and metabolic processes, the Insulin/IGF-1 pathway is also implicated in ageing and longevity. The non-vertebrate roundworm *Caenorhabditis elegans* (*C. elegans*) is an important model organism in lifespan studies because it possesses the ability to exit its reproductive life cycle and enter a dauer larval state, in which it is highly stress resistant, thus extending its lifespan (Kimura et al., 1997). In response to food, *C. elegans* secrete Insulin/IGF-1-like peptides that bind to and activate the DAF-2 receptor, a receptor tyrosine kinase (RTK) the common orthologue of the mammalian IR/IGF-1R. DAF-2 signalling coordinates the growth, differentiation and metabolic changes that are required for survival in a changing environment (van Heemst, 2010). DAF-2 mutations cause either arrest of the larva in the dauer state or retention of some dauer features, thereby greatly increasing the lifespan of the worms (Kenyon et al., 1993, Halaschek-Wiener et al., 2005).

The fruit fly *Drosophila melanogaster* similarly has one common Insulin/IGF-1 receptor tyrosine kinase that can bind multiple Insulin/IGF-1-like peptides inducing intracellular signalling cascades associated with regulation of lifespan (Tatar et al., 2001, Giannakou and Partridge, 2007).

In mammals, Insulin and IGF signals are propagated through distinct RTKs, the IR and IGF-1R, that share significant homology, particularly in their kinase domains. However, the evidence for control of lifespan in mammals is not as compelling in mammals as in worms. In mice, heterozygous knockout of the IGF-1R caused increased lifespan, but the effect was sex-specific (Holzenberger et al., 2003). Mutations in IGF-1R and lower levels of IGFs have been associated with human longevity. However, complex fluctuations in GH and IGF-1 signalling are influenced by many genetic and environmental factors such as age, sex and weight (Veldhuis et al., 2011), so the effects of IGF-1 signalling on longevity in mammals is still a topic of much debate (Vitale et al., 2019). Additionally, IGF-1 signalling is implicated in neuronal function and, thus, healthy ageing. Downregulation of IGF-1 was shown to impair mitochondrial structure and function in astrocytes associated with diminished astrocyte function, which is essential to hippocampal-mediated spatial learning. Therefore, age-dependent downregulation of IGF-1 was proposed as a mechanism for the development of age-related cognitive disorders such as Alzheimer's Disease (AD) (Logan et al., 2018). However, this is an area of some controversy, as blocking IGF-1 signalling was shown to delay AD progression by reducing the accumulation of amyloid-β, which is considered toxic and critical to the development of AD (Freude et al., 2009, Gontier et al., 2015). The complexity of IGF-1 effects on the aging brain is reviewed elsewhere (Gubbi et al., 2018).

1.1.2 Mechanism of IGF-1 receptor activation

Insulin, IGF-1 and IGF-2 can all bind competitively to all three receptors IR, IGF-1R and IGF-2R, although with different affinities with IGF-1 displaying highest affinity for IGF-1R and Insulin for IR-B (Denley et al., 2005). The IGF-1R, was originally

described in 1974 as having distinct properties from the IR (Megyesi et al., 1974, Megyesi et al., 1975). It is synthesized in the cells as a 180 kDa precursor protein that undergoes glycosylation and dimerization prior to proteolytic cleavage, which yields the mature tetrameric receptor linked together by disulphide bonds. As illustrated in Figure 1.1A, this mature receptor is comprised of two extracellular α subunits and two β subunits that extend from the extracellular space, across the cell membrane and into the intracellular space. The α chains interact with the ligand, whereas the tyrosine kinase domain is present within the intracellular section of the β chains. The amino acid precursor consists of 1367 residues with a signal peptide at residues -30-1, the α chain at residues 1-707, a proteolytic cleavage site at residues 708-711 and the β chain at residues 712-1337. The tyrosine kinase domain (residues 973-1229) is present on the intracellular section of the β chains flanked by a juxtamembrane region (930-972) and a C-terminal tail (1230-1337) (Adams et al., 2000).

Activation of the IGF-1R leads to phosphorylation of several receptor substrates including Insulin Receptor Substrates (IRS) and Src Homology Collagen (SHC) initiating signalling cascades to induce cell growth and proliferation while preventing cell death, as illustrated in Figure 1.1B (Hakuno and Takahashi, 2018). Firstly, when bound by IGF-1, the receptor undergoes a conformational change that leads to activation of the tyrosine kinase domain. The exact structural changes that occur during the activation of the receptor are still a topic of research, but it was recently demonstrated that binding of one IGF-1 molecule was sufficient to induce receptor activation due to conformational changes (Pautsch et al., 2001, Li et al., 2019). IGF-1R autophosphorylation is initiated on tyrosine residues 1131, 1135 and 1136 within the kinase domain leading to full receptor activation (Kato et al., 1994). Subsequent autophosphorylation on other sites such as Y950 initiate recruitment of

dockings proteins like IRS or Shc to activate the two major IGF-1 pathways involving Phosphoinositide 3-Kinase (PI 3-K) or Mitogen-Activated Protein Kinase-1 (MAPK), as illustrated in Figure 1.1B (Myers and White, 1996).

All the components and activity of the IR/IGF-1R-PI 3-K axis are highly conserved from worm to mammals to promote cell survival, growth and differentiation. The PI 3-K axis promotes cell survival and differentiation (Hakuno and Takahashi, 2018). One of the main proteins directly recruited by active PI 3-K is AKT, which is recruited to the plasma membrane alongside Phosphoinositide-Dependent Kinase-1 (PDK-1) through their PH domains. PDK-1 phosphorylates AKT on T308, and this is followed by Mammalian Target of Rapamycin Complex 2 (mTORC2)-mediated phosphorylation of S473 leading to maximal activation of AKT (Fruman et al., 2017). As reviewed in detail elsewhere, AKT exerts many cellular effects. These include induction of cell proliferation through activation of Mammalian Target of Rapamycin Complex 1 (mTORC1), alteration of cellular metabolism through inhibition of GSK-3 in addition to anti-apoptotic effects mediated for example by phosphorylating BH3 members of BCL-2 family and Forkhead box class O (FoxO) to suppress transcription of pro-apoptotic and cell cycle regulatory genes (Manning and Cantley, 2007).

Another pathway induced by IGF-1R activation involves Growth Factor Receptor-Bound protein 2 (GRB2) that binds through its Src Homology 2 (SH2) domain to IRS or Shc on the activated IGF-1R. GRB2 interacts with Son of Sevenless (SOS), which is a guanine nucleotide exchange factor for Ras, causing activation of Ras. This can activate the Ras-MAPK/ERK cascade, which ultimately causes phosphorylation and activation of MAPK/ERK and of transcriptional activators (Hakuno and Takahashi, 2018). Ras-MAPK/ERK activation affects several

downstream signalling routes mediated through the Extracellular Signal-Related Kinases 1 and 2 (ERK1/2), Jun Amino-Terminal Kinases (JNK1/2/3), p38-MAPK and ERK5. Unlike the PI 3-K/AKT pathway, activation of the MAPK/ERK signalling by IGF-1 generally requires cell adhesion signals and therefore involves the assembly of signalling complexes containing the IGF-1R, integrins, adapters, particularly SHC or Receptor for Activated C Kinase 1 (RACK1) and adhesion kinases such as SRC Proto-Oncogene Non-Receptor Tyrosine Kinase (Src), Focal Adhesion Kinase (FAK) and Fes-Related Tyrosine Kinase (FER) (Clemmons et al., 1999, Kiely et al., 2006, Andersson et al., 2009, Stanicka et al., 2018). These complexes may also contain Rho family proteins that control cell shape and polarity (Deevi et al., 2014). These pathways are associated with induction of cell cycle/cell proliferation, differentiation or migration in addition to increasing DNA synthesis and enhancing cell survival (Sun et al., 2015).

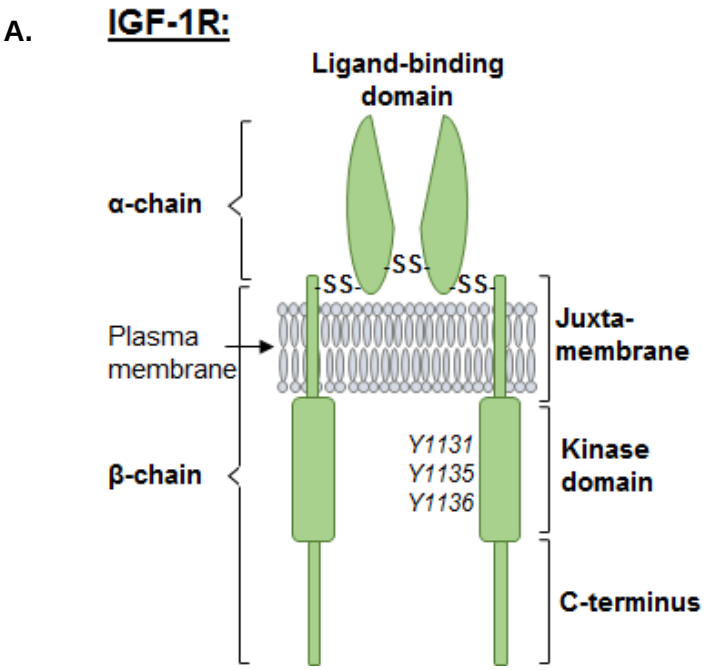

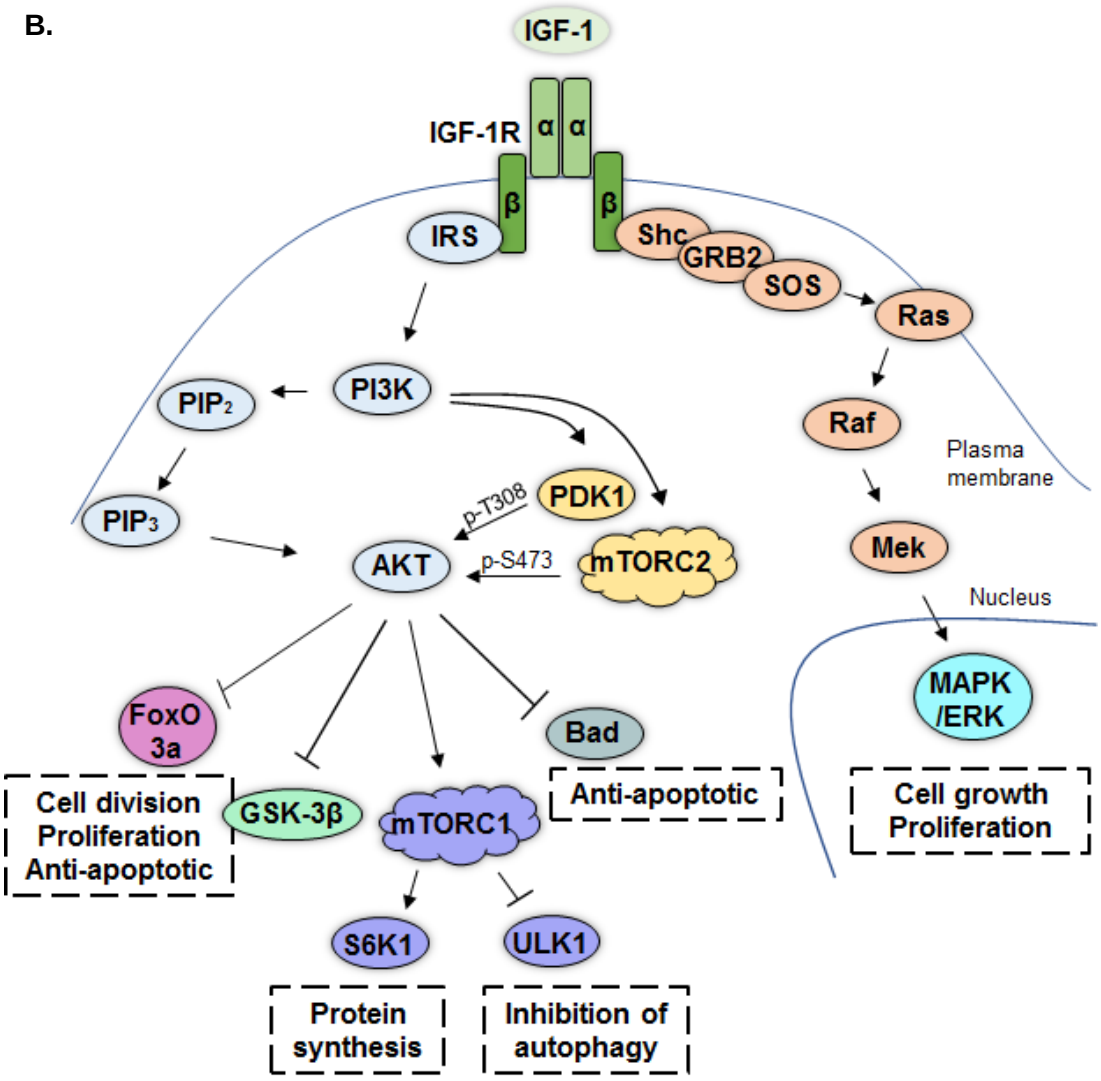

Figure 1.1 Structure of the IGF-1R and the IGF-1 signalling pathways.

A. The IGF-1R consists of a dimer of two α- and β-chains that are bound together by disulphide bonds. The α-symbol binds IGF-1, while the β-chain crosses the plasma membrane with its juxta-membrane domain and protrudes into the cytosol with the kinase domain and C-terminus. **B**. Binding of IGF-1 ligand to the IGF-1R induces two main signalling pathways. One operates through PI 3-K, which induces conversion of PIP2 to PIP3 facilitating activation of AKT that phosphorylates many substrates including the transcription factor FoxO3a, GSK-3β, mTORC1 and Bad. The other pathway involves a phosphorylation cascade resulting in activation of all MAPK/ERK pathways leading to transcriptional activation enhancing cell proliferation and survival.

1.2 IGF-1 signalling in cancer

1.2.1 Implications of IGF-1 in cancer and its therapeutic potential

The genetic disorder Laron Syndrome is caused by mutations in the human GH gene and is associated with low levels of circulating IGF-1. Afflicted individuals present with features such as dwarfism and obesity, but interestingly have a reduced risk of cancer (Shevah and Laron, 2007, Laron and Kauli, 2016). Studies were conducted with a mouse model of Laron Syndrome that lacks the GH receptor/binding protein, which is also associated with reduced IGF-1 levels. The mice exhibited lower incidence and delayed manifestation of fatal tumours compared to wildtype (WT) mice (Ikeno et al., 2009). Similarly, a rat model lacking GH and exhibiting reduced levels of circulating IGF-1, had improved resistance to mammary tumour induction compared to WT rats (Swanson and Unterman, 2002). GH treatment increased the mammary tumour incidence in these rats to the levels of the WT, but when treatment was halted, the tumours regressed, suggesting that the GH/IGF-1 signalling axis is directly implicated in cancer development and progression (Shen et al., 2007).

In humans, IGF-1 signalling particularly related to the levels of circulating IGF-1 has been implicated in many different types of cancer including prostate (Wolk et al., 1998), breast (Peyrat et al., 1993), bladder (Zhao et al., 2003), lung (Yu et al., 1999) and colorectal cancer (Chi et al., 2013). Various studies in IGF-1/IGF-1R levels in human malignancies have yielded conflicting results regarding the clinical and prognostic value of this, as reviewed by Samani *et al.* (Samani et al., 2007). However, IGF signalling is also associated with development of resistance to chemo- and radiotherapy (Juan et al., 2011, Osuka et al., 2013, Cortés-Sempere et al., 2013, Long et al., 2019), so it is clear that IGF-1 pathways are of importance in cancer

deterioration. From a functional point of view, the implication of IGF signalling in cancer is due to its role in tumorigenic processes such as cell growth, proliferation and inhibition of apoptosis. IGFs are also implicated in the promotion of cancer metastasis by enhancing basement membrane breakdown and angiogenesis (Kasprzak et al., 2017). Furthermore, IGF-1 signalling has a significant role in cellular maintenance of stemness features (Teng et al., 2018). It has been proposed that cancer cells acquire such stem cell characteristics to facilitate epithelial-mesenchymal transition (EMT). This process is enhanced by IGF-1 signalling and may contribute to the tumorigenic effects associated with the IGF-1 pathway (Farabaugh et al., 2015, Fajka-Boja et al., 2018).

Promising pre-clinical studies led to the development of anti-cancer treatments targeting the IGF-1 pathway, including anti-IGF-1R and anti-IGF-1 antibodies in addition to small molecule tyrosine kinase inhibitors. However, the drugs proved to be disappointing in clinical trials in unselected patient groups. Much of the current research into IGF-1 signalling aims to better understand the pathway and potential resistance mechanisms and to identify biomarkers that will allow patient stratification to hopefully increase treatment success (Bowers et al., 2015, Werner et al., 2019).

1.2.2 Effects of IGF signalling on mitochondria in cancer cells

Mitochondria health and function is at the centre of cancer development and progression, as many tumorigenic processes result in mitochondria dysfunction that in turn drive further disease progression (Vyas et al., 2016). One of the many mitochondria-associated key characteristics of cancer is metabolic reprogramming. This promotes cancer advancement by inducing a switch to the glycolytic phenotype that was first described by Warburg (Warburg et al., 1927), although this is now known

to be a very complex process (Vander Heiden et al., 2009). It involves uncoupling of oxidative phosphorylation (OXPHOS) for example by regulation of uncoupling protein 2 (UCP2) that can shuttle metabolites out of the mitochondria (Samudio et al., 2008, Vozza et al., 2014, Yu et al., 2019). This reprogramming allows the cancer cells to exploit metabolites to drive different biosynthetic pathways (Vander Heiden et al., 2009, Locasale et al., 2011, Jiang et al., 2011, Nilsson et al., 2014). Growth hormone signalling is associated with regulation of UCP2 and 3 (Pedersen et al., 1999, Futawaka et al., 2016), and circulating IGF-1 was shown to increase UCP1 in cardiomyocytes (Vinciguerra et al., 2009), suggesting that Insulin/IGF-1 may also affect energy metabolism through OXPHOS uncoupling.

Furthermore, Insulin/IGF-2 signalling can mediate metabolic reprogramming in breast cancer cells (Vella et al., 2019). IGF-2 can induce activation and translocation of estrogen receptor (ER)-α and -β to the mitochondria and other subcellular compartments of breast cancer cells (Richardson et al., 2011). At the mitochondria, ERα/β has been linked to induction of mitochondrial DNA (mtDNA) transcription (Song et al., 2006) and regulation of apoptosis (Liang et al., 2015). Estradiol treatment was shown to induce mitochondrial biogenesis (Mattingly et al., 2008) and increase mitochondrial calcium uptake (Lobatón et al., 2005), so possibly, the Insulin/IGF system cross-talks with the ER system to enhance mitochondrial function in tumour cells.

In the neuroblastoma cell line SH-SY5Y and other non-tumour-derived cells, IGF-1 stimulation induces mitochondrial translocation of AKT in a PI 3-K-dependent manner. This is associated with phosphorylation of adenosine triphosphate (ATP) synthase and phosphorylation of mitochondrial GSK-3β (Bijur and Jope, 2003). Phospho-mimetics of ATP Synthase predominantly exhibited reduced dimerization

and ATPase function, although little is known of the effects of such phosphorylations *in vivo* (Kane et al., 2010). GSK-3, on the other hand, can regulate glucose metabolism in different types of cancer (Pal et al., 2014, Momcilovic et al., 2018). It is also involved in regulation of apoptosis (Dickey et al., 2011, Nishimura et al., 2016), can affect mitochondrial permeability (Juhaszova et al., 2004, Tanno et al., 2014) and is implicated in regulation of mitochondrial motility (Ogawa et al., 2016). Thus, the inhibition of mitochondrial GSK-3β mediated by IGF-1, may have many effects on mitochondrial function in cancer as well as other pathologies. As reviewed by Rasola and Chiara (2013), the two homologues GSK-3 isoforms GSK-3α and GSK-3β, collectively referred to as GSK-3, can exert several mitochondrial effects in cancer cells. Active GSK-3 promotes degradation of the anti-apoptotic protein BCL-2 and induces translocation of the pro-apoptotic BCL-2-Associated X protein (BAX) to mitochondria, thus, facilitating apoptosis. Furthermore, GSK-3 downregulates binding of Hexokinase Type II to the outer mitochondrial membrane (OMM), where it is involved in glucose utilization for glycolysis, thereby preventing the metabolic shift often observed in cancer cells (Rasola and Chiara, 2013). Therefore, IGF-1-mediated inhibition of mitochondrial GSK-3 may impair apoptosis and enhance metabolic reprogramming.

IGF-1 induces the mitochondrial pyrimidine carrier (PNC1)/SLC25A33 in cancer cells, and this signal induces cell growth (Floyd et al., 2007). PNC1 suppression leads to mitochondrial dysfunction indicated by reduced OXPHOS and increased reactive oxygen species (ROS) production. Suppression of PNC1 also causes ROS-induced EMT (Favre et al., 2010). Overall, the findings suggest that IGF-1 signalling through regulation of PNC1 protects and maintains mitochondria function. In the cancer setting, this signal enhances mitochondria health and survival of the tumour

cells, but it prevents further tumorigenic transformation to an aggressive mesenchymal phenotype. Thus, most studies indicate a mitochondria-protective role for IGF-1 signalling. However, some conflicting data has also been reported suggesting that heterozygous knockout of the IGF-1R in mice protects against oxidative stress (Holzenberger et al., 2003). These mice also displayed attenuated dextran sulphate sodium (DSS)-induced colitis, which was associated with enhanced mitochondrial resistance to oxidative damage in colorectal mucosal cells in response to azoxymethane (AOM)/DSS and increased OXPHOS (Wang et al., 2019). However, as these mice only exhibited partial reduction in IGF-1 signalling, the phenotypic improvements likely reflect the requirement for balanced IGF-1 signalling. Mice with homozygous knockout of the IGF-1R die immediately post birth and exhibit severe growth retardation (Sell et al., 1994). Furthermore, in patients with GH deficiency, GH therapy dosage can be based on serum IGF-1 levels (Cohen et al., 2007), although different studies have highlighted the difficulty in optimizing IGF-1 levels. High to normal levels of circulating IGF-1 improved waist-circumference as an indicator of obesity and general well-being, but with potentially dangerous adverse effects (van Bunderen et al., 2016), whereas low-normal IGF-1 levels improved cognitive function, but was associated with fatigue (van Bunderen et al., 2018). Thus, enhancing our understanding of IGF-1 effects on mitochondria, is of great importance, given the implication of mitochondria dysfunction in many disease pathologies. Mitochondrial effects of IGF-1 are summarized in Figure 1.2.

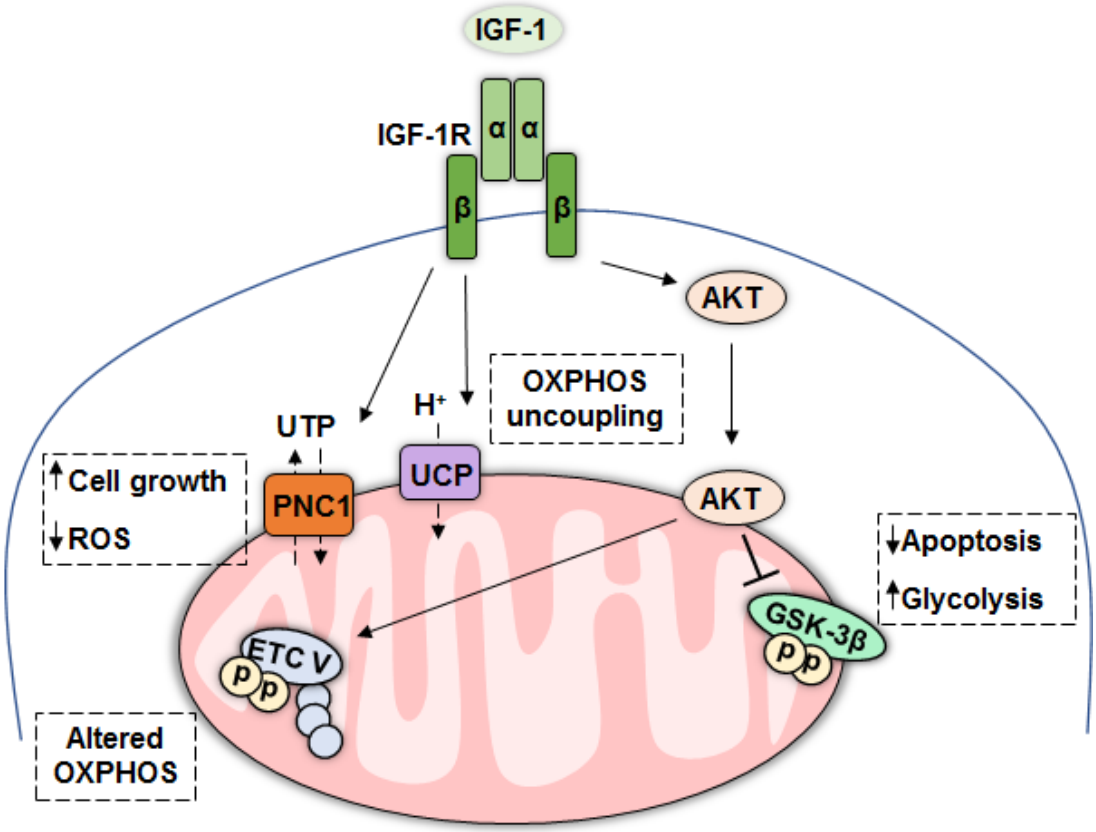

Figure 1.2 IGF-1 effects on mitochondrial function.

IGF-1 induces PNC1 to enhance cellular growth and reduce ROS production. Insulin/IGF-1 can induce UCPs to cause OXPHOS uncoupling, facilitating metabolic reprogramming. IGF-1 can cause mitochondrial translocation of active AKT, which leads to phosphorylation of ATP synthase/electron transport chain components (ETC) V and inhibitory phosphorylation of GSK-3β, which could prevent induction of apoptosis and could enhance metabolic reprogramming due to altered glucose metabolism.

1.3 Mitochondria structure, function and dynamics

1.3.1 Mitochondrial structure and function

Mitochondria originate from α-proteobacterium that were taken up by a predecessor of modern eukaryotic cells approximately 2 billion years ago according to the endosymbiont theory (Gray, 2017). Human mitochondria contain mtDNA that is about 16 kilobases in size and is present in cells in multiple copies. mtDNA encodes 13 proteins that are all essential components of the electron transport chain complexes I-V. Mitochondrial DNA encodes 22 tRNAs and 2 mitochondrial rRNAs. Most

mitochondrial proteins are nuclear encoded, translated on ribosomes in the cytoplasm and subsequently imported through transporters in the mitochondrial membranes (Friedman and Nunnari, 2014).

The structure of mitochondria as double membrane organelles was first described in the 1950's (Palade, 1952, Sjostrand, 1953). They are composed of an outer mitochondrial membrane (OMM) that regulates the overall shape and size of the mitochondria. Encased by the OMM, is the inner mitochondrial membrane (IMM), which is pushed towards the OMM by the central mitochondrial matrix, forcing the IMM into tubular cristae-shaped structures (Frey et al., 2002). OXPHOS mainly occurs at the cristae (Gilkerson et al., 2003). OXPHOS entails the transfer of electrons between the electron transport chain complexes (I-IV) that generates a proton gradient across the IMM, which is exploited by the ATP synthase/Complex V to generate ATP. Complexes I, III and IV pump protons across the IMM into the intermembrane space generating the required proton gradient (Saraste, 1999). Studies have shown that cristae shape is regulated based on the cellular energy requirements, illustrative of the dynamic and adaptable nature of mitochondria (Cogliati et al., 2016).

1.3.2 Reactive Oxygen Species (ROS)

ROS are produced as by-products of OXPHOS (Loschen et al., 1971, Balaban et al., 2005) as well as by peroxisomes (Fransen et al., 2012), the endoplasmic reticulum (Delaunay-Moisan and Appenzeller-Herzog, 2015), NADPH oxidase (Lambeth, 2004) or exposure to external stresses such as ultraviolet radiation (Phaniendra et al., 2015). Mitochondria produce ROS predominantly through Complexes I and III of the electron transport chain (ETC) that are the main sources of mitochondrial superoxide (O_2^-). ROS can be rapidly scavenged by superoxide dismutase (SOD) for example,

leading to the production of H_2O_2 that is subsequently converted to H_2O and O_2 through enzymatic reactions (Mailloux, 2015). Figure 1.3 illustrates some of the detrimental mitochondrial effects of ROS and feedback mechanisms that enhance mitochondrial dysfunction under conditions of elevated ROS.

Elevated levels of ROS are associated with many different diseases. As has been extensively reviewed elsewhere, ROS can enhance inflammation (Naik and Dixit, 2011, Mittal et al., 2014), alter cell signalling (Ray et al., 2012), induce mutations in mitochondrial DNA and promote genomic instability (Srinivas et al., 2019). However, it is now well established that ROS play an important role in normal cell function, such as its involvement in appropriate regulation of some immune responses (West et al., 2011), and it has been proposed that it is exploited for intercellular communication (Cowan et al., 2003, Zhou et al., 2010). Thus, the emerging consensus is that redox homeostasis is essential for physiological health (Ursini et al., 2016).

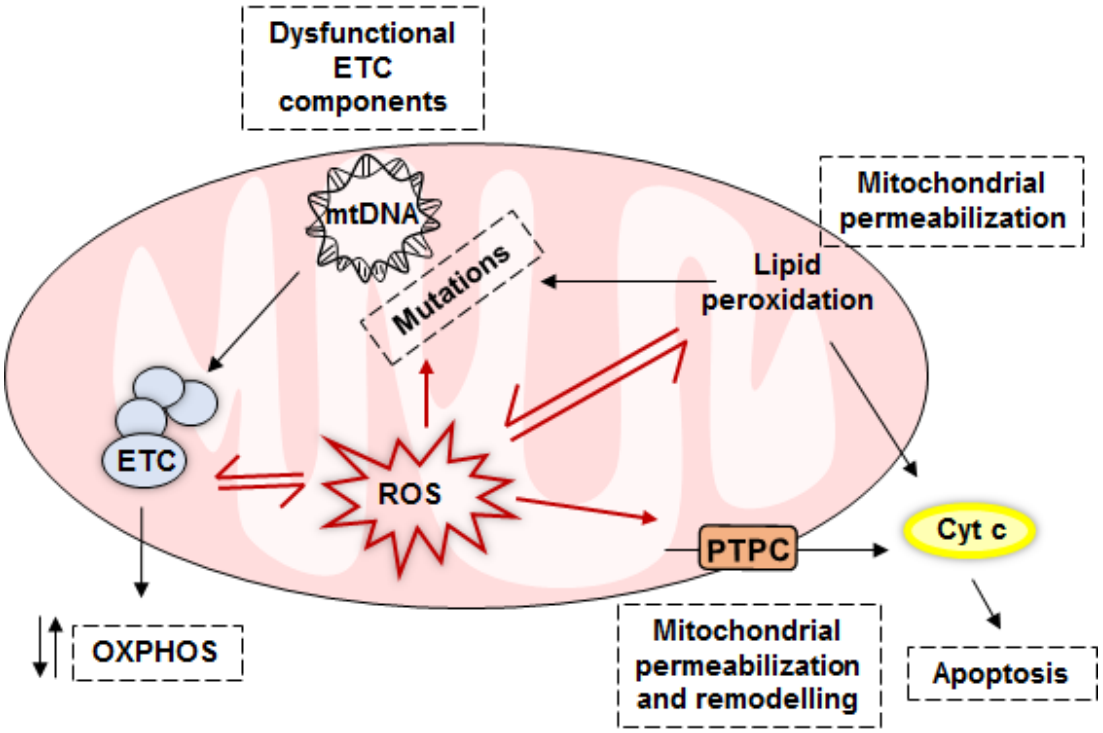

Figure 1.3 The effects of elevated ROS on mitochondrial functions.

ROS can cause mutations in mtDNA leading to impaired synthesis of ETC components, thus altering the quality of mitochondria-derived components of the ETC and the balance between these and imported components, ultimately leading to impaired OXPHOS. ROS can also cause lipid peroxidation leading to mutagenesis and mitochondrial permeabilization. Additionally, ROS can cause cytochrome C release and apoptosis through lipid peroxidation and direct effects on the permeability transition pore complex (PTPC).

1.3.3 Mitochondrial biogenesis

Mitochondrial biogenesis requires the coordinated transcription, translation and import of nuclear encoded mitochondrial proteins alongside translation of the proteins encoded in the mtDNA. This synchronization is mediated by mitochondrial transcription factors such as mitochondrial transcription factor A (TFAM) that are encoded in the nuclear genome (Hock and Kralli, 2009).

Transcription of mtDNA is carried out by mitochondrial RNA polymerase (POLRMT). Mitochondrial Transcription Factor B2 (TFB2M) facilitates interaction between TFAM and POLRMT, and TFAM allows POLRMT to bind promoters within the mtDNA. Once transcribed, mitochondrial mRNA is translated by mt-tRNAs on

the mito-ribosome, a complex consisting of mitochondrial rRNA in addition to both nuclear- and mtDNA-encoded proteins. Unlike, mtDNA-encoded proteins, the nuclear-encoded mitochondrial proteins are translated on cytosolic ribosomes and must be imported into the mitochondria. The most common mitochondrial route involves amino-terminal targeting sequences that are cleaved following import. These targeting sequences enable recognition of the precursor proteins by translocases of the OMM (TOMs) and translocases of the IMM (TIMs) that form pore structures facilitating protein import (Model et al., 2008, Chacinska et al., 2009). Other mitochondrial protein precursors use alternative routes of import that are reviewed elsewhere (Chacinska et al., 2009, Wiedemann and Pfanner, 2017).

Central to the regulation of mitochondrial biogenesis are Nuclear Respiratory Factors 1 and 2 (NRF1/NRF2) that control expression of nuclear encoded mitochondrial proteins such as TFAM, TFB2M and ETC components. NRF1/NRF2 expression, in turn, is regulated by transcriptional activators that are induced under different cellular conditions as illustrated in Figure 1.4. These include peroxisome proliferator-activated receptor-γ (PPAR-γ) coactivator-1 α (PGC-1α) (Puigserver et al., 1998, Wu et al., 1999), PPAR-γ coactivator-1β (PGC-1β) (Shao et al., 2010, Gao et al., 2011), PGC-1-related coactivator (PRC) (Andersson and Scarpulla, 2001) and Nuclear Factor, Erythroid 2 Like 2 (NFE2L2/Nrf2) (Piantadosi et al., 2008). Firstly, it was shown that cold exposure induces PGC-1α in brown fat tissue and muscle leading to increased expression of several genes encoding mitochondrial proteins (Puigserver et al., 1998). Furthermore, in skeletal muscles, increased intracellular concentrations of Ca^{2+} during endurance exercise cause activation of Ca^{2+}/calmodulin-dependent protein kinase (CaMK), which leads to PGC-1α activation (Wu et al., 2002). Additionally, exercise causes activation of p38 mitogen-activated protein kinase (p38

MAPK) in skeletal muscle, which increases PGC-1α expression and mitochondrial biogenesis to facilitate muscle adaptation to increased physiological demands (Akimoto et al., 2005). Similarly, the cellular energy sensor, AMP-activated protein kinase (AMPK), that is activated in response to ATP depletion during exercise for example, causes activation of PGC-1α (Jäger et al., 2007). On the other hand, GSK-3β inactivation increases PGC-1α expression through activation of transcription factor EB (TFEB), suggesting that GSK-3β is a negative regulator of PGC-1α. Thus, physiological inactivation of GSK-3β was proposed to enhance mitochondrial biogenesis during myogenic differentiation (Theeuwes et al., 2018, Theeuwes et al., 2020). Furthermore, in the context of myogenic differentiation, the homologous protein PGC-1β was also shown to induce mitochondrial biogenesis (Shao et al., 2010). 17β-estradiol also stimulates hepatic mitochondrial biogenesis through PGC-1β (Galmes-Pascual et al., 2017). PRC, on the other hand, is cell cycle regulated, as it is ubiquitously expressed and increased under conditions requiring cell proliferation (Andersson and Scarpulla, 2001). NFE2L2/Nrf2 is another transcriptional regulator implicated in mitochondrial biogenesis and health, and various stimuli/stresses can induce this pathway. For example, exercise-induced oxidative stress can stimulate mitochondrial biogenesis by upregulating Nrf2 activity (Merry and Ristow, 2016). Furthermore, recovery from sepsis or from lung injury in response to *Staphylococcus aureus* infection in mice depends on Nrf2-mediated activation of mitochondrial biogenesis (MacGarvey et al., 2012, Athale et al., 2012).

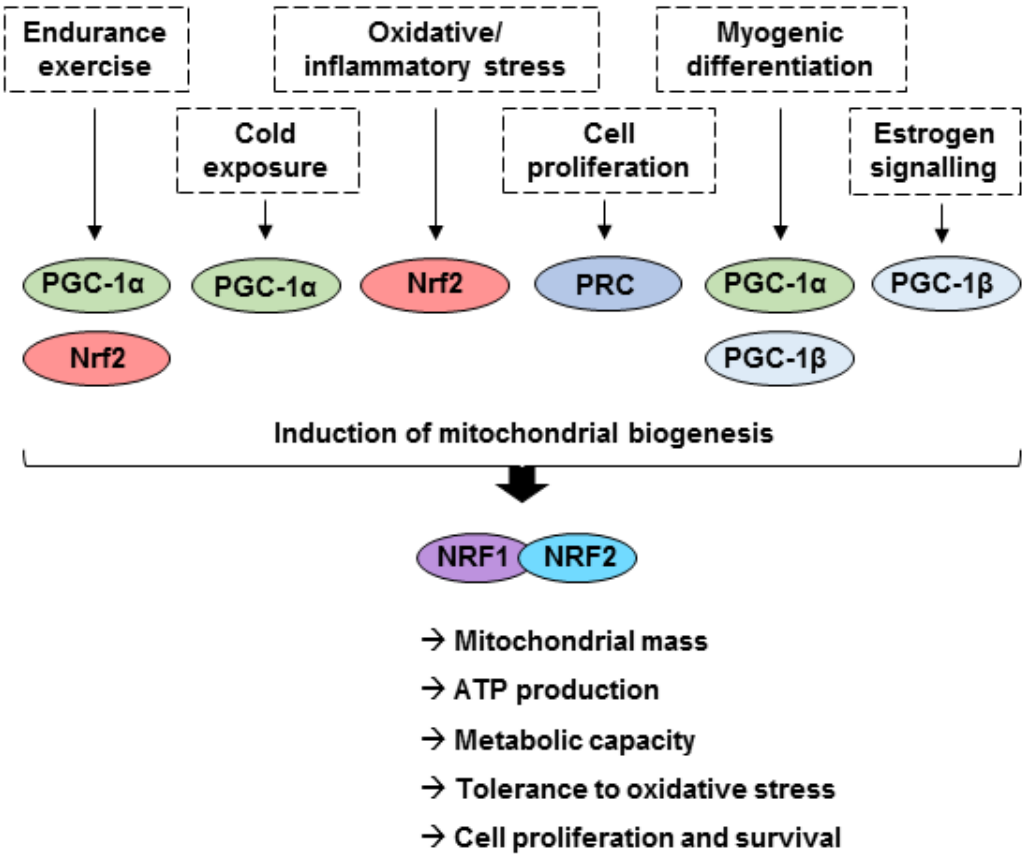

Figure 1.4 Regulators of mitochondrial biogenesis.

Various stresses or stimuli including cold exposure, oxidative/inflammatory stress, induction of cell proliferation, myogenic differentiation and exercise can induce mitochondrial biogenesis through the transcriptional regulators, PGC-1α, PGC-β, PRC or Nrf2. They all converge on induction of NRF1 and NRF2 to mediate this signal.

1.3.4 Mitochondrial dynamics

Mitochondria are dynamic organelles that constantly adapt to the cellular environment by undergoing fusion and fission events. Mitochondrial fusion is mediated mainly by the guanosine triphosphate (GTP)ases optic atrophy gene 1 (OPA1), mitofusin 1 (MFN1) and mitofusin 2 (MFN2). It occurs sequentially, as OPA1 mediates fusion of the IMM, while MFN1 and MFN2 mediate fusion of the OMM (Song et al., 2009). As reviewed by Sebastián and Zorzano (2018), it has been proposed that the mitofusins can dimerize between opposing mitochondrial membranes following GTP binding. Hydrolysis of GTP then causes conformational changes that bring the membranes into

close contact allowing fusion to occur (Qi et al., 2016, Cao et al., 2017, Sebastián and Zorzano, 2018).

Mitochondrial fission on the other hand is mediated by the GTPase DRP1 (Smirnova et al., 2001), which is predominantly cytoplasmic under normal cellular conditions. The protein forms oligomers that upon fission-inducing stimuli can assemble into larger structures at the OMM. Conformational changes in the protein following GTP hydrolysis cause constriction of the OMM leading to mitochondrial division. DRP1 function and localisation is predominantly regulated by post-translational modification such as phosphorylations and sumoylations (Chang and Blackstone, 2010). A recent study revealed that DRP1 is essential for mitochondrial fission, whereas dynamins that were previously proposed to be required for this process are dispensable (Fonseca et al., 2019).

Different growth conditions for *Saccharomyces cerevisiae* were shown to affect mitochondria shape, size and interconnectivity (Visser et al., 1995). Mitochondria can fuse to protect and preserve the existing mitochondria pool in a cell in response to nutrient deprivation (Gomes et al., 2011). Furthermore, exchange of material between different mitochondria facilitates the segregation of mitochondria that are targeted for degradation due to damage (Twig et al., 2008).

Mitochondria dynamics also affect mitochondrial metabolism. Particularly, MFN2 is central to the integration between mitochondria form and function, as MFN2 depletion or mutations in various models was associated with impaired OXPHOS, reduced mitochondrial membrane potential and metabolic reprogramming (Bach et al., 2003, Pich et al., 2005). Hence, it is not surprising that dysregulation of mitochondrial dynamics is associated with various pathologies (Chan, 2019).

1.3.5 Mitochondrial autophagy

1.3.5.1 Autophagy

Autophagy is a catabolic process through which cellular components/organelles are engulfed by autophagosomes and degraded, when the autophagosomes fuse with lysosomes. This process feeds anabolic processes upon recycling of the building blocks (Parzych and Klionsky, 2014). In yeast, the coordinated process of autophagosome biogenesis and cargo recruitment and uptake is carried out by a set of autophagy-related proteins (Atg). The yeast ubiquitin-like protein Atg8 is essential to this process (Shpilka et al., 2011). Mammalian homologues of Atg8 include microtubule-associated protein 1 light chain 3 (LC3), γ-aminobutyric-acid-type-A (GABAA)-receptor-associated protein (GABARAP) and GABAA-receptor-associated protein 2/Golgi-associated ATPase enhancer of 16 kDa (GATE-16). These all become anchored to autophagosome membranes upon conversion from form I to form II through a process believed to involve phosphatidylethanolamine (PE)-conjugation (Kabeya et al., 2004). So-called autophagy adaptors, such as sequestosome 1/p62, NDP52 and optineurin mediate the interaction between these autophagy proteins and the ubiquitinated proteins that target cytoplasmic cargo. To do so, the adaptor proteins contain both ubiquitin-binding domains and LC3-interacting regions (LIR) that can interact with a motif in LC3 and other Atg8-like proteins (Birgisdottir et al., 2013).

The formation of autophagosomes is initiated in response to cellular nutrient/energy stress by the UNC-51 Like Autophagy Activating Kinase 1 (ULK1) protein complex, which is regulated by mTORC1 and AMPK (Lin and Hurley, 2016). mTORC1 associates with and phosphorylates ULK1 causing suppression of its activity. mTORC1 is inhibited upon nutrient deprivation, which triggers the release of

ULK1 and induction of autophagy. Conversely, mTORC1 is activated under nutrient rich conditions due to Insulin/IGF-1 signalling through PI 3-K/AKT leading to inhibition of autophagy (Jung et al., 2010). AMPK is activated in response to increases in the AMP/ADP ratio signalling an unbalanced cellular energy status. It can activate ULK1 by direct phosphorylation or, indirectly, through phosphorylation-dependent inhibition of mTORC1 (Hardie, 2011).

1.3.5.2 Mitophagy

Removal of damaged or aged mitochondria occurs through a selective form of autophagy referred to as mitophagy, which is mediated through various pathways. Mitophagy is typically preceded by mitochondrial fission to facilitate the engulfment of the targeted mitochondria by autophagosomes (Lee et al., 2011).

The different pathways through which mitophagy can occur are illustrated in Figure 1.5. Thus far, the most widely described is ubiquitin-dependent and operates through PTEN-induced putative kinase 1 (PINK1) and Parkin. PINK1 is under normal conditions transported across the OMM to the IMM, where it is cleaved and degraded. However, when mitochondria become depolarized, PINK1 is retained at the OMM and becomes activated due to autophosphorylation, causing Parkin recruitment (Okatsu et al., 2012). Parkin functions as an E3 ligase that poly-ubiquitinates proteins on the OMM (Shimura et al., 2000). These proteins then either undergo proteosomal degradation or interact with autophagy adaptors NDP52 and optineurin that can interact with LC3II on autophagosomes leading to engulfment and degradation of mitochondria. NDP52 and Optineurin also recruit ULK1, triggering autophagosome biosynthesis (Lazarou et al., 2015). It was shown that PINK1 also phosphorylates ubiquitin, contributing to the full activation of the E3 ligase activity of Parkin (Koyano

et al., 2014). Other E3 ligases such as Gp78 can also ubiquitinate OMM proteins facilitating Parkin- independent mitophagy (Fu et al., 2013a).

Alternative routes of mitochondrial clearance involve mitophagy receptors that interact directly with Atg8-like proteins on the autophagosome surface through their LC3-interacting regions. These receptors include IMM protein Prohibitin 2 (PHB2) and OMM proteins, B-cell Lymphoma 2 (BCL-2)/Adenovirus E1B 19 kDa Protein-Interacting Protein 3 (BNIP3), NIP3-like protein X (Nix/BNIP3L) and FUN14 Domain Containing 1 (FUNDC1) (Palikaras et al., 2018). PHB2 was recently shown to function as a mitophagy receptor in PINK1-Parkin mitophagy following permeabilization of the OMM (Wei et al., 2017). FUNDC1 mediates mitophagy in response to hypoxia and is known to regulate mitochondrial morphology as well through interactions with OPA1 and DRP1 (Liu et al., 2012). Similarly, the homologues Nix and BNIP3 are known to induce mitophagy under hypoxic conditions, as Hypoxia Inducible Factor 1 Subunit α (HIF-1α) induces their expression (Sowter et al., 2001, Ney, 2015). Nix is also required for mitochondrial clearance associated with reticulocyte maturation (Schweers et al., 2007).

Activating Molecule in BECN1-Regulated Autophagy protein 1 (AMBRA1) is another mitophagy mediator, which has been shown to localise partly to the mitochondria, where it can interact with LC3 and induce mitophagy (Strappazzon et al., 2015).

Interestingly, BNIP3 was shown to enhance PINK1 stabilisation on the OMM and PINK1-Parkin mitophagy (Zhang et al., 2016). Similarly, BNIP3L is a substrate in Parkin-mediated mitophagy (Gao et al., 2015). This suggests cross talk and potentially redundancy in the different mitophagy pathways

Accurate and appropriate regulation of mitophagy is essential to many different cell functions such as cell differentiation (Lampert et al., 2019), neuronal health and function (Anichtchik et al., 2008, Moisoi et al., 2014) and maturation of immune cells (O'Sullivan et al., 2015).

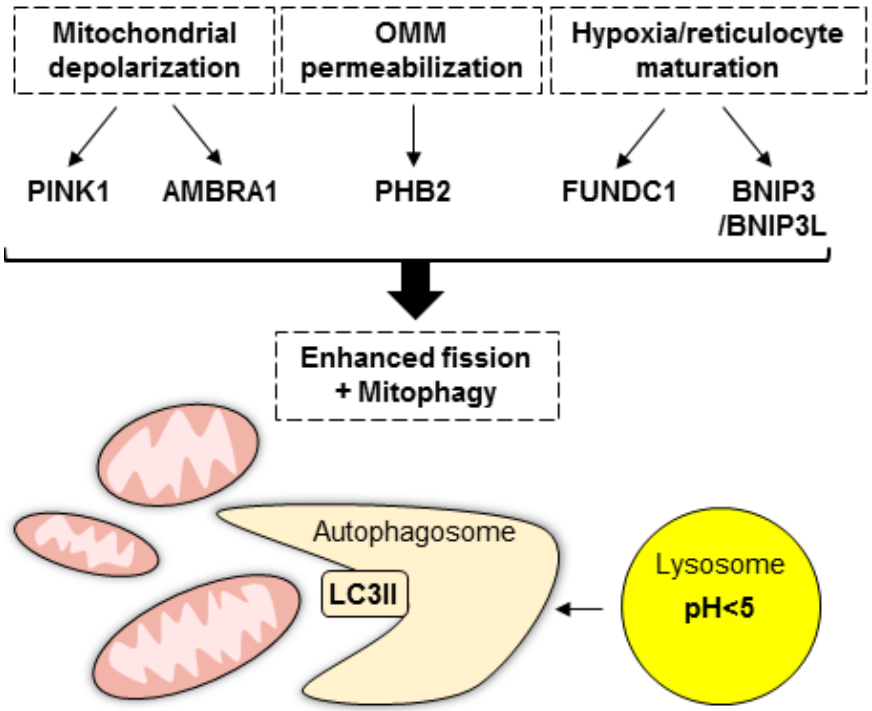

Figure 1.5 Mitophagy triggers and mediators.

Mitochondrial stresses such as depolarization, OMM permeabilization or hypoxia induce mitophagy through a ubiquitin-dependent pathway involving PINK1 or through non-ubiquitin dependent pathways involving the mitophagy receptors, FUNDC1, BNIP3/BNIP3L, PHB2 or AMBRA1.

1.4 BNIP3 functions in cell death and mitophagy

1.4.1 BNIP3 structure and function

BNIP3 was first identified due to its interaction with Adenovirus E1B 19 kDa protein and was shown to localise to mitochondria, when expressed alone. However, BNIP3

translocates to the nucleus upon co-expression with the E1B 19 kDa protein, which protects again apoptosis in response to the viral infection (Boyd et al., 1994).

BNIP3 belongs to the BNIP3 subfamily of the BH3-only BCL-2 family of proteins, consisting of BNIP3 and BNIP3L. The two proteins share approximately 55% sequence homology (Chinnadurai et al., 2008). As illustrated in Figure 1.6, BNIP3 contains an N-terminal proline (P), glutamic acid (E), serine (S), threonine (T) and aspartic acid (D) (PEST) domain that targets it for degradation, a BCL-2 homology (BH3) domain, a conserved domain and a C-terminal transmembrane region that targets it to the OMM of mitochondria (Vasagiri and Kutala, 2014). Through its BH3 domain, it interacts with the anti-apoptotic proteins BCL-2, BCL-x_L and EBV-BHRF1 that are functional homologues of Adenovirus E1B 19 kDa protein. Mutations in the BH3 domain was shown to partially impair the apoptotic functions of BNIP3 and prevent interaction with and subsequent suppression of the anti-apoptotic protein BCL-x_L (Yasuda et al., 1998). A later study revealed that cell death mediated by BNIP3 is independent of caspases and cytochrome C release (Vande Velde et al., 2000). In this study, BNIP3 was shown to induce early plasma membrane permeabilization but prevented the common apoptotic process of phosphatidylserine externalisation. Late DNA fragmentation was induced, but atypically this was independent of apoptosis inducing factor (AIF), which is well-described for its role in DNA fragmentation upon apoptotic stimuli (Susin et al., 1999). BNIP3 expression also led to accumulation of cytoplasmic vacuoles. Taken together, the data suggest that BNIP3 mediates a necrotic type of cell death. Furthermore, BNIP3 induced loss of mitochondria membrane potential due to opening of the permeability transition (PT) pore and increased production of ROS. Inhibition of the PT pore prevented BNIP3-induced cell death, suggesting mitochondria dysfunction is essential to this cell death

pathway (Vande Velde et al., 2000). It has since been shown that BNIP3 can induce cell death through various mechanisms, such as tumour necrosis factor (TNF)-mediated necrosis (Kim et al., 2011), a hypoxia-induced caspase-independent pathway (Ma et al., 2017) and a calpain-dependent cell death pathway activated in response to hypoxia-acidosis mimicking ischemia (Graham et al., 2015). It was also shown that BNIP3 mediated protective mitochondrial autophagy despite ultimately inducing cell death in response to hypoxia (Ma et al., 2017).

In cardiomyocytes the transcription factor Forkhead box O3a (FOXO3a) upregulates BNIP3 causing increased mitochondrial Ca^{2+}, decreased mitochondrial membrane potential and finally cell death, suggesting that FOXO3a specifically promotes the apoptotic/necrotic function of BNIP3 (Chaanine et al., 2016). IGF-1 signalling can phosphorylate FOXO3a via PI 3-K/AKT causing its translocation to the cytoplasm and inhibition of its activity (Yan et al., 2016), suggesting IGF-1 may suppress this cell death-promoting function of BNIP3.

As mentioned above, BNIP3 is induced in response to hypoxia by HIF-1α (Guo et al., 2001). BNIP3 can bind and inhibits RHEB causing inhibition of mTORC1 activity during hypoxia, and this is associated with reduced cell growth (Li et al., 2007).

Perinecrotic regions of tumours are hypoxic and exhibit elevated levels of BNIP3, which may mediate cell death in such areas (Sowter et al., 2001). However, some tumours display impaired BNIP3-induced cell death despite increased BNIP3 expression. It has been proposed that this may be due to retainment of BNIP3 in the nucleus of such tumour cells (Burton et al., 2006). Another study proposed that growth factor signalling might impact on BNIP3 function in tumours. They showed that Epidermal Growth Factor (EGF) and IGF can prevent hypoxia-mediated cell death

through a mechanism dependent on the presence of an intact BH3 domain in BNIP3. Of note, the group did not specify which IGF ligand was applied, and the concentration used in cell cultures was 1µg/ml, thus, exceeding physiological levels (Kothari et al., 2003). However, IGF signalling may be able to alter the expression or function of BNIP3 to mediate protection against cell death.

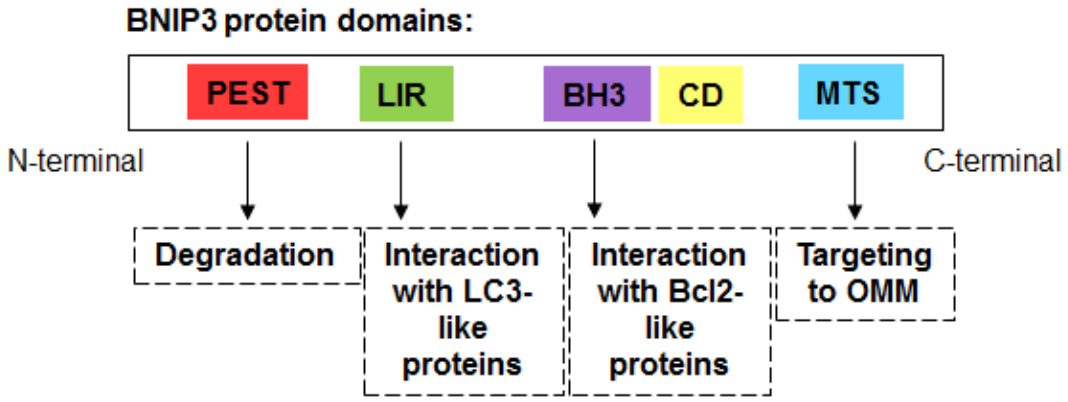

Figure 1.6 The protein domains of BNIP3.

BNIP3 contains an N-terminal PEST domain, which targets BNIP3 for proteosomal degradation, a LIR which interacts with LC3II during mitochondrial clearance, a B-cell Lymphoma 2 (BCL-2) Homology (BH3) domain that is implicated in regulation of apoptosis, a conserved domain (CD) and a C-terminal mitochondrial targeting sequence (MTS).

1.4.2 BNIP3 in mitophagy

BNIP3 also contains a LIR motif in the N-terminus, which is exposed to the cytoplasm, when the C-terminal transmembrane domain is inserted into the OMM. This motif is essential to interaction with LC3, and inactivation of the motif, partially prevented the reduction in mitochondrial mass observed in response to overexpression of WT BNIP3, suggesting that mitochondrial BNIP3 can trigger mitophagy likely through interaction with LC3-like proteins on the autophagosome surface (Hanna et al., 2012). BNIP3 can selectively mediate mitophagy and prevent cell death by impairing OXPHOS without causing permeabilization of the OMM (Rikka et al., 2011). This

suggests a cytoprotective role for BNIP3, when it induces mitophagy, and a cell death promoting role for BNIP3 under other conditions.

Mitophagy mediated by BNIP3 is preceded by recruitment of the mitochondrial fission mediator DRP1 likely to separate the damaged/aged parts of the mitochondrial network that are targeted for degradation (Lee et al., 2011). Furthermore, BNIP3 can interact with OPA1 to inhibit mitochondrial fusion (Landes et al., 2010).

Modulation of serines flanking the LIR domain to generate a phosphomimetic mutant and a non-phosphorylatable mutant revealed a phosphorylation-dependent regulation of BNIP3 activity. The phosphomimetic displayed enhanced interaction with LC3 and GATE-16 and increased mitochondrial degradation, whereas the non-phosphorylatable mutant abolished interaction with LC3/GATE-16. This was associated with anti-apoptotic effects through reduced cellular capacity for cytochrome C release (Zhu et al., 2013). Phosphorylations near the C-terminal transmembrane region were also shown to affect the function of BNIP3, as BNIP3-dependent cell death was downregulated, but mitophagy induction was unaffected (Liu and Frazier, 2015). Similarly, phosphorylation of Nix enhances its mitophagy function (Rogov et al., 2017). Others have demonstrated cellular regulation of BNIP3 function by alternative splicing (Gang et al., 2015).

Consistently, these studies suggest a cytoprotective role of BNIP3-mediated mitophagy. In support of this, it was shown that BNIP3 knockout mice exposed to renal ischemia-reperfusion, had impaired mitophagy, which was associated with accumulation of dysfunctional mitochondria, increased ROS and led to increased cell death in the kidneys (Tang et al., 2019). In addition, the HIF-1α/BNIP3 axis was

shown to induce mitophagy to mediate protection in response to myocardial damage caused by ischemia/reperfusion (Zhang et al., 2019).

In *C. elegans*, the NFE2L2/Nrf2 homologue SKN-1 regulates both mitochondrial biogenesis and mitophagy. In response to mitophagy impairment, which causes ROS accumulation, the redox status sensor SKN-1 was activated and induced mitophagy through DCT-1, which is a homologue of BNIP3/BNIP3L (Palikaras et al., 2015b). Thus, Nrf2 regulates BNIP3 activity in *C. elegans* through a pathway coupling mitochondrial biogenesis and turnover. The different functions of BNIP3 are illustrated in Figure 1.7.

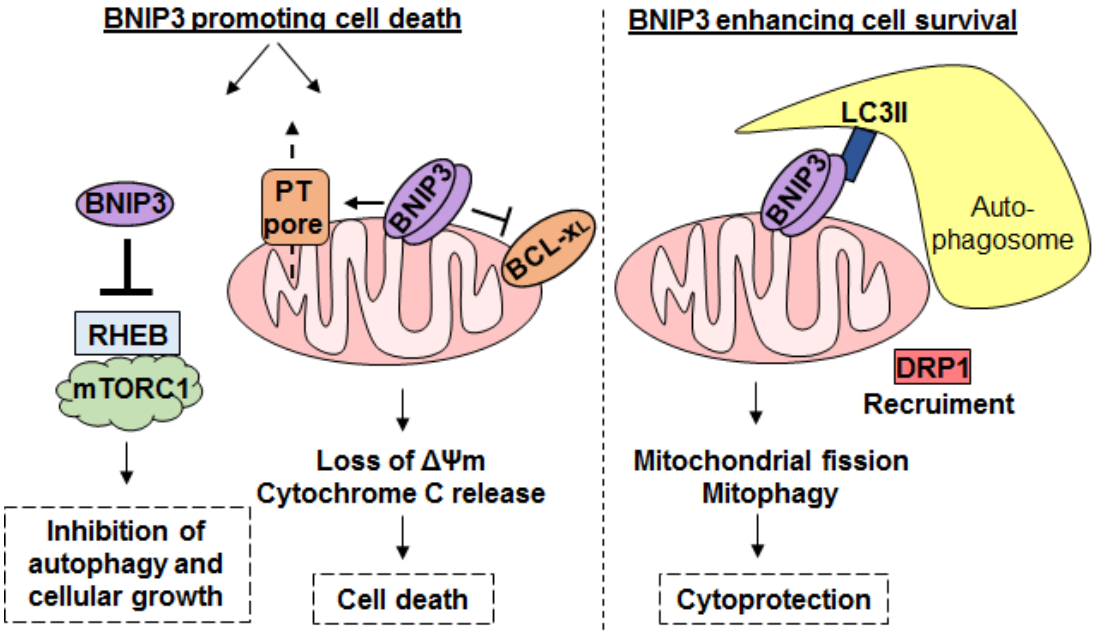

Figure 1.7 Summary of BNIP3 functions.

BNIP3 can inhibit autophagy and cellular growth through inhibition of RHEB. Alternatively, BNIP3 can cause cell death through induction of mitochondrial dysfunction. Finally, BNIP3 can mediate mitophagy by direct interaction with LC3-like proteins on autophagosomes. Δψm: mitochondrial membrane potential.

1.5 Nrf2 function and activity in cancer

1.5.1 Nrf2 function

Nrf2 is a cytoprotective transcription factor that acts as the major mediator of cellular stress responses upon antioxidant stress or toxic insults (Baird and Dinkova-Kostova, 2011). It belongs to a family of basic leucine zipper, cap'n'collar (CNC) transcription factors that in vertebrate consist of NFE2 (Andrews et al., 1993) and the NFE2-related factors Nrf1 (Chan et al., 1993), Nrf2 (Moi et al., 1994) and Nrf3 (Kobayashi et al., 1999). Nrf2 is by far the most studied of the proteins, but, generally, they have important roles in development and are particularly associated with the maintenance of homeostasis during cellular stress responses (Sykiotis and Bohmann, 2010). Nrf2 has been implicated in stem cell differentiation, as it is involved in the metabolic changes required for reprogramming of stem cells (Hawkins et al., 2016). It was shown to regulate the function and longevity of hematopoietic stem cells (Tsai et al., 2013).

Additionally, Nrf2 regulates cellular detoxification in response to various xenobiotics (Köhle and Bock, 2007, McMahon et al., 2001). In cancer cells, these protective functions can be exploited to allow cells to survive in the stressful tumour environment, where nutrients and oxygen levels are low, so, unsurprisingly, Nrf2 is also associated with the development of chemoresistance in bladder cancer (Hayden et al., 2014, Ciamporcero et al., 2018), acute myeloid leukemia (Karathedath et al., 2017), non-small cell lung cancer (Ji et al., 2019) and other cancers (Bai et al., 2016). Furthermore, studies have implicated Nrf2 in metabolic reprogramming, specifically it causes metabolic reprogramming in a HIF-1α-dependent way in breast cancer cells, supporting a role in cancer cell adaptation and progression (Zhang et al., 2018, Wang et al., 2018).

Nrf2 is also strongly associated with mitochondrial health and function, as it has been shown to regulate mitochondrial biogenesis, ATP production and structural integrity for example (Dinkova-Kostova and Abramov, 2015). Furthermore, Nrf2 mediates a homeostatic signalling pathway that impacts both mitochondrial biogenesis and mitophagy, resulting in increased healthy lifespan (Palikaras et al., 2015b). The balance between mitochondrial biogenesis and mitophagy requires strict regulation in healthy cells during aging and in response to stress as well as in cancer cells with their increased dependence on energy production and ROS clearance (Pickles et al., 2018, Wallace, 2012). Therefore, the coordinated regulation of mitochondrial biogenesis and mitochondrial turnover through Nrf2 could enhance tumorigenesis in cancer cells.

Interestingly, an immunohistochemical study of gastric neoplasias ranging from benign to malignant revealed a positive correlation between Nrf2 and IGF-1 with elevated expression of both in premalignant and malignant tumours, potentially linking the two hormetic pathways in cancer (Wang et al., 2011).

1.5.2 Nrf2 activity determined by protein stability

The stability and activity of Nrf2 is mainly regulated at a protein level, as it is bound to inhibitory protein complexes that through interaction with E3 ligases cause rapid ubiquitination and degradation of the protein. Four such complexes have been identified involving Kelch ECH associating protein 1 (KEAP1) interacting with Cullin 3, GSK-3β interacting with SCF/β-TrCP, HMG-CoA reductase degradation 1 homolog (Hrd1) or WDR23 in association with DDB1 and Cullin4 associated factor 11 (DCAF11 or WDR23) (Rojo de la Vega et al., 2018, Park et al., 2019). The protein domain structure of Nrf2 and its interaction with degradative complexes are illustrated in Figure 1.8A-B.

KEAP1 binds as a homodimer to the Neh2 domain of Nrf2 at two distinct sites, the DLG and the ETGE motifs. KEAP1, furthermore, binds Cullin 3, which interacts with Ring-box1 protein, and the three proteins form an E3 ubiquitin ligase complex that ubiquitinates Nrf2. Upon exposure to particularly electrophiles, Keap1 undergoes cysteine modifications that cause the dissociation from Cullin 3, leading to stabilization of Nrf2 (Suzuki and Yamamoto, 2015, Furukawa and Xiong, 2005). Additionally, Nrf2 induction leads to increased levels of its target genes, including p21 and p62, that can bind Nrf2 causing displacement of KEAP1, thus further enhancing Nrf2 stabilization (Taguchi et al., 2011, Ichimura et al., 2013, Komatsu et al., 2010).

Active GSK-3β on the other hand can phosphorylate serines within the Neh6 domain of Nrf2, which also contains a region resembling the SCF/β-TrCP destruction motif that is targeted for ubiquitination. These phosphorylations mediated by GSK-3β enhance degradation of Nrf2 and are necessary for the recruitment of SCF/β-TrCP. It was shown that inhibition of the PI 3-K/AKT pathway increases GSK-3β activity and reduces Nrf2 activation (Rada et al., 2011, Chowdhry et al., 2013). As IGF-1 signalling inhibits GSK-3β by phosphorylating the protein on S9, IGF-1 may potentially cause activation of Nrf2 (Sutherland et al., 1993).

The E3 ubiquitin ligase Hrd1 was shown to regulate Nrf2 degradation in liver cirrhosis (Wu et al., 2014). Finally, WDR23 regulates Nrf2 activity specifically affecting Nrf2 target genes involved in the cytoprotective Nrf2 response. WDR23 is part of an E3 ligase complex with CUL4A-DDB1 that can mediate Nrf2 degradation (Lo et al., 2017). It appears that all these different routes for Nrf2 regulation are complementary and upregulate various Nrf2 response pathways depending on the cellular status.

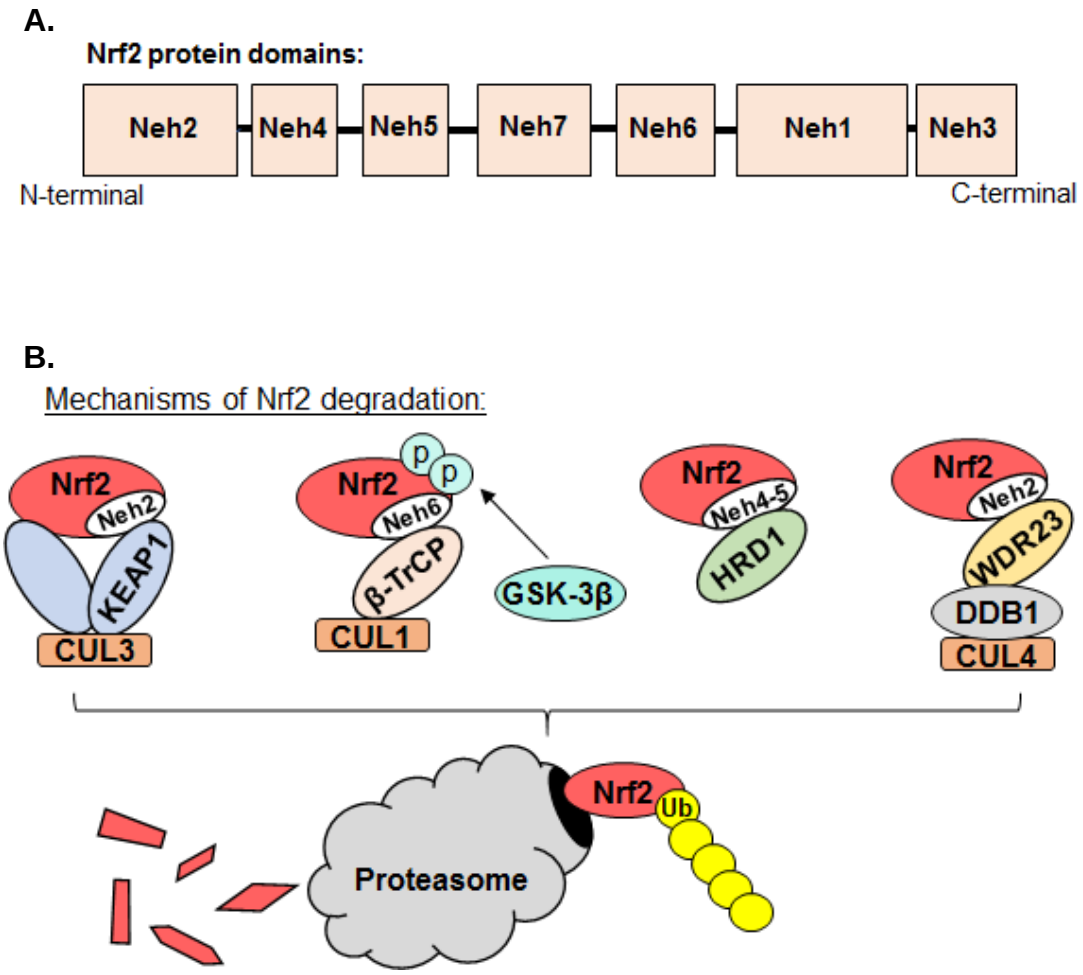

Figure 1.8 The domain structure of Nrf2 and its various routes for degradation.

A. Nrf2 is composed of 7 Neh domains in the illustrated order that can interact with different negative regulators of Nrf2. **B.** KEAP1 or WDR23 can interact with the Neh2 domain of Nrf2 to recruite the E3 ligases CUL3 or CUL4, respectively. Hrd1 binds the Neh4 and Neh5 domains of Nrf2. β-TrCP interacts with the Neh6 domain of Nrf2, and this interaction is enhanced by GSK-3β-mediated phosphorylations. β-TrCP recruits CUL1 to mediate degradation of Nrf2. The recruitment of E3 ligases cause ubiquitination (Ub) and proteosomal degradation of Nrf2.

1.6 Thesis Aims

IGF-1 signalling contributes to cancer development and progression. However, clinical trials with anti-IGF-1 treatments in cancer patients have yielded disappointing results. This has highlighted the need to improve means of stratifying patients and to enhance our understanding of the pathway to target it more efficiently. One approach to improve treatment efficacy while reducing the occurrence of chemoresistance, is to target multiple components of the pathway.

Mitochondrial dysfunction is a key characteristic of cancer cells and can affect metabolism, mitochondrial biogenesis, mitochondrial dynamics or mitophagy. IGF-1 signalling impacts on several aspects of mitochondrial function. We previously characterized the mitochondrial UTP carrier PNC1, which is induced by IGF-1 and implicated in promotion of cell growth. This established a mitochondria protective role for IGF-1 in cancer cells (Floyd et al., 2007, Favre et al., 2010). Thus, inhibition of IGF-1 signalling may render cancer cells vulnerable to targeting of essential mitochondrial proteins representing potential drug targets.

The first aim of this project was to complete a study focusing on the effects of IGF-1 on mitochondrial biogenesis and mitophagy in cancer cells, particularly through the mitophagy receptors BNIP3 and PHB2.

The second aim was to delineate the pathway through which IGF-1 regulates BNIP3 and expand our knowledge on the importance of this signalling pathway in mitochondrial dynamics and turnover.

The third aim was to develop a tool with which to directly measure mitophagy within our cell models and to use this tool to directly assess the effects of IGF-1 on mitophagy.

Chapter 2. Materials and Methods

2.1 Antibodies

Rabbit anti-phospho-IGF-1R (Y1135/1136 #3024), rabbit anti-IGF-1R (#3027), rabbit anti-phospho-AKT (S473, #4060), rabbit anti-AKT (#2920), rabbit anti-NFE2L2/Nrf2 (#12721), rabbit anti-caspase 3 (#9662), rabbit anti-cleaved caspase 3 (#9661), rabbit anti-phospho-GSK-3β (S9, #9336), rabbit anti-phospo-p70 S6 kinase (T371, #9208) and rabbit anti-p70 S6 kinase (#9202) were all obtained from Cell Signalling Technology (Danvers, MA). Rabbit anti-PHB1 (#PA5-19556) and rabbit anti-PHB2 (#PA5-14133) was from Thermo Fisher Scientific (Waltham, MA). Rabbit anti-TOM20 (#sc-11415), mouse anti-TOM20 (#sc-17764), anti-α-tubulin (#sc-23948), and mouse anti-p62 (#sc-28359) were from Santa Cruz Biotechnology (Dallas, TX). Mouse anti-BNIP3 (#ab10433) and mouse Total Human OXPHOS WB antibody cocktail (#ab110411) were from Abcam (Cambridge, UK). Mouse anti-β-actin (#A5441) and rabbit anti-LC3 (#L8918) were from Sigma-Aldrich (St. Louis, MO). Mouse anti-GSK-3 (#610202) was from BD Biosciences (Franklin Lakes, NJ) and Rabbit anti-HIF-1α (#A300-286A) from Bethyl Laboratories Inc (Montgomery, TX). Rabbit anti-PINK1 (#BC-100-494) was purchased from Novus Biologicals (Littleton, CO).

Of note, BNIP3 is known to undergo post translational modification including phosphorylations that can affect the migratory pattern, so by western blotting it presents with a series of bands around 30-35kDa apart from the two dominant bands representing the monomer at ~20-25kDa and the dimer ~55-60kDa, although the profile varies slightly depending on the cell line (Mellor et al., 2010, Graham et al., 2007). For quantification of protein from human cancer cell lysates, densitometry was performed measuring the bottom monomer band only, which was consistently detected with different antibody batches, and was specifically altered by the indicated

culture conditions. For MEFs, all bands in the 25-30kDa range were included for densitometry, due to the different antibody detection profile observed in these cells.

2.2 Cell lines and cell culture

MCF-7, DU145 and U2OS cell lines were all obtained from ATCC (Old Town Manassas, VA). MCF-7 breast cancer cells, U2OS osteosarcoma cells and R- and R+ cells (mouse embryonic fibroblast cell lines (MEFs) derived from IGF-1R knock-out mice (Sell et al., 1994) were cultured in DMEM (#D6429, Sigma) supplemented with 10% heat-inactivated fetal bovine serum (FBS), 10mM L-Glutamine and 5mg/ml penicillin/ streptomycin. DU145 prostate carcinoma cells were cultured in RPMI (#R8758, Sigma) with the same supplements. Cells were cultured in incubators at 37°C and 5% CO_2. Prior to experiments that included IGF-1 stimulation or chemical inhibitors, cells were seeded and cultured for 16h, allowing them to reach a confluence of approximately 70%.

When seeding for experiments, cell counting was performed using a haemocytometer. A small volume of the cell suspension was diluted 1:1 with Trypan Blue Solution (0.4%, #T8154, Sigma-Aldrich) that allows distinction between cells that are alive (unstained) or dead (blue).

For serum-deprivation of cells, they were washed twice with PBS and then cultured in serum-free medium for 4h prior to addition of IGF-1 (Peprotech #100-11) at 10ng/ml for the indicated periods of time unless otherwise stated.

The MCF-7R cell line was generated in our laboratory by Dr. Amy Lyons as described in O'Flanagan *et al.* 2016. MCF-7 cells were maintained in increasing concentrations of the IGF-1R receptor tyrosine kinase inhibitor BMS-754807 (#A-

1013, Active Biochem, Hong Kong), producing a cell line with acquired resistance to the inhibitor (O'Flanagan et al., 2016). Generally, these cells were cultured in DMEM culture medium as described above for MCF-7 cells with the addition of 500nM BMS-754807 until 24h prior to seeding, when the BMS-754807 was removed to prevent cross-actions with other chemicals added during the experiments.

For inhibition of GSK-3, two compounds were used: The GSK-3α/β inhibitor SB415286 (#S3567, Sigma) at 30μM and the GSK-3β inhibitor LiCl at 10mM. They were added to complete medium cultures for the time indicated in figure legends. As the two GSK-3 isoforms (α/β) have overlapping functions with little knowledge of their distinct roles (Doble et al., 2007, Itoh et al., 2012), a specific isoform was only stated in this thesis, when analysing the phosphorylation site at Ser9, which is known to specifically occur on GSK-3β (Cross et al., 1995).

The PI 3-K inhibitor LY294002 (#440204, Merck) was added to complete medium cultures at 20μM 30 min prior to addition of IGF-1. For induction of mitochondrial stress, the iron chelator deferiprone (DFP, #379409, Sigma) was used at 1mM and both of the mitochondrial uncouplers Carbonyl Cyanide 3-Chlorophenylhydrazone (CCCP, #C2759, Sigma) or Carbonyl cyanide 4-(trifluoromethoxy)phenylhydrazone (FCCP, #C2920, Sigma) were used at 10μM concentration. They were added to complete medium cultures for the time indicated in figure legends. 50μM of the lysosomal inhibitor chloroquine (#14774, Sigma) was added for the last 4h of cell culture in the indicated experiments. LY294002, SB415286, CCCP and FCCP were all dissolved in DMSO, and therefore DMSO alone was added as a vehicle control to reach equivalent concentrations to that in control samples (usually 1/1000).

2.3 Polymerase Chain Reaction (PCR) and agarose gel electrophoresis

20µl PCR reactions included: 20ng of DNA template, 1µl each of the forward and reverse primer (10µM working stock), 10µl GoTaq G2 Green All-in-One PCR Master Mix (#M7823, Promega (Maddison, WI, USA)) and nuclease-free water. The following PCR cycle setup was used on a PTC-200 Peltier Thermal Cycler (MJ Research, Waltham, MA, USA):

- 95°C for 2min

Followed by 35 cycles of:

- 94°C for 30s
- X °C for 30s (temperature should be 5°C below lowest primer Tm)
- 72°C for X s (elongation time depends on PCR amplicon size (1min/kb))

The PCR products were separated on 1.0-1.5% agarose gels (DNA grade agarose (#A9539, Sigma) in TAE buffer (40 mM Tris, 20 mM acetic acid, 1 mM EDTA (pH 8.0)) depending on the size of the amplicon with 5µl SafeView Nucleic Acid Stain (#NBS-SV5,NBS Biological, Huntington, UK) per 50ml TAE. DNA Gel Loading Dye (6x) (#R0611, Thermo Fisher Scientific) was added to the samples, and electrophoresis was performed for 10-45min depending on fragment size at 70-90V. The following molecular ladders were used: GeneRuler 100 bp DNA Ladder (#SM0241) and GeneRuler 1 kb DNA Ladder (#SM0311) from Thermo Fisher Scientific. The DNA products were visualised by UV using a Gel Doc EZ Imager with Image Lab software purchased from Bio-Rad.

2.4 Restriction enzyme digestion and ligation of DNA

For restriction enzyme digestions, the enzymes, digestion buffers, T4 DNA Ligase Reaction Buffer and T4 DNA Ligase (#M0202) were all purchased from New England Biolabs (Ipswich, MA, USA). For agarose gel DNA extraction, the KeyPrep Gel Clean Up Kit was used (#AM-113163, Anachem).

Restriction enzyme digestions were prepared as follows per 25µl reaction: 1ug DNA, 2.5µl restriction buffer, 1µl of each restriction enzyme and nuclease-free water. Incubation was typically performed for 1h at 37°C unless otherwise specified for the specific restriction enzyme in use. Agarose gel electrophoresis was performed as described above to confirm successful digestion.

DNA ligations were set up as follows per 20µl reaction: 2µl T4 DNA Ligase Reaction Buffer (10x), 50ng vector DNA, 1µl T4 DNA Ligase, nuclease-free water and varying amounts of insert DNA depending on the sizes of the vector and the insert. The amount of insert to use was calculated using the NEBioCalculator (https://nebiocalculator.neb.com/#!/ligation) typically applying 3:1 and 5:1 insert:vector ratios. Generally, ligations were done at 16°C overnight, and the T4 DNA Ligase was subsequently inactivated by heating the ligation mix to 65°C for 10min.

2.5 Bacterial transformation

Lysogeny broth (LB) (#L3022, Sigma-Aldrich) was prepared in dH_2O and autoclaved. For agar plates, bacteriological agar (#A5306, Sigma-Aldrich) was added to this solution prior to autoclaving. The appropriate antibiotics were added depending on the antibiotic resistance cassette present within the plasmids in use. Ampicillin (#A9518, Sigma-Aldrich) was used at 100µg/ml. Kanamycin (#K1377, Sigma-Aldrich) was used at 30µg/ml.

Competent DH5α *Escherichia Coli* (*E. Coli*) were used for transformation of plasmids. The competent *E. Coli* (stored at -80°C) were allowed to thaw for ~5min on ice. Generally, 1-2µl of DNA (~10ng) was added to 50µl aliquots of the bacteria and left on ice for 30min. The bacteria were then heat-shocked for 1.5min at 42°C and subsequently kept on ice for 2min prior to addition of 950µl of LB medium with no antibiotic. The bacteria were left to grow for 1h at 37°C in a shaking incubator at 150rpm. For supercoiled plasmids, 100µl of this culture was spread onto agar plates with the appropriate selection antibiotic. For non-supercoiled plasmids, the 1ml culture was centrifuged at 3000rpm for 3min, resuspended in 50-100µl LB medium and spread on agar plates with the appropriate selection antibiotic.

The agar plates were kept in an incubator at 37°C overnight (~16h). The following day, colonies were picked using sterile pipette tips and used for inoculation of 2-5ml LB medium cultures with the appropriate selection antibiotic. These were cultured overnight in a shaking incubator (150rpm) at 37°C overnight (~16h) and plasmid DNA extraction was performed using The Plasmid DNA Extraction Kit (#112113, Anachem) to allow analysis of the plasmids. Sequencing of plasmids was performed using Supreme Sanger Sequencing offered by Eurofins Scientific (Luxembourg).

2.6 Plasmid transfection

Plasmid DNA was amplified for transfections using The NucleoBond™ Xtra Midi Plus EF Kit to extract DNA (#12718422, Thermo Fisher Scientific). For this, a 2-5ml culture was inoculated as described above and cultured for ~8h in a shaking incubator (150rpm) at 37°C. From this starter culture, ~100µl was added to 100ml sterile LB medium in a 1L Erlenmeyer flask containing the appropriate selection antibiotic and

grown overnight (~16h) in a shaking incubator (150rpm) at 37°C. The plasmid DNA was extracted per manufacturer's instructions.

DNA transfections were performed using Lipofectamine (#18324-012) for MCF-7 cells or using Lipofectamine 2000 (#11668-019) for DU145, U2OS, R- and R+ cells. Both transfection reagents were purchased from Thermo Fisher Scientific and used following the manufacturer's instructions. Generally, for MCF-7 and DU145 cell lines, 2.5x10^5 cells were seeded per well in a 6-well plate the day before transfection. 1µg/well of DNA was used for transfections with Lipofectamine, whereas 2µg/well was used for transfections with Lipofectamine 2000. The DNA solution and transfection reagent were prepared separately in OptiMEM medium (Thermo Fisher Scientific, #51985026) and left to incubate for 5min at room temperature, before being gently mixed. The mixed transfection reagent and DNA was left to incubate for 20min at room temperature and then added to the cells. For Lipofectamine, the transfection mix (150µl per well) was added diluted in OptiMEM medium (600µl per well) to the cells and an equal volume of complete medium with 20% FBS was added 4-5h post transfection (750µl per well, with final concentration of 10% FBS in the medium). For Lipofectamine 2000, complete medium (1.8ml per well) was added to the cells with the transfection mix (200µl per well). When using either reagent, the transfection mixture was removed 24h post transfection, and the cells were detached and reseeded for experiments.

MCF-7 cells with stable expression of pcDNA3.1-VLCAD(1-40)-mCherry-EGFP, pcDNA3.1-BNIP3 WT or LIR-mutant plasmids were generated by transfection with the plasmids followed by selection with G418/neomycin. A dose-response drug curve for G418 in MCF-7 cells established the concentration at which 70-80% of all cells died after 4-5 days (1mg/ml). This concentration of G418 was subsequently used

to select cells containing the plasmids, and 0.8mg/ml was then used to maintain plasmid expression in culture following the initial selection phase.

The pcDNA3-HA2-KEAP1 plasmid was a kind gift from Yue Xiong (Addgene plasmid # 21556; http://n2t.net/addgene:21556; RRID:Addgene_21556) (Furukawa and Xiong, 2005). pEGFP-LC3 was a kind gift from Tamotsu Yoshimori (Addgene plasmid # 21073; http://n2t.net/addgene:21073; RRID:Addgene_21073) (Kabeya et al., 2000). pTRE-Tight-MitoTimer was a kind gift from Roberta Gottlieb (Addgene plasmid #50547; http://n2t.net/addgene:50547; RRID:Addgene_50547) (Hernandez et al., 2013).

pcDNA3.1-VLCAD(1-40)-mCherry-EGFP and pcDNA3.1-BNIP3 WT and LIR-mutant were all synthesised by GenScript Biotech Corporation (Piscataway, NJ). The pmCherry EV and WT BNIP3 constructs were generated as described below.

2.7 siRNA transfection

siRNAs targeting BNIP3 (L-004636-00-0005), NFE2L2/Nrf2 (L-003755-00-0005), and PHB2 (L-018703-00-0005) were purchased from Dharmacon (Lafayette, CO). As a negative control, Silencer Negative Control 1 (#AM4611) was obtained from Thermo Fisher Scientific (Waltham, MA). siRNA transfections were performed using Lipofectamine RNAiMAX (#13778075) from Thermo Fisher Scientific per manufacturer's instructions using all siRNAs at a concentration of 20nM. Cells were detached and resuspended in penicillin/streptomycin-free medium. For MCF-7 and DU145 cells, $6.5x10^5$ cells were seeded per well of a 6-well plate. For R- and R+ cells, $2.5x10^5$ cells were seeded per well of a 6-well plate. siRNA oligonucleotides were diluted in OptiMEM medium (#51985026) from Thermo Fisher Scientific. RNAiMAX transfection reagent was added to the siRNA/OptiMEM solutions and left

to incubate for 5min at room temperature. This solution was then added to the wells of a 6-well plate, and the cells were added on top of this. Cells were allowed to adhere overnight in the incubator. 24h post transfection, the siRNA solution was removed, and the transfected cells were reseeded for experiments.

2.8 Generation of expression vectors encoding a mitophagy reporter and different forms of BNIP3

To detect and quantify mitophagy in intact cells, we aimed to generate a mitochondria-targeted mCherry-EGFP construct informed by the vector used by Allen and colleagues (Allen et al., 2013). To generate the construct (illustrated in the figure below), we first used the mitochondrial targeting sequence (MTS) from pcDNA3-MTS-WT-c-Src-FLAG, which was a gift from Yoshimi Homma (Addgene plasmid # 44652; http://n2t.net/addgene:44652; RRID:Addgene_44652) (Ogura et al., 2012) to insert this into the pmCherry-EGFP vector, which was a gift from Thomas Leonard & Ivan Yudushkin (Addgene plasmid # 86639; http://n2t.net/addgene:86639; RRID:Addgene_86639) (Ebner et al., 2017). This MTS originates from the IMM protein very-long-chain acyl-CoA dehydrogenase (VLCAD). We attempted to excise the MTS from pcDNA3-MTS-WT-c-Src-FLAG, but it required extensive restriction enzyme incubation (>7h) to efficiently digest it, and subsequent ligations of the extracted sequence into the similarly digested pmCherry-EGFP vector did not yield the correct construct (vector design 1 in Figure 2.1).

Next, we attempted to excise the sequence following the MTS in the pcDNA3-MTS-WT-c-Src-FLAG vector and excise the mCherry-EGFP sequence from of the pmCherry-EGFP vector to insert it into the pcDNA3-MTS backbone (vector design 2 in Figure 2.1). Again, this approach did not generate the correct construct.

Then, we proceeded to design PCR primers flanking the MTS with appropriate restriction sites included to allow restriction enzyme digestion and ligation of the MTS into the pmCherry-EGFP vector. However, ligation of the digested PCR product into the digested pmCherry-EGFP vector did not yield the correct construct (vector design 3 in Figure 2.1).

Finally, primers were designed to amplify the mCherry-EGFP sequence with restriction sites included to allow restriction enzyme digestion and ligation of this fragment alongside the PCR-amplified MTS sequence into an empty pcDNA3 backbone (vector design 4 in Figure 2.1). Still, the correct vector was not obtained. We suspected that technical challenges related to a high GC-content (approximately 78%) in the MTS sequence and high number of repeats in the mCherry and EGFP sequences were causing problems with the PCRs, so after attempting these various strategies without success, we decided to have the vector encoding the reporter sequence synthesised by GenScript Biotech Corporation. Thus, we designed a pcDNA3.1-VLCAD(1-40)-mCherry-EGFP construct encoding the mitochondrial targeting sequence (aa 1-40) of the IMM protein VLCAD, followed by mCherry and EGFP, which was successfully synthesized by GenScript Biotech Corporation and delivered to us.

Plasmids encoding either WT BNIP3 or a LIR-inactive mutant of BNIP3 were designed based on those described by Zhu and colleagues where the LIR domain residues W21 and L23 (mouse BNIP3) were mutated to alanines to effectively abolish BNIP3-LC3 interaction (Zhu et al., 2013). These residues correspond to W83 and L86 in the human WT BNIP3 sequence, and, thus, the human BNIP3 LIR-mutant was designed to encode the W83A/L86A mutations. These custom pcDNA3.1-BNIP3 WT and LIR-mutant vectors were then obtained from GenScript Biotech Corporation. To

generate an empty vector (EV) control plasmid, the BNIP3 insert was excised and the vector was subsequently re-ligated and sequenced to confirm the correct sequence with the BNIP3 insert successfully removed.

To generate a vector encoding an mCherry-tagged version of BNIP3 for use in immunofluorescence, WT BNIP3 was excised from the pcDNA3.1 vector using restriction sites that had been added at either end of the BNIP3 insert during vector design. WT BNIP3 was then ligated into a pmCherry-EGFP backbone, where the EGFP sequence had been excised to generate a pmCherry-BNIP3 WT plasmid. Similarly, EGFP was excised from pmCherry-EGFP allowing self-ligation to generate a pmCherry EV.

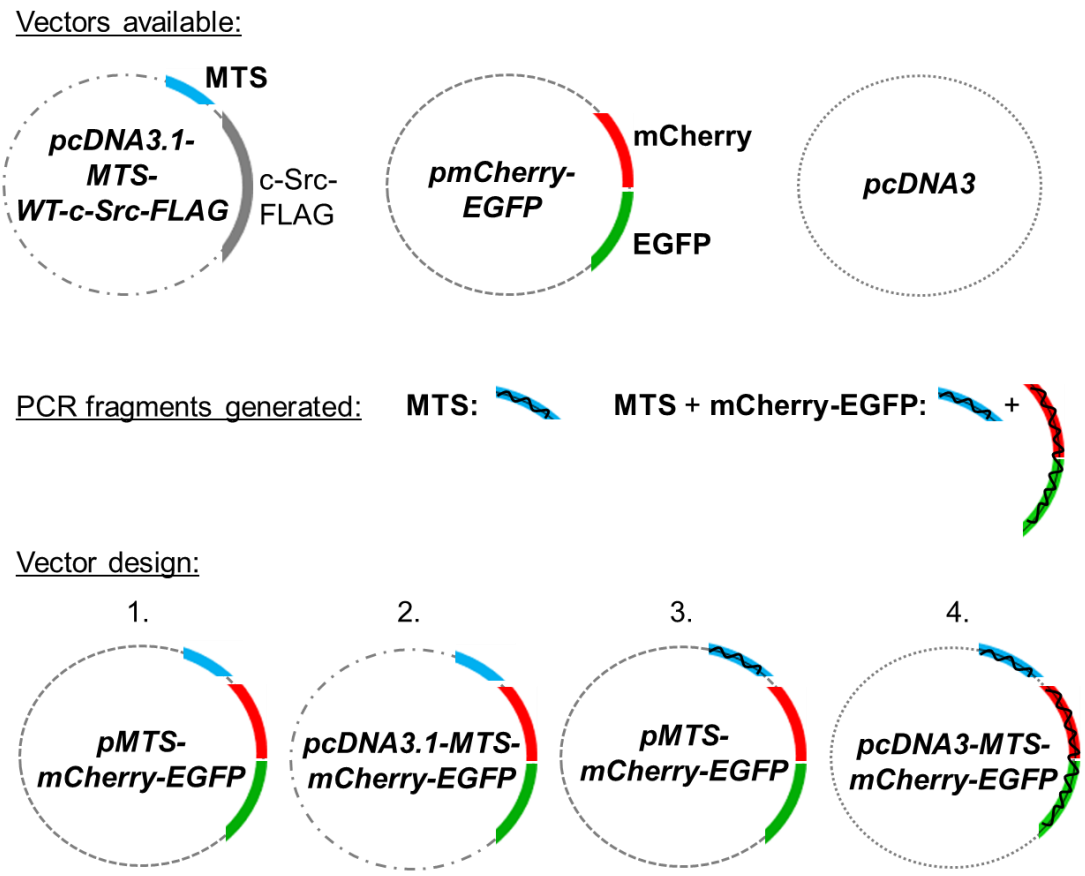

Figure 2.1 Cloning strategies.

A schematic of the cloning strategies attempted in the aim to generate a vector encoding the mitochondrial targeting sequence of VLCAD(1-40) followed by the tandem probe mCherry-EGFP. Details of strategies 1-4 are described in the text. DNA fragments with a line running through them represent PCR-generated fragments.

2.9 Mitophagy detection and quantification in MCF-7-VLCAD(1-40)-mCherry-EGFP cells

Cells stably expressing the fluorescent reporter were seeded onto sterile glass coverslips, cultured according to experimental conditions, fixed with 4% paraformaldehyde in PBS, quenched with 50mM NaCl for 15min and washed with PBS. The glass coverslips were mounted onto glass slides with vinol mounting medium (Celvol #205s: 15% w/v vinol in PBS, 33% v/v glycerol and 0.1% sodium azide). Using a Nikon Eclipse E600 microscope equipped with a Spot digital camera and SPOT software, version 4.6 (Diagnostic Instruments, Sterling Heights, MI), a minimum of 15 images were acquired per condition using a 100x objective. Since each image contains approximately 3-10 cells, an average of approximately 90 cells were analysed per condition. The images were processed and analysed using Adobe Photoshop (CS6). The number of cells considered mitophagy-positive, i.e. positive for red puncta, were quantified as a percentage of the total number of cells counted per experimental condition. Each experiment was carried out three times to ensure reproducibility.

2.10 Immunofluorescence

MCF-7 and DU145 cells (200,000 /well) or MEFs (150,000/well) were seeded on sterile glass coverslips in 6-well plates and cultured according to experimental conditions prior to fixation for 30min (MCF-7) or 1h (DU145, U2OS and MEFs) with 4% paraformaldehyde in PBS, followed by quenching with 50mM NaCl for 15min and washing with PBS. Cells were then permeabilised with 0.1% Triton-X in PBS for 5min, followed by a wash with PBS. 5% donkey serum was included in all buffers to block non-specific interactions with secondary antibodies. The fixed cells were incubated with primary antibodies overnight at 4^0C. The anti-TOM20 antibody was

used at 1:500 dilution (Santa Cruz, #sc-11415 or #sc-17764) and the anti-BNIP3 antibody (Abcam, #ab10433) was used at 1:200 dilution in PBS with 5% donkey serum. Secondary antibodies (Alexa 488-conjugated, #711-545-152 from Jackson ImmunoResearch (West Grove, PA)) were applied at 1:200 dilution in PBS with 5% donkey serum for 1h at room temperature. Hoechst dye was included for nuclear staining (blue). The glass coverslips were washed 2x 10minutes with PBS prior to mounting onto glass slides with vinol mounting medium (Celvol #205s: 15% w/v vinol in PBS, 33% v/v glycerol and 0.1% sodium azide). Images were obtained using a Nikon Eclipse E600 microscope equipped with a Spot digital camera and SPOT software, version 4.6 (Diagnostic Instruments, Sterling Heights, MI) or with a Leica DM LB2 microscope with a Nikon Digital Sight DS-U2 camera using NIS-Elements software version 3.0 (Nikon, Japan). Further analysis by confocal microscopy was performed using an OLYMPUS FV1000 Confocal Laser Scanning Biological Microscope with Olympus Fluoview software FV10-ASW 4.0 (Olympus Corporation, Japan), as indicated in figure legends. For images acquired on the Nikon microscope, contrast and brightness was adjusted in Adobe Photoshop (CS6). For confocal microscopy, maximum intensity projections and z-stacks were processed and analyzed in ImageJ, where brightness and contrast were adjusted.

2.11 Hypoxia cultures for induction of mitophagy

Hypoxia was established in cells using a hypoxia chamber (Stemcell Technologies, Vancouver, Canada). The chamber was flushed with nitrogen for 15–20 min until the oxygen concentration within the chamber reached <1%. The oxygen concentration was measured using an Optical Fluorescence O_2 analyzer (Luxcel Biosciences, Cork,

Ireland). Cell lysis to extract proteins or fixation for immunofluorescence was carried out immediately after opening of the hypoxia chamber to minimise reoxygenation.

2.12 Cell lysis, SDS-PAGE and western blotting

For extraction of total cell protein, cells were washed with PBS and lysed with RIPA lysis buffer (50mM Tris, 150mM NaCl, 0.1% SDS, 0.5% sodium deoxycholate and 1% Nonidet P-40 (pH 7.4)) with protease and phosphatase inhibitors (Pierce Halt Protease Inhibitor Cocktail (#78439, Thermo Scientific, used at 1/100 dilution), $NaVO_4$ (Sigma-Aldrich #S6508, 200mM stock used 1/100 dilution), sodium pyrophosphate (Sigma-Aldrich #221368, 250mM stock used 1/100 dilution), β-glycerophosphate (Merck, #35675, 1M stock used at 1/1000 dilution)) for 20min on ice. The protein concentrations were measured using the Bio-Rad Protein Assay Dye Reagent (#500-0006, Fannin, Dublin, Ireland). Samples were prepared in loading dye (2% SDS, 8% glycerol, 60mM Tris-HCl (pH 6.8), 1.2% β-mercaptoethanol and 0.2-0.4% bromophenol blue powder).

SDS-PAGE was performed on 10% or15% polyacrylamide gels depending on the sizes of the proteins analyzed. Generally, protein samples were loaded in the range of 20-80μg per lane depending on the cell line and the protocols optimized for antibodies used for detection. For western blotting, proteins were transferred to nitrocellulose membrane using a Bio-Rad Mini Trans-Blot electrophoretic transfer cell. Membranes were blocked with 5% non-fat dried milk or BSA in TBS with 0.05% Tween20 (TBS-T) for 1h at room temperature to reduce non-specific antibody binding. Next, blots were incubated with primary antibodies prepared in 5% non-fat dried milk or BSA in TBS-T overnight at 4^0C, washed twice with TBS-T and subsequently incubated with IRdye700- or IRdye800-conjugated secondary antibodies

(LI-COR Biosciences) in 5% non-fat dried milk in TBS-T for 1h at room temperature. Blots were scanned with an Odyssey IR scanner system (LI-COR Biosciences, Cambridge, UK). Approximate protein molecular masses are indicated on all blots in kilodaltons.

2.13 Subcellular fractionation of cell lysates

2.13.1 Nuclear and cytosolic fractions

Cellular fractionation was performed to obtain cytosolic and nuclear fractions following the protocol published by Lau and colleagues (Lau et al., 2007). Lysis buffer A (10mM 4-(2-hydroxyethyl)-1-piperazineethanesulfonic acid (HEPES) pH 7.9, 10mM KCl, 1.5mM $MgCl_2$, 0.34 M Sucrose, 10% glycerol, 1 mM dithiotheitol (DTT), 0.1% Triton X-100) with protease and phosphatase inhibitors (as listed under Cell lysis, SDS-PAGE and western blotting) was added to adherent cells that were then scraped and transferred to cold Eppendorf tubes, and kept on ice for 7min. The lysates were then centrifuged at 4000rpm for 5min at 4°C. The supernatant represents the cytosolic fraction, while the pellet contains the nuclear fraction. The pellet was washed 3x with lysis buffer A without Triton-X100 to minimise contamination from the cytosolic fraction. Between each wash, the pellet was spun down at 4000 rpm for 5min at 4°C and the supernatant subsequently discarded. To extract nuclear proteins from the pellet, lysis buffer B (0.2mM ethylene glycol-bis(β-aminoethyl ether)-N,N,N′,N′-tetraacetic acid (EGTA) pH 8, 3mM ethylenediaminetetraacetic acid (EDTA) pH 8, 1 mM DTT) with protease and phosphatase inhibitors (as listed under Cell lysis, SDS-PAGE and western blotting) was added. Rigorous vortexing was carried out every 5-10min for 1h prior to centrifugation at 4000rpm for 5min at 4°C. The supernatant represented the extracted nuclear proteins. The protein concentration in the cytosolic

fraction was assessed using the Bio-Rad Protein Assay Dye Reagent, and equal amounts of protein were loaded for the different samples (for a given sample, the same volume of the cytosolic and the nuclear fraction was loaded) onto 10% polyacrylamide gels for SDS-PAGE.

2.13.2 Mitochondrial and cytosolic fractions

Cells were seeded into 15cm plates and allowed to reach approx. 80% confluency at the time of lysis. The lysis buffer (20 mM mannitol, 70 mM HEPES, 1 mM EGTA, 0.05% bovine serum albumin (BSA), 0.1 mM PMSF, 1 mM DTT) was added to the cells (typically 80µl per plate), and the cells were scraped and transferred into cold Eppendorf tubes. The lysates were homogenised using a pellet pestle (35 strokes per lysate). The homogenized lysates were centrifuged at 3000rpm for 15min at 4°C. Supernatants were transferred to fresh cold Eppendorf tubes and centrifuged at 9700rpm for 15min at 4°C, yielding the mitochondrial fraction in the pellet. The supernatants from this centrifugation step were transferred to fresh Eppendorf tubes and centrifuged at 14.000rpm for 12min at 4°C to obtain pure cytosolic fractions. The mitochondrial pellets were washed at least 6 times with ice-cold PBS and centrifuged after each step at 9700rpm for 5min. After each wash, the supernatant was discarded. After the final wash, the mitochondria fraction was resuspended in ice-cold sterile dH_2O. Samples were prepared in loading dye (2% SDS, 8% glycerol, 60mM Tris-HCl (pH 6.8), 1.2% β-mercaptoethanol and 0.2-0.4% bromophenol blue powder), and SDS-PAGE was performed on polyacrylamide gels as described above.

2.14 Flow cytometry

Mitochondrial function was assessed by flow cytometry. MitoTracker Green (MTG, Thermo Scientific #M7514) was used to assess mitochondrial mass, MitoSOX

(Thermo Scientific #M36008) was used to quantify mitochondrial ROS levels, and Tetramethylrhodamine, methyl ester (TMRM, Thermo Scientific #T668) dye was used to measure mitochondrial membrane potential, as it accumulates in polarized/active mitochondria. For MTG and MitoSOX assays, 300,000 MCF-7 cells per well in 6-well plates were seeded in triplicate wells per condition. The following day, the cells were incubated with MTG (100nM) for 20min or MitoSOX (5μM) for 30min. For TMRM assays, R- and R+ cells were seeded at 175,000 cells per well in 6-well plates in triplicate wells per condition. Cells were washed in PBS. As a positive control for the function of TMRM, the mitochondrial uncoupler FCCP (20μM) was added to a set of control samples for 10 min prior to addition of TMRM (500nM) prepared in complete medium to all wells for 20 min. For all dyes, the cells were incubated in the dark at 37^0 C for the indicated times, then washed with PBS, and detached using accutase (Sigma #A6964). Harvested cells were centrifuged at 1000rpm for 5 min, resuspended in PBS and were immediately analyzed using a FACSCalibur (BD Bioscences) and the Cellquest Pro software (BD Biosciences). Fluorescence intensity was measured in the FL2 channel for 10,000 events per sample. For each sample, the geometric mean was determined, and the average calculated from triplicate wells for each experimental condition.

2.15 Quantitative real time PCR

Cells for RNA extraction were washed with PBS prior to lysis and RNA purification using a PureLink RNA Mini Kit (Thermo Fisher Scientific, #12183025). RNA concentration and purity were assessed using a NanoDrop Lite spectrophotometer (Thermo Fisher Scientific) and a QuantiTect Reverse Transcription Kit (Qiagen, #205313) was used for cDNA synthesis with 500ng-1μg of RNA. Two negative

controls were included for each cDNA synthesis reaction, either containing no RNA or no reverse transcriptase to confirm no reagent contamination and appropriate elimination of genomic DNA.

A FastStart Essential DNA Green Master Kit (Roche Diagnostics, #6402712001) was used for RT-qPCR amplification using a LightCycler 96 Instrument (Roche Diagnostics). For technical duplicates the following volumes were generally used per RT-qPCR reaction: 7.5µl SYBR green (4x dilution), 3µl forward and reverse primer (10µM), 13.5µl nuclease-free water, 3µl cDNA (diluted 1/3 with nuclease-free water). Relative quantification was performed, and as housekeeping genes, Ubiquitin C (UBC) was used to normalize gene expression levels for cancer cell lines and β-actin was used for MEFs. For RT-qPCR data analysis, Ct values <30 were considered positive. Delta Ct values were calculated by normalisation to the housekeeping gene. Delta delta Ct values were calculated as the difference in delta Ct between the sample of interest and the control sample. Finally, relative fold-change was calculated using the 2^-ΔΔCT method (Livak and Schmittgen, 2001). For all RT-qPCR analyses, three independent experiments were performed for subsequent statistical analysis of reproducibility. For presentation, gene expression levels are presented as relative fold-change with the control sample set to a value of 1. All the primers used for RT-qPCR are listed in Table 2.1.

Table 2.1 RT-qPCR primer sequences and their source of origin.

Gene:		Primer sequence:	Source:
BNIP3	F:	5’-CGTTCCAGCCTCGGTTTCTA-3’	Recognizes: NM_004052.3 yielding a product of 133nt.
	R:	5’-ATCTTGTGGTGTCTGCGAGC-3’	
Drp1	F:	5'-TGAAGGATGTCATGTCGGACC-3'	WAN, Y. Y.et al. 2014. Involvement of Drp1 in hypoxia-induced migration of human glioblastoma U251 cells. Oncol Rep, 32, 619-26.
	R:	5'-GTTGAGGACGTTGACTTGGCT-3'	
GCLC	F:	5'-GGCACAAGGACGTTCTCAAGT-3'	JIANG, M., et al. 2015. BMP-driven NRF2 activation in esophageal basal cell differentiation and eosinophilic esophagitis. The Journal of Clinical Investigation, 125, 1557-1568.
	R:	5'-CAGACAGGACCAACCGGAC-3'	
HO1	F:	5'-CTCAAACCTCCAAAAGCC-3'	ZHONG, Z. & TANG, Y. 2016. Upregulation of Periostin Prevents High Glucose-Induced Mitochondrial Apoptosis in Human Umbilical Vein Endothelial Cells via Activation of Nrf2/HO-1 Signaling. Cellular Physiology and Biochemistry, 39, 71-80.
	R:	5'-TCAAAAACCACCCCAACCC-3'	
KEAP1	F:	5'-TTCAAGGCCATGTTCACCAA-3'	DEVLING, T. W. P. et al. 2005. Utility of siRNA against Keap1 as a strategy to stimulate a cancer chemopreventive phenotype. Proceedings of the National Academy of Sciences of the United States of America, 102, 7280-7285A.
	R:	5'-TGGATACCCTCAATGGACACC-3'	
MFN1	F:	5’-TGTTTTGGTCGCAAACTCTG-3’	RUSSELL, A. P. et al. 2013. Regulation of miRNAs in human skeletal muscle following acute endurance exercise and short-term endurance training. The Journal of physiology, 591, 4637-4653.
	R:	5’-CTGTCTGCGTACGTCTTCCA-3’	
MFN2	F:	5'-ATGCATCCCCACTTAAGCAC-3'	RUSSELL, A. P. et al. 2013. Regulation of miRNAs in human skeletal muscle following acute endurance exercise and short-term endurance training. The Journal of physiology, 591, 4637-4653.
	R:	5'-CCAGAGGGCAGAACTTTGTC-3'	
NRF1	F:	5'-CGCTCTGAGAACTTCATGGAGGAACAC-3'	BORI, Z. et al. 2012. The effects of aging, physical training, and a single bout of exercise on mitochondrial protein expression in human skeletal muscle. Experimental gerontology, 47, 417-424.
	R:	5'-GCCACATGGACCTGCTGCACTT-3'	
UBC	F:	5'-TCGAGAATGTCAAGGCAAAGATC-3'	OHL, F. et al. 2005. Gene expression studies in prostate cancer tissue: which reference gene should be selected for normalization? Journal of molecular medicine (Berlin, Germany), 83, 1014-1024.
	R:	5'-GAGTGGACTCTTTCTGGATGTTGTA-3'	
Ms/hu Nrf2	F:	5'-CTACTCCCAGGTTGCCCACA-3'	SARR, D. et al. 2017. Oxidative Stress: A Potential Therapeutic Target in Placental Malaria. ImmunoHorizons, 1, 29-41.
	R:	5'-CGACTCATGGTCATCTACAAATGG-3'	
Ms actin	F:	5'-ATATCGCTGCGCTGGTCGTC-3'	Recognizes: NM_007393.5 yielding a product of 149nt.
	R:	5'-ATAGGAGTCCTTCTGACCCATT-3'	
Ms BNIP3	F:	5'-GCTCCCAGACACCACAAGAT-3'	CHAVEZ-VALDEZ, R. et al. 2012. Necrostatin-1 attenuates mitochondrial dysfunction in neurons and astrocytes following neonatal hypoxia-ischemia. Neuroscience, 219, 192-203.
	R:	5'-TGAGAGTAGCTGTGCGCTTC-3'	

Chapter 3. IGF-1 Enhances Mitochondrial Turnover and BNIP3 Function in Cancer Cells

Contributions:

Parts of Chapter 3 were published in a manuscript (Lyons et al., 2017). To give a comprehensive account of the work undertaken and the scientific context from which this project arose, the following work from colleagues was included:

- RT-qPCR was performed by Dr Amy Lyons to assess gene expression levels of mitochondrial markers and the two transcriptional co-activators PGC-1β and PRC in MCF-7 cells in response to IGF-1 (Fig. 3.1).
- Dr Amy Lyons generated MCF-7 cells with an acquired resistance to the IGF-1R inhibitor BMS754807, in which she measured levels of BNIP3 under normoxic and hypoxic conditions. The mitochondrial mass and levels of mitochondrial reactive oxygen species in these cells were assessed (Fig. 3.3.A-B), and Dr Michael Coleman performed immunofluorescence staining of these cells to assess their capacity to induce mitophagic clearance in response to hypoxia (Fig. 3.3.C-D).
- The remaining work presented in the chapter was performed by the thesis author.

3.1 Abstract

The Insulin-Like Growth Factor 1 (IGF-1) signalling pathway is implicated in the development and progression of many types of cancer. Importantly, this pathway is also associated with mitochondrial protection. Here, we explored how IGF-1 signalling enhances the biogenesis and turnover of mitochondria in cancer cells. The study revealed that IGF-1 induces mitochondrial biogenesis through the transcriptional regulators, Peroxisome Proliferator-Activated Receptor-γ (PPAR-γ) coactivator-1 β (PGC-1β) and PGC-1-Related Coactivator (PRC), and suppression of both proteins altered mitochondrial dynamics causing mitochondrial elongation. Interestingly, MCF-7 cells with acquired resistance to an IGF-1R tyrosine kinase inhibitor (MCF-7R cells) exhibited impaired induction of the mitophagy receptor (BCL-2)/Adenovirus E1B 19 kDa Protein-Interacting Protein 3 (BNIP3) and impaired mitophagy under hypoxic conditions. Furthermore, IGF-1 induced BNIP3 under normoxic conditions in cancer cells, and suppression of BNIP3 caused accumulation of the mitochondrial marker Prohibitin 1 (PHB1), indicating reduced mitophagy. However, ectopic expression of BNIP3 did not promote survival in response to cellular stress in IGF-1R KO MEFs (R-) cells. Surprisingly, ectopic expression of wildtype (WT) BNIP3 in cancer cells downregulated macro-autophagy, suggesting that BNIP3 may differentially regulate autophagy and mitophagy. Suppression of the mitophagy receptor Prohibitin 2 (PHB2) reduced protein levels of IGF-1 pathway components, but whether it has a role in mitochondrial turnover through this pathway could not be established. Overall, this study demonstrates an essential function for IGF-1 signalling in mitochondrial homeostasis.

3.2 Introduction

IGF-1 signalling is implicated in cancer development, as it is associated with cell growth, proliferation and suppression of cell death (Hakuno and Takahashi, 2018). In recent years, IGF-1 signalling has also been linked to mitochondrial function. We previously characterized an IGF-1-inducible mitochondrial pyrimidine nucleotide carrier (PNC1)/SLC25A33 that is essential for mitochondrial maintenance (Floyd et al., 2007), and whose suppression promotes mitochondrial dysfunction (Favre et al., 2010). These studies suggest a mitochondria protective role for IGF-1. Others have also proposed a mitochondria-protective role for IGF-1, since partial IGF-1 deficiency causes hepatic mitochondrial dysfunction in a mouse model, and IGF-1 therapy in low doses restores mitochondrial function in these animals (Olleros Santos-Ruiz et al., 2017).

Mitochondrial dysfunction is also common in cancer and is associated with cancer progression. Dysfunction in most areas of mitochondrial function including metabolism, mitochondria-mediated cell death, biogenesis and degradation have been observed in cancer (Vyas et al., 2016). To maintain a healthy mitochondria population, a balance between mitochondrial biogenesis and mitophagy is required to ensure that new mitochondria are produced, while aged/damaged ones are removed (Palikaras et al., 2015a). It has been proposed that in cancer cells, mitochondrial biogenesis and mitophagy are uncoupled, because mitophagy is often dysregulated (Drake et al., 2017). While mitochondrial dysfunction promotes disease progression, tumour cells that are highly proliferative also depend on mitochondrial maintenance (Wallace, 2012). Therefore, in cancer, a balance must exist that allows the oncogenic effects of mitochondrial stress and the associated mitochondrial dysfunction, while maintaining

sufficient mitochondrial function to enable tumour cell survival and growth. However, it is still unknown how this balance is achieved.

Here, we asked, if IGF-1 plays a role in promoting mitochondrial biogenesis and/or clearance. Various regulators of mitophagy have been identified. PTEN-Induced Kinase 1 (PINK1) mediates mitophagy in response to mitochondrial depolarization (Matsuda et al., 2010, Kawajiri et al., 2010a, Lazarou et al., 2015), whereas FUN14 Domain Containing 1 (FUNDC1), BNIP3 and (BCL-2)/Adenovirus E1B 19 kDa Protein-Interacting Protein 3-Like (BNIP3L) mediate mitophagy in response to hypoxia, for example (Bellot et al., 2009, Rikka et al., 2011, Liu et al., 2012, Zhang et al., 2019). The complexity of mitophagy regulation has become apparent in recent years, and novel mitophagy mediators such as the inner mitochondrial membrane (IMM) protein PHB2 have been identified. PHB2 is required for Parkin-mediated mitophagy and facilitates the elimination of paternal mitochondria in *C. elegans*, revealing an important role in development (Wei et al., 2017). PHB2 also promotes PINK1/Parkin mitophagy by stabilizing PINK1 at the outer mitochondrial membrane (OMM) through a mechanism that depends on the IMM protease presenilins-associated rhomboid-like protein (PARL) and one of its substrates phosphoglycerate mutase family 5 (PGAM5), which is a mitochondrial phosphatase (Yan et al., 2020).

PHB2 is required for cholestasis-induced hepatic mitophagy, implicating this receptor in different mitophagic pathways (Xiao et al., 2018). Since mitochondrial function is essential to cell survival, it is not surprising that there is crosstalk between different mitophagy pathways to ensure efficient mitochondrial clearance. BNIP3 enhances PINK1-mediated mitophagy by promoting the accumulation of full-length PINK1 at the OMM causing recruitment of Parkin (Zhang et al., 2016), and BNIP3L

can act as a Parkin substrate to facilitate mitophagy (Gao et al., 2015). In cardiomyocytes, BNIP3 can also promote recruitment of Parkin to mitochondria and induce mitophagy through a mechanism dependent on the mitochondrial fission mediator Dynamin-Related Protein 1 (DRP1) (Lee et al., 2011). Interestingly, PHB2 and the homologous protein PHB1 also are implicated in insulin/IGF-1 signalling (Ande and Mishra, 2009, Fu et al., 2013b, Ising et al., 2015), potentially suggesting mitochondrial retrograde communication between these signalling pathways. However, limited research has been carried out on the connections between IGF-1 signalling and prohibitins. Thus, we aimed to explore, whether IGF-1 influences prohibitin functions, and whether the mitophagy receptor PHB2 affects IGF-1 regulation of mitochondrial turnover.

In this study, we delineated an IGF-1 signalling pathway that couples the regulation of biogenesis and degradation of mitochondria in cancer cells. IGF-1 induces mitochondrial biogenesis through the transcriptional co-activators PGC-1β and PRC, while inducing the mitophagy receptor BNIP3. Impaired IGF-1 signalling was associated with reduced BNIP3-mediated mitophagy under hypoxic conditions, suggesting that IGF-1 can regulate mitochondrial degradation through BNIP3 to sustain cell viability. Knockdown of BNIP3 under non-hypoxic conditions caused increased mitochondrial mass, suggesting that BNIP3 increased the levels of mitophagy. However, highlighting the complexity of the cellular autophagic mechanisms, overexpression of WT BNIP3 reduced autophagosome turnover, suggesting its expression inhibits general autophagy. Therefore, the function of IGF-1-induced BNIP3 accumulation in cells under non-hypoxic conditions is complex and may not be limited to promotion of mitophagy.

It was also determined that IGF-1 induces both cytosolic and mitochondrial accumulation of PHB2 protein in cancer cells, and that PHB2 suppression reduced basal levels of Nuclear Factor Erythroid-2 Related Factor (Nrf2/NFE2L2) and BNIP3 but did not impede their induction in response to IGF-1. Thus, our findings also support a role for PHB2 in the IGF-1 signalling pathway, but whether it contributes to mitophagy was not established.

3.3 Results

3.3.1 IGF-1 induces mitochondrial biogenesis through PGC-1β and PRC in cancer cells

To assess how IGF-1 contributes to cellular mitochondrial turnover and function, the effects of IGF-1 signalling on mitochondrial biogenesis were assessed. MCF-7 cells were serum-starved for 4h prior to addition of IGF-1 at either 10ng/ml or 100ng/ml. Both concentrations of IGF-1 increased the mRNA expression levels of various mitochondrial markers including ARALAR, PNC1, TFAM and MFN1 (Fig. 3.1.A). IGF-1 also induced expression of the transcriptional co-activators PGC-1β and PRC that are known to regulate mitochondrial biogenesis (Shao et al., 2010, Gao et al., 2011, Andersson and Scarpulla, 2001). This induction was dependent on PI 3-K, as the PI 3-K inhibitor, LY294002 prevented the induction of each of the two transcriptional regulators (Fig. 3.1.B).

Thus, IGF-1 induces mitochondrial biogenesis in cancer cells through PGC-1β and PRC. Moreover, PGC-1β and PRC have redundant roles in mitochondrial biogenesis, because suppression of both proteins is required to impair IGF-1-mediated induction of the mitochondrial marker ARALAR (Fig. 3.1.C).

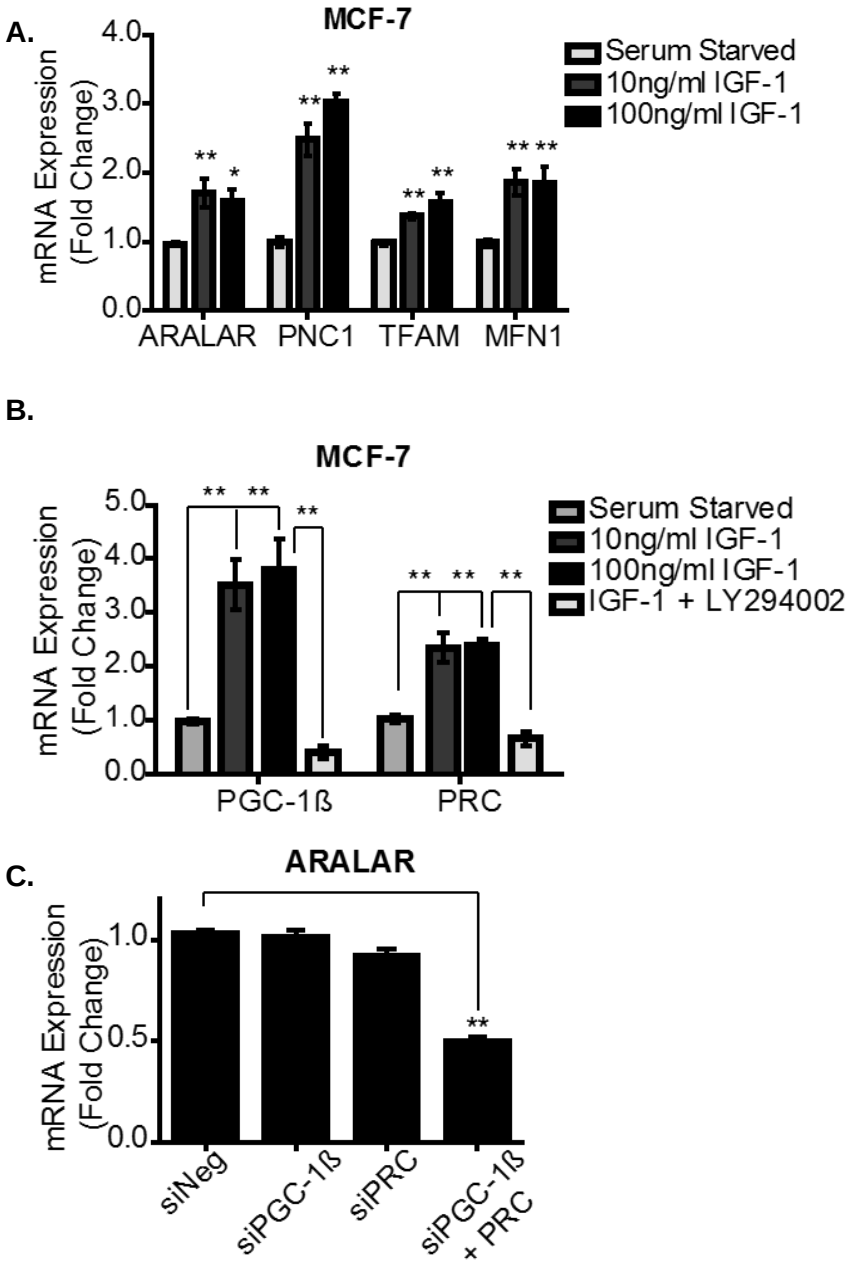

Figure 3.1 IGF-1 induces mitochondrial biogenesis through PGC-1β and PRC.

A. RT-qPCR analysis showing gene expression levels of mitochondrial markers ARALAR, PNC1, TFAM and MFN1 in MCF-7 cells that were serum-starved for 4h prior to addition of IGF-1 for 20h. **B.** RT-qPCR analysis showing gene expression levels of PGC-1β and PRC in MCF-7 cells that were serum-starved for 4h prior to addition of IGF-1 for 20h in the presence or absence of the PI 3-K inibitor LY294002 (20μM), which was added 30min before addition of IGF-1. **C.** RT-qPCR analysis showing gene expression levels of ARALAR. MCF-7 cells were transfected with a control siRNA, siPGC-1β, siPRC or both siPGC-1β and siPRC for 48h prior to RNA extraction. Gene expression levels were normalised to the housekeeping gene UBC and are presented as fold change relative to control conditions set to a value of 1. Results are presented as mean ± SEM from three independent experiments. For statistical analysis, the Student's t-test was performed (*: $p<0.05$, **: $p<0.01$, ***: $p<0.001$).

3.3.2 PGC-1β and PRC are essential to the maintenance of mitochondrial morphology

Based on the observation that IGF-1 induces mitochondrial biogenesis through PGC-1β and PRC (Fig. 3.1), the impact of these proteins on mitochondrial dynamics was tested. Suppression of PGC-1β/PRC with siRNA appeared to reduce mitochondrial mass, as indicated by the mitochondrial marker VDAC1 (Fig.3.2.A). A slight reduction in ETC complex III was observed in response to the knockdown, which may indicate a change in OXPHOS capacity, although there was no clear change in the other components. Furthermore, PGC-1β/PRC suppression caused a slight reduction in mitochondrial membrane potential, as measured by flow cytometric analysis of TMRE staining (Fig. 3.2.B), although this did not reach statistical significance.

Strikingly, suppression of PGC-1β/PRC led to altered mitochondrial morphology in MCF-7 cells, as illustrated by immunofluorescent staining with the mitochondrial marker TOM20 (Fig. 3.2.C). The mitochondria in cells transfected with a control siRNA were rounded and small, whereas suppression of PGC-1β/PRC caused mitochondrial elongation. To ensure the efficiency of the siRNA knockdown, PGC-1β/PRC expression levels were assessed by RT-qPCR (Fig. 3.2.D). The expression of both genes was reduced to approximately 30% of the expression levels in the controls.

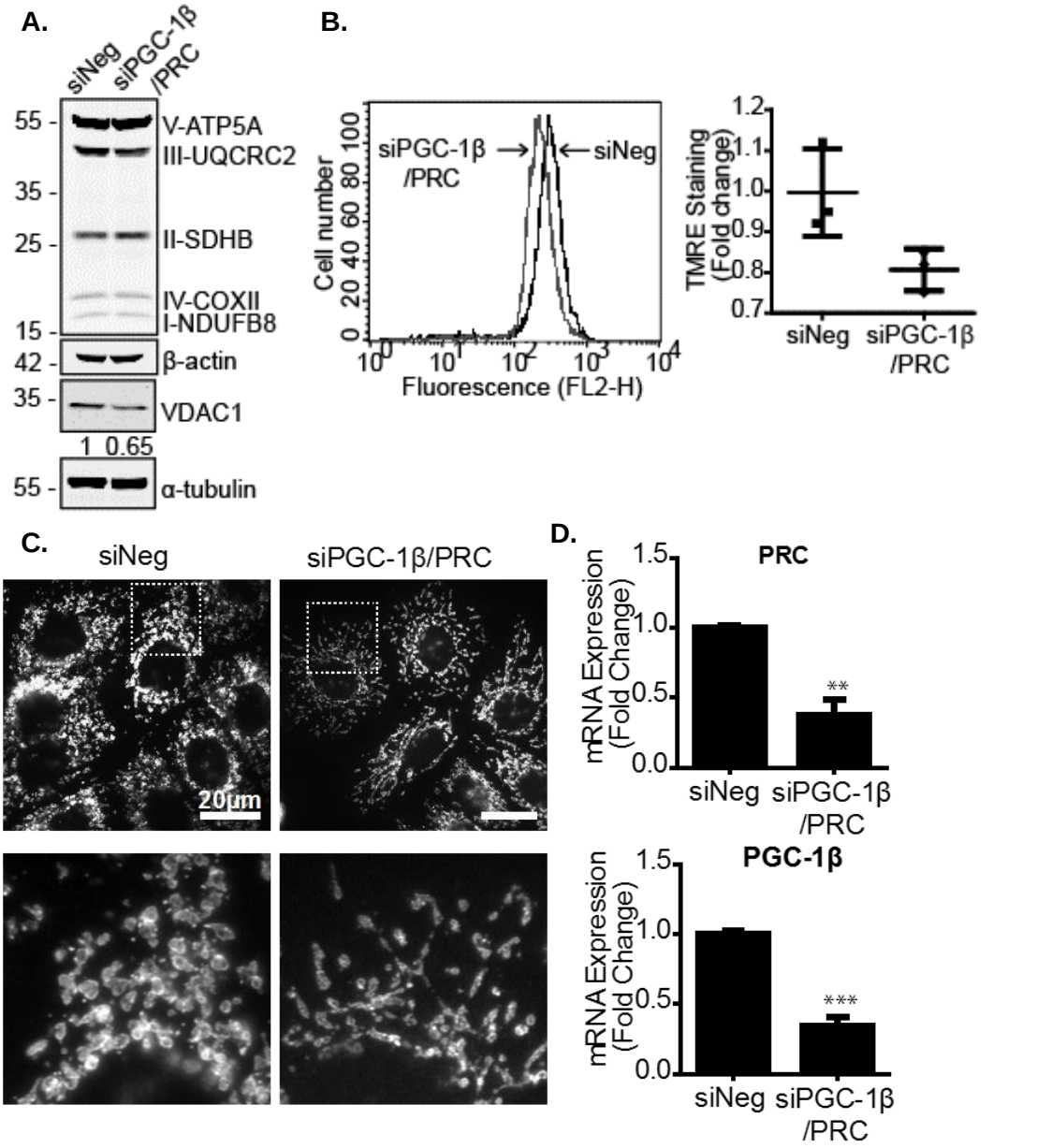

Figure 3.2 Suppression of PGC-1β and PRC reduces mitochondrial mass and causes mitochondrial elongation with no associated changes in OXPHOS components or mitochondrial membrane potential.

A. Western blot showing levels of VDAC1 and components of OXPHOS complexes I-V in MCF-7 cells transfected with a control siRNA or siPGC-1β/siPRC for 48h. For VDAC1, protein levels were normalised to β-actin and the relative fold change to the control is shown. **B**. Mitochondrial membrane potential was assessed by flow cytometry analysis of MCF-7 cells transfected with a control siRNA or siPGC-1β/siPRC for 48h followed by staining with TMRE. Representative histograms are shown alongside the quantification of the relative fold change in geometric means with the control set to a value of 1. **C**. Immunofluorescence staining of MCF-7 cells transfected with a control siRNA or siPGC-1β/siPRC for 72h. The cells were stained with TOM20 and images obtained on a Nikon Eclipse E600 microscope using a 100x objective. **D**. RT-qPCR analysis of MCF-7 cells transfected with a control siRNA or siPGC-1β/siPRC for 48h. Levels of PGC-1β/PRC were normalised to housekeeping gene UBC. Results are presented as mean ± SEM from three independent experiments. For statistical analysis, the Student's t-test was performed (*: $p<0.05$, **: $p<0.01$, ***: $p<0.001$). All experiments were repeated three times.

3.3.3 MCF-7 cells with impaired IGF-1 signalling exhibit accumulation of dysfunctional mitochondria associated with reduced capacity to induce BNIP3 and mitophagy under hypoxic conditions

To further study the effects of IGF-1 signalling in the regulation of mitochondrial turnover and function, a variant cell line with acquired resistance to an IGF-1R inhibitor (BMS-754807) was generated from MCF-7 cells, named MCF-7R cells. MCF-7R cells have impaired IGF-1 signalling due to sustained downregulation in the protein levels of the IGF-1R, even upon removal of BMS-754807 from the culture medium (Lyons et al., 2017). Compared to parental MCF-7 cells, MCF-7R cells exhibited increased mitochondrial mass (Fig.3.3.A) and reactive oxygen species (ROS) (Fig. 3.2.B), indicative of mitochondrial dysfunction. However, the increase in mitochondrial mass was not associated with increased expression of PGC-1β or PRC, suggesting mitochondrial biogenesis was not upregulated (Fig.3.3.B). This raised the question of, whether mitophagy was impaired in these cells leading to an accumulation of aged/damaged mitochondria. Investigations into this revealed that MCF-7R cells had impaired capacity to induce the mitophagy receptor BNIP3 in response to hypoxia compared to parental MCF-7 cells (Fig.3.3.C). As can be seen in Figure 3.3.C, the anti-BNIP3 antibody detects the monomer at ~20-25 kDa and the dimer at ~55-60 kDa. Furthermore, other bands at around 30-35 kDa represent various forms of BNIP3 modified post-translationally by phosphorylations for example, as has been documented before (Graham et al., 2007, Mellor et al., 2010). Importantly, the observed deficiency in BNIP3 induction under hypoxic conditions in the MCF-7R cells was associated with reduced levels of BNIP3-mediated mitophagy, as demonstrated by immunofluorescence colocalisation of the mitochondrial marker Translocase of Outer Mitochondrial Membrane 20 (TOM20) and BNIP3 (Fig. 3.3.D).

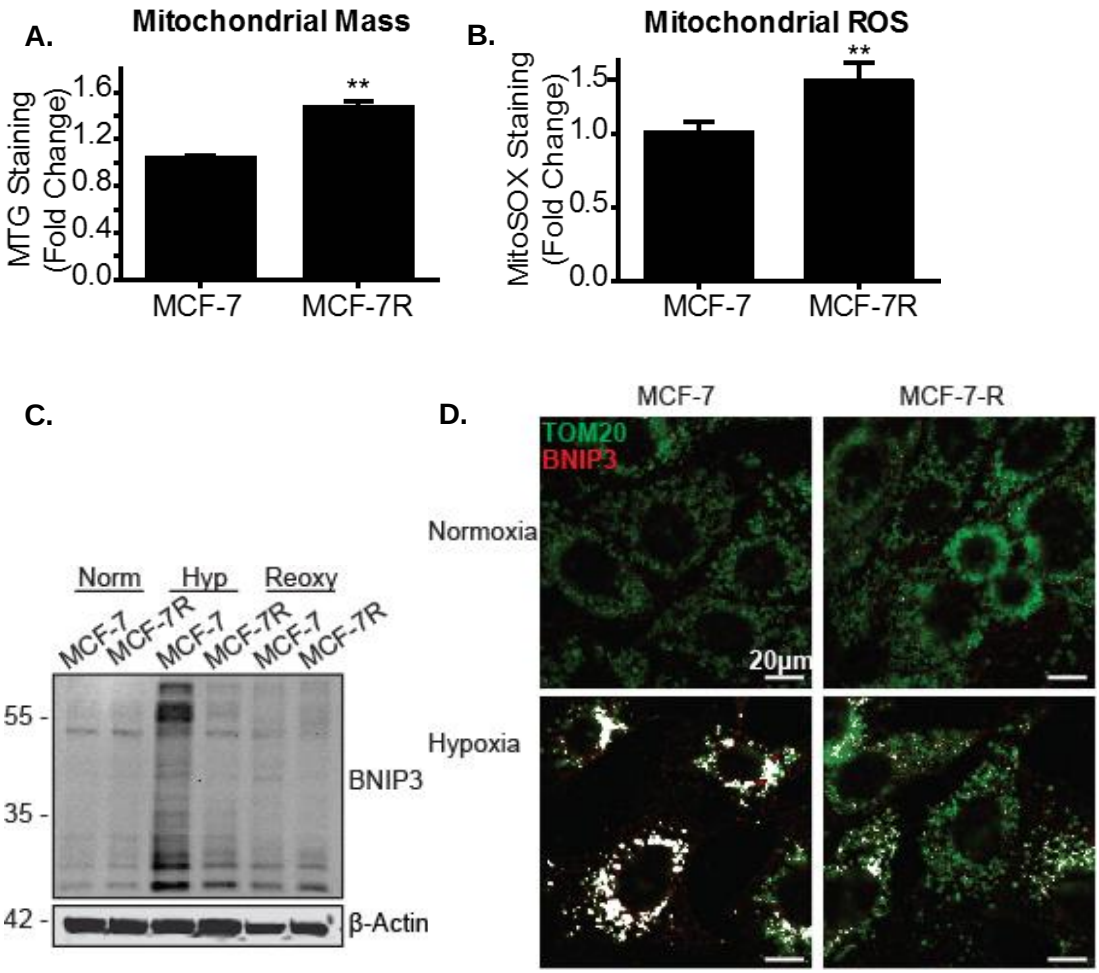

Figure 3.3 MCF-7R cells have increased mitochondrial mass, mitochondrial dysfunction and impaired BNIP3-mediated mitophagy in response to hypoxia.

A. Mitochondrial mass was assessed in MCF-7 and MCF-7R cells by flow cytometry analysis following staining with MitoTracker Green. The fold change in the geometric means is shown relative to the control sample set to a value of 1. **B**. Mitochondrial ROS levels were assessed in MCF-7 and MCF-7R cells by flow cytometry analysis following staining with MitoSOX. The fold change in the geometric means is shown relative to the control sample set to a value of 1. **C**. Western blot showing levels of BNIP3 in MCF-7 and MCF-7R cells under normal culture conditions (Norm), in response to 20h hypoxia (Hyp, 1% O_2) or 20h hypoxia followed by 5h of reoxygenation (reoxy). β-actin is the protein loading control. **D**. Representative images of immunofluorescence staining of MCF-7 and MCF-7R cells showing colocalisation between TOM20 and BNIP3 under normal culture conditions or in response to 20h hypoxia (1% O_2). Colocalisation is highlighted in white. Results are presented as mean ± SEM from three independent experiments. For statistical analysis, the Student's t-test was performed (*: $p<0.05$, **: $p<0.01$, ***: $p<0.001$). All experiments were repeated three times.

3.3.4 IGF-1 induces BNIP3 and Nrf2 expression under normoxic conditions in cancer cells, and impaired IGF-1 signalling causes dysregulation of Nrf2 expression

To test whether IGF-1 also affects BNIP3 protein abundance in cancer cells under non-hypoxic culture conditions, MCF-7 and DU145 cells were serum-deprived for 4h prior to the addition of IGF-1 for 2, 4, 8 or 24h. Indeed, IGF-1 did induce BNIP3 in a time-dependent manner in both cell lines (Fig. 3.4.A-B). Predominantly, bands corresponding to the monomer (25-35 kDa) were induced, whereas the dimer was less prominent. IGF-1 also caused an accumulation of sequestosome 1/p62 protein over time, demonstrating IGF-1-mediated inhibition of general autophagy (Fig. 3.4.A). Since BNIP3 is a dual function protein known to promote either cell death or mitophagy (Zhang and Ney, 2009), and IGF-1 is known to have anti-apoptotic effects (Parrizas et al., 1997, Kang et al., 2003, Jin et al., 2014), we hypothesized that IGF-1 induces BNIP3-dependent mitophagy.

In *C. elegans*, the Nrf2 homologue SKN1 has been coupled to the induction of both mitochondrial biogenesis and to the regulation of mitophagy and the BNIP3 homologue DCT-1 (Palikaras et al., 2015b). Thus, the effects of IGF-1 on Nrf2 expression in parental MCF-7 cells and MCF-7R cells were investigated. In parental MCF-7 cells, IGF-1 induced Nrf2 expression significantly, suggesting its expression is under IGF-1 regulation. MCF-7R cells exhibited higher levels of Nrf2 than parental MCF-7 cells, but this was unaffected by IGF-1 stimulation (Fig. 3.4.C). Due to the role of Nrf2 in antioxidant stress, it was not surprising to observe elevated levels of Nrf2 in MCF-7R cells that also have increased ROS (Fig. 3.3.B). This suggests that Nrf2 is IGF-1-inducible, and that this pathway is dysregulated in MCF-7R cells due to IGF-1R signalling being compromised.

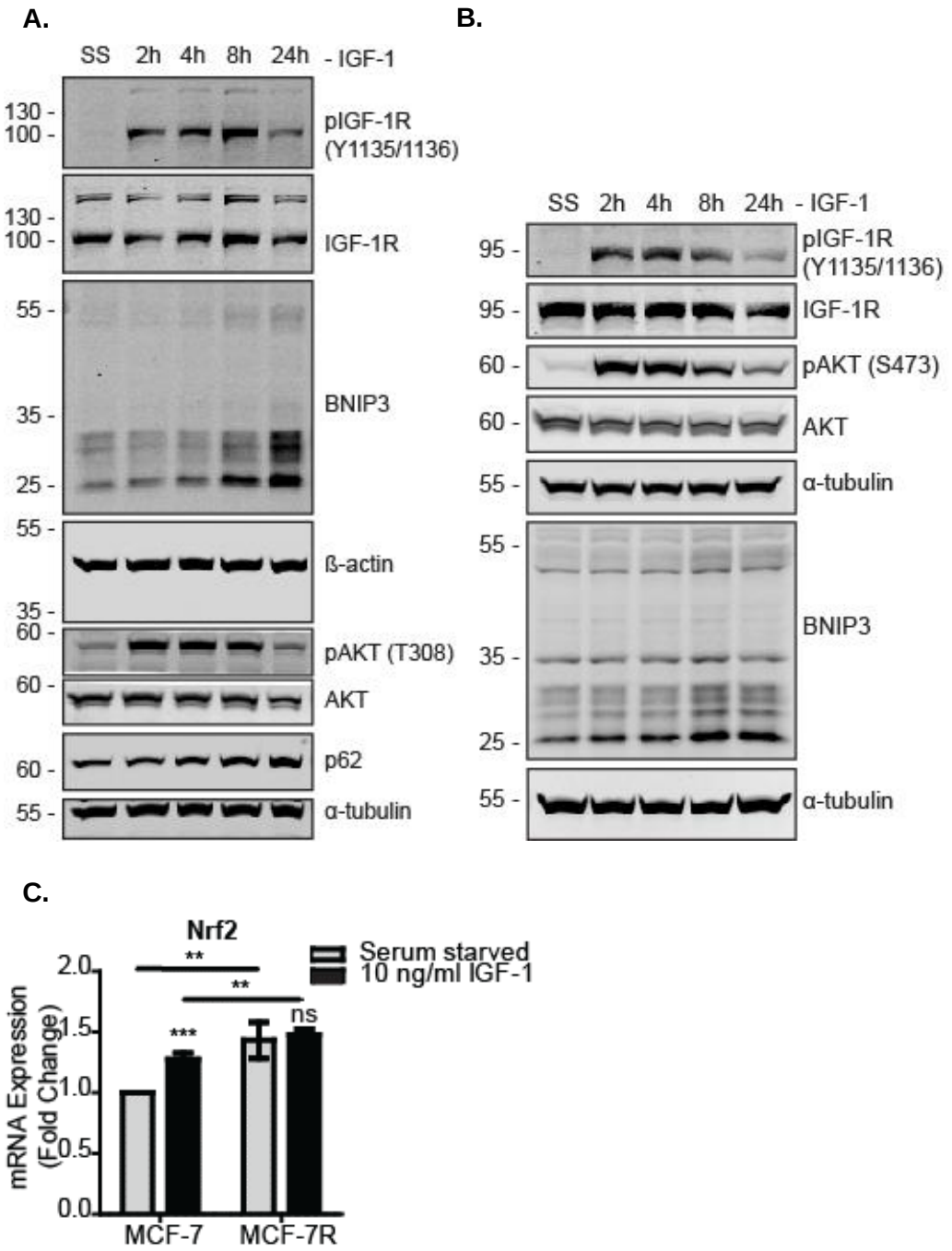

Figure 3.4 IGF-1 induces BNIP3 in a time-dependent manner in MCF-7 and DU145 cells and induces Nrf2 in parental MCF-7 cells, but not MCF-7R cells.

A. Western blot of MCF-7 and (**B**) DU145 cells showing levels of IGF-1R phosphorylation, BNIP3 and p62. Cells were serum-starved for 4h prior to addition of IGF-1 (10ng/ml) for the indicated times. β-actin and α-tubulin are the protein loading controls. **C**. Gene expression levels of Nrf2 in MCF-7 and MCF-7R cells measured by qRT-PCR. Cells were serum-starved for 4h prior to addition of IGF-1 (10ng/ml) for 20h. Gene expression levels were normalised to the housekeeping gene UBC and are presented as fold change relative to control conditions set to a value of 1. Results are presented as mean ± SEM from three independent experiments. For statistical analysis, the Student's t-test was performed (*: $p<0.05$, **: $p<0.01$, ***: $p<0.001$). All experiments were repeated three times.

3.3.5 Suppression of BNIP3 may upregulate mitophagy, while downregulating macro-autophagy

To test whether the observed IGF-1-mediated induction of BNIP3 is associated with mitophagy activation in cancer cells, siRNA was used to suppress BNIP3 in MCF-7 cells. Transient suppression of BNIP3 increased protein levels of the mitochondrial marker PHB1 and reduced levels of the macro-autophagy mediator p62 (Fig. 3.5.A). For both proteins, the difference was statistically significant at 48h post transfection but not at 72h even though the trends remained consistent (Fig. 3.5.B). The increase in PHB1 suggests that suppression of BNIP3 reduces mitophagy and, thus, causes a slight increase in mitochondrial mass. On the other hand, the reduction in p62 could signify enhanced general autophagy, which leads to p62 degradation (Bjørkøy et al., 2005).

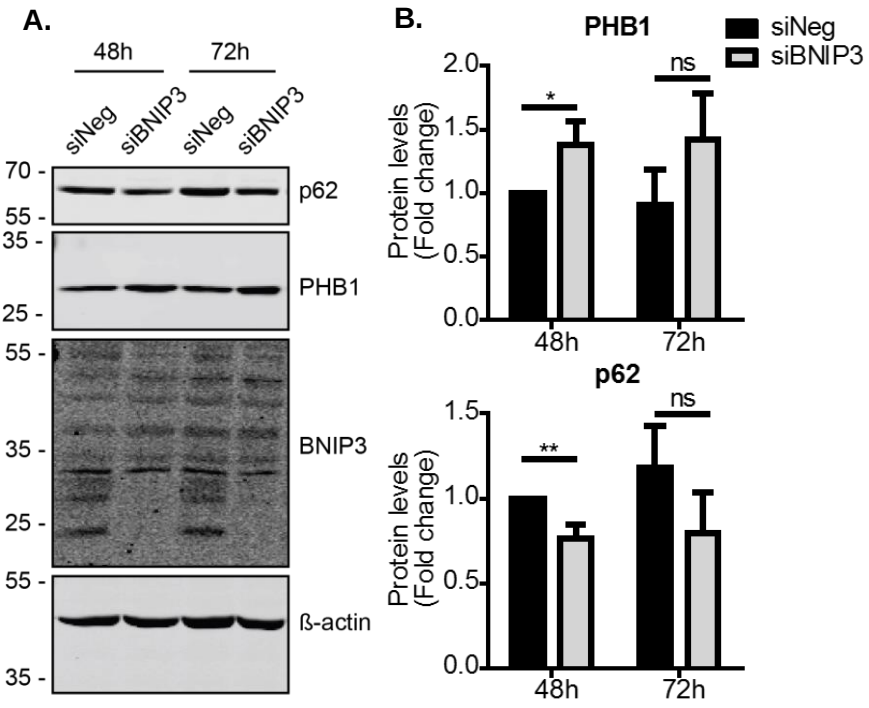

Figure 3.5 Suppression of BNIP3 may affect mitophagy and/or general autophagy in cancer cells

A. Western blot showing levels of BNIP3, p62 and PHB1 in MCF-7 cells transfected with a negative control siRNA or siBNIP3 for 48 or 72h. **B.** Protein levels were normalized to β-actin and are shown as relative fold change compared to the negative control at 48h post transfection. Results are presented as mean ± SEM from three independent experiments. For statistical analysis, the Student's t-test was performed (*: $p<0.05$, **: $p<0.01$, ***: $p<0.001$). A representative blot is shown.

3.3.6 DFP induces BNIP3 and CCCP induces PINK1 to activate mitophagy

A limitation to the experimental conditions, thus far, is that cells were cultured in complete medium, where general autophagy would be low. Cells cultured in conditions, where mitophagy is induced, might provide a better insight into the importance of BNIP3 and the IGF-1 signalling pathway in mitophagy. Therefore, several different chemicals known to induce mitophagy were tested for their effects on BNIP3 expression. These included $CoCl_2$ that mimics hypoxia to induce Hypoxia-Inducible Factor 1α (HIF-1α) and BNIP3 (Wu et al., 2015, Chen et al., 2017b), deferiprone (DFP) that causes iron chelation (Allen et al., 2013) and Carbonyl cyanide 3-chlorophenylhydrazone (CCCP), which causes mitochondrial uncoupling and mitophagy through the PINK1-Parkin pathway (Matsuda et al., 2010, Kawajiri et al., 2010a).

Initial testing in MCF-7 cells to determine the appropriate dosage and time points for these chemicals, revealed that at 24h, $CoCl_2$ induced BNIP3, when applied at 50μM, while DFP potently induced BNIP3 at all three concentrations tested. On the other hand, CCCP, when used at 20 and 50μM, induced PINK1 as expected, with no obvious induction of BNIP3 (Fig. 3.6A). DFP and CCCP are well-established chemical inducers of mitophagy, so to confirm this in the cell cultures, autophagic flux was measured in response to treatment with each compound. If mitophagy was induced, autophagosome turnover should theoretically increase (Chen et al., 2017a). Autophagic flux was assessed by addition of chloroquine (CQ) for the last 4h of the mitophagy stimuli. CQ prevents fusion of autophagosomes with lysosomes causing accumulation of Microtubule-associated Protein 1 Light Chain 3 α (LC3) in its processed form, LC3II, which coats the surface of autophagosomes (Mauthe et al., 2018). As CQ was only added for the last 4h of the incubation, the difference in LC3II

protein levels between a CQ-treated and the equivalent non-CQ-treated sample illustrates the LC3II turnover within that window of time. As can be seen in Fig. 3.6B, both DFP and CCCP increase autophagosome turnover, although DFP appeared to be more potent than CCCP under the conditions applied. Thus, DFP was chosen as a suitable inducer of BNIP3 and mitophagy for subsequent experiments.

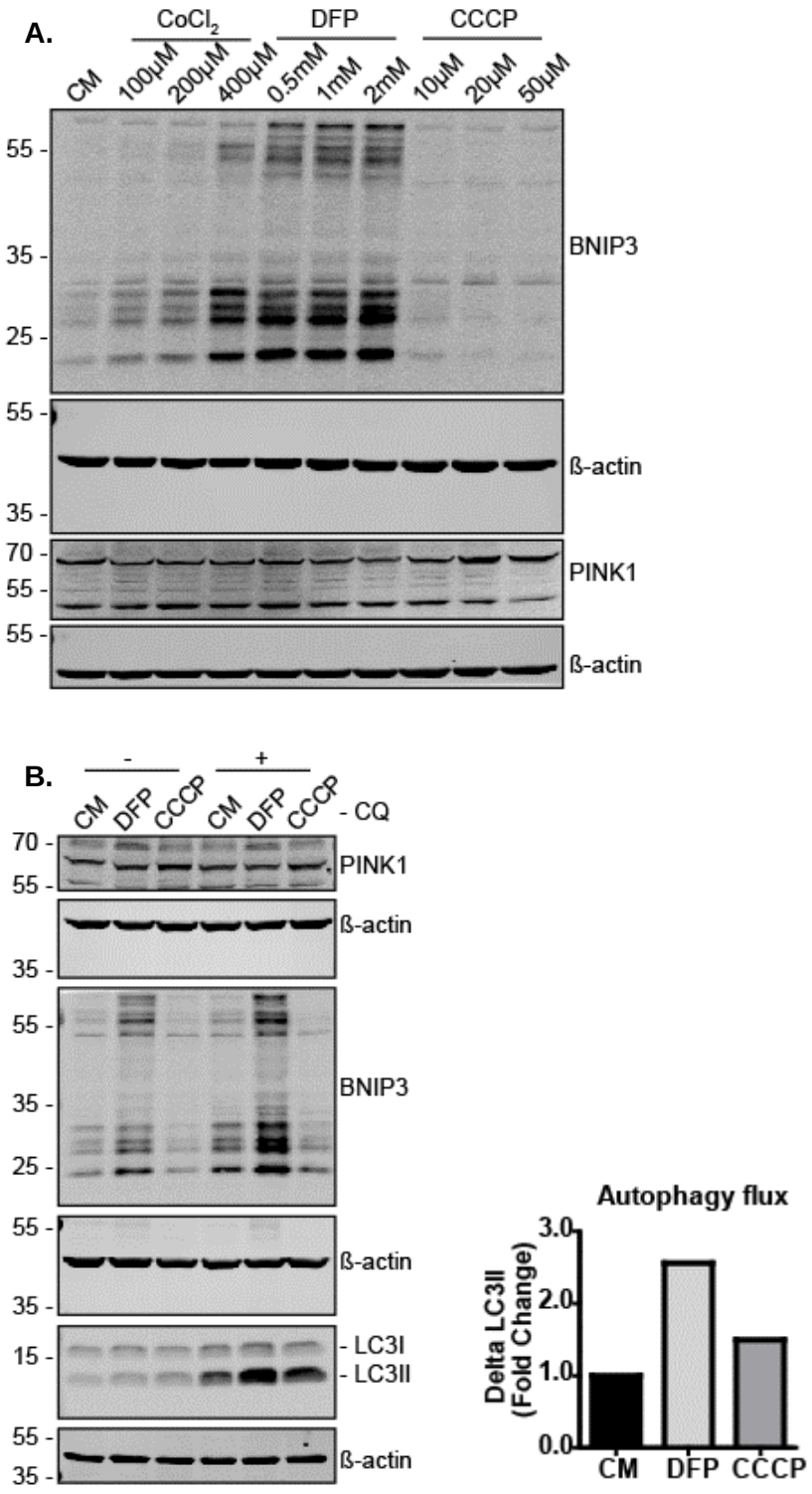

Figure 3.6 DFP induces BNIP3 and increases autophagic flux in MCF-7 cells, while CCCP induces PINK1 and increases autophagic flux to a lesser degree.

A. Western blot showing levels of BNIP3 and PINK1 in MCF-7 cells in response to CoCl2, DFP or CCCP for 24h at the indicated concentrations. β-actin is the protein loading control. **B**. Western blot showing levels of PINK1, BNIP3 and LC3 in MCF-7 cells in response to 24h DFP (1mM) or CCCP (10μM). CQ (50μM) was added for the last 4h. LC3II levels were normalised to β-actin, and autophagic flux was calculated as the difference in LC3II levels between a sample treated with CQ and the same sample non-CQ-treated. The experiments were performed once.

3.3.7 BNIP3 knockdown reduces cell survival in response to nutrient or mitochondrial stress in R- cells, while R+ cells have lower sensitivity to BNIP3 knockdown

To further investigate the importance of BNIP3 and IGF-1 signalling in induction of mitophagy or response to cellular stress, the effects of serum deprivation or mitochondrial stress caused by addition of DFP in complete medium were assessed in IGF-1R KO MEFs (R- cells), and R- cells that stably overexpress the IGF-1R (R+ cells). Levels of apoptosis were assessed by caspase 3 and Poly(ADP-Ribose) Polymerase (PARP) cleavage. In R- cells, both serum starvation and DFP induced apoptosis (Fig. 3.7 and Riis et al., 2020). Interestingly, suppression of BNIP3 further impaired cell survival upon exposure to either treatment, suggesting that in these cells, BNIP3 is important for cell survival under conditions of autophagy/mitophagy induction. R+ cells, on the other hand, showed no induction of apoptosis in response to these stresses, and this was unaffected by BNIP3 suppression. These results suggest that impaired IGF-1 signalling causes R- cells to be more sensitive to these stresses than R+ cells, that are apparently protected due to the overexpression of the IGF-1R and less sensitive to suppression of BNIP3.

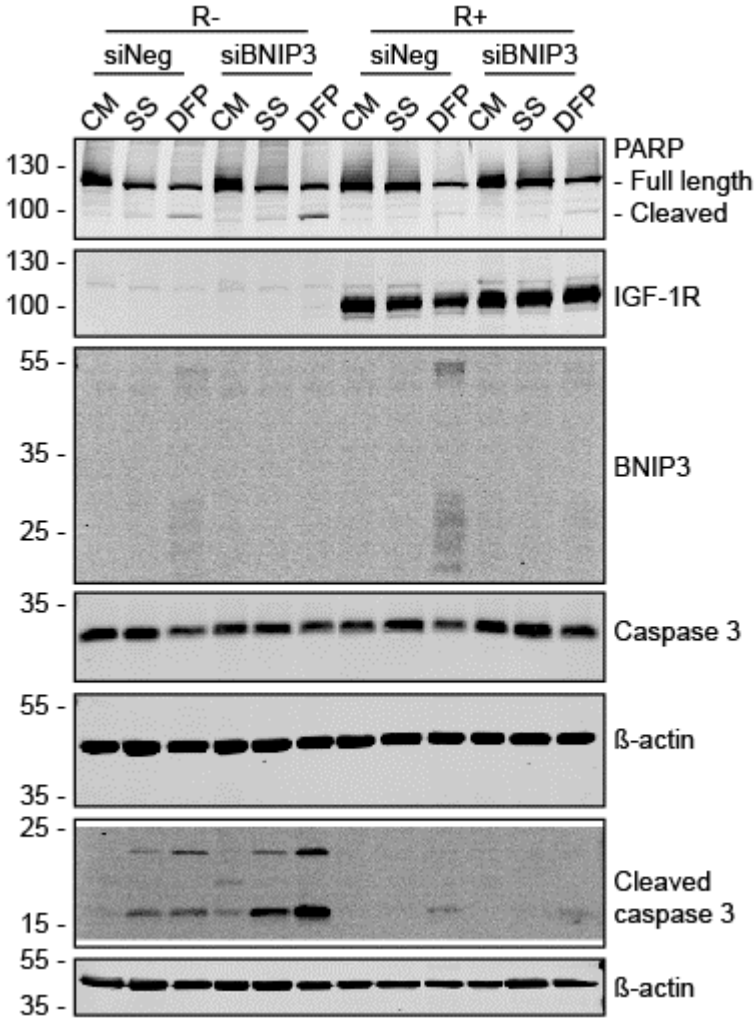

Figure 3.7 Suppression of BNIP3 impairs cell survival upon exposure to serum-deprivation or DFP in R- cells, but not R+ cells.

Western blot showing levels of BNIP3 and cleavage of PARP and caspase 3 in R- and R+ cells. The cells were transfected with a control siRNA or siBNIP3 for 48h prior to addition of serum-free medium or DFP (1mM) for 24h. β-actin is the protein loading control. The experiment was repeated twice, and a representative blot is shown.

3.3.8 Ectopic expression of WT BNIP3 reduces macro-autophagy in cancer cells, but does not improve survival of R- cells exposed to nutrient or mitochondrial stress

Another approach to deciphering the importance of BNIP3 induction in response to IGF-1 signalling, was to compare the effects of ectopically expressing wildtype (WT) BNIP3 and a BNIP3 mutant, which has two mutations in the LIR domain (W83A/L86A). This LIR mutant BNIP3 is incapable of mediating its mitophagy function, as reported by Zhu and colleagues (Zhu et al., 2013). MCF-7 cells transiently

transfected with vectors encoding these BNIP3 constructs were assessed by immunofluorescence with an anti-BNIP3 antibody to assess expression and mitochondrial localisation of BNIP3. Figure 3.8.A shows that endogenous BNIP3 in cells transfected with the empty vector control (EV) was barely detectable, WT or LIR-mutant BNIP3 were clearly overexpressed, and the BNIP3 staining pattern was consistent with mitochondrial morphology, suggesting predominantly mitochondrial localisation. Autophagic flux was measured in these cells in complete medium (Fig. 3.8.B). WT but not LIR-mutant BNIP3 expression caused a reduction in autophagosome turnover compared to the EV control. As indicated by p-p70 S6 kinase (T371) and p62 levels, there was no dramatic change in autophagy levels, and PHB1 levels were similarly not affected, indicating no clear activation of mitophagy (Fig. 3.8.B).

To test whether the lack of mitophagy could be due to the lack of mitophagy-promoting stimuli, the same experiment was performed in complete medium or DFP-containing medium. Again, overexpression of WT BNIP3 but not the LIR-mutant BNIP3 reduced autophagosome turnover in complete medium conditions, and a similar trend was observed in response to DFP (Fig. 3.8.C). This suggests that WT BNIP3 either inhibits the induction of autophagy or enhances the clearance of autophagosomes, and this function requires a functional LIR domain.

Interestingly, the WT and LIR-mutant BNIP3 exhibited slightly different protein bands in western blots. WT BNIP3 presented dominant bands at 30-35kDa, while the LIR-mutant had an additional strong band at approximately 40kDa, suggesting the LIR-mutant undergoes posttranslational modifications that retard its mobility in SDS PAGE compared with the WT protein. Alternatively, the LIR mutant

may be associated in stable protein complexes resulting in an apparently increased molecular weight.

Since it was observed that suppression of BNIP3 in R- cells impaired their tolerance to nutrient deprivation or mitochondria stress (DFP), R- and R+ cells were transfected with either WT or LIR-mutant BNIP3, to assess if they could enhance cell survival in response to mitochondrial stress. However, ectopic expression of BNIP3 was not sufficient to promote cell survival under such conditions as demonstrated by similar levels of cell death between cell lines (Fig 3.8.D).

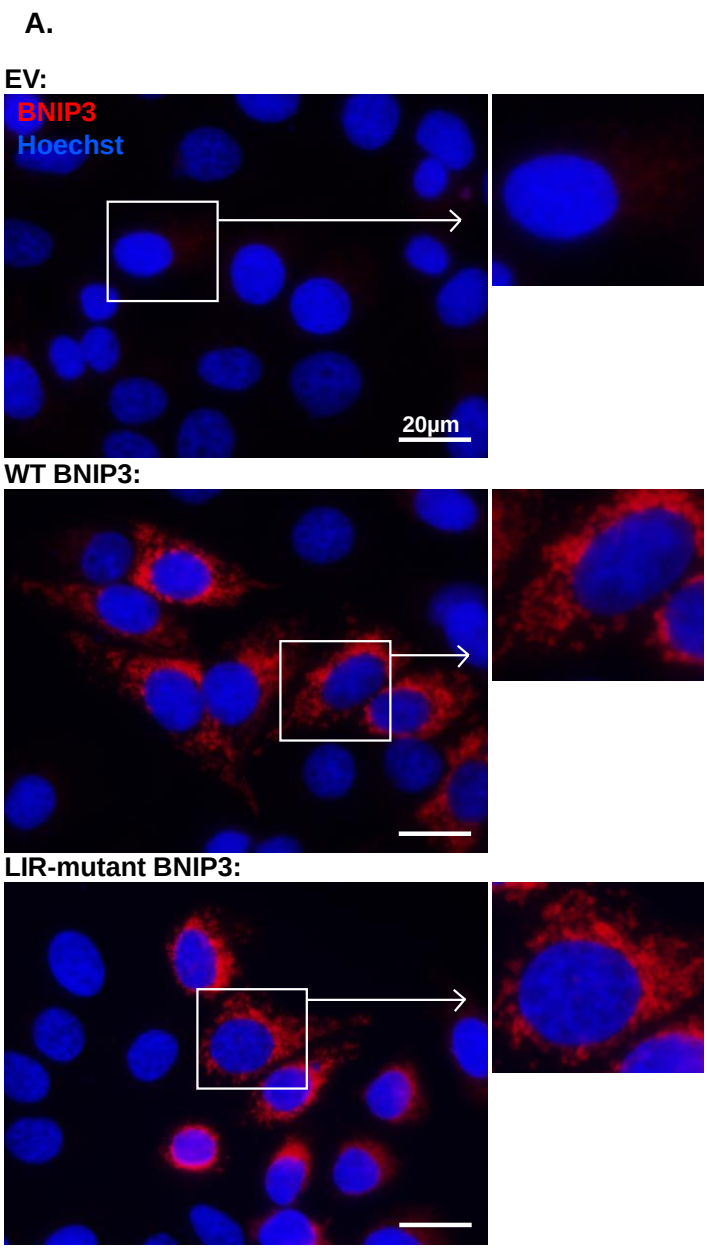

Figure 3.8 Ectopic expression of WT BNIP3 reduces autophagic flux in cancer cells but does not affect cell survival in R- or R+ cells exposed to mitochondrial stress.

A. Immunofluorescent staining of MCF-7 cells transfected with pcDNA3.1 EV, WT or LIR-mutant BNIP3. The cells were stained with an anti-TOM20 antibody and Hoechst. Images were acquired on a Leica DM LB2 microscope using a 100x objective.

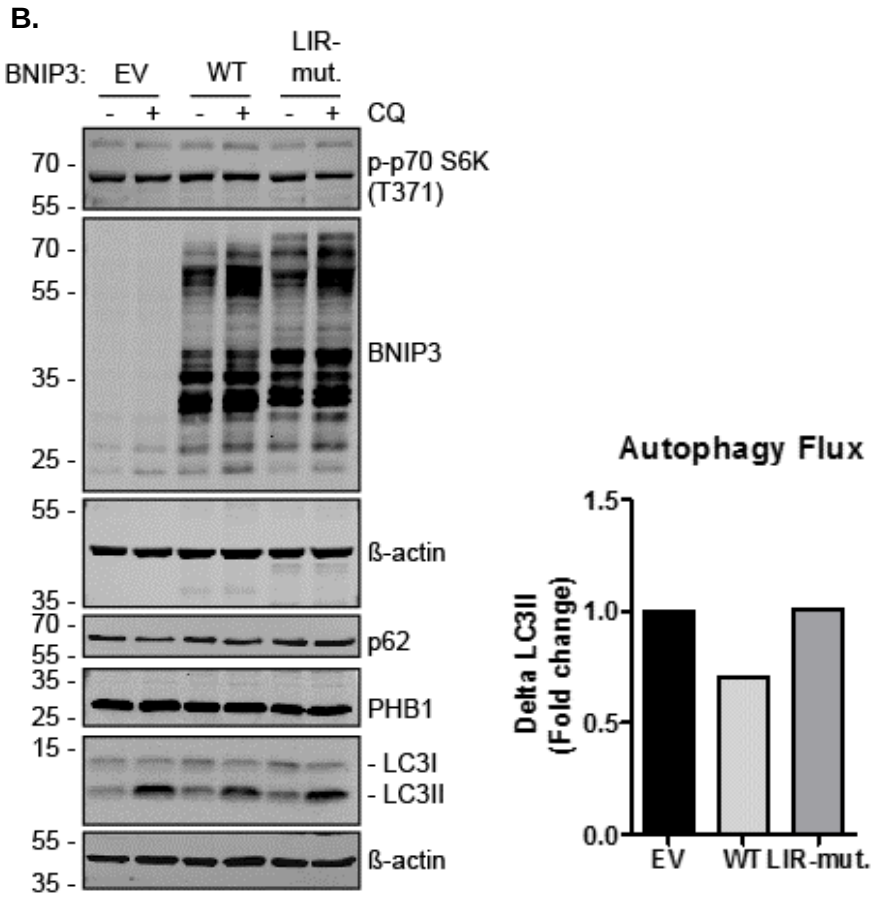

3.8.B. Western blot showing protein levels of BNIP3, LC3, p62 and p-p70 S6 kinase (T371) in MCF-7 cells. The cells were transiently transfected with pcDNA3.1 EV, WT or LIR-mutant BNIP3. 72h post transfection, CQ (50μM) was added to the cells for the last 6h prior to lysis. LC3II levels were quantified and normalised to β-actin. The difference in LC3II levels between a CQ-treated and the corresponding untreated sample was calculated as a measure of autophagic flux, and the relative fold change compared to the EV control is shown in the bar chart.

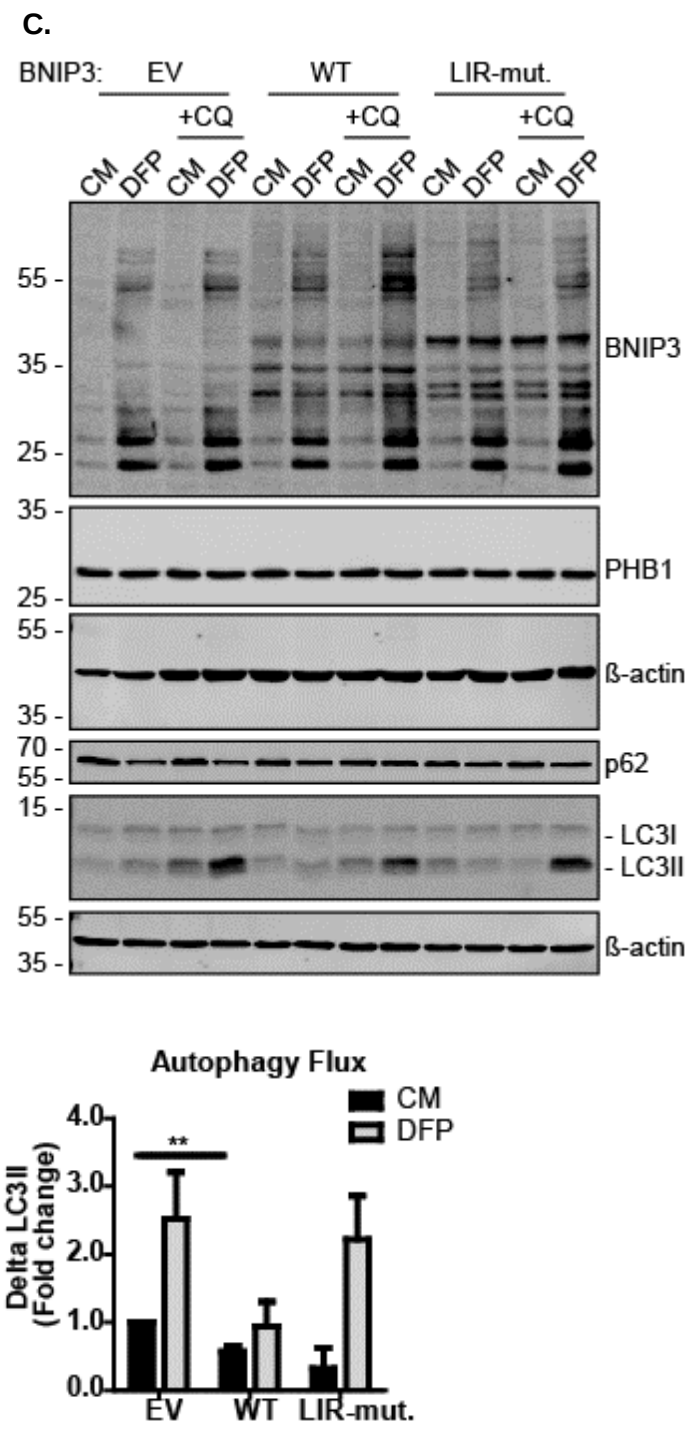

3.8.C. Western blot showing protein levels of BNIP3, p62 and LC3 in MCF-7 cells. The cells were transiently transfected with pcDNA3.1 EV, WT or LIR-mutant BNIP3. 72h post transfection, the cells were maintained in complete medium or exposed to DFP (1mM) for 24h. CQ (50μM) was added for the last 4h. LC3II levels were quantified and normalised to β-actin. Autophagic flux was calculated as for (**B**), and the relative fold change compared to the EV complete medium control is shown in the bar chart. Results are presented as mean ± SEM from three independent experiments. For statistical analysis, the Student's t-test was performed (*: $p<0.05$, **: $p<0.01$, ***: $p<0.001$). A representative blot is shown.

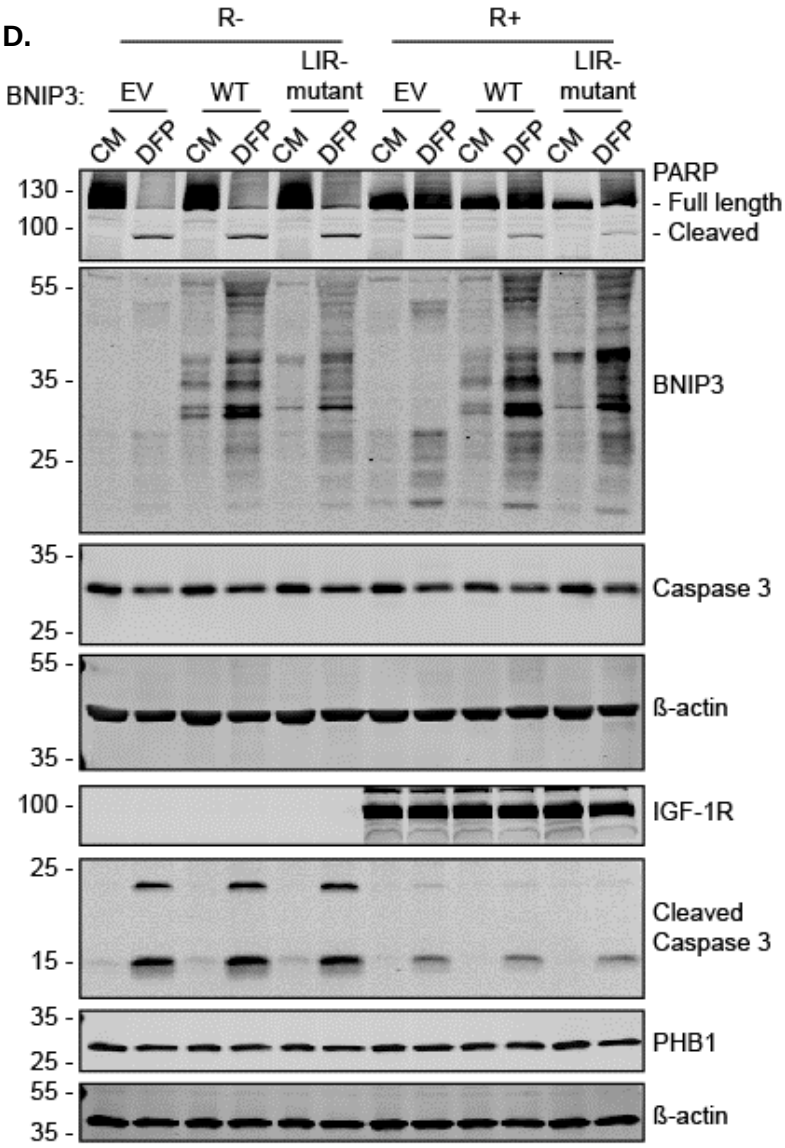

3.8.D. Western blot showing levels of BNIP3, caspase 3, PHB1 and PARP and caspase 3 cleavage in R- and R+ cells. The cells were transfected with pcDNA3.1 EV, BNIP3 WT or BNIP3 LIR-mutant for 48h prior to addition of DFP (1mM) for 24h. β-actin is the protein loading control. The experiment was repeated twice, and a representative blot is shown.

3.3.9 Impaired IGF-1 signalling reduces basal levels of PHB1/PHB2, and IGF-1 induces accumulation of both mitochondrial and cytosolic PHB2 in cancer cells

The potential for crosstalk between BNIP3 and other mitophagy pathways was next considered. PHB2 was recently shown to function as a mitophagy receptor in Parkin-mediated mitophagy. PHB2 is present at the IMM and, thus, requires permeabilization

of the OMM to interact with LC3-like proteins (Wei et al., 2017). Crosstalk between PINK1 and BNIP3-mediated mitophagy has also been documented (Zhang et al., 2016). Therefore, we asked if PHB2 might facilitate BNIP3-mediated mitophagy. PHB2 locates to the IMM in a multimeric complex consisting of several PHB1/PHB2 heterodimers (Nijtmans et al., 2000, Tatsuta et al., 2005). Due to the firmly established functional interaction between the prohibitin proteins, both were examined in this study. To test whether IGF-1 signalling affects PHB1 or PHB2 levels, MCF-7 and MCF-7R cells were serum-starved for 4h prior to addition of IGF-1 for 20h. Consistent with previous findings, BNIP3 was not induced in response to IGF-1 in MCF-7R cells (Lyons et al., 2017), and the cells exhibited reduced levels of the IGF-1R. Parental MCF-7 cells exhibited higher levels of PHB1 and PHB2 in serum-free cultures compared to MCF-7R cells, but neither protein was clearly affected by the addition of IGF-1 (Fig. 3.9.A). Surprisingly, IGF-1 increased levels of both proteins in the MCF-7R cells despite the impairment in IGF-1 signalling in these cells. Of note, upon seeding for the experiment, the MCF-7R cells were maintained in complete medium not containing the IGF-1R inhibitor, BMS-754807. Although, MCF-7R cells were shown to stably maintain reduced levels of the IGF-1R after the removal of the inhibitor from cultures (Lyons et al., 2017), the cells are IGF-1-responsive, as indicated by induction of AKT phosphorylation (Fig. 3.9.A). Thus, perhaps IGF-1 stimulation can restore the prohibitin levels to that observed in the parental cells. However, as the MCF-7R cells clearly exhibited lower basal levels of PHB1/PHB2 than parental cells, this implicates IGF-1 in the regulation of PHB1 and PHB2 protein levels/stability.

To further test the effects of IGF-1 on mitochondrial PHB1/PHB2, cellular fractionations were performed with MCF-7 and DU145 cells to isolate mitochondria-

enriched fractions under complete medium, serum-starved and IGF-1-stimulated cell culture conditions. Interestingly, PHB2 was found in both the mitochondrial and the cytosolic fractions, whereas PHB1 only appeared in mitochondrial fractions. Unlike observations in whole cell lysates from parental MCF-7 cells in Figure 3.9.A, the fractions showed that IGF-1 induced a slight increase in PHB2 protein in both mitochondrial and cytosolic fractions in MCF-7 and DU145 cells. No clear induction or reduction of PHB1 protein was observed in response to IGF-1 (Fig. 3.9.B). The mobility of cytosolic PHB2 protein was retarded in SDS PAGE compared to the mitochondrial PHB2 protein in both cell lines, suggesting a difference in post-translational modifications, for example. Of note, IGF-1 induced the appearance of a second and slightly higher molecular weight PHB1 protein band in the mitochondrial fraction in DU145 cells, indicating differential post-translational modification. However, these effects were not observed in MCF-7 cells.

A.

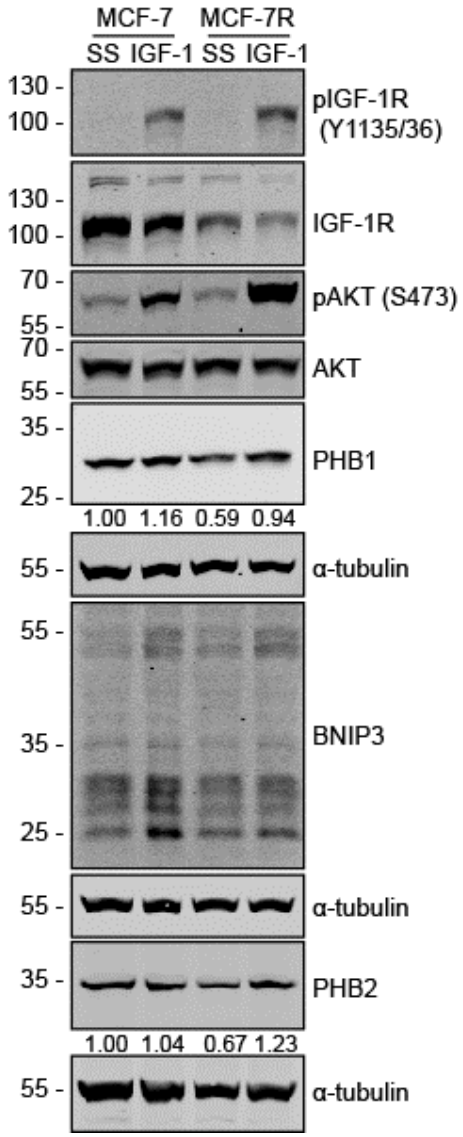

Figure 3.9 MCF-7R cells have lower basal levels of PHB1 and PHB2 than MCF-7 cells, and PHB2 is IGF-1 responsive in cancer cells.

A. Western blot showing levels of PHB1, PHB2 and BNIP3 levels in MCF-7 and MCF-7R cells. MCF-7R cells were maintained in 500nM BMS-754807 until seeding for experiments. The cells were serum-starved for 4h prior to addition of IGF-1 (10ng/ml) for 20h. Protein levels of PHB1/PHB2 were quantified and normalised to the α-tubulin. The relative fold change is shown for each sample compared to the control sample. The experiment was performed once.

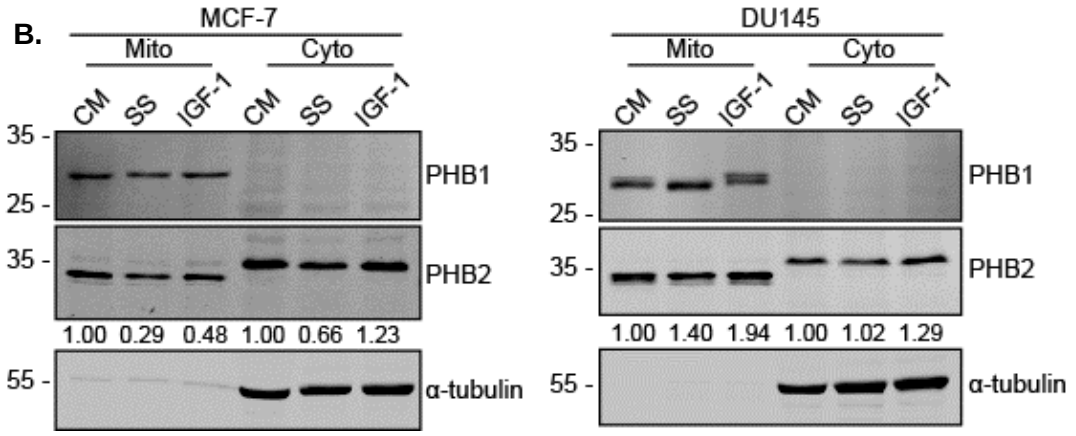

3.9.B. Western blot showing subcellular fractions of MCF-7 and DU145 cells. The cells were kept in complete medium or serum-starved for 4h followed by stimulation with IGF-1 (10ng/ml) for 4h, before mitochondria-enriched fractions were separated from cytosolic fractions. The fractions were probed for PHB1, PHB2 and the cytosolic marker α-tubulin. The bands were quantified, and relative fold changes compared to the controls are shown underneath the blots. The experiment was performed once.

3.3.10 Suppression of PHB2 reduces protein levels of BNIP3 or Nrf2, impairs IGF-1-mediated inhibition of macro-autophagy and causes mitochondrial fragmentation

To further investigate how IGF-1 controls PHB1/PHB2 and the potential role of PHB2 in BNIP3-mediated mitophagy, we used siRNA to reduce PHB2 levels in MCF-7 and DU145 cells. PHB2 suppression reduced protein levels of both PHB1 and PHB2 in both cell lines (Fig. 3.10.A), as has previously been described (Artal-Sanz et al., 2003, Merkwirth et al., 2008, Ising et al., 2015). Furthermore, knockdown of PHB2 reduced levels of both p62 and BNIP3 at 72h in the MCF-7 cells, and while siPHB2-DU145 cells had reduced p62 and Nrf2 protein, there was no apparent reduction in BNIP3 levels. Due to difficulties, detecting endogenous Nrf2 protein levels in MCF-7 cells, Nrf2 levels could not be assessed in these cells. These observations with Nrf2, BNIP3 and p62 suggest that PHB2 may affect both general autophagy and mitophagy.

Suppression of either PHB1 or PHB2 has previously been linked to mitochondrial fragmentation, as the proteins are associated with maintenance of mitochondrial integrity (Artal-Sanz et al., 2003, Merkwirth et al., 2008, Ising et al.,

2015). To test this in cancer cells, MCF-7 and DU145 cells transfected with control siRNA or siPHB2 were stained with an anti-TOM20 antibody (Fig. 3.10.B). Indeed, we did observe mitochondrial fragmentation in both cell lines, even in MCF-7 cells that generally exhibit quite small and rounded mitochondria under control culture conditions. Due to such a dramatic effect on mitochondrial dynamics, we next asked, if PHB2 affects IGF-1-mediated induction of BNIP3 and potentially mitophagy in MCF-7 and DU145 cells. To test this, cells were transfected with a control siRNA or siPHB2, and 24h later were serum-starved for 4h followed by IGF-1 stimulation for 20h (Fig. 3.10.C). In MCF-7 cells, suppression of PHB2 reduced basal BNIP3 levels, but did not impair the IGF-1-mediated induction of BNIP3. PHB2 suppression did, however, prevent p62 accumulation in response to IGF-1 in MCF-7 cells, suggesting impaired IGF-1-mediated inhibition of autophagy. In DU145 cells, suppression of PHB2 reduced basal levels of Nrf2, but the induction in response to IGF-1 was not affected. These cells showed no effect on BNIP3 or p62 levels. Thus, although PHB2 is clearly responsive to IGF-1, it is not immediately clear, why these differences exist between cell lines.

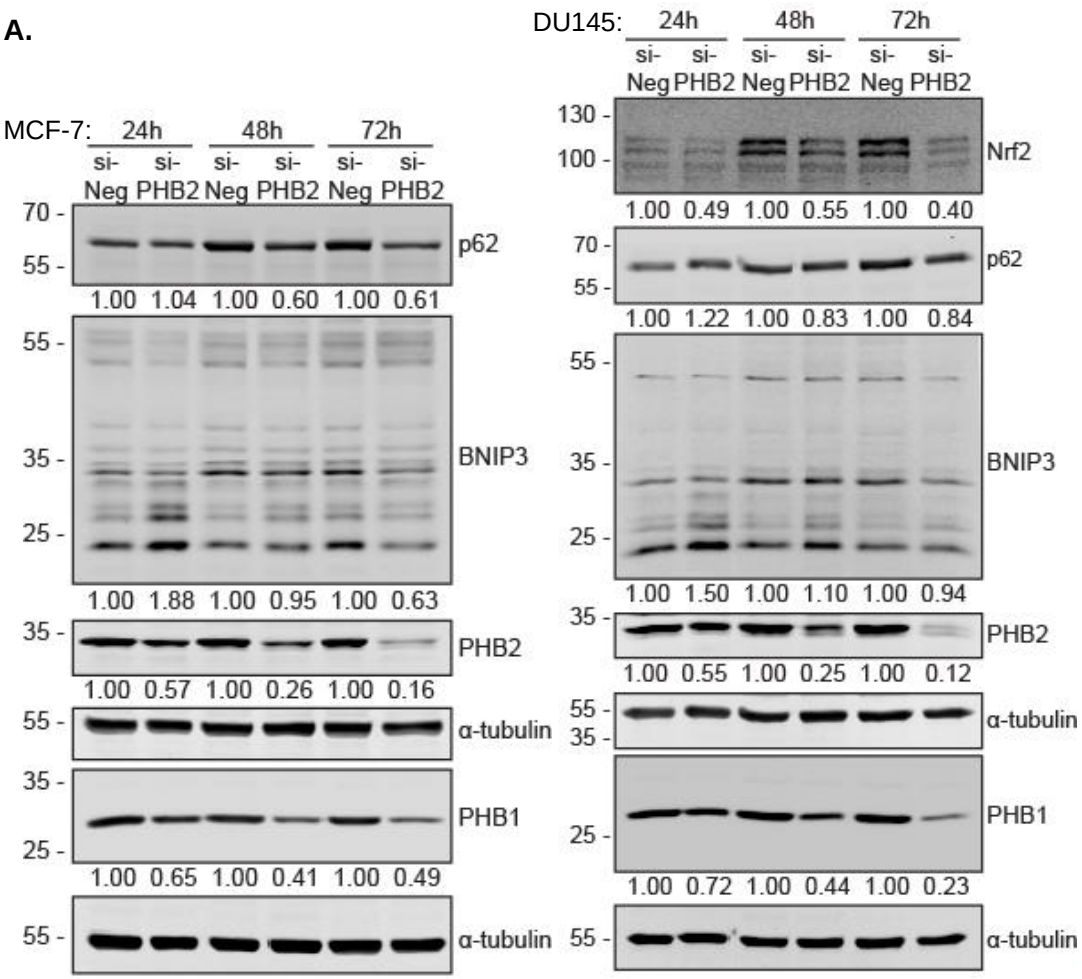

Figure 3.10 Suppression of PHB2 reduces levels of BNIP3 or Nrf2 in cancer cells, impairs IGF-1-mediated inhibition of macro-autophagy and causes mitochondrial fragmentation.

A. Western blot showing levels of p62, BNIP3, Nrf2, PHB1 and PHB2 in MCF-7 and DU145 cells that were transfected with control siRNA or siPHB2 for 24, 48 or 72h as indicated. Protein levels were quantified and normalised to α-tubulin. For each time point, the relative fold change is shown underneath the blots, comparing protein levels in siPHB2-treated cells to the controls.

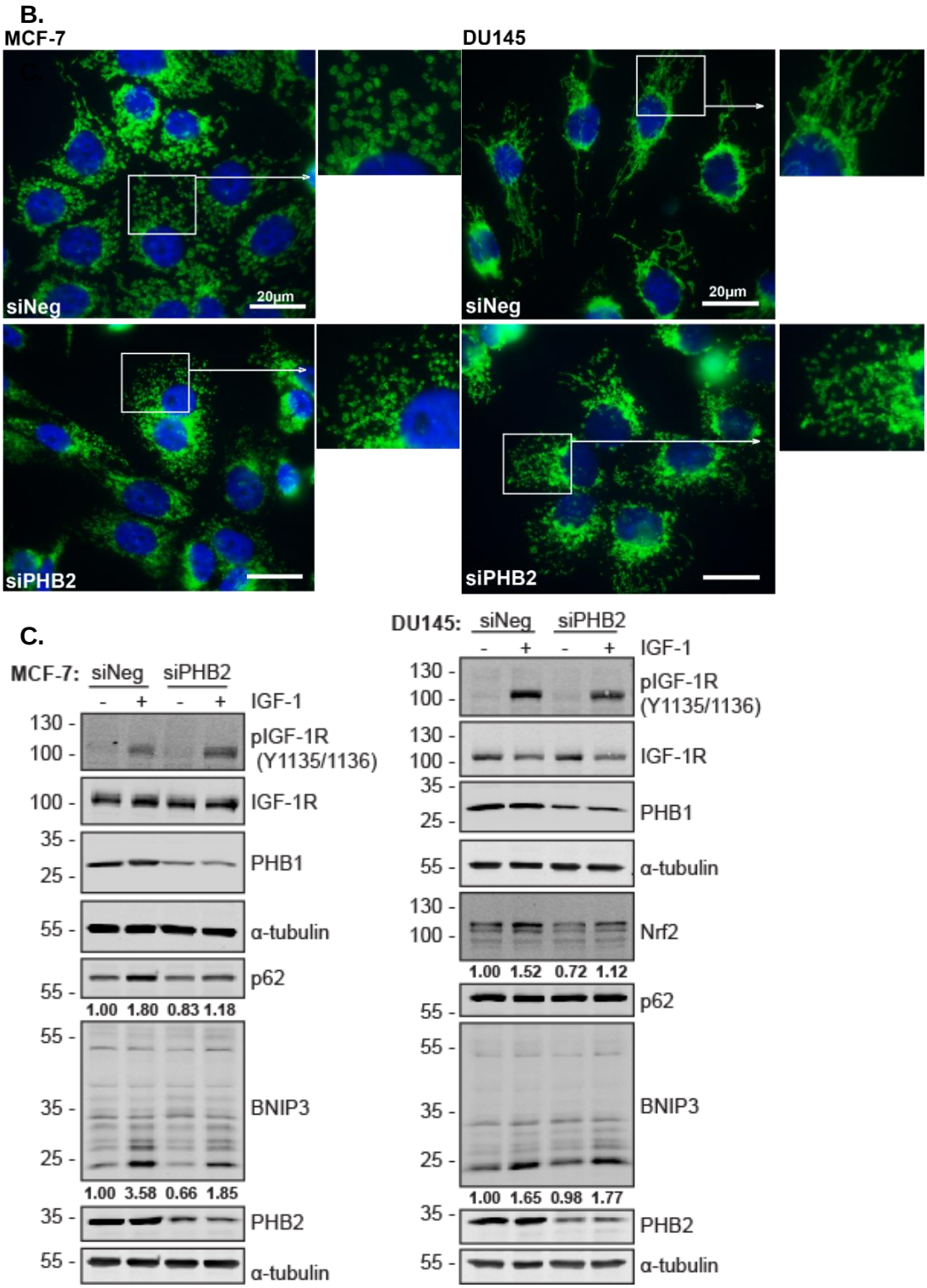

3.10.B. Immunofluorescence images of MCF-7 and DU145 cells stained with anti-TOM20 antibody and Hoechst. Cells were transfected with a control siRNA or siPHB2 for 96h. Images were acquired on a Nikon Eclipse E600 microscope using a 100x objective. **C.** Western blot showing levels of PHB1, PHB2, p62 and BNIP3 in addition to IGF-1R phosphorylation in MCF-7 and DU145 cells. Cells were transfected with a control siRNA or siPHB2. 48h post transfection, cells were serum-starved for 4h prior to addition of IGF-1 (10ng/ml) for 20h. Protein levels of BNIP3 and Nrf2 were quantified and normalised to α-tubulin. The relative fold change for each sample compared to the control sample are shown underneath the blots. All experiments were repeated twice, and representative blots are shown.

3.4 Discussion

Mitochondrial homeostasis depends on a tightly regulated balance of mitochondrial dynamics, which involves the processes of mitochondrial biogenesis, fission and fusion events in addition to mitochondrial degradation. IGF-1 has been implicated in the regulation of mitochondrial function, but its role in mitochondrial turnover has not yet been established. Here, we found that IGF-1 stimulates mitochondrial biogenesis through PGC-1β and PRC, while inducing the mitophagy receptor BNIP3. We demonstrated that PGC-1β/PRC are essential for the maintenance of mitochondrial morphology, as suppression of both transcriptional coactivators, caused mitochondrial elongation compared to rounded mitochondria observed in MCF-7 cells under normal culture conditions. This could reflect a protective mechanism for maintaining the existing pool of mitochondria by inhibiting mitophagy, as mitochondrial fission often facilitates mitochondrial degradation (Gomes and Scorrano, 2008, Frank et al., 2012, Zuo et al., 2014).

The mitophagy receptor BNIP3 is best described for its role in hypoxia, a condition that arises in tumours. Thus, the IGF-1-BNIP3 axis is particularly relevant in cancer. The MCF-7R cells with impaired IGF-1 signalling were unable to mount an effective BNIP3-mediated mitophagy response, suggesting a mitochondrial vulnerability in cancer cells with acquired resistance to IGF-1R inhibitors, which could potentially be exploited therapeutically. Interestingly, IGF-1 induced BNIP3 protein expression under normoxic conditions in cancer cells as well as during hypoxia. Given the anti-apoptotic effects of IGF-1 (Parrizas et al., 1997, Fernández et al., 2004), the IGF-1-mediated induction of BNIP3 is likely not associated with the cell death-inducing capacity of BNIP3 but rather with its ability to induce mitophagy. It has been proposed that the two different BNIP3 functions are regulated by the

phosphorylation status of BNIP3 (Zhu et al., 2013, Liu and Frazier, 2015). We hypothesize that IGF-1 activates both mitochondrial biogenesis and mitophagy to support mitochondria health in cancer cells. This could facilitate ROS clearance and sustain ATP production to meet the elevated energy demands of proliferating tumour cells, whereas induction of mitochondrial biogenesis alone could cause the accumulation of aged and dysfunctional mitochondria, ultimately leading to cell death. Surprisingly, ectopic expression of WT BNIP3 was associated with reduced autophagic flux in response to mitophagy induction by DFP. If the measured autophagosome turnover under these conditions reflects mitophagy levels, this suggests that BNIP3 reduces mitophagy. However, if general autophagy is inhibited by WT BNIP3 this could account for the reduction in autophagic flux, thereby masking an upregulation in mitophagy.

This conclusion is, however, not supported by previous reports that BNIP3 can directly bind to and inhibit Rheb, an activator of the negative autophagy regulator mTOR, thus potentially causing upregulation of autophagy (Li et al., 2007). Furthermore, one study found that BNIP3 was essential for epidermal keratinocyte differentiation and caused activation of autophagy. However, this was associated with removal of mitochondria, suggesting they were in fact detecting mitophagy rather than general autophagy (Moriyama et al., 2014). On the other hand, BNIP3 deficiency was shown to cause increased non-selective autophagy in cortical neurons exposed to oxygen-glucose deprivation followed by reperfusion, suggesting that BNIP3 normally restricts macro-autophagy (Shi et al., 2014). In support of an autophagy-inhibitory role for BNIP3, we found that suppression of BNIP3 in MCF-7 cells caused reduced p62 accumulation, potentially signifying enhanced general autophagy. Importantly, overexpression of WT BNIP3 caused a reduction in autophagic flux in complete

medium conditions with no associated reduction in the mitochondrial marker PHB1, suggesting mitophagy levels were unchanged, but macro-autophagy was impaired. This effect was only observed in response to overexpression of wildtype BNIP3 and not LIR-mutant BNIP3, suggesting that the interaction of BNIP3 with LC3-like proteins affects total autophagosome turnover.

Despite the apparent lack of mitophagy activation in response to overexpression of WT BNIP3, suppression of BNIP3 increased levels of the mitochondrial maker PHB1, suggesting reduced mitophagic activity. Furthermore, the MCF-7R cells displayed significantly reduced capacity for BNIP3-dependent mitophagy under hypoxic conditions, implicating the IGF-1-BNIP3 axis in mitochondrial clearance. Possibly, WT BNIP3 does not enhance mitophagy in complete medium cultures lacking mitophagy stimuli, but loss of BNIP3 reduces endogenous basal levels of mitophagy.

We also sought to establish, whether PHB2 and PHB1 contribute to the IGF-1-BNIP3 axis. Since PHB2 is at the IMM, it may help ensure efficient mitochondrial clearance following mitophagy induction through other pathways. Due to variability across experiments, it was unclear, how IGF-1 affects PHB1/PHB2 protein levels, although MCF-7R cells exhibited reduced basal levels of both PHB2 and PHB1. In parental MCF-7 cells, 20h IGF-1 stimulation had no effect on PHB1/PHB2 protein levels, although 4h IGF-1 stimulation in MCF-7 and DU145 cells appeared to cause a slight increase in both cytosolic and mitochondrial PHB2 levels. This discrepancy could be due to the difference in the timepoints examined. Furthermore, although AKT has been shown to cause mitochondrial translocation of PHB1 (Jiang et al., 2015), this may not affect overall protein levels.

Suppression of PHB2 caused dramatic mitochondrial fragmentation in both MCF-7 and DU145 cells. In MCF-7 cells, suppression of PHB2 reduced BNIP3 and p62 levels. These cells also exhibited reduced autophagic inhibition in response to IGF-1, as indicated by reduced accumulation of p62. However, in DU145 cells, BNIP3 levels were unaffected, while Nrf2 levels were reduced. DU145 cells did not appear to be IGF-1 responsive in terms of p62 accumulation. Of note, DU145 cells have impaired macro-autophagy, because they lack a key protein Autophagy Related 5 (ATG5) (Ouyang et al., 2013), so it is possible that any changes in autophagy might be masked or skewered in these cells. Thus, BNIP3 or Nrf2 protein levels were reduced by suppression of PHB2 but remained IGF-1-responsive. Since, we found here that Nrf2 was induced by IGF-1, and it has been implicated in the regulation of BNIP3-dependent mitophagy in *C. elegans* (Palikaras et al., 2015b), IGF-1 may function through an Nrf2-BNIP3 axis, and the data suggest retrograde signalling from mitochondria to this IGF-1 signalling pathway.

The impairment in mitophagy and reduced tolerance to hypoxia in the MCF-7R cells emphasize the importance of the IGF-1 pathway in maintaining mitochondria health. While it is clear that the IGF-1 signal is mitochondria-protective in cancer cells, further work is required to elucidate the physiological relevance of BNIP3 induction in response to IGF-1 under non-hypoxic conditions, and the effects of the IGF-1 pathway on mitochondrial turnover. A summary is presented in Figure 3.11 of the key IGF-1 effects on mitochondrial biogenesis, turnover and homeostasis established through previous work by our group and the results presented in this chapter.

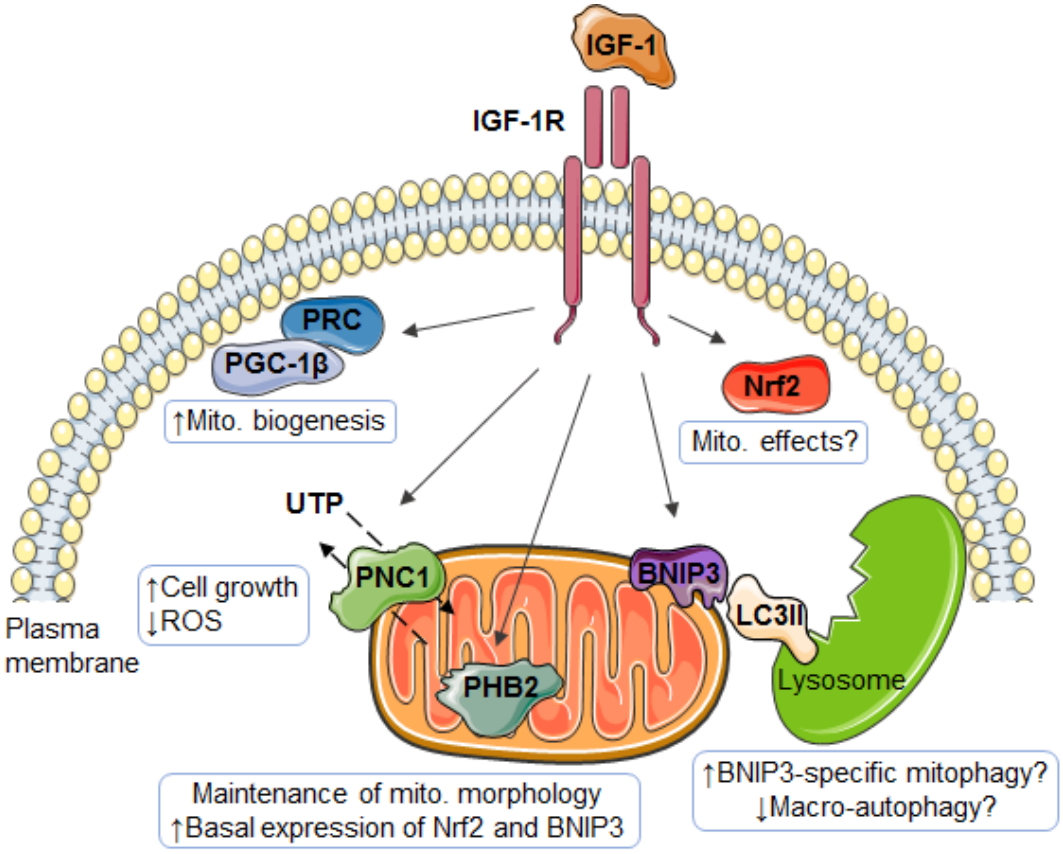

Figure 3.11. Schematic summary of mitochondrial IGF-1 effects.

IGF-1 induces mitochondrial biogenesis through PGC-1β and PRC and promotes cellular growth and redox homeostasis through PNC1. IGF-1 also induces Nrf2 which may affect mitochondrial biogenesis, turnover and health, BNIP3 which may induce mitophagy while inhibiting macro-autophagy and PHB2 which is essential to the maintenance of mitochondrial morphology.

Chapter 4. IGF-1 Signalling Regulates Mitochondrial Dynamics and Turnover Through a Conserved GSK-3β-Nrf2-BNIP3 Pathway

Chapter 4 was published as part of a manuscript: Riis S., Murray J. B., and O'Connor R., IGF-1 Signalling Regulates Mitochondria Dynamics and Turnover through a Conserved GSK-3β-Nrf2-BNIP3 Pathway. Cells, 2020. 9(1).

All experiments in this chapter were performed by the thesis author.

4.2 Abstract

The Insulin-Like Growth Factor I (IGF-1) signalling pathway is essential for cell growth and facilitates tumourogenic processes. We recently reported that IGF-1 induces a transcriptional programme for mitochondrial biogenesis, while also inducing expression of the mitophagy receptor BCL-2/Adenovirus E1B 19 kDa Protein-Interacting Protein 3 (BNIP3), suggesting that IGF-1 has a key mitochondria-protective role in cancer cells. Here we investigated this further and delineated the signaling pathway for BNIP3 induction. It was established that IGF-1 induced BNIP3 expression through a known AKT-mediated inhibitory phosphorylation on Glycogen Synthase Kinase 3β (GSK-3β) leading to activation of Nuclear Factor Erythroid-2 Related Factor (Nrf2/NFE2L2) and acting through the downstream transcriptional regulator Hypoxia-Inducible Factor 1α (HIF-1α). Suppression of IGF-1 signaling, Nrf2, or BNIP3 caused the accumulation of elongated mitochondria and altered mitochondrial dynamics. IGF-1R null mouse embryonic fibroblasts (MEFs) were impaired in BNIP3 expression and in the capacity to mount a cell survival response in response to serum deprivation or mitochondrial stress. IGF-1 signalling enhanced cellular capacity to induce autophagosomal turnover in response to activation of either general autophagy or mitophagy. Overall, the data show that IGF-1 mediates a mitochondria-protective signal that is coordinated through the cytoprotective transcription factor Nrf2. This pathway couples mitochondrial biogenesis with BNIP3 induction, and increases cellular capacity for autophagosome turnover, whilst enhancing survival under conditions of metabolic or mitochondrial stress.

4.3 Introduction

The IGF-1 signalling pathway is essential for cell growth and survival (Hakuno and Takahashi, 2018) and has the potential to enhance tumour growth and cancer progression (Denduluri et al., 2015, Guevara-Aguirre et al., 2018). Anticancer therapies targeting the IGF-1R have overall proved disappointing in clinical trials (Qu et al., 2017, Osher and Macaulay, 2019). However, the compelling evidence for IGF actions in cancer and its central function in human biology and ageing, makes it important to better understand the mechanisms and regulation of this signalling pathway, so that it may be successfully modulated or targeted for therapeutic benefit.

Mitochondrial dysfunction is a common feature of cancer cells that may arise due to altered fusion/fission dynamics, oxidative stress, metabolic reprogramming and other mitochondrial changes (reviewed in (Vyas et al., 2016)). Emerging evidence suggests that dysregulation of mitophagy is common in cancer, and that the accumulation of dysfunctional mitochondria drives cancer progression (Drake et al., 2017). The balance between mitochondrial biogenesis and mitophagy requires strict regulation to maintain a sustainable mitochondria population in healthy cells (Pickles et al., 2018). However, it has been proposed that mitophagy and mitochondrial biogenesis are uncoupled in cancer due to an observed upregulation of mitochondrial biogenesis associated with downregulation of mitophagy (Drake et al., 2017).

We and others have shown that IGF-1 signalling modifies mitochondrial function and fitness including mitochondrial DNA/RNA maintenance, biogenesis, oxidative phosphorylation and suppression of ROS production (Sádaba et al., 2016, Favre et al., 2010, Ribeiro et al., 2014). IGF-1 induces expression of the highly conserved mitochondrial carrier for pyrimidine nucleotides PNC1/SLC25A33, which is a homologue of the essential yeast carrier RIM2 and is essential for mitochondria

DNA and RNA maintenance. Interestingly, suppression of PNC1/SLC25A33 expression in cancer cell lines causes a profound mitochondrial dysfunction, an increase in ROS and induction of epithelial mesenchymal transition (EMT) (Favre et al., 2010). This observation suggested an important function for IGF-1 signaling in the maintenance of healthy mitochondria and suppression of ROS-induced epithelial-to-mesenchymal transition (EMT) in cancer cells. We subsequently reported that IGF-1 promotes mitochondrial biogenesis through upregulation of the transcriptional co-activators PGC-1β and PRC, whilst inducing expression of the mitophagy receptor BNIP3. (Lyons et al., 2017)

BNIP3 was originally described as a BH3-only member of the BCL-2 family that can that can interact with and inhibit pro-survival BCL-2 proteins to induce apoptosis. It is closely related to BCL-2/Adenovirus E1B 19 kDa Protein-Interacting Protein 3-Like (BNIP3L/Nix) with both proteins containing LC3-interacting regions (LIR) that can interact with LC3II on autophagosomes to enable mitophagy (Choe et al., 2015). Although they exhibit distinct tissue-specific expression, BNIP3 and BNIP3L are both induced by hypoxia to promote mitophagy that is independent of PINK1/Parkin. Interestingly, BNIP3 expression has been reported to increase in the early stages of breast cancer but becomes suppressed as tumours become hypoxic. BNIP3 inactivation or suppression has been associated with pancreatic cancer, glioma, breast and prostate cancer, with murine cancer models suggesting a tumour suppressor function (Chourasia et al., 2015, Niu et al., 2019, Du et al., 2017). However, it is still not clear how BNIP3 expression, its induction by IGF-1, or the role of mitophagy in cancer cell metabolism is regulated or integrated with mitochondrial biogenesis and mitochondrial function.

We hypothesized that IGF-1 signaling promotes both mitochondrial biogenesis and mitophagy as an underlying mito-protective feature of all cells (normal or transformed). This highly conserved homeostatic signalling pathway is present in *C. elegans*, where the BNIP3/NIX orthologue DCT-1 couples the regulation of mitochondrial biogenesis with mitophagy to support a healthy lifespan The *C. elegans* pathway is controlled by SKN-1, which is the orthologue of the transcriptional regulator NFE2L2/Nrf2 (Palikaras et al., 2015b, Palikaras et al., 2015c).

Here we delineated the signaling pathway for IGF-1-mediated BNIP3 induction in cancer cell lines and MEFs. We found that IGF-1- induced BNIP3 expression requires Nrf2 acting through HIF-1α, and this pathway is essential for mitochondrial morphology and dynamics. Moreover, IGF-1 signalling is essential for cell tolerance to nutrient deprivation and mitochondrial stress. We conclude that IGF-1 signals couple induction of mitochondrial biogenesis with basal levels of mitochondrial turnover through Nrf2 and BNIP3, thus maintaining mitochondrial homeostasis and facilitating cancer progression.

4.4 Results

4.4.1 R- cells have lower levels of Nrf2 and BNIP3, altered expression of OXPHOS components and lower mitochondrial membrane potential than R+ cells

IGF-1 induces expression of the transcription coactivators PGC-1β and PRC that mediate a mitochondrial biogenesis programme and also induces expression of the mitophagy receptor BNIP3 at the mRNA and protein level (Lyons et al., 2017). Since mitochondrial biogenesis and mitophagy may be coupled, and since Nrf2 promotes transcription of the BNIP3/NIX orthologue DCT-1 in *C. elegans* (Palikaras et al.,

2015c), we hypothesized that Nrf2 activity may be important for IGF-1-mediated induction of BNIP3 in mammalian cells.

To test this, Nrf2 and BNIP3 levels were first compared in IGF-1R knockout MEFs (R- cells) and R- cells stably reconstituted with the IGF-1R (R+ cells). As can be seen in Figure 4.1.A-B, R- cells express statistically significantly lower levels of both Nrf2 and BNIP3 protein and mRNA than R+ cells, suggesting a requirement for IGF-1 signalling in the expression of these proteins. Expression levels of the mitochondrial marker PHB1 were similar in the two cell lines, indicating that the difference observed in BNIP3 expression was not due to a significant difference in mitochondrial mass (Fig. 4.1.B). Interestingly, expression levels of electron transport chain components were different in R- and R+ cells, with R+ cells exhibiting lower levels of Complex III, but higher levels of Complex V/ATP synthase, suggesting altered capacity for oxidative phosphorylation in R+ cells. This was associated with a slightly higher mitochondria membrane potential in R+ cells compared to R- cells as measured by flow cytometric analysis of the cells stained with the dye TMRM (Fig. 4.1.C). These data suggest that IGF-1 is important in the regulation of mitochondria function and potentially turnover.

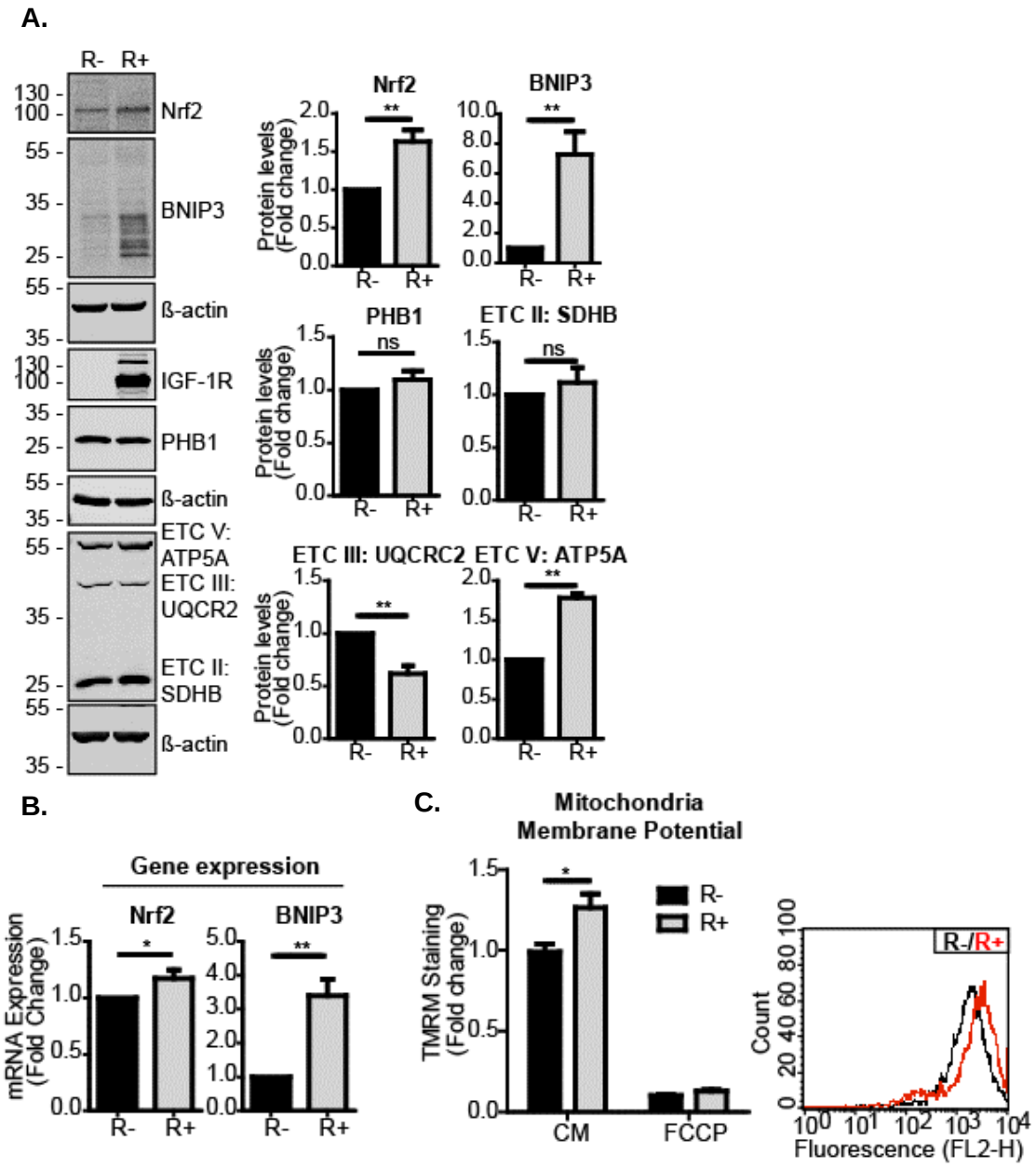

Figure 4.1 IGF-1R KO MEFs exhibit lower levels of Nrf2 and BNIP3 in addition to a slightly reduced mitochondrial membrane potential, compared to these cells overexpressing the IGF-1R.

A. Western blot showing levels of Nrf2, BNIP3, PHB1 and OXPHOS components in R- and R+ cells in complete medium. Protein levels were normalised to β-actin and presented as fold change relative to the control sample set to a value of 1. **B**. Gene expression levels of Nrf2 and BNIP3 in R- and R+ cells in complete medium measured by RQ -PCR. Gene expression levels were normalised to the housekeeping gene β-actin and presented as fold change relative to the control set at a value of 1. **C**. Mitochondrial membrane potential measured by flow cytometry in R- and R+ cells using TMRM dye. The average geometric means are shown as fold change compared to R- set to a value of 1 for the first biological repeat. FCCP positive controls were included. A representative graph illustrating the fluorescence intensity of R+ cells (red) and R- cells (black) is also shown. Results are presented as mean ± SEM from three independent experiments. For statistical analysis, the Student's t-test was performed (*: $p<0.05$, **: $p<0.01$, ***: $p<0.001$).

4.4.2 IGF-1 induces Nrf2 and BNIP3 in multiple cancer cell lines and causes nuclear translocation of Nrf2

IGF-1-mediated induction of BNIP3 expression was observed in all cancer cell lines tested, including MCF-7 cells (Lyons et al., 2017). Here, it was observed that IGF-1 stimulation increased the amount of Nrf2 present in the nuclear fraction of MCF-7 cells, suggesting that IGF-1 causes activation of Nrf2 to induce its activity as a transcription factor (Fig. 4.2.A). IGF-1 also induced Nrf2 and BNIP3 in DU145 cells, where serum-starvation reduced levels of both Nrf2 and BNIP3, and subsequent IGF-1 stimulation induced expression of both proteins (Fig. 4.2.B). The human osteosarcoma cell line U2OS also exhibited a slight but statistically significant increase in BNIP3 expression in response to IGF-1 (Fig. 4.2.C).

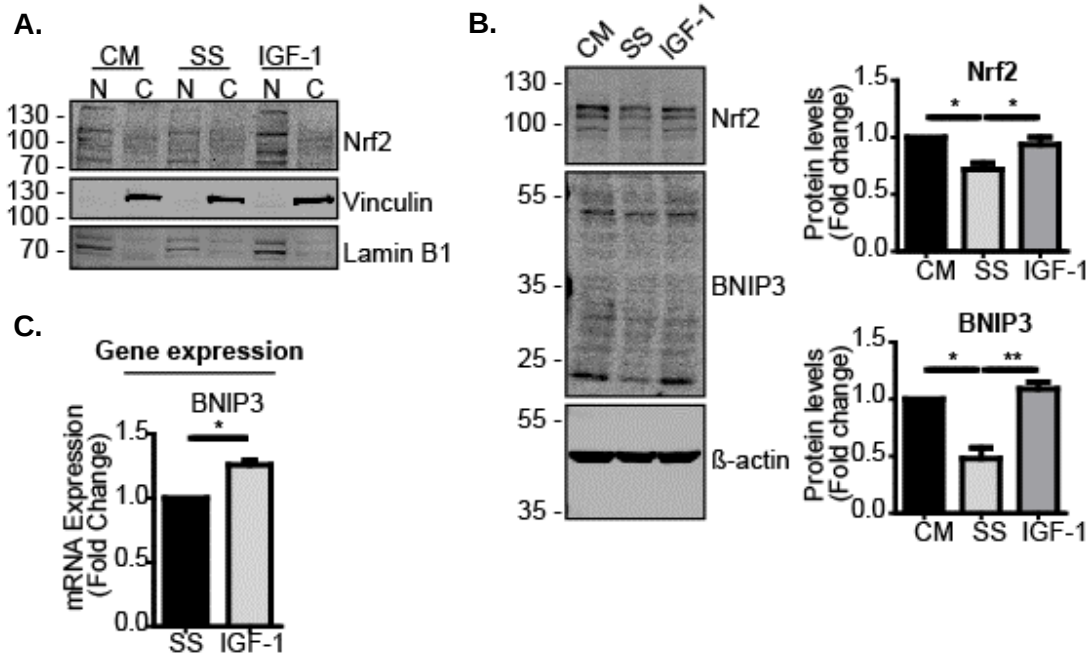

Figure 4.2 IGF-1 induces nuclear translocation of Nrf2 in MCF-7 cells and causes BNIP3 induction in both DU145 and U2OS cells.

A. Western blot showing Nrf2 levels in nuclear (N) and cytosolic (C) fractions of MCF-7 cells maintained in control medium or serum-starved for 4h followed by 4h IGF-1 stimulation (10ng/ml). **B**. Western blot showing Nrf2 and BNIP3 levels in DU145 cells. The cells were kept in complete medium or serum-starved for 4h prior to addition of IGF-1 (10ng/ml) for 20h. **C**. Gene expression levels of BNIP3 in U2OS cells measured by RQ -PCR. The cells were serum-starved for 4h prior to stimulation with IGF-1 (10ng/ml) for 20h. In all panels the data is derived from three independent experiments. Protein levels were normalised to β-actin and presented as fold change relative to the control sample set to a value of 1. For RQ -PCR, gene expression levels were normalised to the housekeeping gene UBC and presented as fold change relative to control conditions set at a value of 1. Results are presented as mean ± SEM from three independent experiments. For statistical analysis, a one-way ANOVA (B) and The Student's t-test (C) were performed (*: $p<0.05$, **: $p<0.01$, ***: $p<0.001$).

4.4.3 Nrf2 is required for IGF-1-mediated induction of the mitophagy receptor BNIP3

To test whether Nrf2 is required for IGF-1-mediated induction of BNIP3, Nrf2 was suppressed with siRNA in MCF-7 and DU145 cells. This caused significantly impaired BNIP3 induction by IGF-1, implicating Nrf2 in the IGF-1-BNIP3 axis (Fig. 4.3.A). A similar result was observed with BNIP3 transcription, because although IGF-1 induced expression of both Nrf2 and BNIP3 mRNA in MCF-7 cells transfected with a control siRNA, Nrf2 suppression resulted in loss of IGF-1-mediated

BNIP3 induction (Fig. 4.3.B). These results demonstrate that Nrf2 is required for induction of BNIP3 in response to IGF-1.

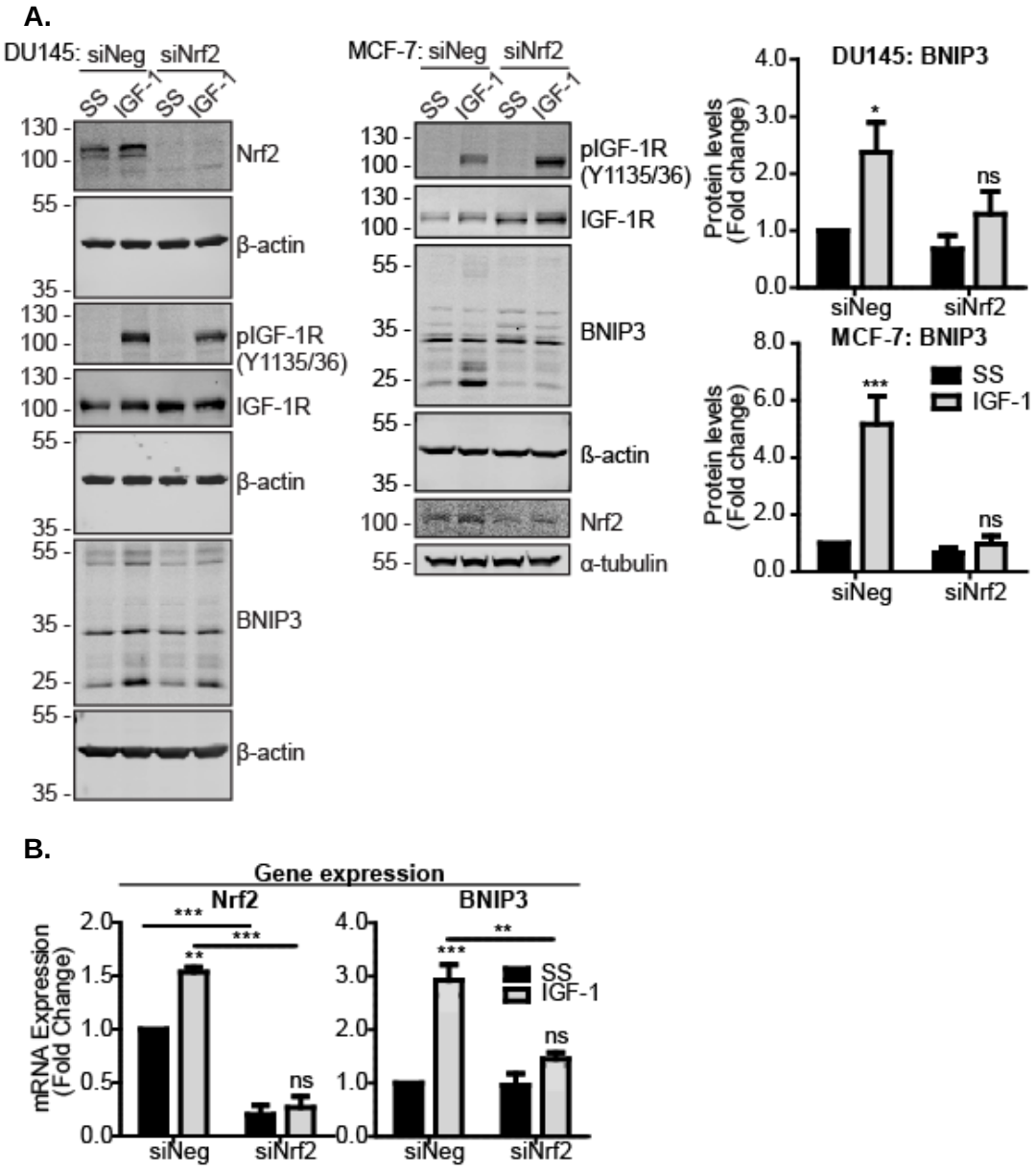

Figure 4.3 IGF-1-mediated induction of BNIP3 is dependent on Nrf2.

A. Western blot showing levels of Nrf2 and BNIP3 in MCF-7 and DU145 cells that were transfected with a control siRNA or siNrf2. At 48h post transfection cells were serum-starved for 4h prior to addition of IGF-1 (10ng/ml) for 20h. Protein levels were normalised to β-actin and presented as fold change relative to the control sample set to a value of 1. **B.** Gene expression levels of Nrf2 and BNIP3 in MCF-7 cells transfected with a control siRNA or siNrf2 measured by RQ-PCR. 48h post transfection, the cells were serum-starved for 4h prior to addition of IGF-1 at 10ng/ml for 20h prior to RNA extraction. Gene expression levels were normalised to the housekeeping gene UBC and presented as fold-change relative to control conditions set at a value of 1. Results are presented as mean ± SEM from three independent experiments. For statistical analysis, two-way ANOVAs were performed (*: $p<0.05$, **: $p<0.01$, ***: $p<0.001$).

4.4.4 IGF-1 induces BNIP3 through an inhibitory phosphorylation of GSK-3β

Next it was investigated how the IGF-1 signaling pathway intersects with induction of Nrf2 expression and activity. Nrf2 protein stability, and thereby its activity, is tightly regulated in cells through inhibitory cytoplasmic protein complexes that may include KEAP1 or GSK-3β (Kansanen et al., 2013, Chowdhry et al., 2013, Tebay et al., 2015), resulting in degradation of Nrf2. IGF-1-stimulated activation of AKT via PI 3-K can mediate an inhibitory phosphorylation on serine 9 in GSK-3β (Sutherland et al., 1993), so we next tested, whether IGF-1 activates Nrf2 by inhibiting GSK-3β-mediated Nrf2 degradation. As expected, IGF-1 enhanced S9 phosphorylation on GSK-3β in MCF-7 cells in a PI 3-K-dependent manner, because PI 3-K inhibition with LY294002 impaired this IGF-1-mediated phosphorylation (Fig. 4.4.A). Moreover, pharmacological inhibition of GSK-3α/β with SB415286 in control medium resulted in higher BNIP3 protein levels in DU145 and MCF-7 cells (Fig. 4.4.B), although the induction appeared to be transient in MCF-7 cells.

Importantly, SB415286 did not alter the activity of mTORC1 as indicated by maintenance of p-p70 S6 kinase (T371) levels, nor did it cause a significant reduction in p62/sequestosome (Fig. 4.4.B) 1 levels, suggesting that general autophagy is unaffected. Similarly, DU145 and MCF-7 cells (Fig. 4.4.C) exposed to LiCl, a known inhibitor of GSK-3β and inducer of Nrf2 (Stambolic et al., 1996, Salazar et al., 2006), exhibited increased BNIP3 expression without associated induction of general autophagy. Thus, these data show that inhibition of GSK-3β may selectively activate BNIP3 and potentially induce BNIP3-mediated mitophagy.

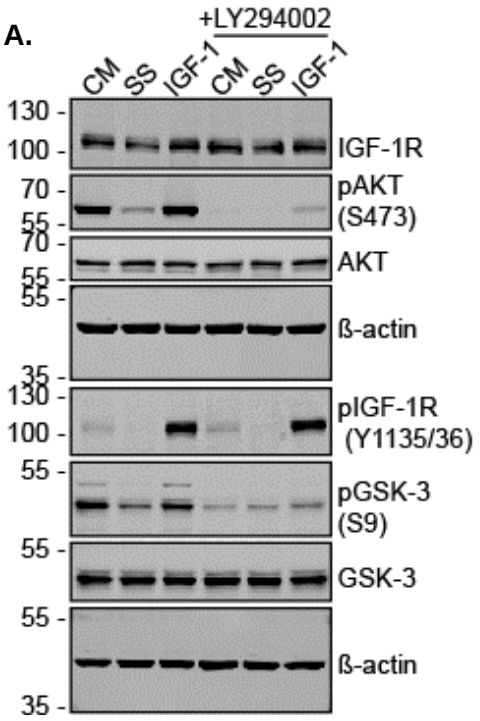

Figure 4.4 IGF-1 phosphorylates GSK-3β on S9, and inhibition of GSK-3β causes induction of BNIP3 with no associated induction of general autophagy.

A. Western blot of MCF-7 cells showing levels of AKT phosphorylated on S473 and GSK-3β phosphorylated on S9. Cells were serum-starved for 4h prior to stimulation with IGF-1 (10ng/ml) for 4h in the absence or presence of the PI 3-K inhibitor LY294002, which was added 30 min prior to stimulation. The experiment was repeated three times, and a representative blot is shown.

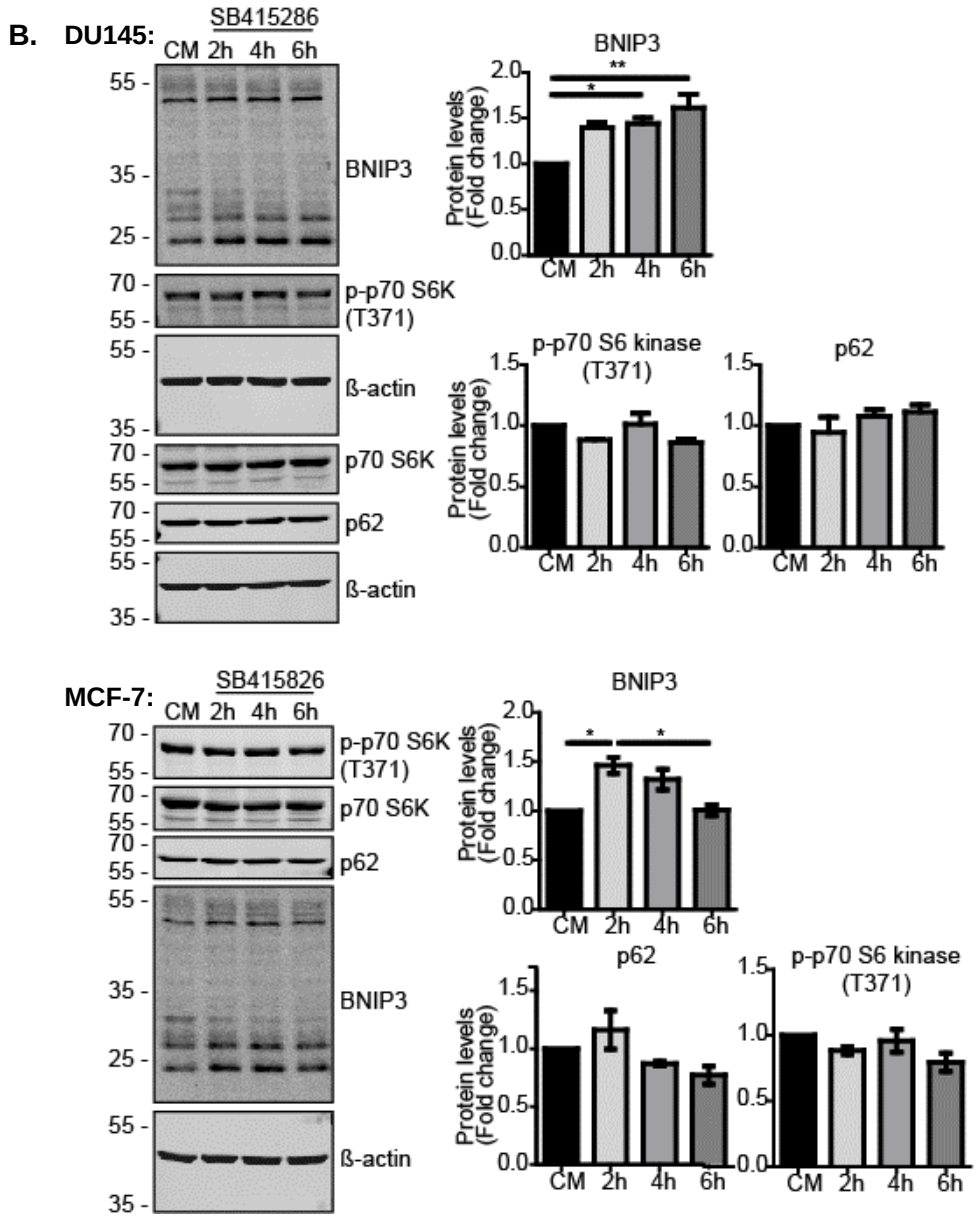

4.4.B. Western blot showing levels of Nrf2, BNIP3, p62 and p-p70 S6 kinase (T371) in DU145 and MCF-7 cells. Cells were cultured in complete medium in the presence or absence of 30μM SB415286 for 2, 4 or 6h.

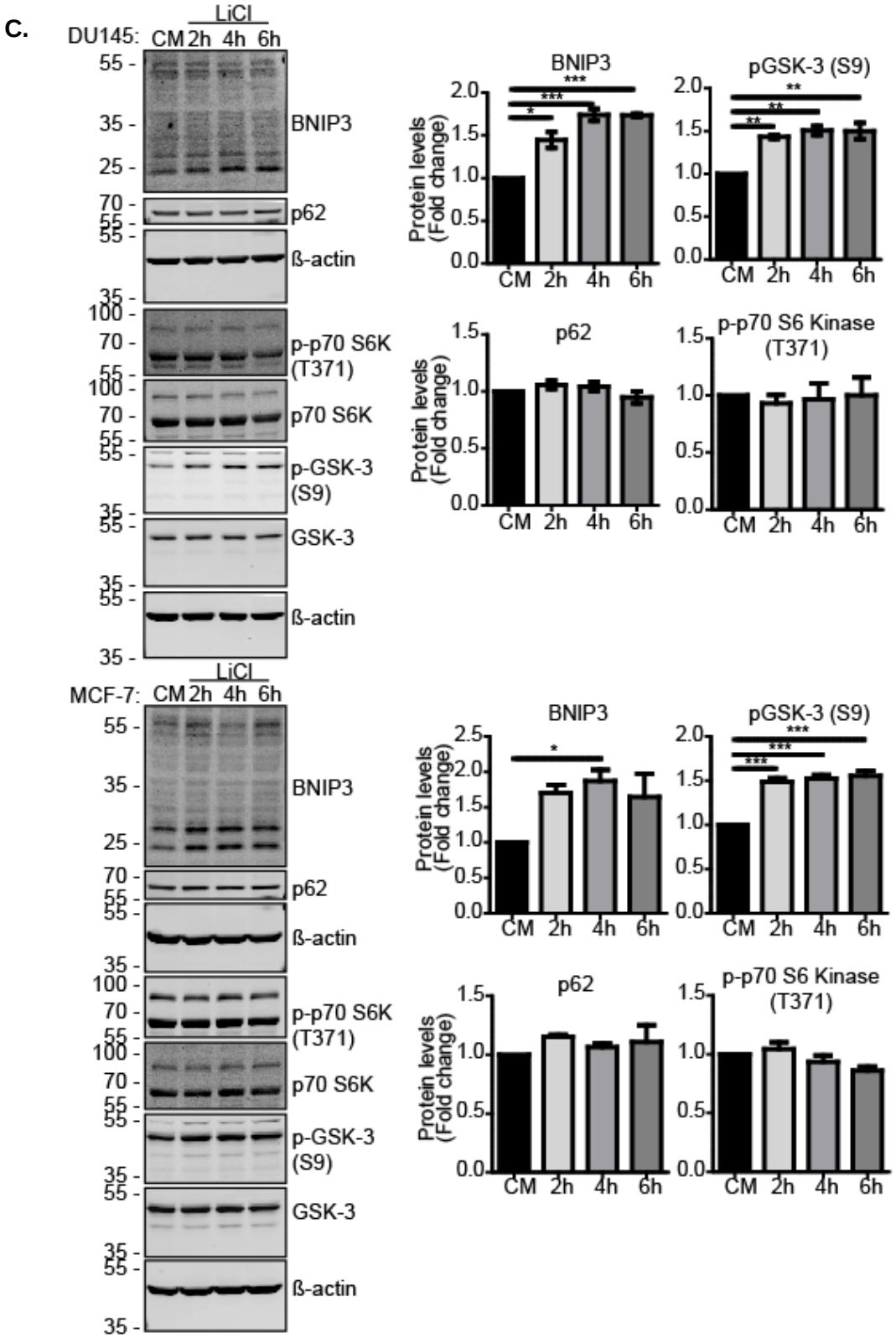

4.4.C. Western blots showing levels of BNIP3, pGSK-3β (S9), p62 and p-p70 S6K in DU145 and MCF-7 cells. Cells were cultured in complete medium in the absence or presence of 10mM LiCl for 2, 4 or 6h. Protein levels were normalised to β-actin and presented as fold change relative to the control sample set to a value of 1. Results are presented as mean ± SEM from three independent experiments. For statistical analysis, one-way ANOVAs were performed (*: $p<0.05$, **: $p<0.01$, ***: $p<0.001$).

4.4.5 Ectopic expression of KEAP1 does not affect the induction of BNIP3 in response to IGF-1 and KEAP1 is not differentially expressed in R- and R+ cells

It was also tested, whether activity of the negative Nrf2 regulator KEAP1 was implicated in IGF-1-mediated BNIP3 induction. Ectopic expression of KEAP1 in either DU145 or MCF-7 cells (Fig. 4.5.A) did not significantly alter the induction of BNIP3, indicating that IGF-1 effects on Nrf2 activity are independent of KEAP1. It is possible that the IGF-1-induced accumulation of sequestosome 1/p62 that occurs due to autophagy inhibition (Korolchuk et al., 2009) and is evident in Figure 4.5.A, could impair KEAP1 inhibition of Nrf2, because p62 competes with KEAP1 for binding to Nrf2 (Komatsu et al., 2010). Such effects would indirectly enhance Nrf2 stabilization. Furthermore, there was no significant difference in expression levels of KEAP1 between R- and R+ cells (Fig. 4.5.B), and levels of the known Nrf2 target genes Glutamate-Cysteine Ligase Catalytic Subunit (GCLC), Heme Oxygenase 1 (HO1) and Nuclear Respiratory Factor 1 (NRF1) were not significantly affected by KEAP1 overexpression in complete medium in DU145 or MCF-7 cells, except for a slight reduction observed in GCLC levels in the MCF-7 cells (Fig. 4.5.C).

Overall, these data indicate that IGF-1 signaling induces Nrf2 expression and protein stabilization through PI 3-K/AKT-mediated phosphorylation of GSK-3β on S9, which prevents GSK-3β-mediated Nrf2 degradation, while KEAP1 appears to have no significant impact on the IGF-1-induced effects on Nrf2 activity.

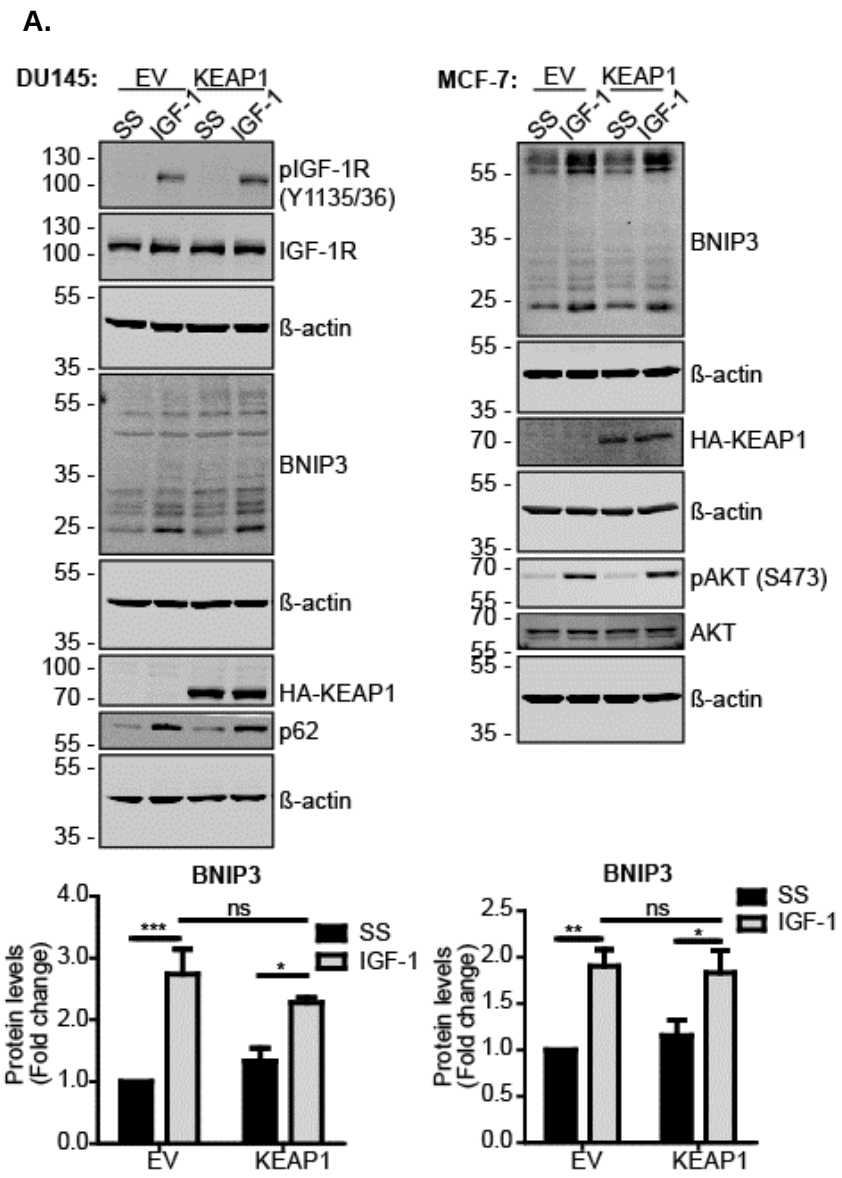

Figure 4.5 Ectopic KEAP1 does not affect IGF-1-mediated BNIP3 induction and does not significantly affect Nrf2 activity in complete media conditions.

A. Western blot of DU145 and MCF-7 cells transiently transfected with pcDNA3 EV or pcDNA3-HA2-KEAP1. The cells were serum-starved for 4h prior to stimulation with IGF-1 (10ng/ml) for 20h. Protein levels were normalised to β-actin and presented as fold change relative to the control sample set to a value of 1.

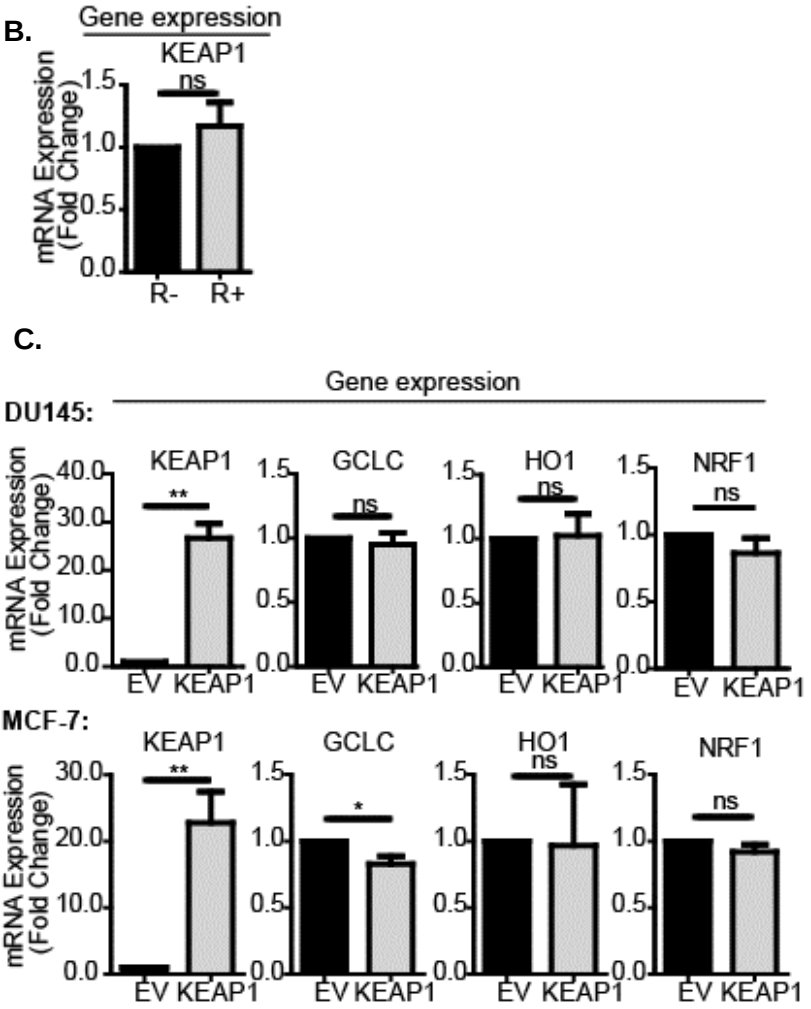

4.5.B. KEAP1 expression levels in R- and R+ cells in control media measured by RT-qPCR. **C**. mRNA expression levels of KEAP1 and Nrf2 target genes, GCLC, HO1 and NRF1 in DU145 and MCF-7 cells transfected with pcDNA3.1 empty vector or pcDNA3.1-HA2-KEAP1 for 48h and cultured in complete medium. mRNA expression levels were measured by RT-qPCR. Gene expression levels were normalised to the housekeeping gene UBC (human cell lines) or β-actin (MEFs) and presented as fold change relative to control conditions set at a value of 1. Results are presented as mean ± SEM from three independent experiments. For statistical analysis, two-way ANOVAs (A) and the Student's t-test (B-C) were performed (*: $p<0.05$, **: $p<0.01$, ***: $p<0.001$).

4.4.6 IGF-1 induces HIF-1α under normoxic conditions in cancer cells through an axis dependent on Nrf2

To further investigate how Nrf2 mediates induction of BNIP3 in response to IGF-1, we asked whether other downstream transcription factors are involved in the Nrf2-dependent induction of BNIP3. It has been shown that HIF-1α induces BNIP3, and HIF-1α binding sites in the BNIP3 promoter have been identified (Bellot et al., 2009,

Peng et al., 2019). Furthermore, inhibition of HIF-1α impairs IGF-1-mediated BNIP3 induction, implicating HIF-1α in this pathway (Lyons et al., 2017). Silencing of Nrf2 has been linked to impaired HIF-1α activity in breast cancer (Lee et al., 2019), so Nrf2 may regulate HIF-1α expression and/or function. Therefore, HIF-1α levels were investigated under conditions of Nrf2 suppression in MCF-7 and DU145 cells.

Interestingly, IGF-1 induced HIF-1α in MCF-7 cells transfected with a control siRNA under conditions of normal oxygen levels, suggesting a role for HIF-1α in this pathway that is not dependent on hypoxia. This induction was significantly impaired, when Nrf2 was suppressed (Fig. 4.6). A similar effect of Nrf2 suppression was observed in DU145 cells. Although HIF-1α induction in response to IGF-1 was approximately three-fold, this did not reach statistical significance. Thus, IGF-1 induces both HIF-1α and BNIP3 in a Nrf2-dependent manner, suggesting Nrf2 induces BNIP3 through HIF-1α.

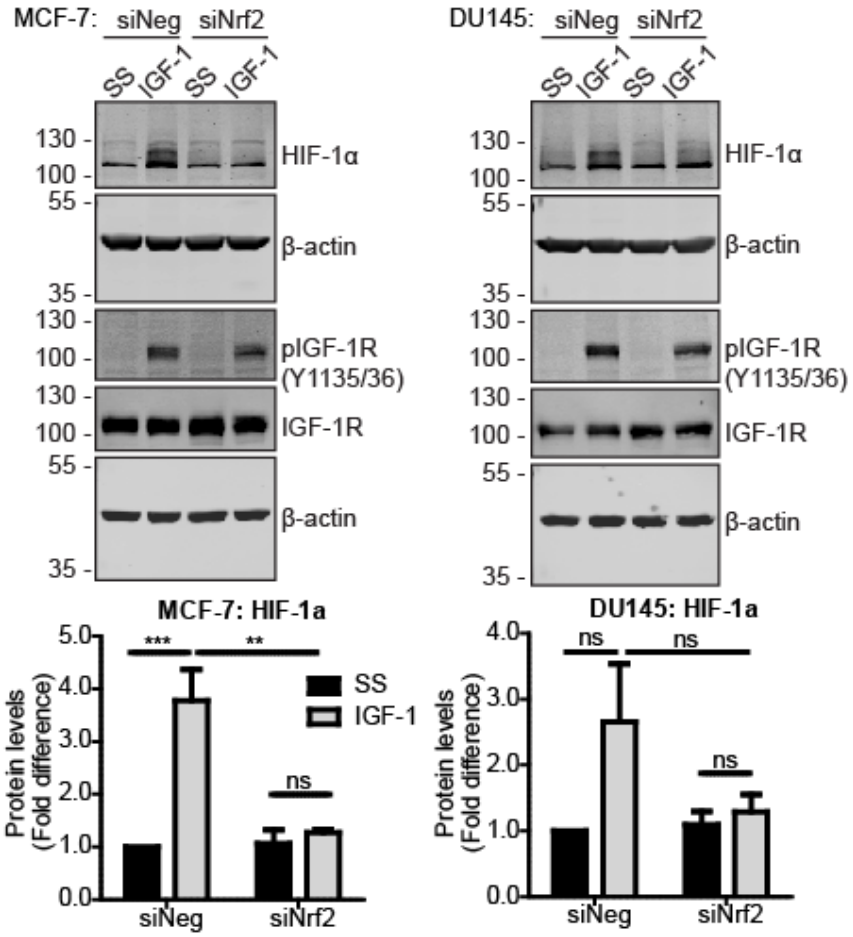

Figure 4.6 IGF-1 induces HIF-1α in a Nrf2-dependent way.

Western blot showing levels of HIF-1α and IGF-1R in MCF-7 and DU145 cells transfected with a control siRNA or siNrf2. At 48h post transfection, cells were serum-starved for 4h prior to stimulation with IGF-1 (10ng/ml) for 20h. Protein levels were normalised to β-actin and presented as fold change relative to the control sample set to a value of 1. Results are presented as mean ± SEM from three independent experiments. For statistical analysis, two-way ANOVAs were performed (*: $p<0.05$, **: $p<0.01$, ***: $p<0.001$).

4.4.7 The IGF-1-Nrf2-BNIP3 pathway regulates mitochondrial dynamics

The next objective was to study the effects of Nrf2 activity on mitochondrial dynamics and mitophagy/autophagy. It was observed that Nrf2 suppression in MCF-7 cells had a strong effect on mitochondrial morphology, as shown by immunofluorescence staining with the mitochondrial marker Translocase of Outer Mitochondrial Membrane 20 (TOM20). Cells in which Nrf2 was suppressed exhibited more fused and elongated mitochondria than control cells (Fig. 4.7.A). The efficiency of the Nrf2

suppression was assessed by RT-qPCR, alongside expression levels of the mitochondrial fission mediator Dynamin-Related Protein 1 (DRP1), which was significantly reduced (Fig. 4.7.B), suggesting the mitochondrial elongation observed may be due to reduced mitochondrial fission. Similarly, suppression of BNIP3 resulted in mitochondrial elongation (Fig. 4.7.C). Since accumulation of elongated mitochondria could be due to reduced mitochondrial fission or enhanced mitochondrial fusion, we proceeded to analyse expression levels of several known regulators of mitochondrial dynamics. It was observed that BNIP3 suppression also resulted in lower levels of DRP1 with no change in Mitofusin 1 or Mitofusin 2 (MFN1/MFN2) levels (Fig. 4.7.D).

DRP1 is known to be recruited by BNIP3 to facilitate mitophagy (Lee et al., 2011, Burman et al., 2017). The results presented here indicate that impaired IGF-1 signalling leads to reduced mitochondrial fission and potentially impaired mitochondrial turnover as a result of mitochondrial elongation. Thus, the IGF-1-Nrf2-BNIP3 signalling pathway is required for regulation of mitochondrial morphology and dynamics, potentially affecting cell capacity to induce mitochondrial clearance. Interestingly, R- cells also exhibited more elongated mitochondria than R+ cells, indicating a requirement for IGF-1 signals in mitochondrial dynamics (Fig. 4.7.E).

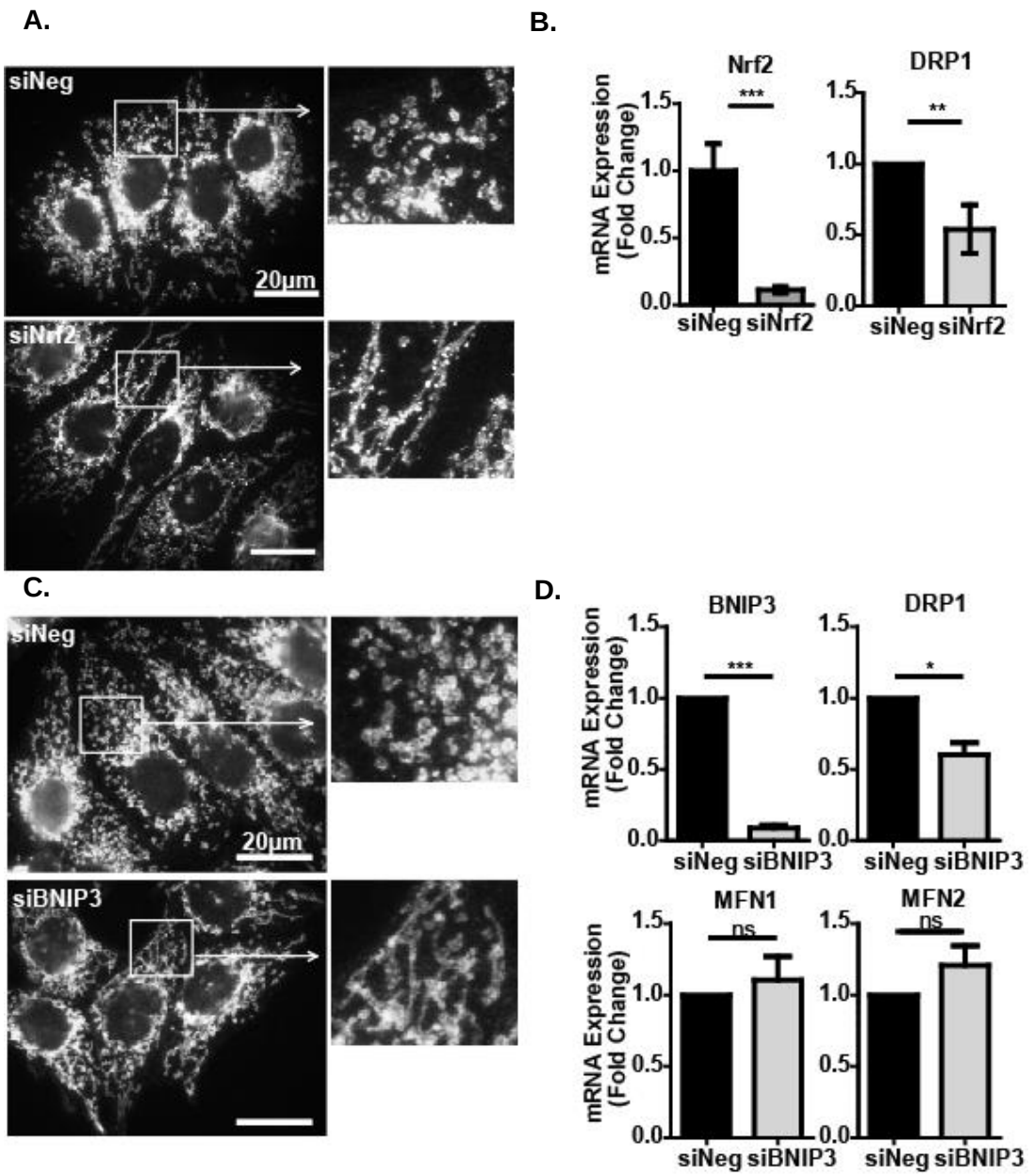

Figure 4.7 Suppression of Nrf2, BNIP3 or the IGF-1R pathway causes mitochondrial elongation and is associated with downregulation of DRP1 expression levels.

A. Immunofluorescence showing TOM20 in MCF-7 cells transfected with a control siRNA or siNrf2 and cultured in complete medium for 72h. Images were acquired on a Nikon Eclipse E600 microscope using a 100x objective. **B**. Gene expression levels of Nrf2 in response to transfection with a control siRNA or siNrf2 in MCF-7 cells measured by RT-qPCR. **C**. Immunofluorescence showing TOM20 in MCF-7 cells transfected with a control siRNA or siBNIP3 and cultured in complete medium for 72h. Images were acquired on a Nikon Eclipse E600 microscope using a 100x objective. **D**. Gene expression levels of BNIP3 and the mitochondria dynamics regulatory genes DRP1, MFN1 and MFN2 measured by RT-qPCR in MCF-7 cells transfected with a control siRNA or siBNIP3 for 72h. Gene expression levels were normalised to the housekeeping gene UBC and presented as fold change relative to control conditions set at a value of 1. Results are presented as mean ± SEM from three independent experiments. For statistical analysis, the Student's t-test was performed (*: $p<0.05$, **: $p<0.01$, ***: $p<0.001$).

E.

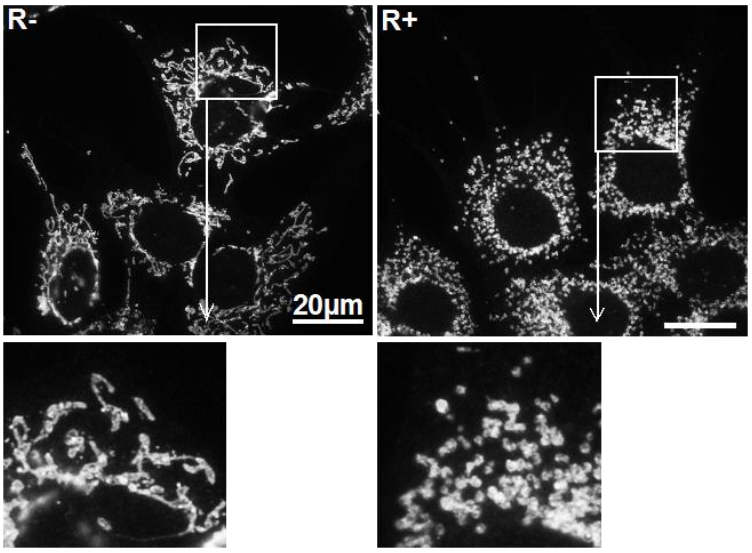

4.7.E. Immunofluorescence showing TOM20 in R- and R+ cells cultured in complete medium. Images were acquired on an OLYMPUS FV1000 Confocal Laser Scanning Biological Microscope with a 100x objective. All experiments were repeated three times, and representative images are shown.

4.4.8 Lack of IGF-1R signalling renders MEFs more sensitive to nutrient or mitochondrial stress

Next, we sought to investigate the physiological relevance of IGF-1 signalling in mitophagy induction during cellular stress responses. To test this, R- and R+ cells were exposed to serum-starvation to induce metabolic stress, or to either the iron chelator deferiprone (DFP) or the mitochondrial uncoupler carbonyl cyanide m-chlorophenyl hydrazine (CCCP) to induce mitochondrial stress. Interestingly, DFP induced BNIP3 expression in both cell lines, suggesting that DFP induces mitophagy via BNIP3. However, DFP-induced BNIP3 expression was clearly more evident in R+ cells, than in R- cells. Furthermore, R- cells exhibited a significantly lower tolerance to serum-starvation and DFP, than R+ cells, and accumulated higher levels of cleaved caspase 3 indicative of apoptosis (Fig. 4.8). These results show that loss of IGF-1R signalling results in impaired cellular stress responses leading to cell death.

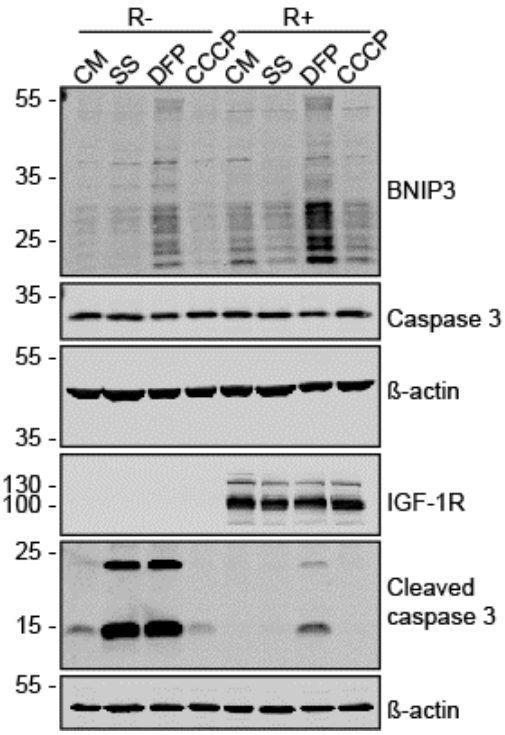

Figure 4.8 IGF-1R KO MEFS display impaired survival under conditions of nutrient or mitochondrial stress compared to these cells reconstituted with IGF-1R.

Western blot showing BNIP3 and cleaved caspase 3 levels in complete medium, serum-starvation or the addition of DFP (1mM) or CCCP (10μM) to complete medium for 24h. Three independent experiments were carried out, and a representative blot is shown.

4.4.9 IGF-1 regulates cellular capacity for autophagosomal turnover in response to metabolic and mitochondrial stress

To get a more complete picture of the effects of IGF-1 signalling on cellular autophagy including mitophagy, the levels of autophagosomal turnover were assessed, by measuring autophagic flux in R- and R+ cells exposed to stress. Autophagic flux was quantified as described in Chapter 3 (section 3.3.6). As can be seen in Figure 4.9.A, R- cells display higher levels of autophagosomal turnover than R+ cells in control cultures. However, when the cells were exposed to serum-starvation or DFP, R+ cells exhibited a higher capacity to induce autophagosome turnover, suggesting that IGF-1 signalling promotes cellular capacity for both general autophagy and mitophagy in response to stress (Fig. 4.9.B).

Taken together, these data indicate that IGF-1 signalling supports cell survival in response to autophagic and mitophagic stresses, and that this is mediated by increasing the capacity of the cell to induce autophagosome turnover. IGF-1-mediated induction of BNIP3 in a Nrf2-dependent manner may, therefore, be a component of an overall cell survival and stress protective response.

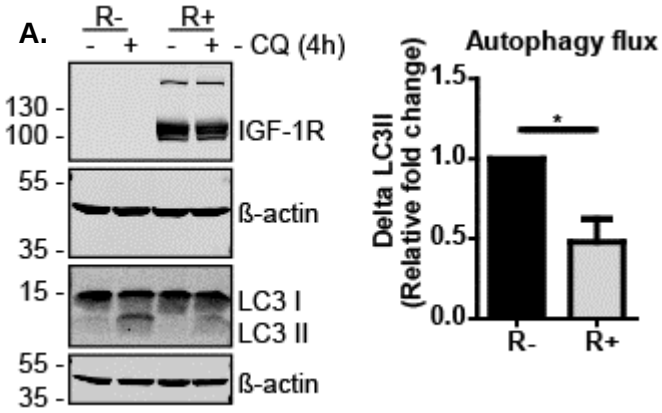

Figure 4.9 R- cells exhibit higher levels of autophagic flux under complete medium conditions but impaired induction of autophagosome turnover in response to nutrient deprivation or mitochondrial stress compared to R+ cells.

A. Western blots showing LC3 levels in R- and R+ cells. Cells were cultured in complete medium in the absence or presence of chloroquine (CQ, 50μM) added 4h before harvesting. Autophagic flux was calculated as ΔLC3II for each condition in the presence and absence of CQ and presented as fold change relative to the R- sample.

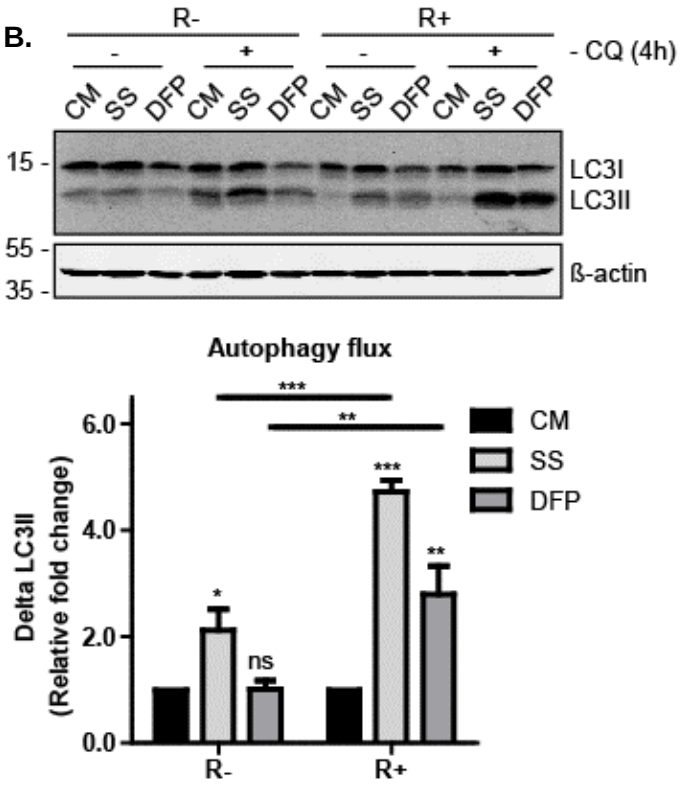

4.9.B. Western blot showing LC3 levels in R- and R+ cells cultured in complete medium with or without DFP (1mM) or in response to serum-starvation for 24h. CQ (50μM) was added to the indicated cultures for the last 4h before harvesting. Protein levels were normalised to β-actin and presented as fold change relative to the control sample set to a value of 1. Results are presented as mean ± SEM from three independent experiments. For statistical analysis, the Student's t-test (A) or a two-way ANOVA (B) was performed (*: $p<0.05$, **: $p<0.01$, ***: $p<0.001$).

4.5 Discussion

IGF-1 signalling is essential for growth, promotes tumourigenesis, cancer cell survival and proliferation, and it also has a highly conserved and potent effect on mitochondrial function and homeostasis (Denduluri et al., 2015, Sádaba et al., 2016, Hakuno and Takahashi, 2018). Loss of IGF-1 signals leads to impaired mitochondrial capacity for ATP production and antioxidant capacity. However, these effects can be reversed with IGF-1 therapy, suggesting that IGF-1 signalling is mitochondria protective (Sádaba et al., 2016).

In this study, it was established that IGF-1 mediates a conserved signal through Nrf2 for induction of BNIP3 expression in cancer cells and MEFs. Nrf2 has a well described cytoprotective function in antioxidant stress response and detoxification. In cancer cells, this may be exploited to allow cells to better survive in stressful environments and facilitate the development of chemoresistance (Wang et al., 2008, Rojo de la Vega et al., 2018). We observed that IGF-1-mediated induction of BNIP3 (Lyons et al., 2017) can occur through HIF-1α which is induced by Nrf2 (Zhang et al., 2018, Lee et al., 2019), suggesting that BNIP3 may be a secondary, rather than a direct, Nrf2 target gene.

Mitophagy is important for the overall maintenance of cellular health, and mitophagy dysregulation is common in many diseases (Um and Yun, 2017). Mitophagy is also a key event in cell differentiation, which requires careful regulation of mitochondrial mass and distribution to ensure that the mitochondrial function of the cell matches the specific cellular requirements concerning energy production and reactive oxygen species clearance, for example (Esteban-Martinez and Boya, 2017, Fu et al., 2019). BNIP3 was found to enhance mitochondrial function under hypoxic conditions in stem cells and to facilitate differentiation of epidermal keratinocytes (Lee et al., 2017, Moriyama et al., 2017). However, this central role of mitophagy in the differentiation of various cell types enables mitophagic processes to induce de-differentiation of otherwise fully differentiated cells in cancer progression, allowing cancer cells to acquire stemness features (Reya et al., 2001). Interestingly, the IGF-1 signalling pathway has been proposed to maintain both stem-like qualities and to enhance cell survival during cell differentiation (Huat et al., 2014, Teng et al., 2018).

Our finding suggest that IGF-1 signals are essential for maintenance of mitochondrial homeostasis. Suppression of either Nrf2 or BNIP3 in MCF-7 cells

caused a dramatically altered mitochondrial appearance with more fused and elongated mitochondria, a morphological difference that was also evident in R- cells compared to R+ cells. Suppression of BNIP3 was also associated with reduced expression of the mitochondrial fission mediator DRP1, which is known to be recruited by BNIP3 to facilitate mitophagy (Lee et al., 2011). Thus, IGF-induced BNIP3 can regulate mitochondrial dynamics. Interestingly, the punctate mitochondria and higher levels of DRP1 observed in control MCF-7 cells compared to cells with suppressed Nrf2 or BNIP3 have also been described as characteristics of stem cells (Fu et al., 2019).

BNIP3 is a protein of at least dual function with the ability to promote cell death under certain conditions and to induce mitophagy particularly under hypoxic conditions (Zhang and Ney, 2009). It has also been implicated in regulating cell proliferation (Singh et al., 2018). Since, IGF-1 induces BNIP3 in serum-deprived cells, but is also known to protect against apoptosis, it is likely that BNIP3 facilitates mitophagy under these conditions. This conclusion is supported by our observations regarding autophagic flux in R- and R+ cells. Higher basal levels of autophagic flux were present in R- cells compared to R+ cells, as could be expected due to activation of mTORC1 by IGF-1 leading to inhibition of general autophagy (Jung et al., 2010). However, R+ cells induced autophagosomal turnover in response to either metabolic or mitochondrial stress significantly more potently than R- cells, suggesting that IGF-1 signalling increases the capacity of cells to induce both autophagy and mitophagy in response to cellular stresses. A striking difference between R- and R+ cells was also observed in terms of tolerance to either serum-starvation or DFP. R+ cells clearly displayed lower levels of apoptosis under these conditions than R- cells, suggesting that the IGF-1 pathway enhances cellular survival under such stresses. The elevated

levels of BNIP3 in R+ cells would be expected to mediate efficient mitophagic clearance in response to DFP.

BNIP3 has previously been shown to enhance cell survival under conditions of nutrient deprivation (Macher-Goeppinger et al., 2017), which may contribute to the increased survival of R+ cells in serum-deprived culture conditions observed here. It is also interesting that neither R- nor R+ cells exhibited cell death in response to CCCP, which is known to upregulate mitophagy through the PINK1-Parkin-mediated pathway (Matsuda et al., 2010, Kondapalli et al., 2012), despite an observed CCCP-mediated induction of PINK1 (Fig. 3.6.A). This suggests that R- cells that lack IGF-1 signaling may be uniquely impaired in BNIP3-mediated mitophagy. Therefore, although alternative functions of BNIP3 cannot yet be excluded, we propose that BNIP3 expression levels are central to the dramatic differences observed in autophagic flux and stress tolerance between R- and R+ cells in response to either serum-starvation or DFP.

In conclusion, this study demonstrates that IGF-1 signalling has an essential function in mitochondrial dynamics and turnover through the activity of Nrf2 and BNIP3. This mitochondria-protective role may be a key vulnerability of this essential growth pathway and offer potential for novel therapeutic intervention in cancer.

Chapter 5. IGF-1 Signalling Induces BNIP3-Specific Mitophagy but Reduces Total Cellular Mitophagy

5.1 Abstract

While we established that IGF-1 induces both mitochondrial biogenesis and the mitophagy receptor BNIP3 in a coordinated manner to maintain mitochondrial health and function (Lyons et al., 2017), it remains to be established whether IGF-1 directly triggers mitophagy in cancer cells. Here, we developed a fluorescent probe with which to study mitophagy in live cells. This VLCAD(1-40)-mCherry-EGFP probe enables both visualisation and quantification of mitophagy in response to various stimuli. In MCF-7 cells expressing this probe, 20-30% of cells exhibited active mitophagy in complete medium conditions, while in serum-starvation, hypoxia or the presence of the mitochondrial stressors DFP and CCCP the percentage of mitophagy-positive cells increased. In serum-starved cells, the addition of IGF-1 reduced overall levels of mitophagy. However, by analysing the colocalisation of BNIP3 and LC3, which indicates BNIP3-specific mitophagy, it was observed that IGF-1 increased BNIP3 and LC3 interaction, suggesting that even when cells are deprived of serum, IGF-1 can induce a basal level of mitophagy through BNIP3. IGF-1R null mouse embryonic fibroblasts (MEFs) named R- cells exhibited a similar capacity for mitophagy to IGF-1R-expressing (R+) cells. However, in response to mitochondrial stress, mitophagic vesicles were observed to accumulate over time in R- cells and this was associated with cell death. In contrast, R+ cells apparently eliminated mitochondria efficiently and exhibited less cell death than R- cells. Thus, we propose that IGF-1 maintains a low level of mitophagy to prevent accumulation of damaged mitochondria, while enabling cells to control total autophagy levels to enhance cell survival.

5.2 Introduction

Detection and quantification of mitophagy in cells is greatly limited by the available tools and technologies. For *in vitro* studies, these include transmission electron microscopy (TEM) that allows visualisation of mitochondria contained within autophagosomes, western blotting analysis of mitochondrial markers and mitophagy/autophagy mediators, flow cytometric analysis of mitochondrial mass using mitochondrial dyes or microscopy analysis of fluorescent probes such as mt-Keima, as reviewed by Chen and colleagues (Chen et al., 2017a). TEM is still considered the superior technique, but is not widely available or easily quantifiable, unlike techniques such as flow cytometry and western blotting. However, these measurements are indirect and cannot assess mitophagy in live cells, so the scope of their interpretation is limited. Autophagosome turnover can be assessed by measuring LC3II levels, but this does not distinguish between general autophagy and mitophagy (Mauthe et al., 2018, Mizushima and Yoshimori, 2007).

Fluorescent probes have emerged as promising mitophagy detection tools because they enable specific visualisation of ongoing mitophagy using standard microscopy. Visualising the colocalisation of GFP-LC3 and mitochondrial markers is a measure of the recruitment of autophagosomes to mitochondria. GFP fluorescence, however becomes quenched within lysosomes due to low pH (Shinoda et al., 2018), and therefore, it does not allow detection of late-stage mitophagy. Mt-Keima is a probe that targets the Keima protein to the mitochondrial matrix (Katayama et al., 2011). Keima is resistant to proteases but is pH-sensitive and it undergoes a shift in excitation wavelength within lysosomes (Kogure et al., 2006, Katayama et al., 2011). This can be exploited to measure the fluorescence intensity at each wavelength to calculate a ratio between the two, which reflects mitophagy levels (Sun et al., 2017). Another

mitophagy probe was developed by Allen and colleagues. This is a tandem mCherry-GFP probe that includes a mitochondrial targeting sequence (MTS) from the outer mitochondrial membrane (OMM) protein Fis1. In this case, GFP quenching within lysosomes can be exploited because healthy mitochondria emit both red and green fluorescence to yield a yellow staining pattern. On the other hand, degrading mitochondria within lysosomes can only emit red fluorescence from the pH-insensitive mCherry tag, when the green signal becomes quenched. Thus, in cells expressing this reporter, red puncta represent mitochondria undergoing degradation (Allen et al., 2013).

The results presented in this thesis show that IGF-1 clearly induces accumulation of the BNIP3 mitophagy receptor in cells and suggest that this enhances cellular capacity for mitophagy. However, to better establish the contribution of IGF1-induced BNIP3 in mitophagy it was necessary to assess mitophagy with a reporter in living cells. Therefore, we sought to develop a mitophagy reporter by using the probe described by Allen and colleagues as a guide (Allen et al., 2013). Rather than using the OMM-targeting sequence they described, we opted to use the mitochondrial targeting sequence from the inner mitochondrial membrane (IMM) protein, very-long-chain acyl-CoA dehydrogenase (VLCAD). This, we hypothesized, would ensure sensitive detection of fully engulfed mitochondria better than an OMM targeting sequence that may be less specific. The new probe VLCAD(1-40)-mCherry-EGFP was then used to assess mitophagy levels in cancer cells and how this was affected by IGF-1 signalling, in addition to the effects of IGF-1R deficiency on mitophagy induction and clearance in MEFs.

In cancer cells, serum starvation induced mitochondrial as well as autophagic clearance, while IGF-1 inhibited both. However, IGF-1 also induced colocalisation of

EGFP-LC3 with BNIP3, suggesting that IGF-1 induces a specific mitophagic response mediated by BNIP3. Supporting a mitophagic role for BNIP3 in cancer cells, ectopic expression of wildtype (WT) BNIP3 but not a mitophagy-incompetent BNIP3 mutant enhanced mitophagy in response to mitochondrial uncoupling. Furthermore, R- cells exhibited impaired capacity to recover from mitophagic stress responses compared to R+ cells leading to cell death.

The findings demonstrate the importance of mito- and cyto-protective IGF-1 signalling in transformed cells, and also identifies a previously undescribed vulnerability in cells with impaired IGF-1 signalling.

5.3 Results

5.3.1 Design of VLCAD(1-40)-mCherry-EGFP reporter and validation of mitochondrial targeting sequence

The mitochondria-targeted tandem mCherry-GFP probe used by Allen and colleagues (Allen et al., 2013) was used as a model to design a new probe. It is likely that depending on the orientation of the probe once inserted into the OMM, some unspecific detection of mitophagy would occur, if the mCherry-GFP tandem tag is exposed to the cytosolic side of the mitochondria. To avoid such issues, an IMM targeting sequence was employed here. The IMM mitochondrial targeting sequence (MTS) from very-long-chain acyl-CoA dehydrogenase (VLCAD) (aa 1-40) has previously been used to target proteins to the mitochondria, as described for the pcDNA3-MTS-CA-c-Src-FLAG construct (Ogura et al., 2012). The sequence and functional concept of the probe is illustrated in Figure 5.1.A.

To test whether efficient mitochondrial targeting could be observed using this MTS, the pcDNA3-MTS-CA-c-Src-FLAG plasmid was transfected into MCF-7 cells,

which were counterstained with an antibody to detect the mitochondrial marker TOM20. As can be seen in Figure 5.1.B, fluorescence images of these cells demonstrated a high level of specific mitochondrial targeting of the Src-FLAG protein. This confirmed that the VLCAD sequence was appropriate for inclusion in a mitochondria-targeting probe.

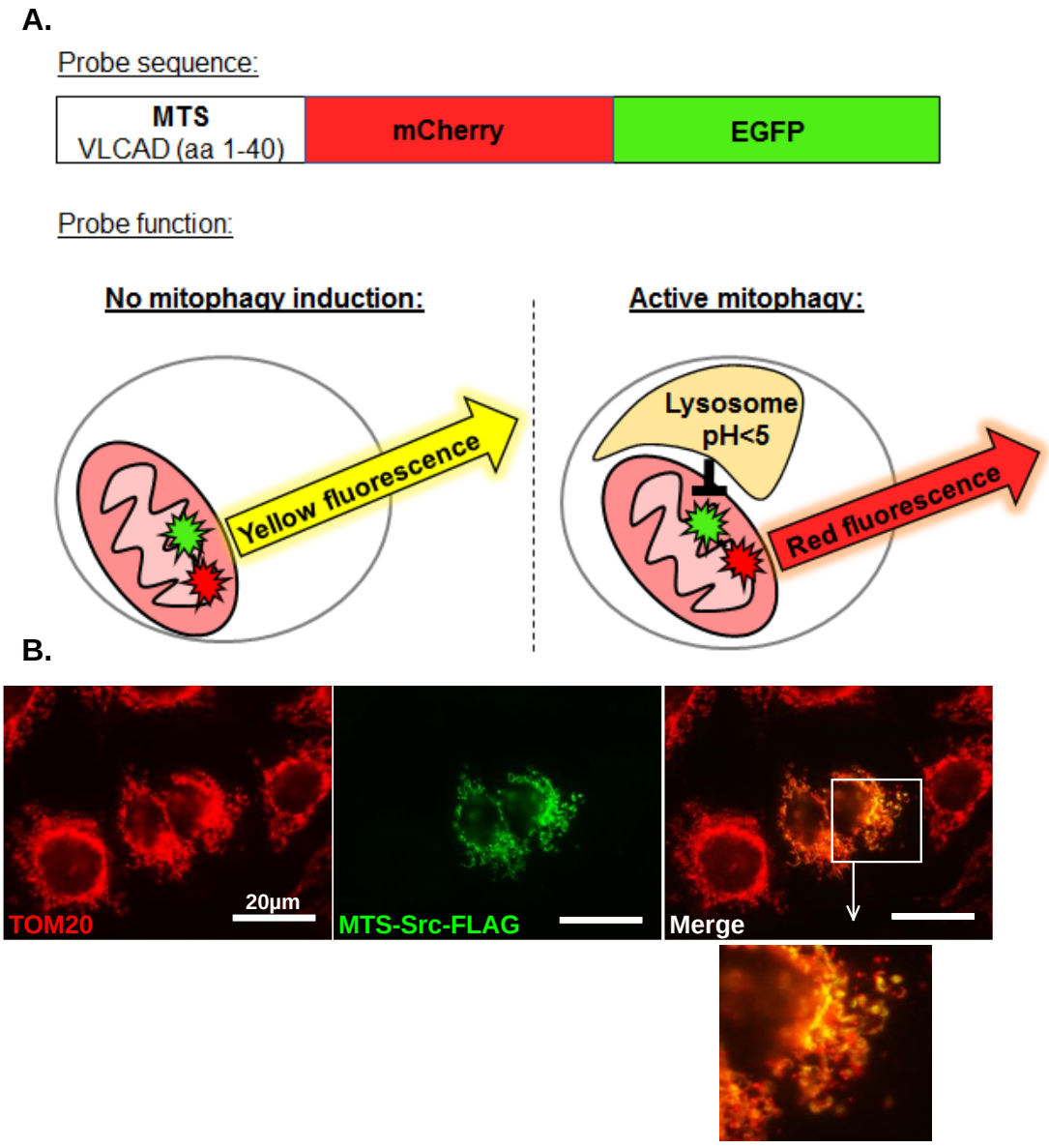

Figure 5.1 The VLCAD(1-40) mitochondrial targeting sequence efficiently targets proteins to the mitochondria.

A. Schematic illustration of the sequence and function of the VLCAD(1-40)-mCherry-EGFP probe. **B**. MCF-7 cells transiently transfected with pcDNA3-MTS-CA-c-Src-FLAG were fixed at 24h post transfection. The cells were stained with anti-TOM20 antibody and images were obtained using a Nikon Eclipse E600 microscope with a 100x objective. The experiments were performed once, and a representative image is shown.

5.3.2 Validation of mitochondrial localisation of VLCAD(1-40)-mCherry-EGFP probe

The MTS from VLCAD was then used to design the tandem probe encoding mCherry and EGFP. This pcDNA3.1-VLCAD(1-40)-mCherry-EGFP vector was synthesized by GenScript (see Chapter 2. Methods and Materials). To test the reporter, it was first transfected into U2OS cells and its localisation to mitochondria was assessed by counterstaining for TOM20. Images were acquired with a confocal microscope. Figure 5.2.A shows that both the EGFP and the mCherry tag localise predominantly to mitochondria that are labelled with TOM20.

Next, MCF-7 cells were stably transfected with the plasmid encoding the reporter, to generate the MCF-7-VLCAD(1-40)-mCherry-EGFP cell line, which was selected and maintained in medium containing neomycin/G418 (see section 3.6 in Materials and Methods). Localisation of the reporter to the mitochondria was again confirmed by counterstaining for TOM20 followed by confocal microscopy (Fig. 5.2.B).

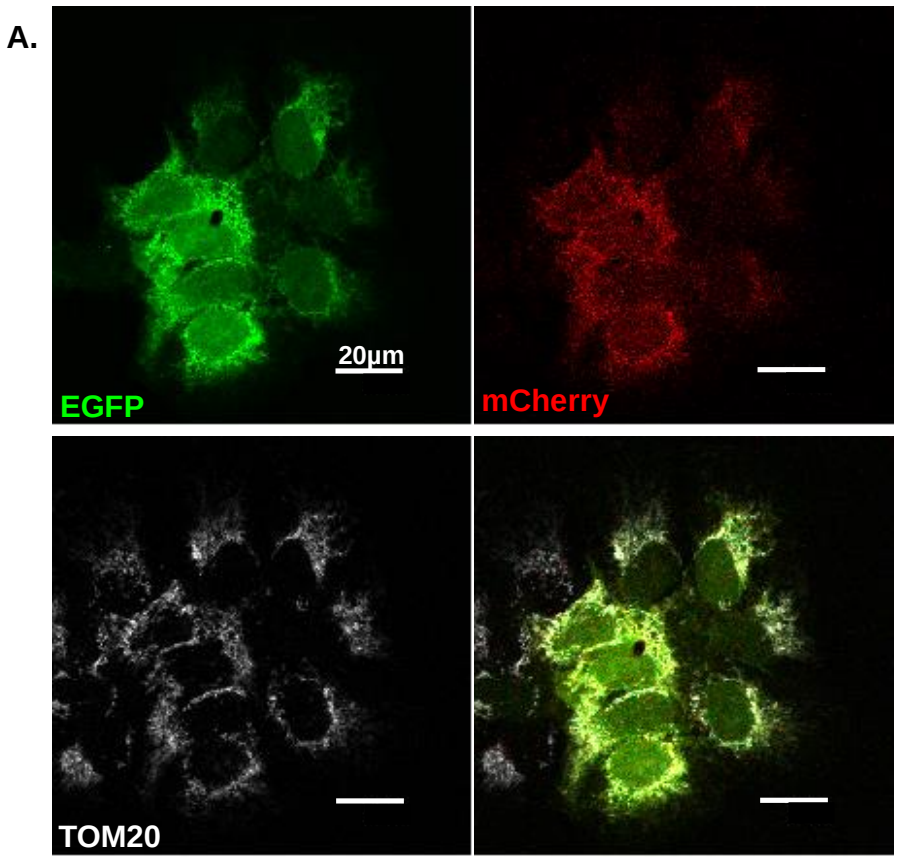

Figure 5.2 The VLCAD(1-40)-mCherry-EGFP probe localises to mitochondria in U2OS and MCF-7 cells.

A. U2OS cells were transiently transfected with the pcDNA3.1-VLCAD(1-40)-mCherry-EGFP construct. At 48h post transfection, the cells were fixed and stained with a TOM20 antibody. Images were obtained using an OLYMPUS FV1000 Confocal Laser Scanning Biological Microscope with a 100x objective.

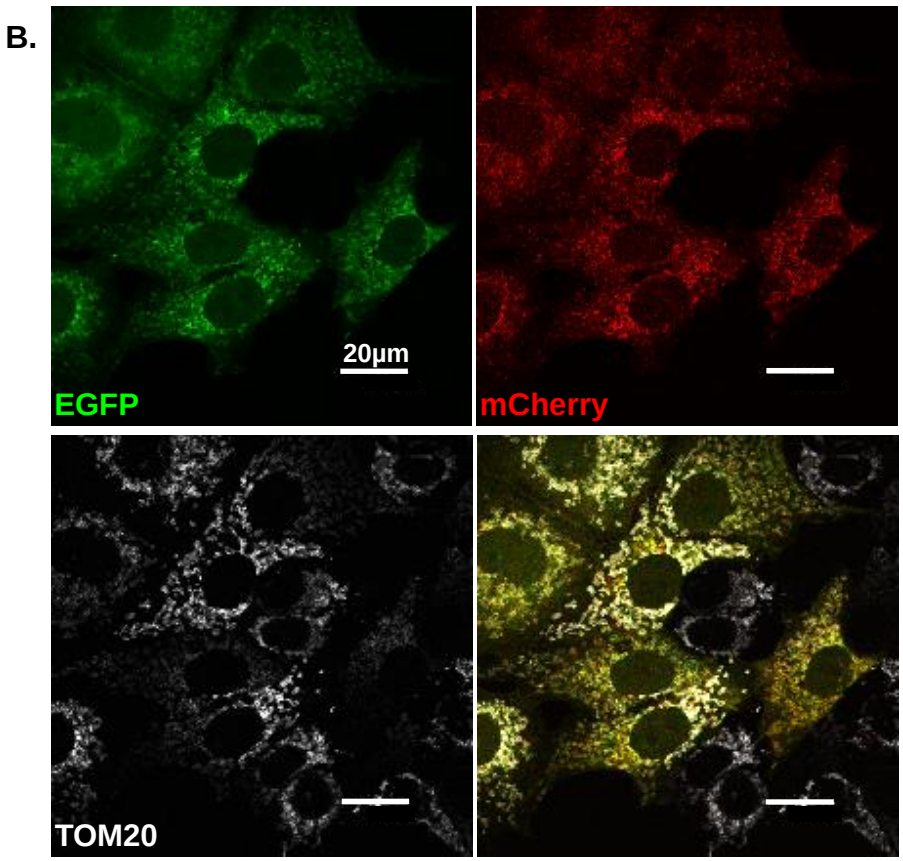

5.2.B. MCF-7 cells were transfected with the pcDNA3.1-VLCAD(1-40)-mCherry-EGFP plasmid, and a stable cell line was generated. Cells were maintained in normal growth medium with G418. Cells were fixed, stained with a TOM20 antibody, and imaged using an OLYMPUS FV1000 Confocal Laser Scanning Biological Microscope with a 100x objective. The experiments were performed once, and representative images are shown.

5.3.3 The VLCAD(1-40)-mCherry-EGFP reporter enables visualisation of mitophagy induction in response to serum-starvation, DFP or CCCP

To assess the capacity of the probe to detect mitophagy in the MCF-7-VLCAD(1-40)-mCherry-EGFP stable cell line, mitophagy was induced in several different ways including 24h serum deprivation or the addition of DFP or CCCP to cells in complete medium. The cells were fixed, and the fluorescence images captured were then assessed for presence of red-only puncta representing engulfed mitochondria undergoing lysosomal degradation. Representative images shown in Figure 5.3 demonstrate the relative low number of red puncta in complete medium conditions, and the appearance of red puncta in response to all mitophagy-inducing conditions.

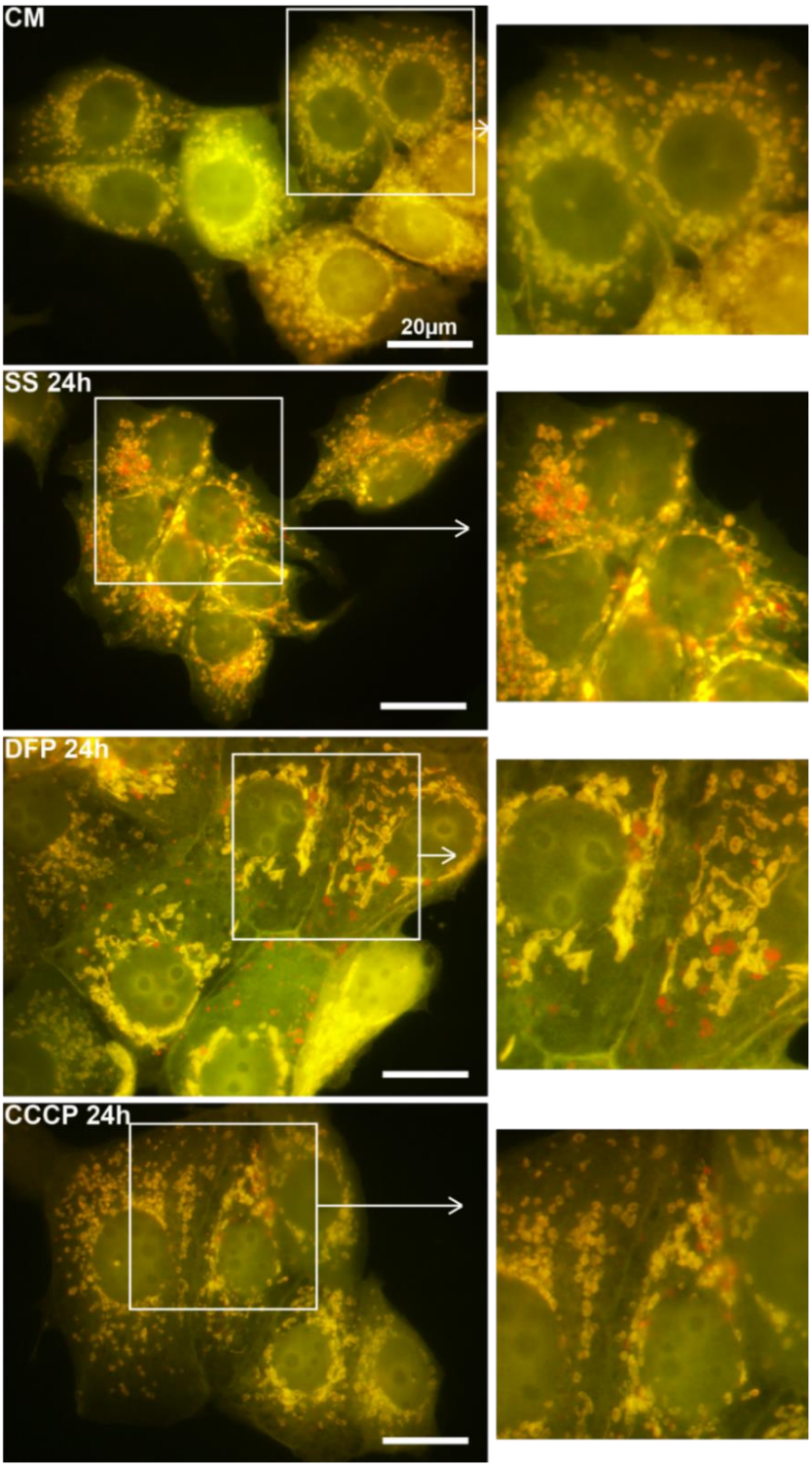

Figure 5.3 Serum deprivation, DFP or CCCP induce mitophagy in MCF-7 cells, which can be visualised with the VLCAD(1-40)-mCherry-EGFP probe.

MCF-7-VLCAD(1-40)-mCherry-EGFP cells were maintained in complete medium, exposed to DFP (1mM) or CCCP (10µM) for 24h or kept in serum-free medium for 24h. The cells were fixed, and images obtained using a Nikon Eclipse E600 microscope with a 100x objective. The experiment was performed once, and 20 fields of view were imaged per conditions. Representative images are shown.

5.3.4 The VLCAD(1-40)-mCherry-EGFP reporter detects mitophagy induction in response to hypoxia

The MCF-7-VLCAD(1-40)-mCherry-EGFP cells were next exposed to hypoxia, which is known to induce mitophagy (Zhang et al., 2008, Liu et al., 2012). Cells in normal culture conditions were compared to cells exposed to hypoxia (<1% O_2) for 6h prior to fixation. Figure 5.4.A shows the appearance of red puncta under hypoxic conditions compared to non-hypoxic conditions. In this case, some cells presented with larger and more prominent red puncta than was observed in Figure 5.3.A. This indicates that hypoxia is a more potent inducer of mitochondrial clearance than the other mitophagy stimuli tested, or perhaps that mitochondrial clearance under hypoxic conditions involves degradation of larger mitochondria. As a control to ensure that the hypoxia was induced in these cells, western blotting was carried out with cell lysates to measure induction of HIF-1α and BNIP3 in response to 6h hypoxia compared to control conditions (Fig. 5.3.B). This confirmed that the cells were hypoxic and that 6h hypoxia was sufficient time to induce BNIP3 and mitophagy.

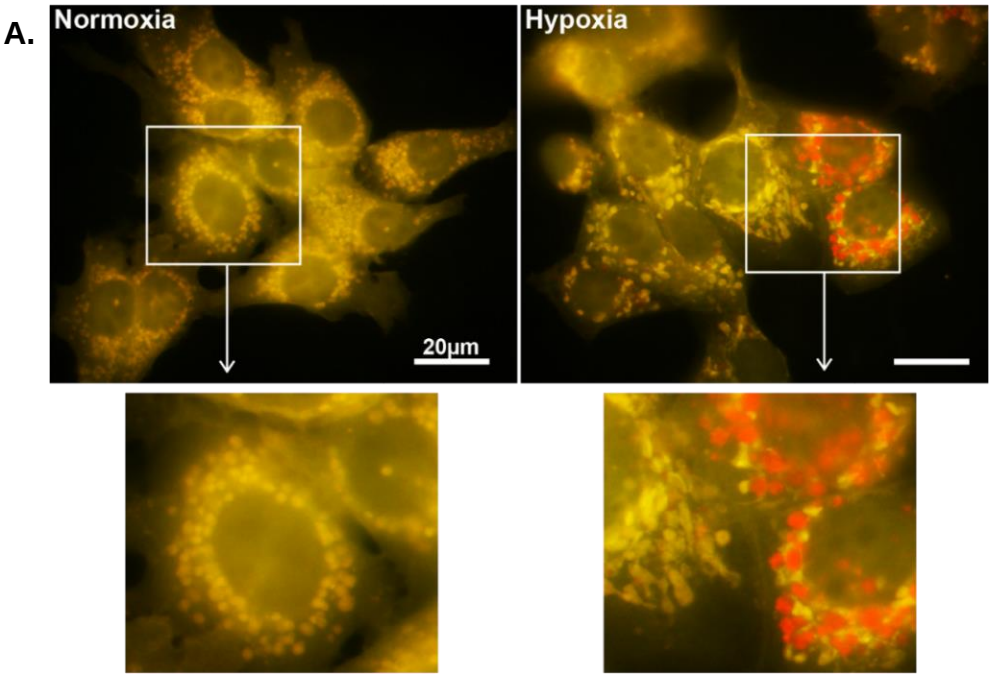

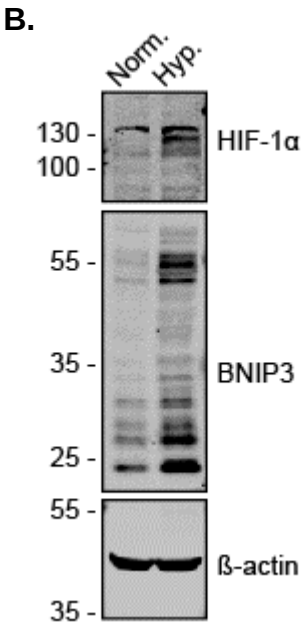

Figure 5.4 Hypoxia induces HIF-1α, BNIP3 and mitophagy in MCF-7-VLCAD(1-40)-mCherry-EGFP cells.

A. MCF-7-VLCAD(1-40)-mCherry-EGFP cells were kept under normal culture conditions or exposed to hypoxia (<1% O_2) for 6h. The cells were fixed and imaged using a Nikon Eclipse E600 microscope with a 100x objective. **B**. Western blot from cell lysates derived from the same cultures show levels of HIF-1α and BNIP3 in MCF-7-VLCAD(1-40)-mCherry-EGFP cells under normal culture conditions or exposed to hypoxia (<1% O_2) for 6h. β-actin is the protein loading control. The experiment was performed once, and 15 fields of view were imaged per conditions. Representative images are shown.

5.3.5 Mitophagy detection using the VLCAD(1-40)-mCherry-EGFP reporter depends on a low lysosomal pH

The next step was to test whether the red puncta truly represented mitochondria undergoing degradation and that their appearance was due to quenching of EGFP within lysosomes. For this, we used bafilomycin A1, which inhibits the lysosomal proton pump (Crider et al., 1994). Bafilomycin raises the pH within lysosomes, which should reduce the number of red puncta that appear in response to mitophagy stimuli. MCF-7-VLCAD(1-40)-mCherry-EGFP cells were cultured in complete medium or in complete medium with DFP for 24h in the absence or presence of bafilomycin A1 for the last 4h prior to fixing. Representative images are shown in Figure 5.5.A, and it is clear that there were fewer red puncta in the cells incubated with DFP that were also exposed to bafilomycin A1 compared to cells exposed to DFP alone. By quantifying the number of cells considered mitophagy-positive, i.e. positive for red puncta, as a percentage of the total number of cells counted, it was determined that approximately 20% of the cells were undergoing mitophagy under normal culture conditions (Fig. 5.5B). Addition of DFP increased the percentage of mitophagy-positive cells to approximately 70%, thus, clearly inducing mitochondrial clearance. The addition of bafilomycin A1 significantly reduced the number of mitophagy-positive cells both in complete medium conditions and in response to DFP. Therefore, it was concluded that the appearance of red puncta is indicative of active mitophagy, and that the function of the probe depends on the quenching of EGFP, which occurs due to the acidic pH of lysosomes.

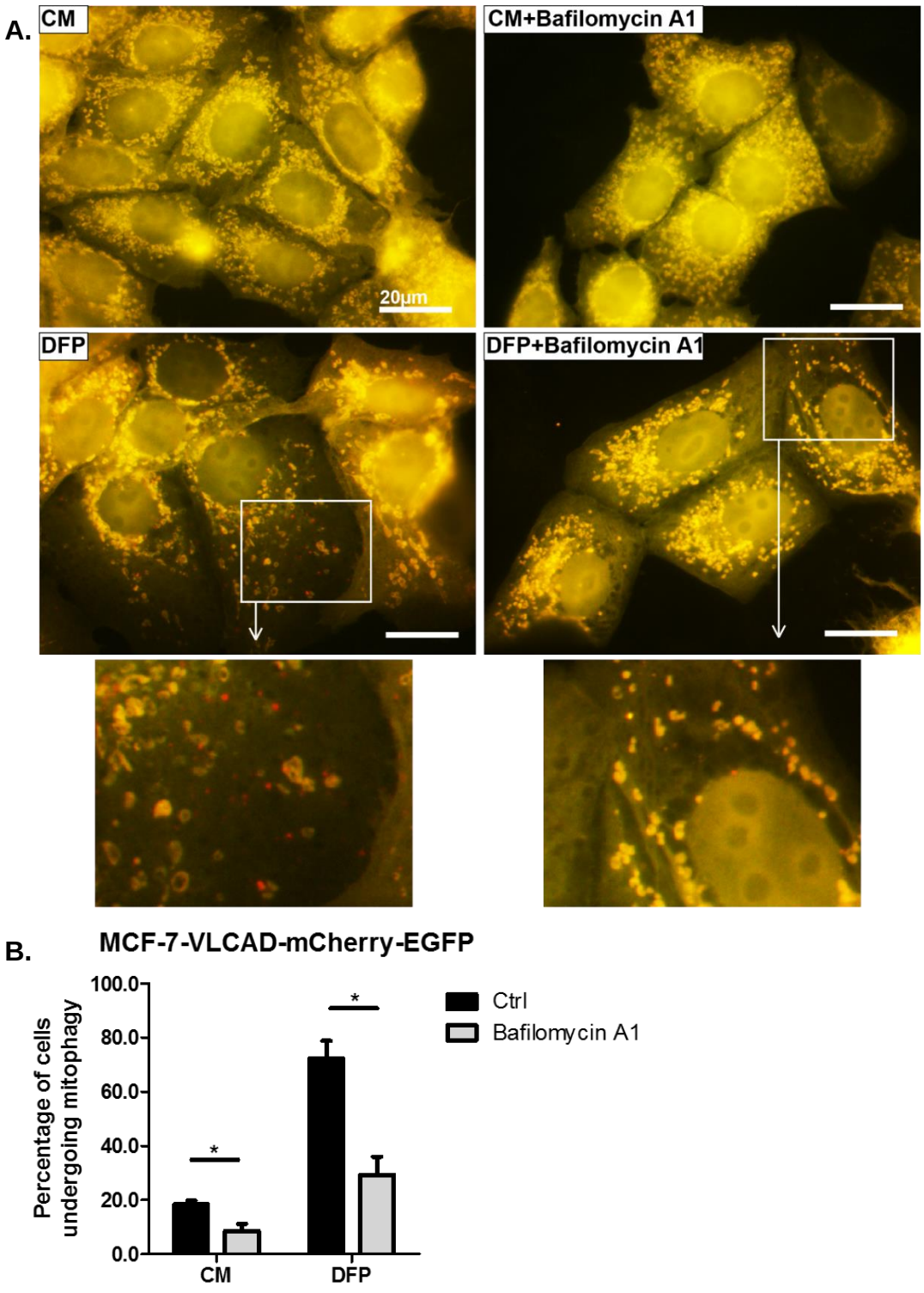

Figure 5.5 The accumulation of red puncta in response to mitophagy induction is dependent on low lysosomal pH.

A. MCF-7-VLCAD(1-40)-mCherry-EGFP cells were kept in complete medium or exposed to DFP (1mM) for 24h followed by addition of bafilomycin A1 (100nM) for the last 4h. The cells were fixed, and images obtained using a Nikon Eclipse E600 microscope with a 100x objective. **B**. The percentage of mitophagy-positive cells per condition in (A) was quantified, and results are presented as mean ± SEM from three independent experiments. For each experiment, 15 fields of view were imaged per conditions. For statistical analysis, the Student's t-test was performed (*: $p<0.05$, **: $p<0.01$, ***: $p<0.001$).

5.3.6 Inhibition of GSK-3β induces mitophagy

Having demonstrated the function and sensitivity of the mitophagy probe, the next objective was to use the MCF-7-VLCAD(1-40)-mCherry-EGFP cell line to assess the effects of IGF-1 signalling and BNIP3 on mitophagy induction. First, we wanted to measure the effects of GSK-3β inhibition on mitophagy, because IGF-1 induces BNIP3 through inhibition of GSK-3β activity. GSK-3β inhibition with LiCl or SB415286 also resulted in induction of BNIP3 (Fig. 4.4.B-C and Riis et al., 2020) thus indicating that GSK-3β inhibition could be used to mimic IGF-1 signalling in complete medium conditions rather than using serum-deprived cells. MCF-7-VLCAD(1-40)-mCherry-EGFP cell cultures incubated with LiCl or SB415286 for 2 or 6h were assessed for the number of cells undergoing mitophagy. In complete medium, approximately 20% of the cells showed signs of active mitophagy and both GSK-3β inhibitors increased the percentage of cells undergoing mitophagy to approximately 50% (Fig. 5.6A-B). This reached statistical significance for SB415286 at both timepoints, but only at 2h for LiCl. Mitophagy was induced to a similar extent by both compounds, and levels of mitophagy in cells exposed to the inhibitors for 2 or 6h were similar, suggesting that the induction of mitophagy had already occurred at 2h and was sustained at this level up to 6h.

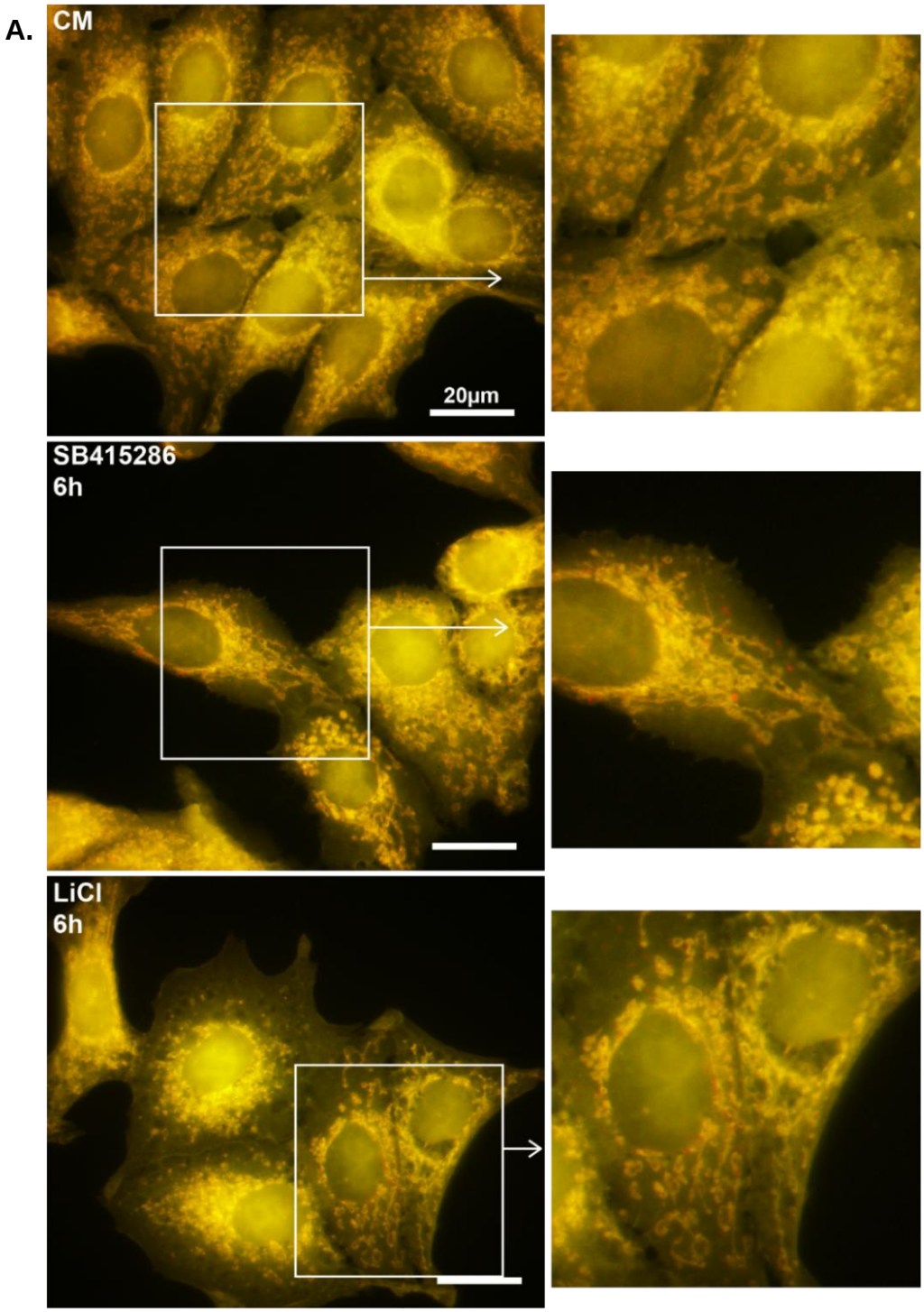

Figure 5.6 GSK-3β inhibition induces mitophagy in MCF-7 cells.

A. MCF-7-VLCAD(1-40)-mCherry-EGFP cells cultured in complete medium were incubated with SB415286 (30µM) or LiCl (10mM) for 2 or 6h. The cells were then fixed and images were obtained using a Nikon Eclipse E600 microscope with a 100x objective. Representative images are shown.

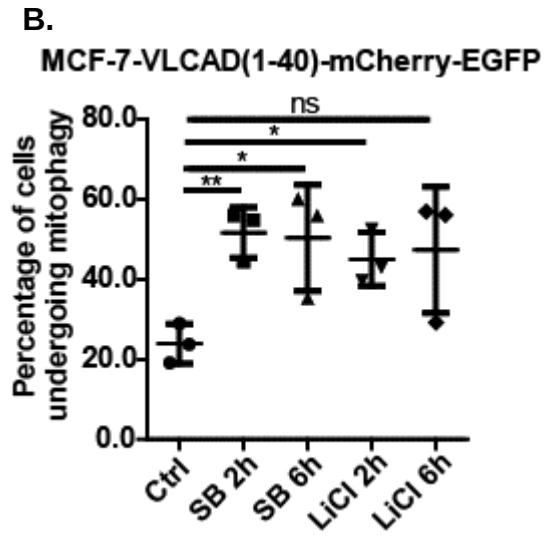

5.6.B. The percentage of mitophagy-positive cells per condition in (A) was quantified, and results are presented as mean ± SEM from three independent experiments. For each experiment, 15 fields of view were imaged per conditions. For statistical analysis, the Student's t-test was performed (*: $p<0.05$, **: $p<0.01$, ***: $p<0.001$).

5.3.7 IGF-1 stimulation reduces total mitophagy in serum-free cultures

In all cell assays used to assess direct effects of IGF-1 on mitophagy, it is necessary to deprive the cells of serum prior to addition of IGF-1. This is to avoid confounding signals from other factors such as insulin, epidermal growth factor, testosterone and growth hormone that are present in foetal bovine serum (Honn et al., 1975, Barnes and Sato, 1980). Here, MCF-7-VLCAD(1-40)-mCherry-EGFP cells were maintained in complete medium or serum-starved for 4h before addition of IGF-1 for 1, 2, 4 or 24h. To assess the extent to which serum-deprivation induced mitophagy, an additional control culture was included, where the cells were maintained in serum-free medium for 24h. The results are shown in Figure 5.7.A and B and indicate that in complete medium, active mitophagy was detected in approximately 30% of cells (Fig. 5.7.B). After 4h of serum-deprivation, approximately 65% of the cells exhibited mitophagy. At 24h serum deprivation, the percentage of mitophagy-positive cells approached 100%. Interestingly, the addition of IGF-1

appeared to reduce mitophagy, as the percentage of mitophagy-positive cells declined over time upon exposure to IGF-1, reaching statistical significance at 4h. After 24h of IGF-1 stimulation, this was further reduced to approximately 15% of the cells, which was a lower percentage of mitophagy-positive cells than that observed in complete medium. Thus, it appears that IGF-1 stimulation of serum-starved cells reduces the levels of total mitophagy, while at the same time inducing BNIP3, (shown in Fig. 3.4.A-B and Lyons et al., 2017). Since 24h of IGF-1 stimulation clearly suppressed the potent induction of mitophagy observed after 24h of serum-starvation, this raises the question, of what the function of BNIP3 is, when it is induced in response to IGF-1 in serum-free conditions. It is possible that IGF-1- mediated suppression of general autophagy (via mTORC1) also suppresses total cellular mitophagy, while maintaining a basal level of BNIP3-specific mitophagy that cannot be detected in serum-starved cells using this mitophagy probe. This hypothesis is supported by our finding that inhibition of GSK-3β (which may mimic IGF-1 stimulation in complete medium) induced expression of both BNIP3 and mitophagy. Alternatively, IGF-1-induced BNIP3 may have other unknown functions in these cells.

A.

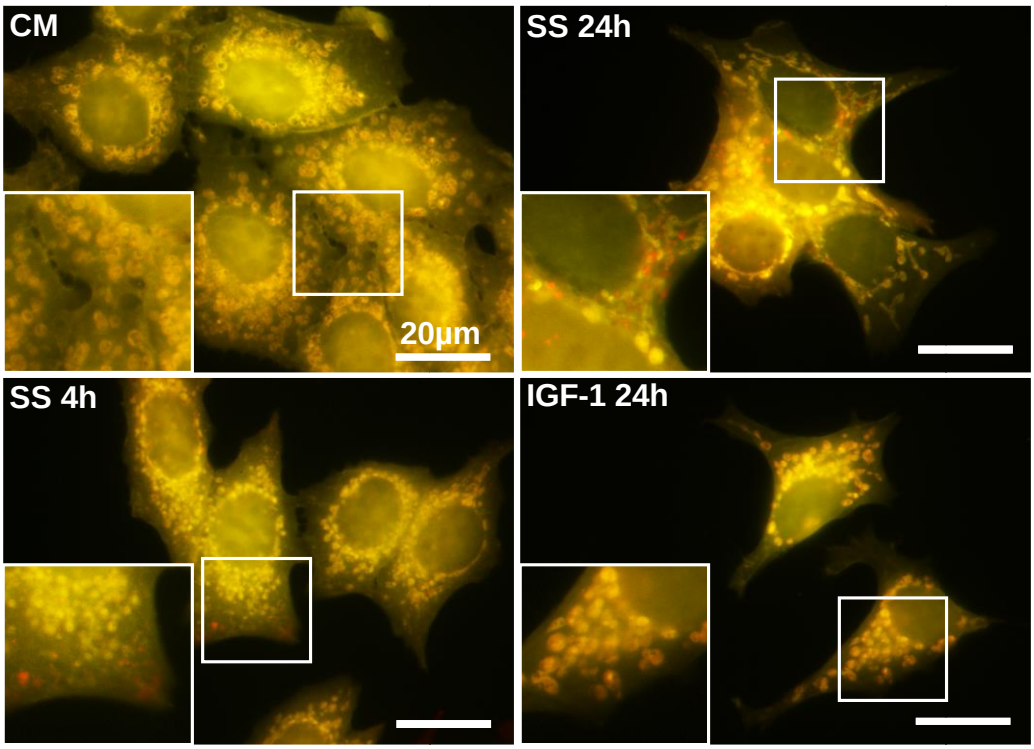

B.

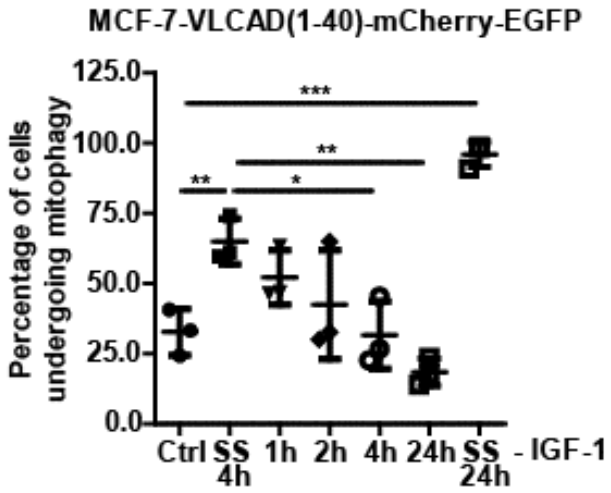

Figure 5.7 IGF-1 protects against mitophagy in MCF-7 cells.

A. MCF-7-VLCAD(1-40)-mCherry-EGFP were kept in complete medium, serum deprived for 4 or 24h or serum deprived for 4h followed by IGF-1 stimulation (10ng/ml) for 1, 2, 4, or 24h. The cells were fixed and imaged using a Nikon Eclipse E600 microscope with a 100x objective. **B**. The percentage of mitophagy-positive cells per condition in (A) was quantified, and results are presented as mean ± SEM from three independent experiments. For each experiment, 15 fields of view were imaged per conditions. For statistical analysis, the Student's t-test was performed (*: $p<0.05$, **: $p<0.01$, ***: $p<0.001$).

5.3.8 Ectopic expression of WT BNIP3 enhances CCCP- but not DFP-induced mitophagy

To further investigate BNIP3 function in mitophagy and IGF-1 signalling we sought to ectopically express wildtype (WT) or LC3-interacting region (LIR)-mutant BNIP3 (see section 2.8 in Materials and Methods), the latter being mitophagy-incompetent, in the MCF-7-VLCAD-mCherry-EGFP cell line. These cells were subsequently maintained in complete medium or exposed to CCCP or DFP for 24h to induce mitophagy, and the number of cells undergoing mitochondrial clearance was quantified (Fig. 5.8.A-B). CCCP and DFP induced mitophagy to a similar extent in cells expressing either an empty vector (EV) control, WT or LIR-mutant BNIP3, where approximately, 50% or 70%, respectively, of the cells exhibited active mitophagy. When comparing effects of the three different plasmids on mitophagy levels, it was clear that in cells expressing WT BNIP3 in CCCP-induced cultures there was a significantly higher number of mitophagy-positive cells present than in the empty vector control (Fig. 5.7.B, $p=0.032$). Under these conditions, there was also a trend towards higher mitophagy levels in cells expressing WT BNIP3 than in cells expressing the LIR-mutant ($p=0.062$), suggesting that this effect may depend on a functional LIR domain (Fig. 5.8.B). There was, however, no statistically significant difference in mitophagy levels between cells transfected with either of the three plasmids following incubation with DFP.

BNIP3 protein overexpression in these cells was confirmed by western blotting (Fig. 5.8.C). Ectopic expression of BNIP3 did not cause any apparent change in levels of general autophagy, since p70 S6 kinase phosphorylation (T371) and p62 levels were similar in all cell cultures (Fig. 5.8.C). Furthermore, there was no alteration in the levels of the mitochondrial marker PHB1, suggesting no induction of mitochondrial degradation in response to the overexpression of BNIP3 in complete medium cultures.

This was consistent with the quantification of mitophagy levels in control conditions in Figure 5.8.B. Overall, the results show that WT but not LIR-mutant BNIP3 increased mitophagy levels in response to mitochondrial uncoupling, supporting a mitophagic role for BNIP3 in cancer cells.

A.

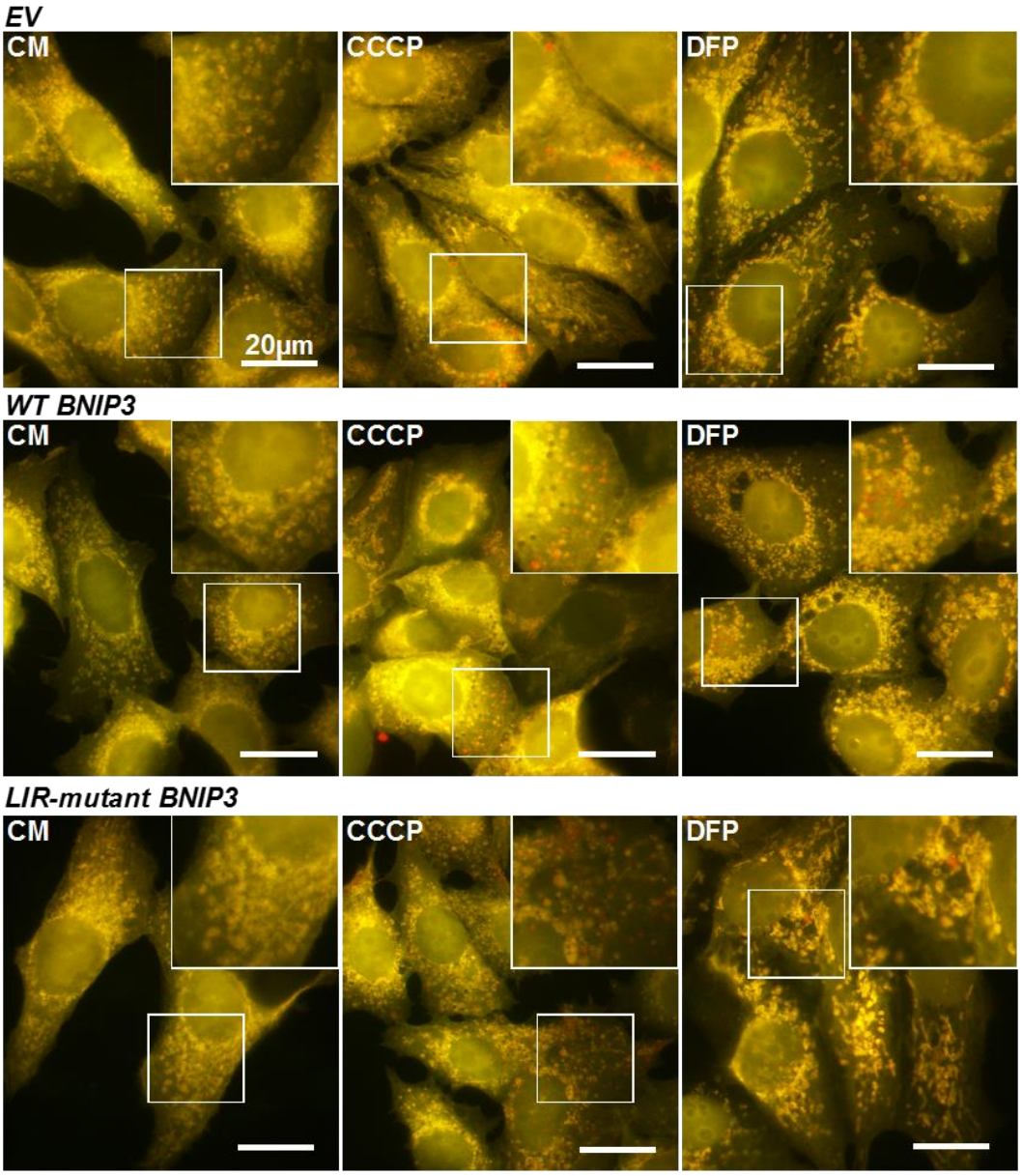

Figure 5.8 Ectopic expression of WT BNIP3 enhances mitophagy induced by CCCP but not DFP.

A. MCF-7-VLCAD(1-40)-mCherry-EGFP cells were transiently transfected with pcDNA3.1 EV, WT or LIR-mutant BNIP3. 48h post transfection, the cells were kept in complete medium or treated with CCCP (10µM) or DFP (1mM) for 24h. The cells were fixed and imaged using a Nikon Eclipse E600 microscope with a 100x objective.

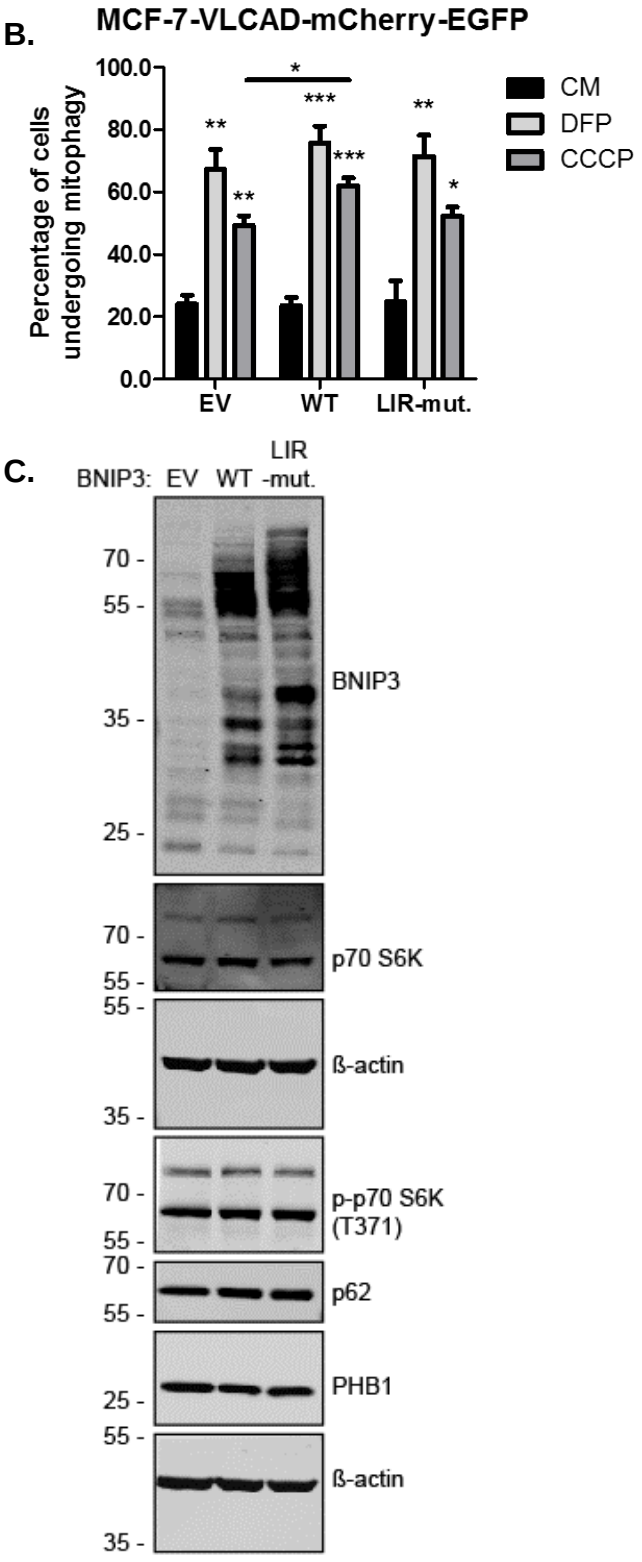

5.8.B. The percentage of mitophagy-positive cells per condition in (A) was quantified, and results are presented as mean ± SEM from three independent experiments. For each experiment, 15 fields of view were imaged per conditions. For statistical analysis, the Student's t-test was performed (*: $p<0.05$, **: $p<0.01$, ***: $p<0.001$). **C**. Western blot showing levels of BNIP3, p-p70 S6K (T371) and p62 in the transfected MCF-7-VLCAD(1-40)-mCherry-EGFP cells in A-B. Cells were lysed 48h post transfection. β-actin is the protein loading control. Three independent experiments were carried out, and a representative blot is shown.

5.3.9 IGF-1 induces colocalisation of endogenous BNIP3 with EGFP-LC3

To further investigate the paradox that IGF-1 stimulation suppressed total mitophagy while at the same time inducing accumulation of BNIP3, we sought to more specifically detect BNIP3-mediated mitophagy in cells by assessing colocalisation of BNIP3 with LC3 on autophagosomes. To do so, pEGFP-LC3 was transfected into MCF-7 cells that were subsequently counterstained for endogenous BNIP3. Co-localisation of EGFP-LC3 and BNIP3 was assessed in cells cultured in complete medium, serum-starved for 4h or 24h, or serum-starved for 4h followed by 20h IGF-1 stimulation (Fig. 5.9). In complete medium cultures, relatively low levels of EGFP-LC3/autophagosome formation were observed, as would be expected under non-stressed conditions (Fig. 5.9). In response to serum-deprivation, LC3-coated autophagosomes appeared after 4h, indicating autophagy, and these accumulated further after 24h. However, no clear colocalisation of EGFP-LC3 with BNIP3 was observed at either time point (Fig. 5.9). The addition of IGF-1 to cultures for 20h reduced the number of autophagosomes indicating suppression of autophagy, as expected. Furthermore, a more orange fluorescence staining was apparent in IGF-1-stimulated cells compared to serum-starved cells, suggesting that there was more colocalisation of LC3 with BNIP3 in response to IGF-1 stimulation in these cells.

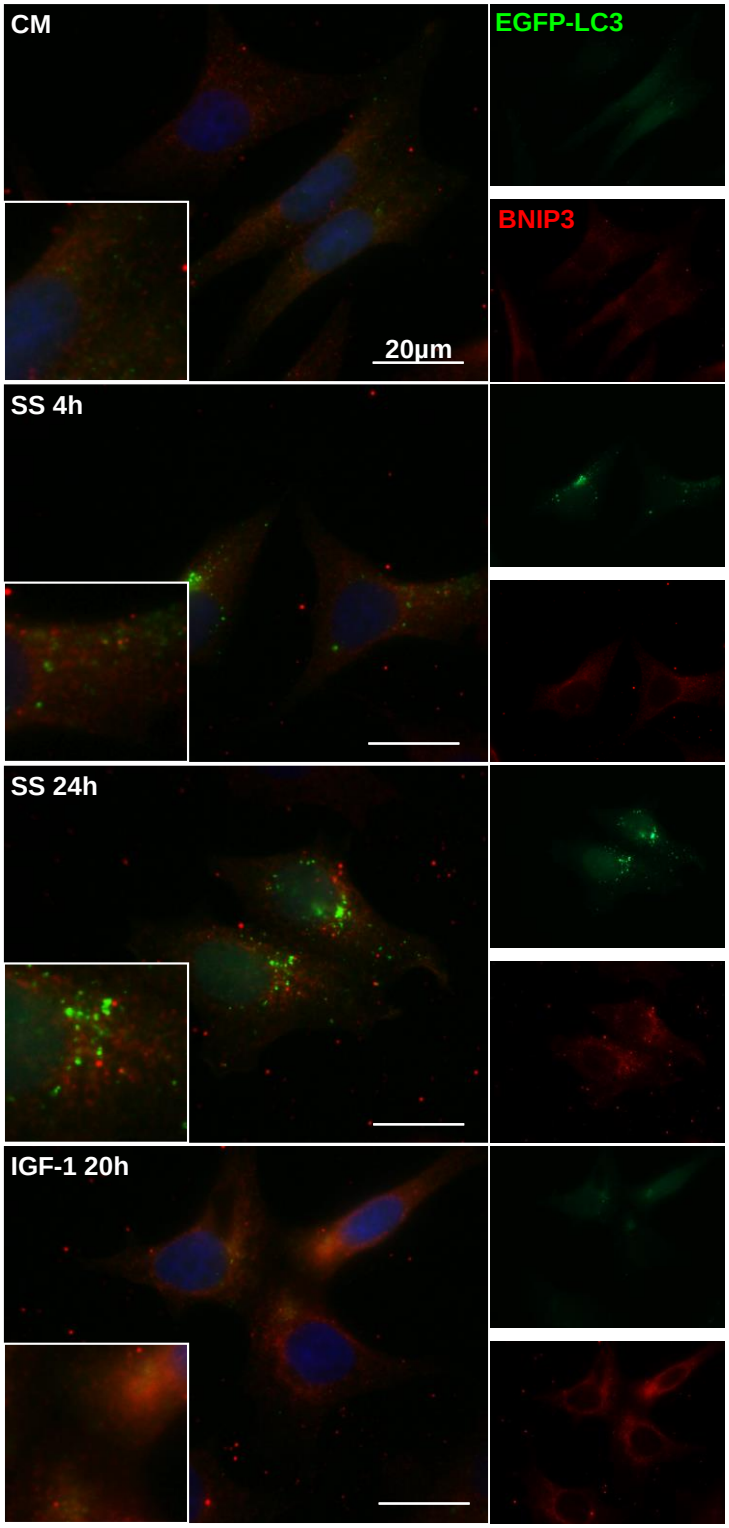

Figure 5.9 IGF-1 stimulation reduces autophagosome accumulation in response to serum-starvation and increases colocalisation between LC3 and endogenous BNIP3.

Immunofluorescence staining of MCF-7 cells. The cells were transfected with pEGFP-LC3 for 48h. Next, they were maintained in complete medium, were serum-starved for 4h or 24h, or were serum-starved for 4h followed by 20h IGF-1 (10ng/ml) stimulation. The cells were fixed and stained with anti-BNIP3 antibody (red) and Hoechst (blue) for nuclear staining. Images were acquired on a Leica DM LB2 microscope using a 100x objective. The experiment was performed three times, and 8 fields of view were imaged per condition per experiment. Representative images are shown.

5.3.10 IGF-1 induces colocalisation of mCherry-BNIP3 with EGFP-LC3

BNIP3 and LC3 colocalization was further investigated by generating and transfecting a plasmid encoding mCherry-BNIP3 WT (see section 2.8 in Methods and Materials). It was anticipated that a clearer indication of colocalisation with pEGFP-LC3 could be observed by ectopically expressing mCherry-tagged BNIP3 than by staining for endogenous BNIP3.

First, MCF-7 cells were transiently transfected with either pmCherry EV or pmCherry-BNIP3 to ensure that the BNIP3 fusion protein was appropriately expressed and located in cells. Immunofluorescence showed that the mCherry-BNIP3 signal had a mitochondrial profile, indicating that BNIP3 was appropriately expressed and the cellular location was not altered by fusion with the mCherry tag (Fig. 5.10.A). Next, MCF-7 cells were transiently co-transfected with pmCherry-BNIP3 and pEGFP-LC3. The cells were maintained in complete medium, were serum-deprived for 4h or 24h, or were serum-deprived for 4h prior to addition of IGF-1 for 20h. Fluorescence images showed that in complete medium cultures, the cells exhibited a low level of EGFP-LC3-indicated autophagy (green puncta) and this was largely unaffected by BNIP3 overexpression (Fig. 5.10.B). In agreement with observations in Figure 5.9, serum-deprivation induced the formation of LC3-coated autophagosomes after either 4h or 24h (Fig. 5.10.C-D). This effect of serum starvation also appeared to be mostly unaffected by the ectopic expression of BNIP3, but some colocalisation of mCherry-BNIP3 with EGFP-LC3 was apparent after 24h serum-starvation. As was observed with endogenous BNIP3 (Fig. 5.9), IGF-1 stimulation increased the colocalisation of mCherry-BNIP3 with EGFP-LC3 as illustrated by increased orange staining (Fig. 5.10.E) compared to serum-starved conditions. This result suggests that IGF-1 increases BNIP3 interaction with LC3 and, thus, mitophagy.

A.

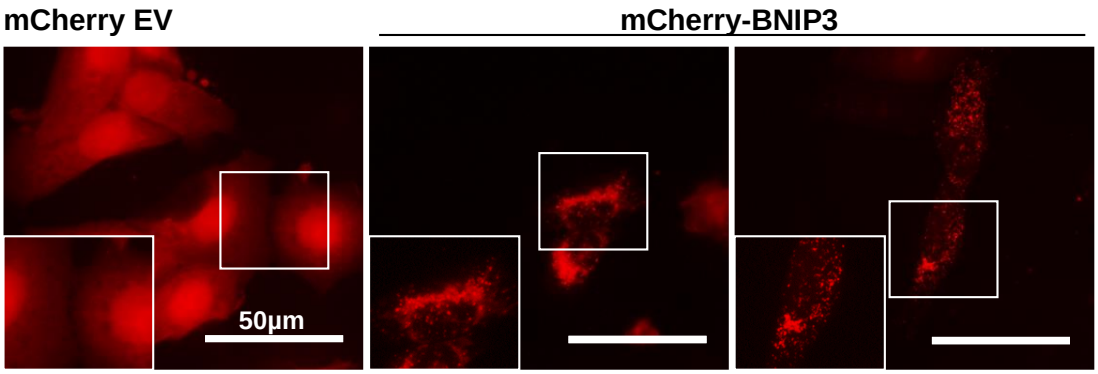

Figure 5.10 Serum deprivation induces autophagosome formation in MCF-7 cells in either the presence or absence of ectopically expressed WT BNIP3, and IGF-1 increases colocalisation between LC3 and BNIP3.

A. Immunofluorescence imaging of MCF-7 cells transfected with pmCherry EV or pmCherry-BNIP3 WT. At 48h post transfection, the cells were fixed, and images were acquired using a Nikon Eclipse E600 microscope with a 40x objective.

B.

Complete medium:

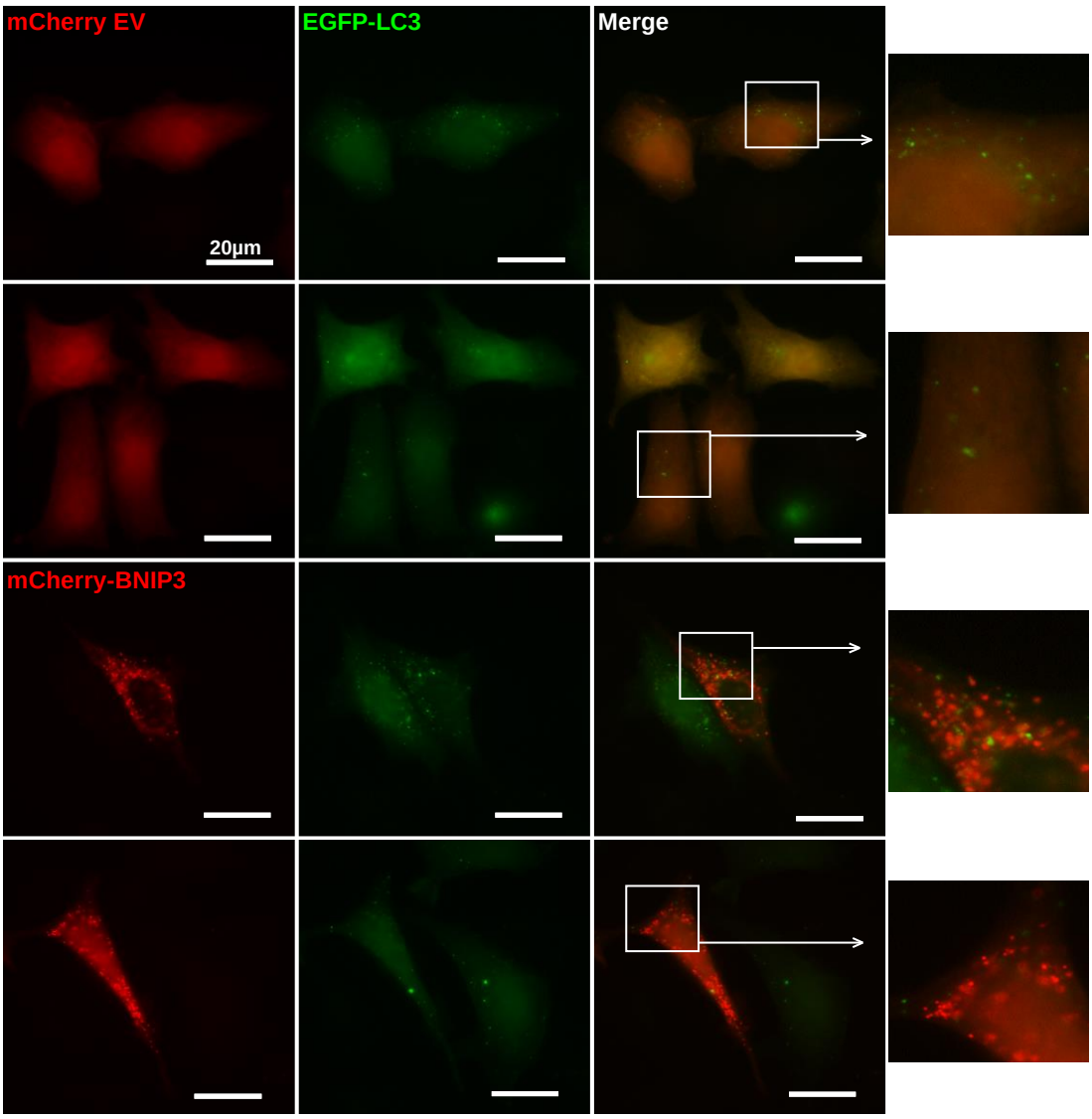

5.10.B-E. MCF-7 cells were transiently co-transfected with pEGFP-LC3 and pmCherry EV or BNIP3 WT. The cells were maintained in complete medium or serum deprived for (**C**) 4h or (**D**) 24h or (**E**) serum deprived for 4h followed by IGF-1 stimulation (10ng/ml) for 20h. The cells were fixed and imaged using a Nikon Eclipse E600 microscope with a 100x objective. The experiment was performed once, and 8 fields of view were imaged per conditions. Representative images are shown.

C.

Serum starvation 4h:

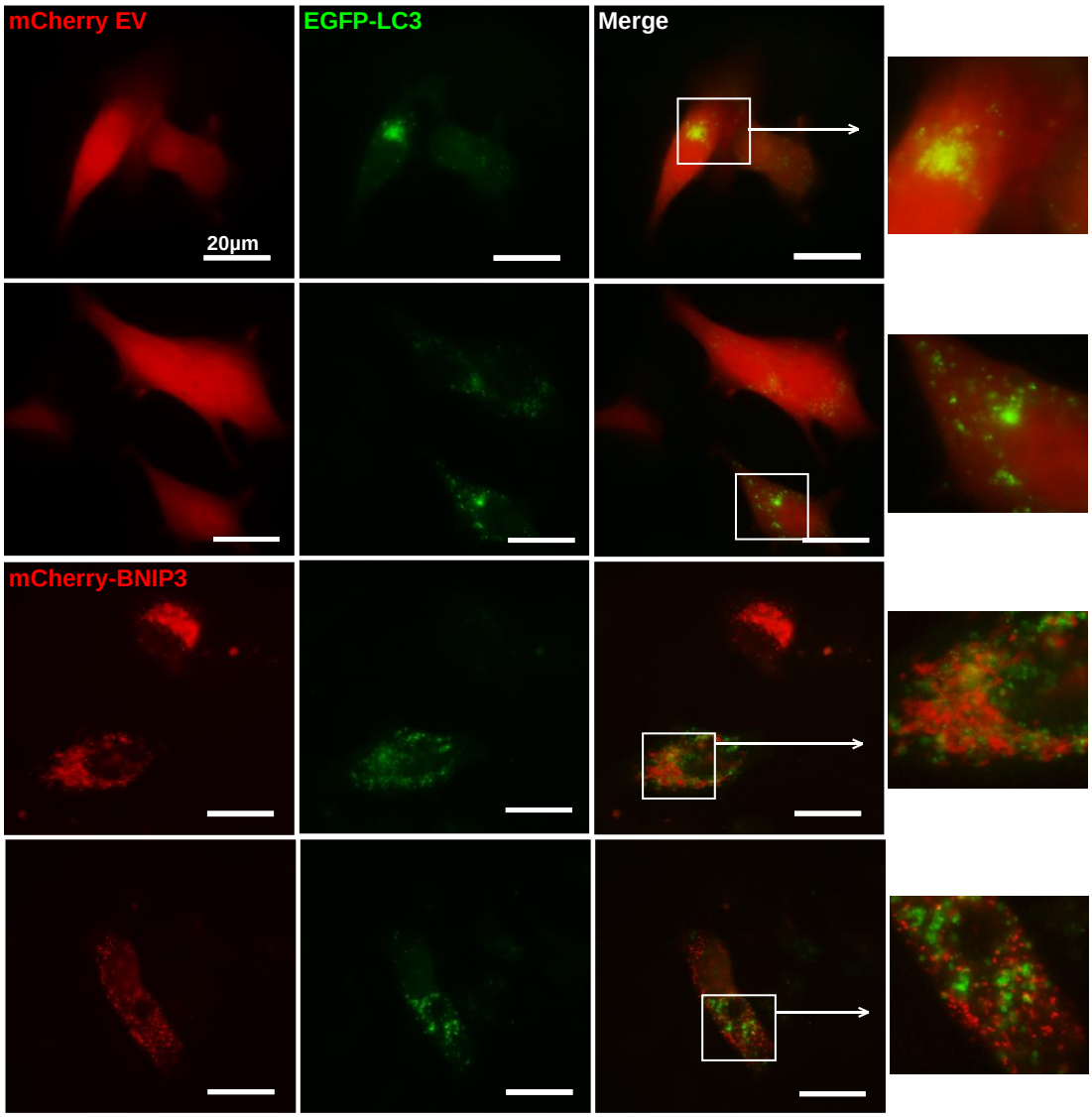

D.

Serum starvation 24h:

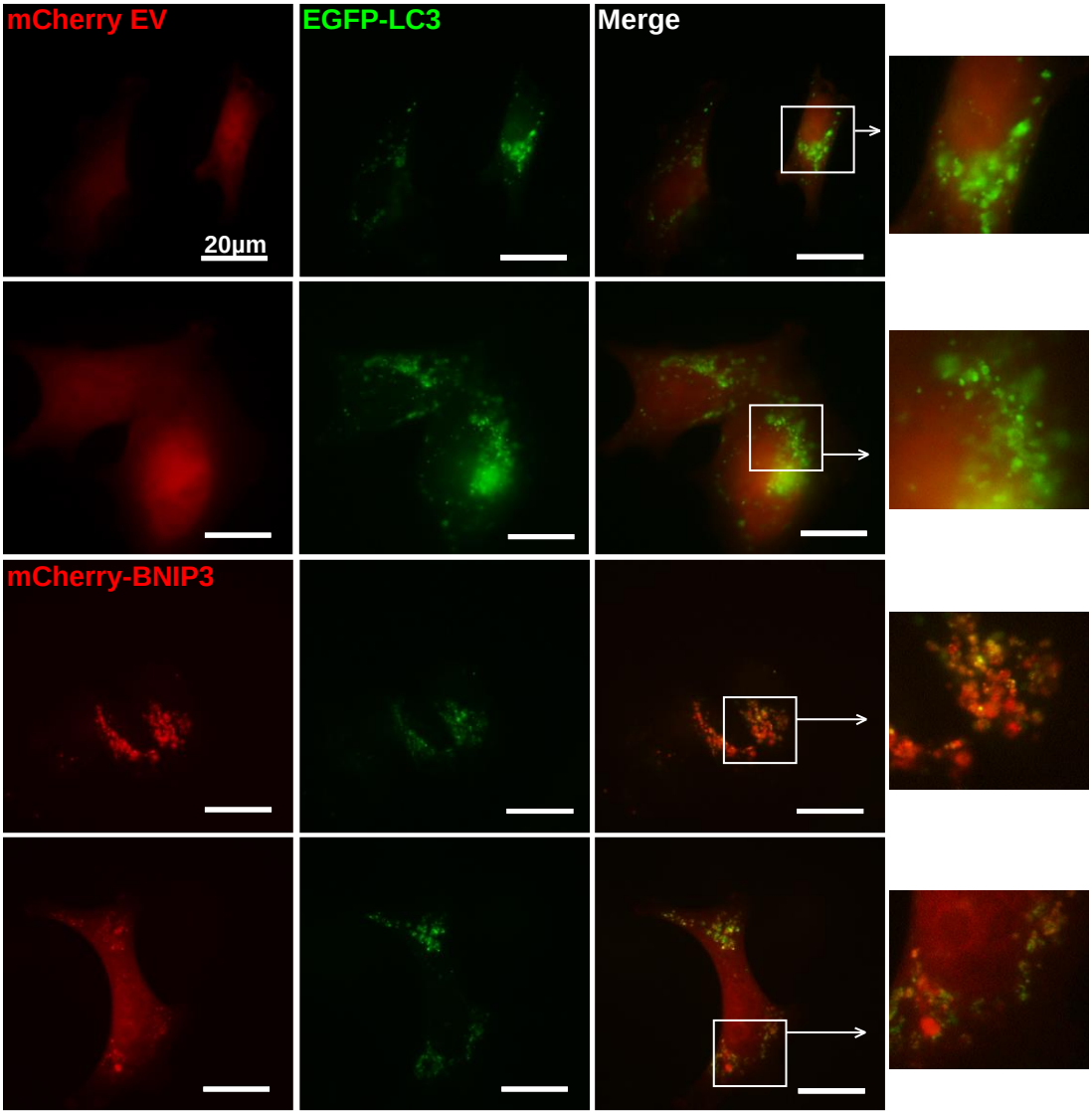

E.

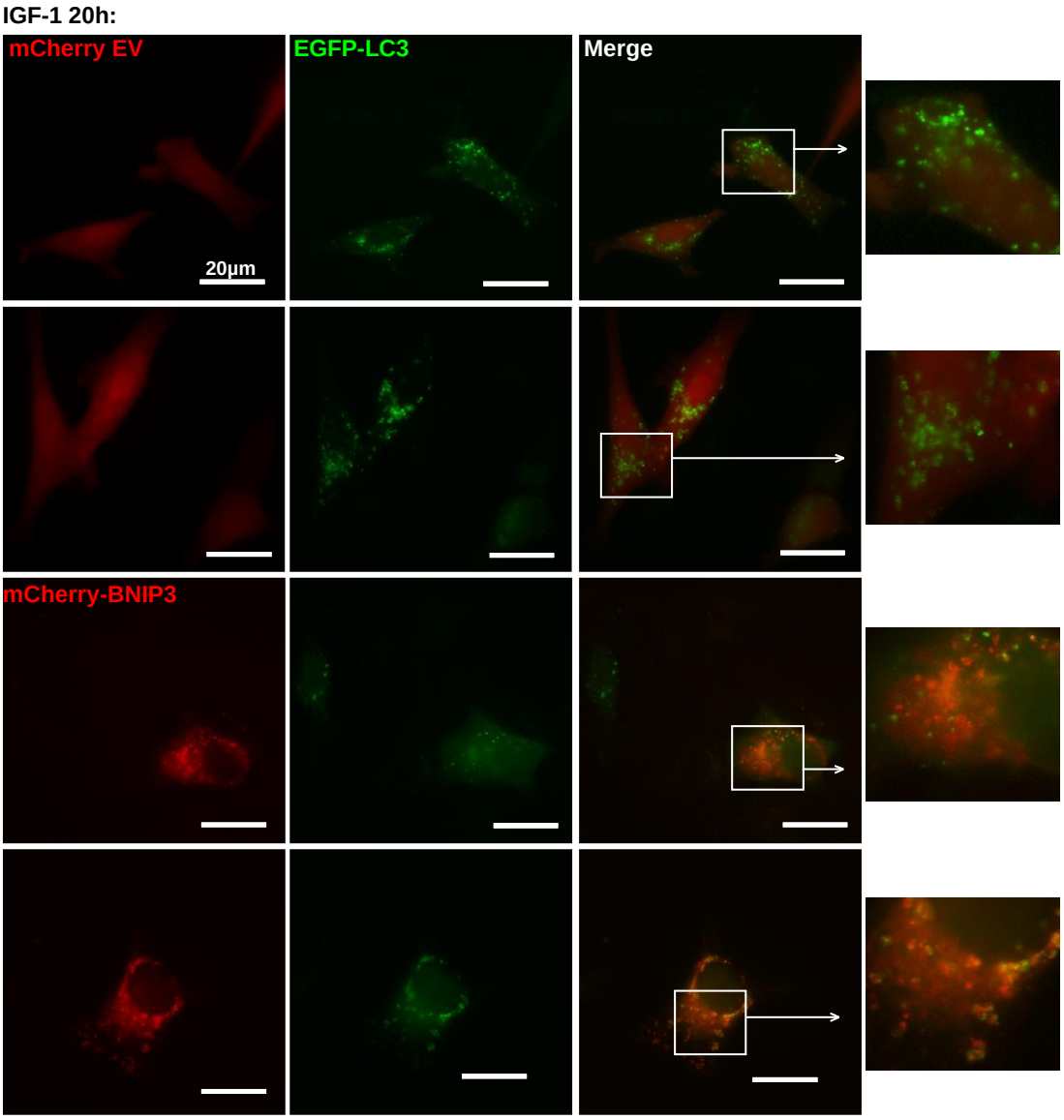

5.3.11 R- cells have reduced capacity to eliminate mitophagic vesicles compared to R+ cells leading to cell death

As an alternative approach to investigate how IGF-1 signalling affects cellular mitophagy capacity, we asked whether intrinsic differences in mitophagy induction and mitochondrial clearance could be observed in IGF-1R-expressing R+ cells compared to IGF-1R knockout R- cells.

R- and R+ cells were transiently transfected with the mitophagy probe (pcDNA3.1-VLCAD(1-40)-mCherry-EGFP) and were maintained in complete

medium in the absence or presence of DFP for 24h or 48h. In complete medium, both cell lines exhibited quite high levels of mitophagy as indicated by red puncta (Fig. 5.11.A.), when compared to MCF-7 cells (Figs 5.1-5.10). Most cells analysed exhibited some level of mitophagy under all conditions, as can be seen in the images in Figure 5.11, suggesting that MEFs generally exhibit higher levels of basal mitophagy than cancer cells. DFP addition for 24h further increased the number of red puncta per cell, indicating induction of mitophagy in both cell lines. In R- cells the appearance of clear large vacuoles indicated cellular stress that may typically precede cell death (Shubin et al., 2016) (Fig. 5.11.A.). At 48h DFP exposure, R- cells exhibited high levels of cell stress with cells apparently dying and accumulating mitophagic vesicles (5.11.B.). R+ cells on the other hand, appeared to recover from the DFP-induced stress. Mitophagy was potently induced at 24h, but at 48h the cells had fewer mitophagic vesicles, indicating efficient clearance, and also exhibited a morphological appearance that resembled cells cultured in complete medium.

This supports our previous observation that R- cells but not R+ cells show substantial levels of cell death upon exposure to DFP for 24h (Fig. 4.8 and Riis et al., 2020). Overall, these results also support the conclusion that IGF-1 signalling is essential for the efficient clearance of mitophagic vesicles and cell survival under conditions of cellular and mitochondrial stress.

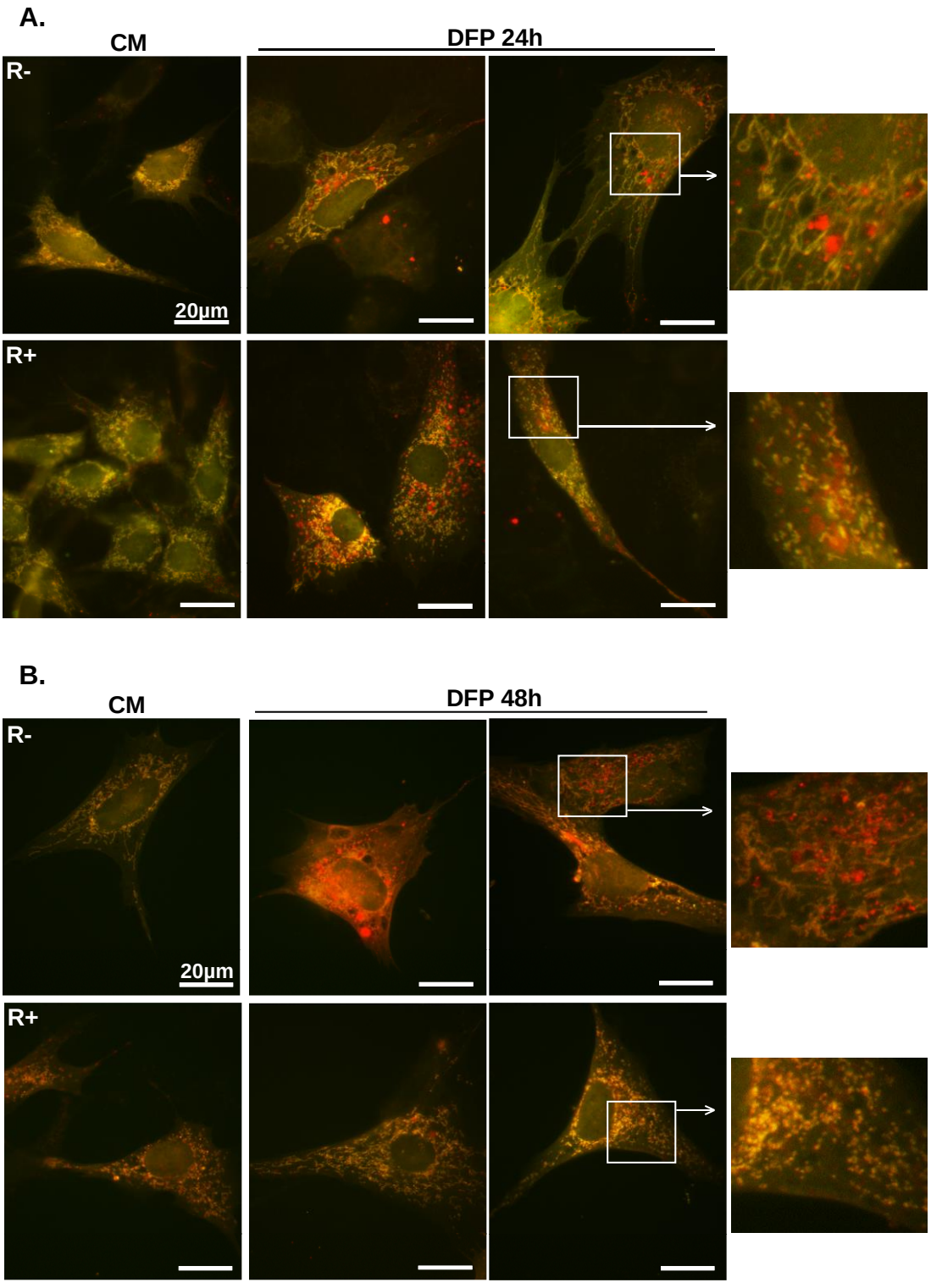

Figure 5.11 R- cells exhibit an impaired response to DFP-induced mitophagic stress compared to R+ cells.

A. R- and R+ cells were transiently transfected with the pcDNA3.1-VLCAD(1-40)-mCherry-EGFP probe. 48h post transfection the cells were kept in complete medium or treated with DFP (1mM) for 24h or (**B**.) 48h. The cells were fixed, and images obtained using a Nikon Eclipse E600 microscope with a 100x objective.

5.4 Discussion

Directly visualising and quantifying mitophagy remains a challenge, despite recent advances including the development of probes such as mt-Keima, which has been used in several studies (Cornelissen et al., 2018, Devi et al., 2019, Sun et al., 2017). In our work thus far, exploring the functional relevance of BNIP3 induction in response to IGF-1, a limitation has been the lack of tools with which to assess mitophagy. Here, we developed and validated a probe named VLCAD(1-40)-mCherry-EGFP that enabled us to directly measure the levels of mitophagy in cells. To ensure accurate and sensitive mitophagy detection, extensive validation was performed. We confirmed a) mitochondrial localisation of the probe, b) sensitive detection of mitophagy in response to mitophagic stimuli and c) that the function of the probe was dependent on the low pH of lysosomes, ensuring that it specifically detects mitochondria undergoing degradation.

Interestingly, analysis of MCF-7 cells expressing the probe revealed that approximately 20-30% of cells exhibited mitophagy in complete medium, thus enabling quantification of mitophagy-positive cells to indicate mitophagy levels. In MEFs, on the other hand, the percentage of cells undergoing mitophagy approached 100% in complete medium, and a qualitative analysis was required instead. Intriguingly, the probe clearly indicated induction of mitophagy in response to all mitophagy-inducing conditions tested, including serum deprivation, hypoxia and mitochondrial stress induced by either iron chelation (DFP) or mitochondrial uncoupling (CCCP). Thus, this novel mitophagy probe is functional and has the potential to contribute to a rapidly evolving area of research. It enables sensitive and specific detection of mitophagy, and because it produced very clear fluorescence

signals in fixed cells, it has the potential to be widely used in different experimental settings.

With this new probe, we wished to assess the cellular effects of IGF-1 signalling on mitophagy, having already established a pathway linking IGF-1 to Nrf2 activation and an associated induction of the mitophagy receptor BNIP3 (Lyons et al., 2017, Riis et al., 2020). A confounding issue in these studies is the necessity to serum starve cells in order to detect IGF-1 signalling response. Serum deprivation causes activation of general autophagy including mitophagy (Yang and Klionsky, 2010), and addition of IGF-1 inhibits general autophagy (Jung et al., 2010). Thus, the question we wished to address was, whether IGF-1 can induce mitophagy through BNIP3, while inhibiting general autophagy through regulation of mTORC1.

By mimicking the IGF-1-mediated inhibition of GSK-3β with associated induction of BNIP3 through addition of either LiCl or SB415286 to complete medium (Riis et al., 2020), we could demonstrate that this was also associated with induction of mitophagy. However, direct IGF-1 stimulation of serum-starved cells, which is also associated with induction of BNIP3 (Lyons et al., 2017), reduced total levels of mitophagy rather than increasing mitophagy. Interestingly, ectopic expression of WT BNIP3 enhanced mitophagy induction in MCF-7 cells only in response to CCCP. We would not necessarily expect increased BNIP3-mediated mitophagy in response to CCCP, because it is known to rely on the PINK1/Parkin pathway (Narendra et al., 2008, Kondapalli et al., 2012, Kawajiri et al., 2010a). However, BNIP3 can facilitate PINK1-mediated mitophagy (Zhang et al., 2016), so, possibly, WT BNIP3 supports PINK1 in mediating a more efficient mitophagy response. On the other hand, since DFP induces BNIP3 (Riis et al., 2020), we predicted that overexpression of WT BNIP3 would enhance DFP-mediated mitophagy, but this was not the case. Previous

work revealed that MCF-7 cells potently induced BNIP3 in response to DFP, and this stimulus led to similar endogenous expression levels to those observed in cells overexpressing BNIP3 (Fig. 3.8.C). Thus, it is possible that MCF-7 cells reached maximal mitophagy capacity without ectopic BNIP3 expression, and no further increase could be observed, when BNIP3 was overexpressed. This might also explain, why WT BNIP3 enhanced CCCP-mediated mitophagy. CCCP induced mitophagy in a lower number of cells in the cultures than DFP, and therefore, there was possibly a greater capacity for enhancement by BNIP3 overexpression in CCCP-containing cultures.

The conclusion that IGF-1 induces the mitophagic function of BNIP3 is supported by previous results showing that IGF-1 specifically increases levels of BNIP3 at the mitochondria (Lyons et al., 2017). It is also supported by the observations here of enhanced colocalisation of endogenous BNIP3 and mCherry-BNIP3 with EGFP-LC3 in response to IGF-1 stimulation compared to little colocalisation observed in serum-starved cells.

R- and R+ cells were further used to explore the role of IGF-1 in mitophagic processes. Both cell lines exhibited high levels of mitophagy in complete medium conditions, suggesting that the overall capacity of the cells to induce mitophagy is unaffected by IGF-1 signalling. However, upon nutrient or mitochondrial stress mediated by serum deprivation or DFP, respectively, the mitophagy response in the R- cells was clearly associated with cellular stress, demonstrated by an accumulation of clear vacuoles indicative of cell death, R- cells were apparently unable to clear the mitophagic vesicles at 48h post addition of DFP. R+ cells, on the other hand, eliminated DFP-induced mitophagic vesicles and maintained cell survival.

In conclusion, the VLCAD(1-40)-mCherry-EGFP probe provided novel insights into how IGF-1 signalling affects mitophagy in transformed cells. IGF-1 downregulates total macro-autophagy and mitophagy as a cyto-protective signal in response to nutrient deprivation. However, the data presented here provide evidence to indicate that IGF-1 induces basal levels of mitophagy through the mitophagy receptor BNIP3. Furthermore, the IGF-1 pathway is essential for cellular tolerance to mitochondrial stress and is required for the efficient clearance of mitophagic vesicles.

General Discussion

Although IGF-1 has been extensively studied in cancer, relatively little is known of its mitochondrial effects. Mitochondria are essential organelles for the maintenance of cell proliferation and survival and are, therefore, of particular importance in tumour cells (Vyas et al., 2016). The results of this thesis expand our knowledge of IGF-1 effects on mitochondrial dynamics and turnover in cancer cells.

The results presented here and in Lyons et al. 2017 show that IGF-1 induces mitochondrial biogenesis through transcriptional regulators PGC-1β and PRC, while inducing the mitophagy receptor BNIP3 in all cancer cell lines tested. Furthermore, re-expressing the IGF-1R in mouse embryonic fibroblasts (MEFs) lacking the IGF-1R, caused an increase in BNIP3 mRNA and protein levels. This suggests that this is a conserved signal and implicates IGF-1 signalling in the regulation of mitophagy. The major transcription factor, Nrf2, was previously identified as a BNIP3-regulator in *C. elegans*, and here we established that Nrf2 is required for IGF-1-mediated induction of BNIP3 in cancer cells as well. It does so through a pathway dependent on HIF-1α, a known transcriptional inducer of BNIP3 under hypoxic conditions. Interestingly, we found that Nrf2 can induce HIF-1α and BNIP3 under normoxic conditions in cancer cells, suggesting that this pathway can operate in a hypoxia-independent manner. However, since tumours often exist in a hypoxic environment, it is likely that this pathway is of greater importance in the physiological tumour setting. In support of this, MCF-7 cancer cells with impaired IGF-1 signalling exhibited reduced capacity to induce BNIP3 and a mitophagic response under hypoxic conditions.

Here, we established a link between IGF-1 signalling and the regulation of Nrf2 function. Like IGF-1, Nrf2 can induce mitochondrial biogenesis and affect other aspects of mitochondria function (Dinkova-Kostova and Abramov, 2015), so we propose that IGF-1 enhances mitochondria health and mediates coordination of the generation and turnover of mitochondria through Nrf2. This would be advantageous to tumour cells, because the maintenance of a healthy mitochondria population enables cancer cells to survive in a stressful tumour environment, where nutrients and oxygen levels are low. Furthermore, Nrf2 regulates cellular detoxification in response to various xenobiotics including chemotherapeutics (McMahon et al., 2001, Köhle and Bock, 2007), and is therefore also associated with the development of chemoresistance (Karathedath et al., 2017, Ciamporcero et al., 2018, Khamari et al., 2018, Ji et al., 2019). Similarly, IGF-1 signalling is implicated in chemoresistance in several different types of cancer (Liu et al., 2002, Juan et al., 2011, Tian et al., 2013, Long et al., 2019). Thus, some of these effects observed in cancer models may be due to overlap between these two potent cytoprotective pathways.

Studies aimed at determining the precise function of BNIP3 that is induced in cells in response to IGF-1 proved to be challenging. IGF-1 promotes potent anti-apoptotic signals (Dunn et al., 1997, Kang et al., 2003, Maldonado et al., 2005, Baregamian et al., 2006), and it is, therefore, highly unlikely that the increase in BNIP3 expression caused by IGF-1 promotes cell death. BNIP3 also functions as a mitophagy receptor that has been implicated predominantly in hypoxia-induced mitochondrial clearance (Bellot et al., 2009, Rikka et al., 2011, Hanna et al., 2012, Ishihara et al., 2013). Thus, we hypothesized that IGF-1 induces a specific form of mitophagy through BNIP3 that it coordinates with induction of mitochondrial biogenesis to ensure the maintenance of mitochondrial homeostasis or health.

However, this hypothesis was not supported by observations with the VLCAD(1-40)-mCherry-EGFP mitophagy reporter, which we developed for mitophagy detection and quantification. This clearly indicated that IGF-1 stimulation in serum-starved cultures in fact suppressed total mitophagy levels. Ectopic expression of WT BNIP3 in MCF-7 cells also reduced autophagic flux in response to DFP-induced mitophagy, suggesting that BNIP3 reduces autophagosome turnover and potentially mitophagy under these conditions. However, WT BNIP3 did not affect the degree of mitophagy induced by DFP (measured with the VLCAD(1-40)-mCherry-EGFP reporter), indicating that the observed reduction in autophagic flux must be due to downregulation of general autophagy, not mitochondrial clearance. WT BNIP3 also reduced overall autophagic flux in complete medium cultures lacking mitophagy stimuli, and suppression of BNIP3 with siRNA reduced protein levels of the autophagy marker p62. These results implicate BNIP3 in the regulation of general autophagy. One explanation for these observations is that IGF-1 reduces total levels of mitophagy by inhibiting macro-autophagy (as would be expected from mTORC1 activation), and this masks a low level of mitophagy that is mediated by BNIP3 in serum-starved cultures.

A mitophagy-activating role for BNIP3 in cancer cells is further supported by the observation that suppression of BNIP3 caused accumulation of the mitochondrial marker PHB1 in MCF-7 cells. Furthermore, with the VLCAD(1-40)-mCherry-EGFP mitophagy reporter it was demonstrated that in complete medium cultures, inhibition of GSK-3β, which was associated with induction of BNIP3, increased mitophagy. Colocalisation studies with endogenous BNIP3 or ectopically expressed mCherry-BNIP3 and EGFP-LC3, which coats autophagosomes, also indicated that IGF-1 induces BNIP3-mediated mitophagy in cancer cells.

Interestingly, ectopic expression of WT BNIP3 enhanced CCCP-induced mitophagy as measured using the VLCAD(1-40)-mCherry-EGFP reporter. This was not observed with LIR-mutant BNIP3, indicating this effect required the LIR domain in BNIP3 to recruit autophagosomes to mitochondria. It was somewhat surprising that BNIP3 enhanced CCCP-induced mitophagy because this is associated with PINK1/Parkin mitophagy (Kawajiri et al., 2010b, Matsuda et al., 2010). However, BNIP3 can enhance PINK1-mediated mitophagy (Zhang et al., 2016), suggesting cross-talk between the two pathways. Potential overlap in the BNIP3 and PHB2 pathways for mitophagy was also suggested by the observation that suppression of PHB2 affected the Nrf2-BNIP3 axis in MCF-7 cells by reducing basal levels of both proteins. The existence of such a multitude of mitophagy pathways and the potential for crosstalk between them highlights the importance of mitochondrial maintenance.

Overall, the results suggest that IGF-1 induces low levels of mitophagy through BNIP3 in a highly controlled and specific manner, while downregulating macro-autophagy. The pathway through which IGF-1 regulates BNIP3 was established in this thesis and Riis et al. 2020 and is illustrated in Figure 6.1. However, it remains to be firmly demonstrated that IGF-1 promotes only the mitophagy function of BNIP3. Interestingly, a truncated version of BNIP3 exists, which lacks the cell death promoting domains and thus predominantly mediates mitophagy. This truncated version was found to be highly expressed in MCF-7 cells and other cancer cell lines, which further supports the involvement of IGF-1-induced BNIP3 in mitophagy promotion in these cells (Gang et al., 2015). Furthermore, as BNIP3 function has been shown to depend on its phosphorylation status (Zhu et al., 2013, Liu and Frazier, 2015), it is possible that IGF-1 signalling could promote phosphorylation of BNIP3 to enhance its mitophagy activity rather than inducing cell death. Besides its implications

in mitophagy and cell death, it was shown that BNIP3 can regulate the actin cytoskeleton to promote cell migration in tumour cells (Maes et al., 2014), similar to its role in promoting hypoxia-induced keratinocyte migration during wound healing (Zhang et al., 2017). If IGF-1-induced BNIP3 supports cell migration, this could contribute to the pro-tumourogenic aspects of IGF-1 signalling. Due to these complexities, further studies are required to fully elucidate the role of the IGF-1-Nrf2-BNIP3 pathway.

In these mitophagy studies, we employed various tools including colocalisation studies, western blotting, and the newly developed VLCAD(1-40)-mCherry-EGFP reporter, emphasizing the complexity of mitophagic mechanisms and the importance of expanding the existing repertoire of mitophagy-detection tools to enable us to interpret data in an informed and comprehensive way. When designing the reporter, we opted to use an IMM targeting sequence rather than an OMM targeting sequence. This was to ensure the sensitive detection of fully engulfed mitochondria and to prevent potentially detecting other mitochondria-associated organelles such as the endoplasmic reticulum (Copeland and Dalton, 1959, Csordas et al., 2006). A limitation to use of the reporter is that it requires thorough analysis of each field of view, which is time-consuming. Attempts at automating the detection and quantification of cells with red-only puncta were unsuccessful but such software would likely improve both the speed and objectivity of the analyses. Of note, the commercially available MitoTimer plasmid (Hernandez et al., 2013) was also tested but to no success. This is an inducible mitochondria-targeted fluorescent reporter. It fluoresces green initially, but this changes to red over time due to oxidation at the mitochondria. Thus, green mitochondria are newly synthesised, whereas red mitochondria represent aged ones. Therefore, the ratio of green to red fluorescence

should theoretically be informative of the speed at which mitochondria are turned over in the cells. Unfortunately, this reporter did not work in our setup and led us to further pursue the other approach, in which the function of the reporter was pH-dependent rather than time-dependent.

Due to time restrictions, the colocalisation experiments with ectopic mCherry-BNIP3 and EGFP-LC3 could unfortunately not be repeated thoroughly. However, the results were consistent with the observations from the colocalisation experiment of endogenous BNIP3 and EGFP-LC3 and, in conjunction with the other results presented in this thesis, they support our hypothesis.

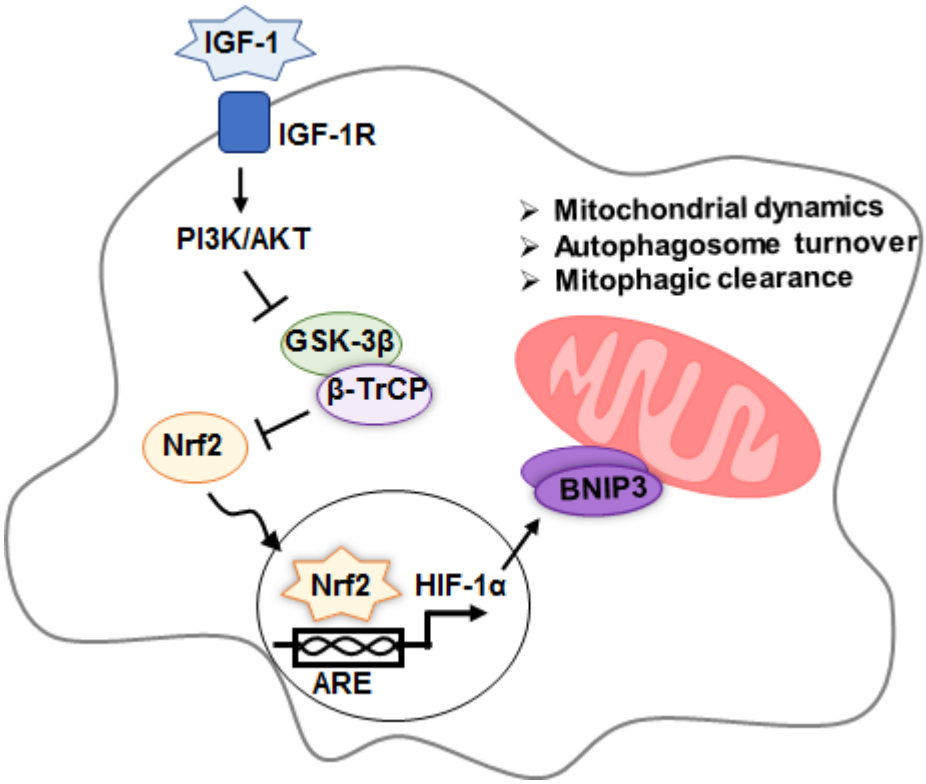

Figure 6.1 IGF-1 induces a mitophagy pathway through Nrf2 and BNIP3.

Schematic illustrating IGF-1-mediated inhibition of GSK-3β, which reduces interaction between β-TrCP and Nrf2, leading to Nrf2 activation. Nrf2 induces HIF-1α, and the induction of BNIP3 expression depends on both Nrf2 and HIF-1α. This pathway is associated with maintenance of mitochondrial morphology, autophagosome turnover in response to stress and efficient elimination of mitophagic vesicles.

The R- and R+ MEFs were used as an alternative model system to study how the presence or absence of IGF-1R signalling in a non-tumour model impacts on mitochondrial turnover. R- cells clearly exhibited reduced tolerance to both nutrient and mitochondrial stress compared to R+ cells, as indicated by induction of apoptosis. Of note, overexpression of BNIP3 in R- cells did not affect cell survival under these conditions, suggesting that increasing levels of this one component of the IGF-1 pathway is not sufficient to improve cellular capacity for stress responses.

Interestingly, both R- and R+ cell lines exhibited a high capacity for mitophagy induction. However, R- cells appeared unable to efficiently eliminate mitophagic vesicles and also accumulated vacuoles that indicated profound cell stress in response to mitophagy induction. R+ cells, on the other hand, recovered from these stresses over time. In general, IGF-1R signalling in R+ cells was associated with improved survival and enhanced induction of autophagosome turnover under conditions of cellular stress, as well as reduced sensitivity to BNIP3 suppression. Mitochondrial dynamics were also affected by IGF-1R signalling, as R- cells exhibited elongated mitochondria compared to small and rounded mitochondria in R+ cells. Similarly, suppression of components of the IGF-1R-Nrf2-BNIP3 pathway resulted in mitochondrial elongation in cancer cells. The IGF-1-mediated effects on mitochondrial biogenesis, dynamics and degradation are summarized in Figure 6.2.

We propose that IGF-1R signalling renders cells more stress-responsive by maintaining high levels of mitochondrial biogenesis and mitochondrial fission leading to a mitochondrial population that can be rapidly turned over when required. This could enhance mitochondrial function under non-stressed conditions and provide a strong overall survival signal in the challenging tumour environment.

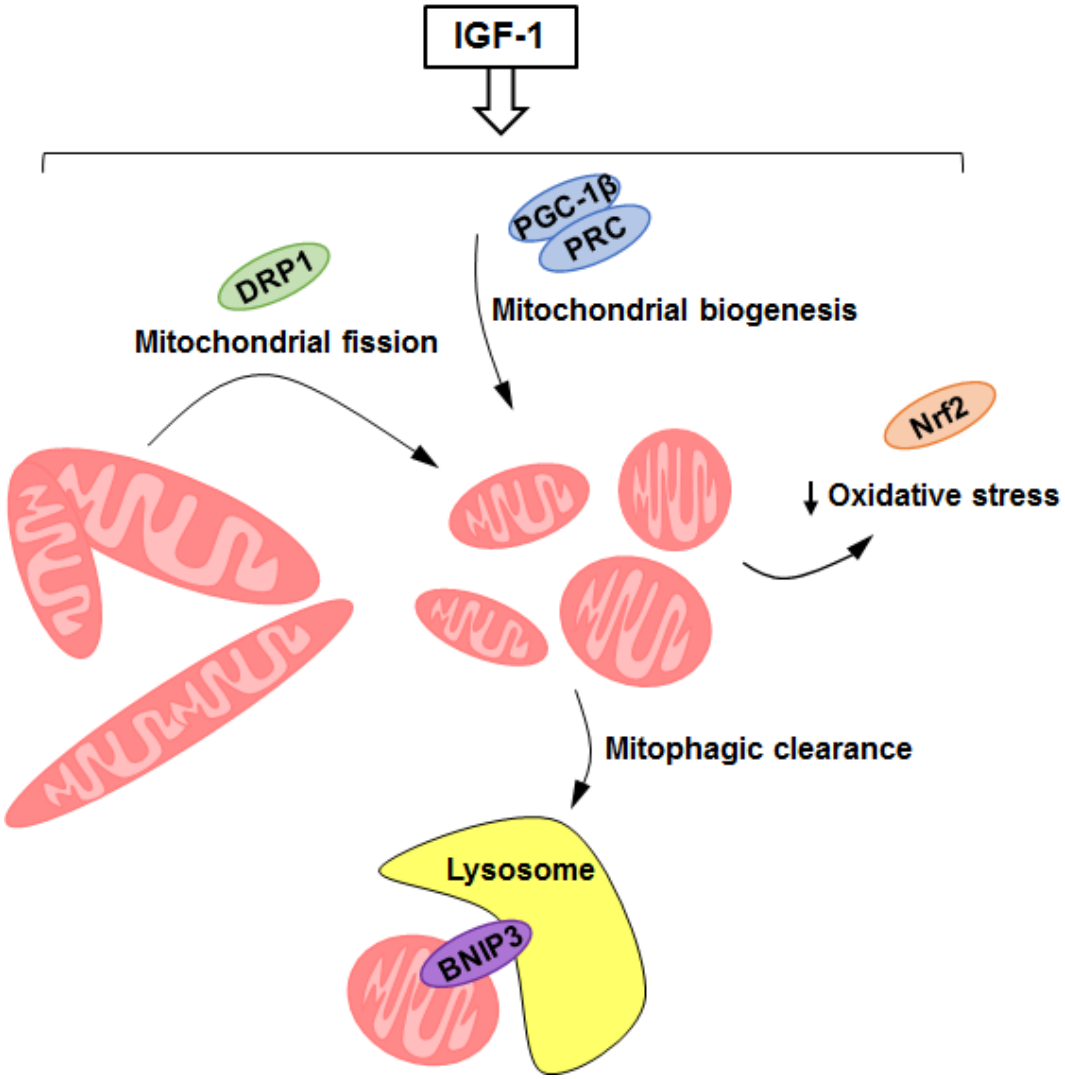

Figure 6.2 IGF-1 induces mitochondrial biogenesis, fission and mitophagy.

Schematic of the IGF-1 effects on mitochondrial dynamics and health. IGF-1 induces mitochondrial biogenesis through transcriptional co-activators PGC-1β and PRC, mitochondrial fission at least in part through regulation of DRP1, and mitophagy through BNIP3. This is associated with induction of Nrf2, which also mediates oxidative stress responses.

Overall, the results presented in this thesis reveal novel IGF-1 effects associated with the maintenance of mitochondrial health. IGF-1 couples the induction of mitochondrial biogenesis with the tightly controlled induction of BNIP3-specific mitophagy, likely to prevent accumulation of aged and dysfunctional mitochondria. This mitophagy pathway is mediated through Nrf2, placing this cytoprotective transcription factor under the regulation of IGF-1. Lack of IGF-1R signalling reduces

the capacity of cancer cells to mount a hypoxic mitophagy response and impairs mitophagic clearance and cell survival during stress responses in MEFs. This exposes a previously unknown vulnerability in these cells and suggest that combining IGF-1R inhibition with induction of mitochondrial stress may offer a promising therapeutic strategy for patients with IGF-1-responsive cancers. Combination therapies have been proposed to enhance the efficacy of IGF-1R inhibitors and reduce the likelihood of chemoresistance (Zhang et al., 2015, Ramcharan et al., 2015, O'Flanagan et al., 2016). While combination strategies involving IGF-1R inhibitors have shown some promise in clinical trials, there is still limited data showing a potent anti-cancer effect of such treatments (Quek et al., 2011, Schwartz et al., 2013, Wilky et al., 2015, Vlahovic et al., 2018). This emphasises that further work is required to determine which aspects of cellular function to co-target and how best to stratify patients for IGF-1R inhibitors.

Mitochondrial research has received a lot of attention in recent years, as mitochondrial dysfunction is implicated in numerous diseases including neurodegenerative disorders and diabetes, affecting many people worldwide (Annesley and Fisher, 2019). Dysregulation of the IGF-1 pathway has also been linked to these conditions (Torres Aleman, 2012, Nambam and Schatz, 2018), so perhaps we should ask, if IGF-1-effects on mitochondria may be of great importance to cellular health?

Here, we describe one mitophagy receptor, BNIP3, and the pathway through which it is regulated by IGF-1. However, it is likely that IGF-1 impacts on other mitophagy pathways as well. Nrf2 can regulate PINK1 expression, suggesting that IGF-1 may indirectly affect PINK1 activity through Nrf2 (Murata et al., 2015, Xiao et al., 2017). Interestingly, studies have indicated that PINK1 enhances IGF-1R and AKT activation to mediate neuronal protection, indicating retrograde communication from

the mitochondria to this signalling pathway (Akundi et al., 2012, Contreras-Zárate et al., 2015, Furlong et al., 2019). Besides mitophagy, there are several other aspects of mitochondrial function that IGF-1 appears able to regulate such as OXPHOS capacity (Aghanoori et al., 2019) and the mitochondrial apoptosis programme (Kang et al., 2003, Pang et al., 2007). Hopefully, future research will add to this thesis work and enlighten us regarding this complex signalling pathway and how to effectively modulate it to improve the management and outcome of the many diseases it affects.

Publications

Lyons A., Coleman M., **Riis S.**, Favre C., O'Flanagan C. H., Zhdanov A. V., Papkovsky D. B. Hursting S.D. and O'Connor R., Insulin-like growth factor 1 signaling is essential for mitochondrial biogenesis and mitophagy in cancer cells. J Biol Chem, 2017. 292(41):16983-16998.

Riis S., Murray J. B., and O'Connor R., IGF-1 Signalling Regulates Mitochondria Dynamics and Turnover through a Conserved GSK-3beta-Nrf2-BNIP3 Pathway. Cells, 2020. 9(1).

Bibliography

ADAMS, T. E., EPA, V. C., GARRETT, T. P. J. & WARD*, C. W. 2000. Structure and function of the type 1 insulin-like growth factor receptor. *Cellular and Molecular Life Sciences CMLS,* 57**,** 1050-1093.

AGHANOORI, M. R., SMITH, D. R., SHARIATI-IEVARI, S., AJISEBUTU, A., NGUYEN, A., DESMOND, F., JESUS, C. H. A., ZHOU, X., CALCUTT, N. A., ALIANI, M. & FERNYHOUGH, P. 2019. Insulin-like growth factor-1 activates AMPK to augment mitochondrial function and correct neuronal metabolism in sensory neurons in type 1 diabetes. *Mol Metab,* 20**,** 149-165.

AKIMOTO, T., POHNERT, S. C., LI, P., ZHANG, M., GUMBS, C., ROSENBERG, P. B., WILLIAMS, R. S. & YAN, Z. 2005. Exercise stimulates Pgc-1alpha transcription in skeletal muscle through activation of the p38 MAPK pathway. *J Biol Chem,* 280**,** 19587-93.

AKUNDI, R. S., ZHI, L. & BÜELER, H. 2012. PINK1 enhances insulin-like growth factor-1-dependent Akt signaling and protection against apoptosis. *Neurobiology of Disease,* 45**,** 469-478.

ALLEN, G. F., TOTH, R., JAMES, J. & GANLEY, I. G. 2013. Loss of iron triggers PINK1/Parkin-independent mitophagy. *EMBO Rep,* 14**,** 1127-35.

ANDE, S. R. & MISHRA, S. 2009. Prohibitin interacts with phosphatidylinositol 3,4,5-triphosphate (PIP3) and modulates insulin signaling. *Biochemical and Biophysical Research Communications,* 390**,** 1023-1028.

ANDERSSON, S., D'ARCY, P., LARSSON, O. & SEHAT, B. 2009. Focal adhesion kinase (FAK) activates and stabilizes IGF-1 receptor. *Biochemical and Biophysical Research Communications,* 387**,** 36-41.

ANDERSSON, U. & SCARPULLA, R. C. 2001. Pgc-1-related coactivator, a novel, serum-inducible coactivator of nuclear respiratory factor 1-dependent transcription in mammalian cells. *Molecular and cellular biology,* 21**,** 3738-3749.

ANDREWS, N. C., ERDJUMENT-BROMAGE, H., DAVIDSON, M. B., TEMPST, P. & ORKIN, S. H. 1993. Erythroid transcription factor NF-E2 is a haematopoietic-specific basic–leucine zipper protein. *Nature,* 362**,** 722-728.

ANICHTCHIK, O., DIEKMANN, H., FLEMING, A., ROACH, A., GOLDSMITH, P. & RUBINSZTEIN, D. C. 2008. Loss of PINK1 Function Affects Development and Results in Neurodegeneration in Zebrafish. 28**,** 8199-8207.

ANNESLEY, S. J. & FISHER, P. R. 2019. Mitochondria in Health and Disease. *Cells,* 8.

ARTAL-SANZ, M., TSANG, W. Y., WILLEMS, E. M., GRIVELL, L. A., LEMIRE, B. D., VAN DER SPEK, H. & NIJTMANS, L. G. 2003. The mitochondrial prohibitin complex is essential for embryonic viability and germline function in Caenorhabditis elegans. *J Biol Chem,* 278**,** 32091-9.

ATHALE, J., ULRICH, A., MACGARVEY, N. C., BARTZ, R. R., WELTY-WOLF, K. E., SULIMAN, H. B. & PIANTADOSI, C. A. 2012. Nrf2 promotes alveolar mitochondrial biogenesis and resolution of lung injury in Staphylococcus aureus pneumonia in mice. *Free radical biology & medicine,* 53**,** 1584-1594.

BACH, D., PICH, S., SORIANO, F. X., VEGA, N., BAUMGARTNER, B., ORIOLA, J., DAUGAARD, J. R., LLOBERAS, J., CAMPS, M., ZIERATH, J. R., RABASA-LHORET, R., WALLBERG-HENRIKSSON, H., LAVILLE, M., PALACíN, M., VIDAL, H., RIVERA, F., BRAND, M. & ZORZANO, A. 2003. Mitofusin-2 Determines Mitochondrial Network Architecture and Mitochondrial Metabolism: A NOVEL REGULATORY MECHANISM ALTERED IN OBESITY. 278**,** 17190-17197.

BAI, X., CHEN, Y., HOU, X., HUANG, M. & JIN, J. 2016. Emerging role of NRF2 in chemoresistance by regulating drug-metabolizing enzymes and efflux transporters. *Drug Metabolism Reviews,* 48**,** 541-567.

BAIRD, L. & DINKOVA-KOSTOVA, A. T. J. A. O. T. 2011. The cytoprotective role of the Keap1–Nrf2 pathway. 85**,** 241-272.

BALABAN, R. S., NEMOTO, S. & FINKEL, T. 2005. Mitochondria, Oxidants, and Aging. *Cell,* 120**,** 483-495.

BAREGAMIAN, N., SONG, J., JESCHKE, M. G., EVERS, B. M. & CHUNG, D. H. 2006. IGF-1 protects intestinal epithelial cells from oxidative stress-induced apoptosis. *The Journal of surgical research,* 136**,** 31-37.

BARNES, D. & SATO, G. 1980. Serum-free cell culture: a unifying approach. *Cell,* 22**,** 649-55.

BELLOT, G., GARCIA-MEDINA, R., GOUNON, P., CHICHE, J., ROUX, D., POUYSSÉGUR, J. & MAZURE, N. M. 2009. Hypoxia-Induced Autophagy Is Mediated through Hypoxia-Inducible Factor Induction of BNIP3 and BNIP3L via Their BH3 Domains. 29**,** 2570-2581.

BIJUR, G. N. & JOPE, R. S. 2003. Rapid accumulation of Akt in mitochondria following phosphatidylinositol 3-kinase activation. *Journal of Neurochemistry,* 87**,** 1427-1435.

BIRGISDOTTIR, Å. B., LAMARK, T. & JOHANSEN, T. 2013. The LIR motif – crucial for selective autophagy. 126**,** 3237-3247.

BJØRKØY, G., LAMARK, T., BRECH, A., OUTZEN, H., PERANDER, M., OVERVATN, A., STENMARK, H. & JOHANSEN, T. 2005. p62/SQSTM1 forms protein aggregates degraded by autophagy and has a protective effect on huntingtin-induced cell death. *J Cell Biol,* 171**,** 603-14.

BOWERS, L. W., ROSSI, E. L., O'FLANAGAN, C. H., DEGRAFFENRIED, L. A. & HURSTING, S. D. 2015. The Role of the Insulin/IGF System in Cancer: Lessons Learned from Clinical Trials and the Energy Balance-Cancer Link. 6.

BOYD, J. M., MALSTROM, S., SUBRAMANIAN, T., VENKATESH, L. K., SCHAEPER, U., ELANGOVAN, B., D'SA-EIPPER, C. & CHINNADURAI, G. 1994. Adenovirus E1B 19 kDa and Bcl-2 proteins interact with a common set of cellular proteins. *Cell,* 79**,** 341-351.

BURMAN, J. L., PICKLES, S., WANG, C., SEKINE, S., VARGAS, J. N. S., ZHANG, Z., YOULE, A. M., NEZICH, C. L., WU, X., HAMMER, J. A. & YOULE, R. J. 2017. Mitochondrial fission facilitates the selective mitophagy of protein aggregates. 216**,** 3231-3247.

BURTON, T. R., HENSON, E. S., BAIJAL, P., EISENSTAT, D. D. & GIBSON, S. B. 2006. The pro-cell death Bcl-2 family member, BNIP3, is localized to the nucleus of human glial cells: Implications for glioblastoma multiforme tumor cell survival under hypoxia. 118**,** 1660-1669.

CAO, Y.-L., MENG, S., CHEN, Y., FENG, J.-X., GU, D.-D., YU, B., LI, Y.-J., YANG, J.-Y., LIAO, S., CHAN, D. C. & GAO, S. 2017. MFN1 structures reveal nucleotide-triggered dimerization critical for mitochondrial fusion. *Nature,* 542**,** 372-376.

CARTER-SU, C., SCHWARTZ, J. & SMIT, L. S. 1996. Molecular mechanism of growth hormone action. *Annu Rev Physiol,* 58**,** 187-207.

CHAANINE, A. H., KOHLBRENNER, E., GAMB, S. I., GUENZEL, A. J., KLAUS, K., FAYYAZ, A. U., NAIR, K. S., HAJJAR, R. J. & REDFIELD, M. M. 2016. FOXO3a regulates BNIP3 and modulates mitochondrial calcium, dynamics, and function in cardiac stress. *American Journal of Physiology - Heart and Circulatory Physiology,* 311**,** H1540-H1559.

CHACINSKA, A., KOEHLER, C. M., MILENKOVIC, D., LITHGOW, T. & PFANNER, N. 2009. Importing Mitochondrial Proteins: Machineries and Mechanisms. *Cell,* 138**,** 628-644.

CHAN, D. C. 2019. Mitochondrial Dynamics and Its Involvement in Disease. *Annual review of pathology*, 10.1146/annurev-pathmechdis-012419-032711.
CHAN, J. Y., HAN, X. L. & KAN, Y. W. 1993. Cloning of Nrf1, an NF-E2-related transcription factor, by genetic selection in yeast. 90, 11371-11375.
CHANG, C.-R. & BLACKSTONE, C. 2010. Dynamic regulation of mitochondrial fission through modification of the dynamin-related protein Drp1. *Annals of the New York Academy of Sciences,* 1201, 34-39.
CHEN, L., MA, K., HAN, J., CHEN, Q. & ZHU, Y. 2017a. Monitoring Mitophagy in Mammalian Cells. *Methods Enzymol,* 588, 187-208.
CHEN, R., JIANG, T., SHE, Y., XU, J., LI, C., ZHOU, S., SHEN, H., SHI, H. & LIU, S. 2017b. Effects of Cobalt Chloride, a Hypoxia-Mimetic Agent, on Autophagy and Atrophy in Skeletal C2C12 Myotubes. *Biomed Res Int,* 2017, 7097580.
CHI, F., WU, R., ZENG, Y.-C., XING, R. & LIU, Y. 2013. Circulation insulin-like growth factor peptides and colorectal cancer risk: an updated systematic review and meta-analysis. *Molecular biology reports,* 40, 3583-3590.
CHINNADURAI, G., VIJAYALINGAM, S. & GIBSON, S. B. 2008. BNIP3 subfamily BH3-only proteins: mitochondrial stress sensors in normal and pathological functions. *Oncogene,* 27, S114-S127.
CHOE, S. C., HAMACHER-BRADY, A. & BRADY, N. R. 2015. Autophagy capacity and sub-mitochondrial heterogeneity shape Bnip3-induced mitophagy regulation of apoptosis. *Cell communication and signaling : CCS,* 13, 37-37.
CHOURASIA, A. H., BOLAND, M. L. & MACLEOD, K. F. 2015. Mitophagy and cancer. *Cancer & Metabolism,* 3, 4.
CHOWDHRY, S., ZHANG, Y., MCMAHON, M., SUTHERLAND, C., CUADRADO, A. & HAYES, J. D. 2013. Nrf2 is controlled by two distinct beta-TrCP recognition motifs in its Neh6 domain, one of which can be modulated by GSK-3 activity. *Oncogene,* 32, 3765-81.
CIAMPORCERO, E., DAGA, M., PIZZIMENTI, S., ROETTO, A., DIANZANI, C., COMPAGNONE, A., PALMIERI, A., ULLIO, C., CANGEMI, L., PILI, R. & BARRERA, G. 2018. Crosstalk between Nrf2 and YAP contributes to maintaining the antioxidant potential and chemoresistance in bladder cancer. *Free Radical Biology and Medicine,* 115, 447-457.
CLEMMONS, D. R., HORVITZ, G., ENGLEMAN, W., NICHOLS, T., MORALEZ, A. & NICKOLS, G. A. 1999. Synthetic alphaVbeta3 antagonists inhibit insulin-like growth factor-I-stimulated smooth muscle cell migration and replication. *Endocrinology,* 140, 4616-4621.
COGLIATI, S., ENRIQUEZ, J. A. & SCORRANO, L. 2016. Mitochondrial Cristae: Where Beauty Meets Functionality. *Trends in Biochemical Sciences,* 41, 261-273.
COHEN, P., ROGOL, A. D., HOWARD, C. P., BRIGHT, G. M., KAPPELGAARD, A.-M., ROSENFELD, R. G. & AMERICAN NORDITROPIN STUDY, G. 2007. Insulin growth factor-based dosing of growth hormone therapy in children: a randomized, controlled study. *The Journal of clinical endocrinology and metabolism,* 92, 2480-2486.
CONTRERAS-ZÁRATE, M. J., NIÑO, A., ROJAS, L., ARBOLEDA, H. & ARBOLEDA, G. 2015. Silencing of PINK1 Inhibits Insulin-Like Growth Factor-1-Mediated Receptor Activation and Neuronal Survival. *Journal of Molecular Neuroscience,* 56, 188-197.
COPELAND, D. E. & DALTON, A. J. 1959. An association between mitochondria and the endoplasmic reticulum in cells of the pseudobranch gland of a teleost. *J Biophys Biochem Cytol,* 5, 393-6.
CORNELISSEN, T., VILAIN, S., VINTS, K., GOUNKO, N., VERSTREKEN, P. & VANDENBERGHE, W. 2018. Deficiency of parkin and PINK1 impairs age-dependent mitophagy in Drosophila. *Elife,* 7.

CORTÉS-SEMPERE, M., DE MIGUEL, M. P., PERNÍA, O., RODRIGUEZ, C., DE CASTRO CARPEÑO, J., NISTAL, M., CONDE, E., LÓPEZ-RÍOS, F., BELDA-INIESTA, C., PERONA, R. & DE CACERES, I. I. 2013. IGFBP-3 methylation-derived deficiency mediates the resistance to cisplatin through the activation of the IGFIR/Akt pathway in non-small cell lung cancer. *Oncogene,* 32**,** 1274-1283.

COWAN, D. B., JONES, M., GARCIA, L. M., NORIA, S., NIDO, P. J. D. & MCGOWAN, F. X. 2003. Hypoxia and Stretch Regulate Intercellular Communication in Vascular Smooth Muscle Cells Through Reactive Oxygen Species Formation. 23**,** 1754-1760.

CRIDER, B. P., XIE, X. S. & STONE, D. K. 1994. Bafilomycin inhibits proton flow through the H+ channel of vacuolar proton pumps. *J Biol Chem,* 269**,** 17379-81.

CROSS, D. A. E., ALESSI, D. R., COHEN, P., ANDJELKOVICH, M. & HEMMINGS, B. A. 1995. Inhibition of glycogen synthase kinase-3 by insulin mediated by protein kinase B. *Nature,* 378**,** 785-789.

CSORDAS, G., RENKEN, C., VARNAI, P., WALTER, L., WEAVER, D., BUTTLE, K. F., BALLA, T., MANNELLA, C. A. & HAJNOCZKY, G. 2006. Structural and functional features and significance of the physical linkage between ER and mitochondria. *J Cell Biol,* 174**,** 915-21.

DEEVI, R. K., COX, O. T. & O'CONNOR, R. 2014. Essential function for PDLIM2 in cell polarization in three-dimensional cultures by feedback regulation of the β1-integrin-RhoA signaling axis. *Neoplasia (New York, N.Y.),* 16**,** 422-431.

DELAUNAY-MOISAN, A. & APPENZELLER-HERZOG, C. 2015. The antioxidant machinery of the endoplasmic reticulum: Protection and signaling. *Free Radical Biology and Medicine,* 83**,** 341-351.

DENDULURI, S. K., IDOWU, O., WANG, Z., LIAO, Z., YAN, Z., MOHAMMED, M. K., YE, J., WEI, Q., WANG, J., ZHAO, L. & LUU, H. H. 2015. Insulin-like growth factor (IGF) signaling in tumorigenesis and the development of cancer drug resistance. *Genes & Diseases,* 2**,** 13-25.

DENLEY, A., COSGROVE, L. J., BOOKER, G. W., WALLACE, J. C. & FORBES, B. E. 2005. Molecular interactions of the IGF system. *Cytokine & Growth Factor Reviews,* 16**,** 421-439.

DEVI, T. S., YUMNAMCHA, T., YAO, F., SOMAYAJULU, M., KOWLURU, R. A. & SINGH, L. P. 2019. TXNIP mediates high glucose-induced mitophagic flux and lysosome enlargement in human retinal pigment epithelial cells. *Biol Open,* 8.

DICKEY, A., SCHLEICHER, S., LEAHY, K., HU, R., HALLAHAN, D. & THOTALA, D. K. 2011. GSK-3β inhibition promotes cell death, apoptosis, and in vivo tumor growth delay in neuroblastoma Neuro-2A cell line. *Journal of neuro-oncology,* 104**,** 145-153.

DINKOVA-KOSTOVA, A. T. & ABRAMOV, A. Y. 2015. The emerging role of Nrf2 in mitochondrial function. *Free Radical Biology and Medicine,* 88, Part B**,** 179-188.

DOBLE, B. W., PATEL, S., WOOD, G. A., KOCKERITZ, L. K. & WOODGETT, J. R. 2007. Functional redundancy of GSK-3alpha and GSK-3beta in Wnt/beta-catenin signaling shown by using an allelic series of embryonic stem cell lines. *Developmental cell,* 12**,** 957-971.

DRAKE, L. E., SPRINGER, M. Z., POOLE, L. P., KIM, C. J. & MACLEOD, K. F. 2017. Expanding perspectives on the significance of mitophagy in cancer. *Seminars in Cancer Biology,* 47**,** 110-124.

DU, Y., LI, J., XU, T., ZHOU, D.-D., ZHANG, L. & WANG, X. 2017. MicroRNA-145 induces apoptosis of glioma cells by targeting BNIP3 and Notch signaling. *Oncotarget,* 8**,** 61510-61527.

DUNN, S. E., HARDMAN, R. A., KARI, F. W. & BARRETT, J. C. 1997. Insulin-like growth factor 1 (IGF-1) alters drug sensitivity of HBL100 human breast cancer cells by inhibition of apoptosis induced by diverse anticancer drugs. *Cancer research,* 57**,** 2687-2693.

EBNER, M., LUCIC, I., LEONARD, T. A. & YUDUSHKIN, I. 2017. PI(3,4,5)P3 Engagement Restricts Akt Activity to Cellular Membranes. *Mol Cell,* 65**,** 416-431 e6.

ESTEBAN-MARTINEZ, L. & BOYA, P. 2017. BNIP3L/NIX-dependent mitophagy regulates cell differentiation via metabolic reprogramming. *Autophagy***,** 0.

FAJKA-BOJA, R., MARTON, A., TÓTH, A., BLAZSÓ, P., TUBAK, V., BÁLINT, B., NAGY, I., HEGEDŰS, Z., VIZLER, C. & KATONA, R. L. 2018. Increased insulin-like growth factor 1 production by polyploid adipose stem cells promotes growth of breast cancer cells. *BMC Cancer,* 18**,** 872.

FARABAUGH, S. M., BOONE, D. N. & LEE, A. V. 2015. Role of IGF1R in Breast Cancer Subtypes, Stemness, and Lineage Differentiation. 6.

FAVRE, C., ZHDANOV, A., LEAHY, M., PAPKOVSKY, D. & O'CONNOR, R. 2010. Mitochondrial pyrimidine nucleotide carrier (PNC1) regulates mitochondrial biogenesis and the invasive phenotype of cancer cells. *Oncogene,* 29**,** 3964-3976.

FEINBERG, M. S., SCHEINOWITZ, M. & LARON, Z. 2000. Echocardiographic dimensions and function in adults with primary growth hormone resistance (Laron Syndrome). *The American Journal of Cardiology,* 85**,** 209-213.

FERNÁNDEZ, M., SÁNCHEZ-FRANCO, F., PALACIOS, N., SÁNCHEZ, I., FERNÁNDEZ, C. & CACICEDO, L. 2004. IGF-I inhibits apoptosis through the activation of the phosphatidylinositol 3-kinase/Akt pathway in pituitary cells. *Journal of molecular endocrinology,* 33**,** 155-163.

FERNANDEZ, R., TABARINI, D., AZPIAZU, N., FRASCH, M. & SCHLESSINGER, J. 1995. The Drosophila insulin receptor homolog: a gene essential for embryonic development encodes two receptor isoforms with different signaling potential. *EMBO J,* 14**,** 3373-84.

FLOYD, S., FAVRE, C., LASORSA, F. M., LEAHY, M., TRIGIANTE, G., STROEBEL, P., MARX, A., LOUGHRAN, G., O'CALLAGHAN, K., MAROBBIO, C. M., SLOTBOOM, D. J., KUNJI, E. R., PALMIERI, F. & O'CONNOR, R. 2007. The insulin-like growth factor-I-mTOR signaling pathway induces the mitochondrial pyrimidine nucleotide carrier to promote cell growth. *Mol Biol Cell,* 18**,** 3545-55.

FONSECA, T. B., SÁNCHEZ-GUERRERO, Á., MILOSEVIC, I. & RAIMUNDO, N. 2019. Mitochondrial fission requires DRP1 but not dynamins. *Nature,* 570**,** E34-E42.

FOWDEN, A. L. 2003. The Insulin-like Growth Factors and feto-placental Growth. *Placenta,* 24**,** 803-812.

FRANK, M., DUVEZIN-CAUBET, S., KOOB, S., OCCHIPINTI, A., JAGASIA, R., PETCHERSKI, A., RUONALA, M. O., PRIAULT, M., SALIN, B. & REICHERT, A. S. 2012. Mitophagy is triggered by mild oxidative stress in a mitochondrial fission dependent manner. *Biochimica et Biophysica Acta (BBA) - Molecular Cell Research,* 1823**,** 2297-2310.

FRANSEN, M., NORDGREN, M., WANG, B. & APANASETS, O. 2012. Role of peroxisomes in ROS/RNS-metabolism: Implications for human disease. *Biochimica et Biophysica Acta (BBA) - Molecular Basis of Disease,* 1822**,** 1363-1373.

FREUDE, S., HETTICH, M. M., SCHUMANN, C., STÖHR, O., KOCH, L., KÖHLER, C., UDELHOVEN, M., LEESER, U., MÜLLER, M., KUBOTA, N., KADOWAKI, T., KRONE, W., SCHRÖDER, H., BRÜNING, J. C. & SCHUBERT, M. 2009. Neuronal IGF-1 resistance reduces Abeta accumulation and protects against premature death in a model of Alzheimer's disease. *FASEB journal : official publication of the Federation of American Societies for Experimental Biology,* 23**,** 3315-3324.

FREY, T. G., RENKEN, C. W. & PERKINS, G. A. 2002. Insight into mitochondrial structure and function from electron tomography. *Biochimica et Biophysica Acta (BBA) - Bioenergetics,* 1555**,** 196-203.

FRIEDMAN, J. R. & NUNNARI, J. 2014. Mitochondrial form and function. *Nature,* 505**,** 335.

FRUMAN, D. A., CHIU, H., HOPKINS, B. D., BAGRODIA, S., CANTLEY, L. C. & ABRAHAM, R. T. 2017. The PI3K Pathway in Human Disease. *Cell,* 170**,** 605-635.

FU, M., ST-PIERRE, P., SHANKAR, J., WANG, P. T. C., JOSHI, B. & NABI, I. R. 2013a. Regulation of mitophagy by the Gp78 E3 ubiquitin ligase. *Molecular biology of the cell,* 24**,** 1153-1162.

FU, P., YANG, Z. & BACH, L. A. 2013b. Prohibitin-2 binding modulates insulin-like growth factor-binding protein-6 (IGFBP-6)-induced rhabdomyosarcoma cell migration. *J Biol Chem,* 288**,** 29890-900.

FU, W., LIU, Y. & YIN, H. 2019. Mitochondrial Dynamics: Biogenesis, Fission, Fusion, and Mitophagy in the Regulation of Stem Cell Behaviors. *Stem cells international,* 2019**,** 9757201-9757201.

FURLONG, R. M., LINDSAY, A., ANDERSON, K. E., HAWKINS, P. T., SULLIVAN, A. M. & O'NEILL, C. 2019. The Parkinson's disease gene PINK1 activates Akt via PINK1 kinase-dependent regulation of the phospholipid PI(3,4,5)P3. *J Cell Sci,* 132.

FURUKAWA, M. & XIONG, Y. 2005. BTB protein Keap1 targets antioxidant transcription factor Nrf2 for ubiquitination by the Cullin 3-Roc1 ligase. *Mol Cell Biol,* 25**,** 162-71.

FUTAWAKA, K., TAGAMI, T., FUKUDA, Y., KOYAMA, R., NUSHIDA, A., NEZU, S., IMAMOTO, M., KASAHARA, M. & MORIYAMA, K. 2016. Growth hormone regulates the expression of UCP2 in myocytes. *Growth hormone & IGF research : official journal of the Growth Hormone Research Society and the International IGF Research Society,* 29**,** 57-62.

GALMES-PASCUAL, B. M., NADAL-CASELLAS, A., BAUZA-THORBRUGGE, M., SBERT-ROIG, M., GARCIA-PALMER, F. J., PROENZA, A. M., GIANOTTI, M. & LLADO, I. 2017. 17beta-estradiol improves hepatic mitochondrial biogenesis and function through PGC1B. *J Endocrinol,* 232**,** 297-308.

GANG, H., DHINGRA, R., LIN, J., HAI, Y., AVIV, Y., MARGULETS, V., HAMEDANI, M., THANASUPAWAT, T., LEYGUE, E., KLONISCH, T., DAVIE, J. R. & KIRSHENBAUM, L. A. 2015. PDK2-mediated alternative splicing switches Bnip3 from cell death to cell survival. *J Cell Biol,* 210**,** 1101-15.

GAO, F., CHEN, D., SI, J., HU, Q., QIN, Z., FANG, M. & WANG, G. 2015. The mitochondrial protein BNIP3L is the substrate of PARK2 and mediates mitophagy in PINK1/PARK2 pathway. *Hum Mol Genet,* 24**,** 2528-38.

GAO, M., WANG, J., LU, N., FANG, F., LIU, J. & WONG, C. W. 2011. Mitogen-activated protein kinase kinases promote mitochondrial biogenesis in part through inducing peroxisome proliferator-activated receptor gamma coactivator-1beta expression. *Biochim Biophys Acta,* 1813**,** 1239-44.

GIANNAKOU, M. E. & PARTRIDGE, L. 2007. Role of insulin-like signalling in Drosophila lifespan. *Trends in Biochemical Sciences,* 32**,** 180-188.

GILKERSON, R. W., SELKER, J. M. L. & CAPALDI, R. A. 2003. The cristal membrane of mitochondria is the principal site of oxidative phosphorylation. 546**,** 355-358.

GLUCKMAN, P. D., JOHNSON-BARRETT, J. J., BUTLER, J. H., EDGAR, B. W. & GUNN, T. R. 1983. Studies of insulin-like growth factor -I and -II by specific radioligand assays in umbilical cord blood. *Clin Endocrinol (Oxf),* 19**,** 405-13.

GOMES, L. C., BENEDETTO, G. D. & SCORRANO, L. 2011. During autophagy mitochondria elongate, are spared from degradation and sustain cell viability. *Nat Cell Biol,* 13**,** 589-598.

GOMES, L. C. & SCORRANO, L. 2008. High levels of Fis1, a pro-fission mitochondrial protein, trigger autophagy. *Biochimica et Biophysica Acta (BBA) - Bioenergetics,* 1777**,** 860-866.

GONTIER, G., GEORGE, C., CHAKER, Z., HOLZENBERGER, M. & AÏD, S. 2015. Blocking IGF Signaling in Adult Neurons Alleviates Alzheimer's Disease Pathology through

Amyloid-β Clearance. *The Journal of neuroscience : the official journal of the Society for Neuroscience,* 35**,** 11500-11513.
GRAHAM, R. M., THOMPSON, J. W. & WEBSTER, K. A. 2015. BNIP3 promotes calcium and calpain-dependent cell death. *Life sciences,* 142**,** 26-35.
GRAHAM, R. M., THOMPSON, J. W., WEI, J., BISHOPRIC, N. H. & WEBSTER, K. A. 2007. Regulation of Bnip3 death pathways by calcium, phosphorylation, and hypoxia-reoxygenation. *Antioxid Redox Signal,* 9**,** 1309-15.
GRAY, M. W. 2017. Lynn Margulis and the endosymbiont hypothesis: 50 years later. *Molecular Biology of the Cell,* 28**,** 1285-1287.
GUBBI, S., QUIPILDOR, G. F., BARZILAI, N., HUFFMAN, D. M. & MILMAN, S. 2018. 40 YEARS of IGF1: IGF1: the Jekyll and Hyde of the aging brain. *Journal of molecular endocrinology,* 61**,** T171-T185.
GUEVARA-AGUIRRE, J., GUEVARA, A., PALACIOS, I., PÉREZ, M., PRÓCEL, P. & TERÁN, E. 2018. GH and GHR signaling in human disease. *Growth Hormone & IGF Research,* 38**,** 34-38.
GUO, K., SEARFOSS, G., KROLIKOWSKI, D., PAGNONI, M., FRANKS, C., CLARK, K., YU, K. T., JAYE, M. & IVASHCHENKO, Y. 2001. Hypoxia induces the expression of the pro-apoptotic gene BNIP3. *Cell Death & Differentiation,* 8**,** 367-376.
HAKUNO, F. & TAKAHASHI, S. I. 2018. IGF1 receptor signaling pathways. *J Mol Endocrinol,* 61**,** T69-T86.
HALASCHEK-WIENER, J., KHATTRA, J. S., MCKAY, S., POUZYREV, A., STOTT, J. M., YANG, G. S., HOLT, R. A., JONES, S. J. M., MARRA, M. A., BROOKS-WILSON, A. R. & RIDDLE, D. L. 2005. Analysis of long-lived C. elegans daf-2 mutants using serial analysis of gene expression. 15**,** 603-615.
HANNA, R. A., QUINSAY, M. N., OROGO, A. M., GIANG, K., RIKKA, S. & GUSTAFSSON, Å. B. 2012. Microtubule-associated Protein 1 Light Chain 3 (LC3) Interacts with Bnip3 Protein to Selectively Remove Endoplasmic Reticulum and Mitochondria via Autophagy. 287**,** 19094-19104.
HARDIE, D. G. 2011. AMPK and autophagy get connected. *The EMBO journal,* 30**,** 634-635.
HAWKINS, KATE E., JOY, S., DELHOVE, JULIETTE M. K. M., KOTIADIS, VASSILIOS N., FERNANDEZ, E., FITZPATRICK, LORNA M., WHITEFORD, JAMES R., KING, PETER J., BOLANOS, JUAN P., DUCHEN, MICHAEL R., WADDINGTON, SIMON N. & MCKAY, TRISTAN R. 2016. NRF2 Orchestrates the Metabolic Shift during Induced Pluripotent Stem Cell Reprogramming. *Cell Rep,* 14**,** 1883-1891.
HAYDEN, A., DOUGLAS, J., SOMMERLAD, M., ANDREWS, L., GOULD, K., HUSSAIN, S., THOMAS, G. J., PACKHAM, G. & CRABB, S. J. 2014. The Nrf2 transcription factor contributes to resistance to cisplatin in bladder cancer. *Urologic Oncology: Seminars and Original Investigations,* 32**,** 806-814.
HERNANDEZ, G., THORNTON, C., STOTLAND, A., LUI, D., SIN, J., RAMIL, J., MAGEE, N., ANDRES, A., QUARATO, G., CARREIRA, R. S., SAYEN, M. R., WOLKOWICZ, R. & GOTTLIEB, R. A. 2013. MitoTimer: a novel tool for monitoring mitochondrial turnover. *Autophagy,* 9**,** 1852-61.
HOCK, M. B. & KRALLI, A. 2009. Transcriptional Control of Mitochondrial Biogenesis and Function. 71**,** 177-203.
HOLZENBERGER, M., DUPONT, J., DUCOS, B., LENEUVE, P., GÉLOËN, A., EVEN, P. C., CERVERA, P. & LE BOUC, Y. 2003. IGF-1 receptor regulates lifespan and resistance to oxidative stress in mice. *Nature,* 421**,** 182-187.
HONN, K. V., SINGLEY, J. A. & CHAVIN, W. 1975. Fetal bovine serum: a multivariate standard. *Proc Soc Exp Biol Med,* 149**,** 344-7.

HUAT, T. J., KHAN, A. A., PATI, S., MUSTAFA, Z., ABDULLAH, J. M. & JAAFAR, H. 2014. IGF-1 enhances cell proliferation and survival during early differentiation of mesenchymal stem cells to neural progenitor-like cells. *BMC Neuroscience,* 15**,** 91.

ICHIMURA, Y., WAGURI, S., SOU, Y.-S., KAGEYAMA, S., HASEGAWA, J., ISHIMURA, R., SAITO, T., YANG, Y., KOUNO, T., FUKUTOMI, T., HOSHII, T., HIRAO, A., TAKAGI, K., MIZUSHIMA, T., MOTOHASHI, H., LEE, M.-S., YOSHIMORI, T., TANAKA, K., YAMAMOTO, M. & KOMATSU, M. 2013. Phosphorylation of p62 Activates the Keap1-Nrf2 Pathway during Selective Autophagy. *Molecular Cell,* 51**,** 618-631.

IKENO, Y., HUBBARD, G. B., LEE, S., CORTEZ, L. A., LEW, C. M., WEBB, C. R., BERRYMAN, D. E., LIST, E. O., KOPCHICK, J. J. & BARTKE, A. 2009. Reduced Incidence and Delayed Occurrence of Fatal Neoplastic Diseases in Growth Hormone Receptor/Binding Protein Knockout Mice. *The Journals of Gerontology: Series A,* 64A**,** 522-529.

ISHIHARA, M., URUSHIDO, M., HAMADA, K., MATSUMOTO, T., SHIMAMURA, Y., OGATA, K., INOUE, K., TANIGUCHI, Y., HORINO, T., FUJIEDA, M., FUJIMOTO, S. & TERADA, Y. 2013. Sestrin-2 and BNIP3 regulate autophagy and mitophagy in renal tubular cells in acute kidney injury. *Am J Physiol Renal Physiol,* 305**,** F495-509.

ISING, C., KOEHLER, S., BRAHLER, S., MERKWIRTH, C., HOHNE, M., BARIS, O. R., HAGMANN, H., KANN, M., FABRETTI, F., DAFINGER, C., BLOCH, W., SCHERMER, B., LINKERMANN, A., BRUNING, J. C., KURSCHAT, C. E., MULLER, R. U., WIESNER, R. J., LANGER, T., BENZING, T. & BRINKKOETTER, P. T. 2015. Inhibition of insulin/IGF-1 receptor signaling protects from mitochondria-mediated kidney failure. *EMBO Mol Med,* 7**,** 275-87.

ITOH, S., SAITO, T., HIRATA, M., USHITA, M., IKEDA, T., WOODGETT, J. R., ALGÜL, H., SCHMID, R. M., CHUNG, U. I. & KAWAGUCHI, H. 2012. GSK-3α and GSK-3β proteins are involved in early stages of chondrocyte differentiation with functional redundancy through RelA protein phosphorylation. *J Biol Chem,* 287**,** 29227-36.

JÄGER, S., HANDSCHIN, C., ST-PIERRE, J. & SPIEGELMAN, B. M. 2007. AMP-activated protein kinase (AMPK) action in skeletal muscle via direct phosphorylation of PGC-1alpha. *Proceedings of the National Academy of Sciences of the United States of America,* 104**,** 12017-12022.

JI, L., ZHANG, R., CHEN, J., XUE, Q., MOGHAL, N. & TSAO, M.-S. 2019. PIDD interaction with KEAP1 as a new mutation-independent mechanism to promote NRF2 stabilization and chemoresistance in NSCLC. *Scientific Reports,* 9**,** 12437.

JIANG, L., DONG, P., ZHANG, Z., LI, C., LI, Y., LIAO, Y., LI, X., WU, Z., GUO, S., MAI, S., XIE, D., LIU, Z. & ZHOU, F. 2015. Akt phosphorylates Prohibitin 1 to mediate its mitochondrial localization and promote proliferation of bladder cancer cells. *Cell Death Dis,* 6**,** e1660.

JIANG, P., DU, W., WANG, X., MANCUSO, A., GAO, X., WU, M. & YANG, X. 2011. p53 regulates biosynthesis through direct inactivation of glucose-6-phosphate dehydrogenase. *Nature Cell Biology,* 13**,** 310-316.

JIN, C., GUO, J., QIU, X., MA, K., XIANG, M., ZHU, X. & GUO, J. 2014. IGF-1 induces iNOS expression via the p38 MAPK signal pathway in the anti-apoptotic process in pulmonary artery smooth muscle cells during PAH. *J Recept Signal Transduct Res,* 34**,** 325-31.

JUAN, H.-C., TSAI, H.-T., CHANG, P.-H., HUANG, C.-Y. F., HU, C.-P. & WONG, F.-H. 2011. Insulin-like growth factor 1 mediates 5-fluorouracil chemoresistance in esophageal carcinoma cells through increasing survivin stability. *Apoptosis : an international journal on programmed cell death,* 16**,** 174-183.

JUHASZOVA, M., ZOROV, D. B., KIM, S. H., PEPE, S., FU, Q., FISHBEIN, K. W., ZIMAN, B. D., WANG, S., YTREHUS, K. & ANTOS, C. L. 2004. Glycogen synthase kinase-3beta

mediates convergence of protection signaling to inhibit the mitochondrial permeability transition pore. *J Clin Invest,* 113.

JUNG, C. H., RO, S. H., CAO, J., OTTO, N. M. & KIM, D. H. 2010. mTOR regulation of autophagy. *FEBS Lett,* 584**,** 1287-95.

KABEYA, Y., MIZUSHIMA, N., UENO, T., YAMAMOTO, A., KIRISAKO, T., NODA, T., KOMINAMI, E., OHSUMI, Y. & YOSHIMORI, T. 2000. LC3, a mammalian homologue of yeast Apg8p, is localized in autophagosome membranes after processing. *The EMBO journal,* 19**,** 5720-5728.

KABEYA, Y., MIZUSHIMA, N., YAMAMOTO, A., OSHITANI-OKAMOTO, S., OHSUMI, Y. & YOSHIMORI, T. 2004. LC3, GABARAP and GATE16 localize to autophagosomal membrane depending on form-II formation. *Journal of cell science,* 117**,** 2805-2812.

KANE, L. A., YOUNGMAN, M. J., JENSEN, R. E. & VAN EYK, J. E. 2010. Phosphorylation of the F(1)F(o) ATP synthase beta subunit: functional and structural consequences assessed in a model system. *Circulation research,* 106**,** 504-513.

KANG, B. P., URBONAS, A., BADDOO, A., BASKIN, S., MALHOTRA, A. & MEGGS, L. G. 2003. IGF-1 inhibits the mitochondrial apoptosis program in mesangial cells exposed to high glucose. *Am J Physiol Renal Physiol,* 285**,** F1013-24.

KANSANEN, E., KUOSMANEN, S. M., LEINONEN, H. & LEVONEN, A. L. 2013. The Keap1-Nrf2 pathway: Mechanisms of activation and dysregulation in cancer. *Redox Biol,* 1**,** 45-9.

KARATHEDATH, S., RAJAMANI, B. M., MUSHEER AALAM, S. M., ABRAHAM, A., VARATHARAJAN, S., KRISHNAMURTHY, P., MATHEWS, V., VELAYUDHAN, S. R. & BALASUBRAMANIAN, P. 2017. Role of NF-E2 related factor 2 (Nrf2) on chemotherapy resistance in acute myeloid leukemia (AML) and the effect of pharmacological inhibition of Nrf2. *PloS one,* 12**,** e0177227-e0177227.

KASPRZAK, A., KWASNIEWSKI, W., ADAMEK, A. & GOZDZICKA-JOZEFIAK, A. 2017. Insulin-like growth factor (IGF) axis in cancerogenesis. *Mutation Research/Reviews in Mutation Research,* 772**,** 78-104.

KATAYAMA, H., KOGURE, T., MIZUSHIMA, N., YOSHIMORI, T. & MIYAWAKI, A. 2011. A sensitive and quantitative technique for detecting autophagic events based on lysosomal delivery. *Chem Biol,* 18**,** 1042-52.

KATO, H., FARIA, T. N., STANNARD, B., ROBERTS, C. T., JR. & LEROITH, D. 1994. Essential role of tyrosine residues 1131, 1135, and 1136 of the insulin-like growth factor-I (IGF-I) receptor in IGF-I action. *Molecular endocrinology (Baltimore, Md.),* 8**,** 40-50.

KAWAJIRI, S., SAIKI, S., SATO, S., SATO, F., HATANO, T., EGUCHI, H. & HATTORI, N. 2010a. PINK1 is recruited to mitochondria with parkin and associates with LC3 in mitophagy. *FEBS Lett,* 584**,** 1073-9.

KAWAJIRI, S., SAIKI, S., SATO, S., SATO, F., HATANO, T., EGUCHI, H. & HATTORI, N. 2010b. PINK1 is recruited to mitochondria with parkin and associates with LC3 in mitophagy. 584**,** 1073-1079.

KENYON, C., CHANG, J., GENSCH, E., RUDNER, A. & TABTIANG, R. 1993. A C. elegans mutant that lives twice as long as wild type. *Nature,* 366**,** 461-464.

KHAMARI, R., TRINH, A., GABERT, P. E., CORAZAO-ROZAS, P., RIVEROS-CRUZ, S., BALAYSSAC, S., MALET-MARTINO, M., DEKIOUK, S., JONCQUEL CHEVALIER CURT, M., MABOUDOU, P., GARÇON, G., RAVASI, L., GUERRESCHI, P., MORTIER, L., QUESNEL, B., MARCHETTI, P. & KLUZA, J. 2018. Glucose metabolism and NRF2 coordinate the antioxidant response in melanoma resistant to MAPK inhibitors. *Cell Death & Disease,* 9**,** 325.

KIELY, P. A., O'GORMAN, D., LUONG, K., RON, D. & O'CONNOR, R. 2006. Insulin-Like Growth Factor I Controls a Mutually Exclusive Association of RACK1 with Protein Phosphatase 2A and β1 Integrin To Promote Cell Migration. 26**,** 4041-4051.

KIM, J.-Y., KIM, Y.-J., LEE, S. & PARK, J.-H. 2011. BNip3 is a mediator of TNF-induced necrotic cell death. *Apoptosis : an international journal on programmed cell death,* 16**,** 114-126.

KIMURA, K. D., TISSENBAUM, H. A., LIU, Y. & RUVKUN, G. 1997. daf-2, an insulin receptor-like gene that regulates longevity and diapause in Caenorhabditis elegans. *Science,* 277**,** 942-6.

KOBAYASHI, A., ITO, E., TOKI, T., KOGAME, K., TAKAHASHI, S., IGARASHI, K., HAYASHI, N. & YAMAMOTO, M. 1999. Molecular Cloning and Functional Characterization of a New Cap'n' Collar Family Transcription Factor Nrf3. 274**,** 6443-6452.

KOGURE, T., KARASAWA, S., ARAKI, T., SAITO, K., KINJO, M. & MIYAWAKI, A. 2006. A fluorescent variant of a protein from the stony coral Montipora facilitates dual-color single-laser fluorescence cross-correlation spectroscopy. *Nat Biotechnol,* 24**,** 577-81.

KÖHLE, C. & BOCK, K. W. 2007. Coordinate regulation of Phase I and II xenobiotic metabolisms by the Ah receptor and Nrf2. *Biochemical Pharmacology,* 73**,** 1853-1862.

KOMATSU, M., KUROKAWA, H., WAGURI, S., TAGUCHI, K., KOBAYASHI, A., ICHIMURA, Y., SOU, Y.-S., UENO, I., SAKAMOTO, A., TONG, K. I., KIM, M., NISHITO, Y., IEMURA, S.-I., NATSUME, T., UENO, T., KOMINAMI, E., MOTOHASHI, H., TANAKA, K. & YAMAMOTO, M. 2010. The selective autophagy substrate p62 activates the stress responsive transcription factor Nrf2 through inactivation of Keap1. *Nat Cell Biol,* 12**,** 213-223.

KONDAPALLI, C., KAZLAUSKAITE, A., ZHANG, N., WOODROOF, H. I., CAMPBELL, D. G., GOURLAY, R., BURCHELL, L., WALDEN, H., MACARTNEY, T. J., DEAK, M., KNEBEL, A., ALESSI, D. R. & MUQIT, M. M. 2012. PINK1 is activated by mitochondrial membrane potential depolarization and stimulates Parkin E3 ligase activity by phosphorylating Serine 65. *Open Biol,* 2**,** 120080.

KOROLCHUK, V. I., MANSILLA, A., MENZIES, F. M. & RUBINSZTEIN, D. C. 2009. Autophagy Inhibition Compromises Degradation of Ubiquitin-Proteasome Pathway Substrates. *Molecular Cell,* 33**,** 517-527.

KOTHARI, S., CIZEAU, J., MCMILLAN-WARD, E., ISRAELS, S. J., BAILES, M., ENS, K., KIRSHENBAUM, L. A. & GIBSON, S. B. 2003. BNIP3 plays a role in hypoxic cell death in human epithelial cells that is inhibited by growth factors EGF and IGF. *Oncogene,* 22**,** 4734-4744.

KOYANO, F., OKATSU, K., KOSAKO, H., TAMURA, Y., GO, E., KIMURA, M., KIMURA, Y., TSUCHIYA, H., YOSHIHARA, H., HIROKAWA, T., ENDO, T., FON, E. A., TREMPE, J.-F., SAEKI, Y., TANAKA, K. & MATSUDA, N. 2014. Ubiquitin is phosphorylated by PINK1 to activate parkin. *Nature,* 510**,** 162-166.

LAMBETH, J. D. 2004. NOX enzymes and the biology of reactive oxygen. *Nature Reviews Immunology,* 4**,** 181-189.

LAMPERT, M. A., OROGO, A. M., NAJOR, R. H., HAMMERLING, B. C., LEON, L. J., WANG, B. J., KIM, T., SUSSMAN, M. A. & GUSTAFSSON, Å. B. 2019. BNIP3L/NIX and FUNDC1-mediated mitophagy is required for mitochondrial network remodeling during cardiac progenitor cell differentiation. *Autophagy,* 15**,** 1182-1198.

LANDES, T., EMORINE, L. J., COURILLEAU, D., ROJO, M., BELENGUER, P. & ARNAUNÉ-PELLOQUIN, L. 2010. The BH3-only Bnip3 binds to the dynamin Opa1 to promote mitochondrial fragmentation and apoptosis by distinct mechanisms. *EMBO Reports,* 11**,** 459-465.

LARON, Z., GINSBERG, S., LILOS, P., ARBIV, M. & VAISMAN, N. 2006. Body composition in untreated adult patients with Laron syndrome (primary GH insensitivity). 65**,** 114-117.

LARON, Z. & KAULI, R. 2016. Fifty seven years of follow-up of the Israeli cohort of Laron Syndrome patients-From discovery to treatment. *Growth hormone & IGF research : official journal of the Growth Hormone Research Society and the International IGF Research Society,* 28**,** 53-56.

LASSARRE, C., HARDOUIN, S., DAFFOS, F., FORESTIER, F., FRANKENNE, F. & BINOUX, M. 1991. Serum Insulin-Like Growth Factors and Insulin-Like Growth Factor Binding Proteins in the Human Fetus. Relationships with Growth in Normal Subjects and in Subjects with Intrauterine Growth Retardation. *Pediatric Research,* 29**,** 219-225.

LAU, L., HANSFORD, L. M., CHENG, L. S., HANG, M., BARUCHEL, S., KAPLAN, D. R. & IRWIN, M. S. 2007. Cyclooxygenase inhibitors modulate the p53/HDM2 pathway and enhance chemotherapy-induced apoptosis in neuroblastoma. *Oncogene,* 26**,** 1920-1931.

LAZAROU, M., SLITER, D. A., KANE, L. A., SARRAF, S. A., WANG, C., BURMAN, J. L., SIDERIS, D. P., FOGEL, A. I. & YOULE, R. J. 2015. The ubiquitin kinase PINK1 recruits autophagy receptors to induce mitophagy. *Nature,* 524**,** 309-314.

LEE, H. J., JUNG, Y. H., CHOI, G. E., KO, S. H., LEE, S.-J., LEE, S. H. & HAN, H. J. 2017. BNIP3 induction by hypoxia stimulates FASN-dependent free fatty acid production enhancing therapeutic potential of umbilical cord blood-derived human mesenchymal stem cells. *Redox Biology,* 13**,** 426-443.

LEE, S., HALLIS, S. P., JUNG, K.-A., RYU, D. & KWAK, M.-K. 2019. Impairment of HIF-1α-mediated metabolic adaption by NRF2-silencing in breast cancer cells. *Redox Biology,* 24**,** 101210.

LEE, Y., LEE, H. Y., HANNA, R. A. & GUSTAFSSON, A. B. 2011. Mitochondrial autophagy by Bnip3 involves Drp1-mediated mitochondrial fission and recruitment of Parkin in cardiac myocytes. *Am J Physiol Heart Circ Physiol,* 301**,** H1924-31.

LI, J., CHOI, E., YU, H. & BAI, X.-C. 2019. Structural basis of the activation of type 1 insulin-like growth factor receptor. *Nature Communications,* 10**,** 4567.

LI, Y., WANG, Y., KIM, E., BEEMILLER, P., WANG, C.-Y., SWANSON, J., YOU, M. & GUAN, K.-L. 2007. Bnip3 Mediates the Hypoxia-induced Inhibition on Mammalian Target of Rapamycin by Interacting with Rheb. 282**,** 35803-35813.

LIANG, J., XIE, Q., LI, P., ZHONG, X., CHEN, Y. J. M. & BIOCHEMISTRY, C. 2015. Mitochondrial estrogen receptor β inhibits cell apoptosis via interaction with Bad in a ligand-independent manner. 401**,** 71-86.

LIN, M. G. & HURLEY, J. H. 2016. Structure and function of the ULK1 complex in autophagy. *Current Opinion in Cell Biology,* 39**,** 61-68.

LIU, J. P., BAKER, J., PERKINS, A. S., ROBERTSON, E. J. & EFSTRATIADIS, A. 1993. Mice carrying null mutations of the genes encoding insulin-like growth factor I (Igf-1) and type 1 IGF receptor (Igf1r). *Cell,* 75**,** 59-72.

LIU, K. E. & FRAZIER, W. A. 2015. Phosphorylation of the BNIP3 C-Terminus Inhibits Mitochondrial Damage and Cell Death without Blocking Autophagy. *PLoS One,* 10**,** e0129667.

LIU, L., FENG, D., CHEN, G., CHEN, M., ZHENG, Q., SONG, P., MA, Q., ZHU, C., WANG, R., QI, W., HUANG, L., XUE, P., LI, B., WANG, X., JIN, H., WANG, J., YANG, F., LIU, P., ZHU, Y., SUI, S. & CHEN, Q. 2012. Mitochondrial outer-membrane protein FUNDC1 mediates hypoxia-induced mitophagy in mammalian cells. *Nat Cell Biol,* 14**,** 177-85.

LIU, Y. C., LEU, C. M., WONG, F. H., FONG, W. S., CHEN, S. C., CHANG, C. & HU, C. 2002. Autocrine Stimulation by Insulin-Like Growth Factor I Is Involved in the Growth, Tumorigenicity and Chemoresistance of Human Esophageal Carcinoma Cells. *Journal of Biomedical Science,* 9**,** 665-674.

LIVAK, K. J. & SCHMITTGEN, T. D. 2001. Analysis of Relative Gene Expression Data Using Real-Time Quantitative PCR and the 2−ΔΔCT Method. *Methods,* 25**,** 402-408.

LO, J. Y., SPATOLA, B. N. & CURRAN, S. P. 2017. WDR23 regulates NRF2 independently of KEAP1. *PLoS Genet,* 13**,** e1006762.

LOBATÓN, C. D., VAY, L., HERNÁNDEZ-SANMIGUEL, E., SANTODOMINGO, J., MORENO, A., MONTERO, M. & ALVAREZ, J. 2005. Modulation of mitochondrial Ca(2+) uptake by estrogen receptor agonists and antagonists. *British journal of pharmacology,* 145**,** 862-871.

LOCASALE, J. W., GRASSIAN, A. R., MELMAN, T., LYSSIOTIS, C. A., MATTAINI, K. R., BASS, A. J., HEFFRON, G., METALLO, C. M., MURANEN, T., SHARFI, H., SASAKI, A. T., ANASTASIOU, D., MULLARKY, E., VOKES, N. I., SASAKI, M., BEROUKHIM, R., STEPHANOPOULOS, G., LIGON, A. H., MEYERSON, M., RICHARDSON, A. L., CHIN, L., WAGNER, G., ASARA, J. M., BRUGGE, J. S., CANTLEY, L. C. & VANDER HEIDEN, M. G. 2011. Phosphoglycerate dehydrogenase diverts glycolytic flux and contributes to oncogenesis. *Nature Genetics,* 43**,** 869-874.

LOGAN, S., PHARAOH, G. A., MARLIN, M. C., MASSER, D. R., MATSUZAKI, S., WRONOWSKI, B., YEGANEH, A., PARKS, E. E., PREMKUMAR, P., FARLEY, J. A., OWEN, D. B., HUMPHRIES, K. M., KINTER, M., FREEMAN, W. M., SZWEDA, L. I., VAN REMMEN, H. & SONNTAG, W. E. 2018. Insulin-like growth factor receptor signaling regulates working memory, mitochondrial metabolism, and amyloid-β uptake in astrocytes. *Molecular metabolism,* 9**,** 141-155.

LONG, X., XIONG, W., ZENG, X., QI, L., CAI, Y., MO, M., JIANG, H., ZHU, B., CHEN, Z. & LI, Y. 2019. Cancer-associated fibroblasts promote cisplatin resistance in bladder cancer cells by increasing IGF-1/ERβ/Bcl-2 signalling. *Cell Death & Disease,* 10**,** 375.

LOSCHEN, G., FLOHÉ, L. & CHANCE, B. 1971. Respiratory chain linked H2O2 production in pigeon heart mitochondria. *FEBS Letters,* 18**,** 261-264.

LYONS, A., COLEMAN, M., RIIS, S., FAVRE, C., O'FLANAGAN, C. H., ZHDANOV, A. V., PAPKOVSKY, D. B., HURSTING, S. D. & O'CONNOR, R. 2017. Insulin-like growth factor 1 signaling is essential for mitochondrial biogenesis and mitophagy in cancer cells. *J Biol Chem,* 292**,** 16983-16998.

MA, Z., CHEN, C., TANG, P., ZHANG, H., YUE, J. & YU, Z. 2017. BNIP3 induces apoptosis and protective autophagy under hypoxia in esophageal squamous cell carcinoma cell lines: BNIP3 regulates cell death. *Diseases of the Esophagus,* 30**,** 1-8.

MACGARVEY, N. C., SULIMAN, H. B., BARTZ, R. R., FU, P., WITHERS, C. M., WELTY-WOLF, K. E. & PIANTADOSI, C. A. 2012. Activation of mitochondrial biogenesis by heme oxygenase-1-mediated NF-E2-related factor-2 induction rescues mice from lethal Staphylococcus aureus sepsis. *American journal of respiratory and critical care medicine,* 185**,** 851-861.

MACHER-GOEPPINGER, S., KEITH, M., HATIBOGLU, G., HOHENFELLNER, M., SCHIRMACHER, P., ROTH, W. & TAGSCHERER, K. E. 2017. Expression and Functional Characterization of the BNIP3 Protein in Renal Cell Carcinomas. *Translational oncology,* 10**,** 869-875.

MAES, H., VAN EYGEN, S., KRYSKO, D. V., VANDENABEELE, P., NYS, K., RILLAERTS, K., GARG, A. D., VERFAILLIE, T. & AGOSTINIS, P. 2014. BNIP3 supports melanoma cell migration and vasculogenic mimicry by orchestrating the actin cytoskeleton. *Cell Death & Disease,* 5**,** e1127-e1127.

MAILLOUX, R. J. 2015. Teaching the fundamentals of electron transfer reactions in mitochondria and the production and detection of reactive oxygen species. *Redox Biology,* 4**,** 381-398.

MALDONADO, C., CEA, P., ADASME, T., COLLAO, A., DÍAZ-ARAYA, G., CHIONG, M. & LAVANDERO, S. 2005. IGF-1 protects cardiac myocytes from hyperosmotic stress-induced apoptosis via CREB. *Biochemical and biophysical research communications,* 336**,** 1112-1118.

MANNING, B. D. & CANTLEY, L. C. 2007. AKT/PKB signaling: navigating downstream. *Cell,* 129**,** 1261-1274.

MATSUDA, N., SATO, S., SHIBA, K., OKATSU, K., SAISHO, K., GAUTIER, C. A., SOU, Y. S., SAIKI, S., KAWAJIRI, S., SATO, F., KIMURA, M., KOMATSU, M., HATTORI, N. & TANAKA, K. 2010. PINK1 stabilized by mitochondrial depolarization recruits Parkin to damaged mitochondria and activates latent Parkin for mitophagy. *J Cell Biol,* 189**,** 211-21.

MATTINGLY, K. A., IVANOVA, M. M., RIGGS, K. A., WICKRAMASINGHE, N. S., BARCH, M. J. & KLINGE, C. M. 2008. Estradiol stimulates transcription of nuclear respiratory factor-1 and increases mitochondrial biogenesis. *Mol Endocrinol,* 22**,** 609-22.

MAUTHE, M., ORHON, I., ROCCHI, C., ZHOU, X., LUHR, M., HIJLKEMA, K. J., COPPES, R. P., ENGEDAL, N., MARI, M. & REGGIORI, F. 2018. Chloroquine inhibits autophagic flux by decreasing autophagosome-lysosome fusion. *Autophagy,* 14**,** 1435-1455.

MCMAHON, M., ITOH, K., YAMAMOTO, M., CHANAS, S. A., HENDERSON, C. J., MCLELLAN, L. I., WOLF, C. R., CAVIN, C. & HAYES, J. D. 2001. The Cap 'n' Collar Basic Leucine Zipper Transcription Factor Nrf2 (NF-E2 p45-related Factor 2) Controls Both Constitutive and Inducible Expression of Intestinal Detoxification and Glutathione Biosynthetic Enzymes. 61**,** 3299-3307.

MEGYESI, K., KAHN, C. R., ROTH, J., FROESCH, E. R., HUMBEL, R. E., ZAPF, J. & NEVILLE, D. M., JR. 1974. Insulin and non-suppressible insulin-like activity (NSILA-s): evidence for separate plasma membrane receptor sites. *Biochemical and biophysical research communications,* 57**,** 307-315.

MEGYESI, K., KAHN, C. R., ROTH, J., NEVILLE, D. M., JR., NISSLEY, S. P., HUMBEL, R. E. & FROESCH, E. R. 1975. The NSILA-s receptor in liver plasma membranes. Characterization and comparison with the insulin receptor. *The Journal of biological chemistry,* 250**,** 8990-8996.

MELLOR, H. R., ROUSCHOP, K. M., WIGFIELD, S. M., WOUTERS, B. G. & HARRIS, A. L. 2010. Synchronised phosphorylation of BNIP3, Bcl-2 and Bcl-xL in response to microtubule-active drugs is JNK-independent and requires a mitotic kinase. *Biochemical Pharmacology,* 79**,** 1562-1572.

MERKWIRTH, C., DARGAZANLI, S., TATSUTA, T., GEIMER, S., LOWER, B., WUNDERLICH, F. T., VON KLEIST-RETZOW, J. C., WAISMAN, A., WESTERMANN, B. & LANGER, T. 2008. Prohibitins control cell proliferation and apoptosis by regulating OPA1-dependent cristae morphogenesis in mitochondria. *Genes Dev,* 22**,** 476-88.

MERRY, T. L. & RISTOW, M. 2016. Nuclear factor erythroid-derived 2-like 2 (NFE2L2, Nrf2) mediates exercise-induced mitochondrial biogenesis and the anti-oxidant response in mice. *J Physiol,* 594**,** 5195-207.

MITTAL, M., SIDDIQUI, M. R., TRAN, K., REDDY, S. P. & MALIK, A. B. 2014. Reactive oxygen species in inflammation and tissue injury. *Antioxid Redox Signal,* 20**,** 1126-67.

MIZUSHIMA, N. & YOSHIMORI, T. 2007. How to interpret LC3 immunoblotting. *Autophagy,* 3**,** 542-5.

MODEL, K., MEISINGER, C. & KÜHLBRANDT, W. 2008. Cryo-Electron Microscopy Structure of a Yeast Mitochondrial Preprotein Translocase. *Journal of Molecular Biology,* 383**,** 1049-1057.

MOI, P., CHAN, K., ASUNIS, I., CAO, A. & KAN, Y. W. 1994. Isolation of NF-E2-related factor 2 (Nrf2), a NF-E2-like basic leucine zipper transcriptional activator that binds to the tandem NF-E2/AP1 repeat of the beta-globin locus control region. 91**,** 9926-9930.

MOISOI, N., FEDELE, V., EDWARDS, J. & MARTINS, L. M. 2014. Loss of PINK1 enhances neurodegeneration in a mouse model of Parkinson's disease triggered by mitochondrial stress. *Neuropharmacology,* 77.

MØLLER, N. & JØRGENSEN, J. O. L. 2009. Effects of growth hormone on glucose, lipid, and protein metabolism in human subjects. *Endocrine reviews,* 30**,** 152-177.

MOMCILOVIC, M., BAILEY, S. T., LEE, J. T., FISHBEIN, M. C., BRAAS, D., GO, J., GRAEBER, T. G., PARLATI, F., DEMO, S., LI, R., WALSER, T. C., GRICOWSKI, M., SHUMAN, R., IBARRA, J., FRIDMAN, D., PHELPS, M. E., BADRAN, K., ST JOHN, M., BERNTHAL, N. M., FEDERMAN, N., YANAGAWA, J., DUBINETT, S. M., SADEGHI, S., CHRISTOFK, H. R. & SHACKELFORD, D. B. 2018. The GSK3 Signaling Axis Regulates Adaptive Glutamine Metabolism in Lung Squamous Cell Carcinoma. *Cancer cell,* 33**,** 905-921.e5.

MORIYAMA, M., MORIYAMA, H., UDA, J., KUBO, H., NAKAJIMA, Y., GOTO, A., MORITA, T. & HAYAKAWA, T. 2017. BNIP3 upregulation via stimulation of ERK and JNK activity is required for the protection of keratinocytes from UVB-induced apoptosis. *Cell Death Dis,* 8**,** e2576.

MORIYAMA, M., MORIYAMA, H., UDA, J., MATSUYAMA, A., OSAWA, M. & HAYAKAWA, T. 2014. BNIP3 plays crucial roles in the differentiation and maintenance of epidermal keratinocytes. *J Invest Dermatol,* 134**,** 1627-1635.

MURATA, H., TAKAMATSU, H., LIU, S., KATAOKA, K., HUH, N. H. & SAKAGUCHI, M. 2015. NRF2 Regulates PINK1 Expression under Oxidative Stress Conditions. *PLoS One,* 10**,** e0142438.

MYERS, M. G., JR. & WHITE, M. F. 1996. Insulin signal transduction and the IRS proteins. *Annu Rev Pharmacol Toxicol,* 36**,** 615-58.

NAIK, E. & DIXIT, V. M. 2011. Mitochondrial reactive oxygen species drive proinflammatory cytokine production. *The Journal of experimental medicine,* 208**,** 417-420.

NAMBAM, B. & SCHATZ, D. 2018. Growth hormone and insulin-like growth factor-I axis in type 1 diabetes. *Growth Horm IGF Res,* 38**,** 49-52.

NARENDRA, D., TANAKA, A., SUEN, D. F. & YOULE, R. J. 2008. Parkin is recruited selectively to impaired mitochondria and promotes their autophagy. *J Cell Biol,* 183**,** 795-803.

NEY, P. A. 2015. Mitochondrial autophagy: Origins, significance, and role of BNIP3 and NIX. *Biochimica et Biophysica Acta (BBA) - Molecular Cell Research,* 1853**,** 2775-2783.

NIJTMANS, L. G. J., DE JONG, L., ARTAL SANZ, M., COATES, P. J., BERDEN, J. A., BACK, J. W., MUIJSERS, A. O., VAN DER SPEK, H. & GRIVELL, L. A. 2000. Prohibitins act as a membrane-bound chaperone for the stabilization of mitochondrial proteins. 19**,** 2444-2451.

NILSSON, R., JAIN, M., MADHUSUDHAN, N., SHEPPARD, N. G., STRITTMATTER, L., KAMPF, C., HUANG, J., ASPLUND, A. & MOOTHA, V. K. 2014. Metabolic enzyme expression highlights a key role for MTHFD2 and the mitochondrial folate pathway in cancer. *Nature Communications,* 5**,** 3128.

NISHIMURA, H., NAKAMURA, O., YAMAGAMI, Y., MORI, M., HORIE, R., FUKUOKA, N. & YAMAMOTO, T. 2016. GSK-3 inhibitor inhibits cell proliferation and induces apoptosis in human osteosarcoma cells. *Oncology reports,* 35**,** 2348-2354.

NIU, Y., LIN, Z., WAN, A., CHEN, H., LIANG, H., SUN, L., WANG, Y., LI, X., XIONG, X.-F., WEI, B., WU, X. & WAN, G. 2019. RNA N6-methyladenosine demethylase FTO promotes breast tumor progression through inhibiting BNIP3. *Molecular cancer,* 18**,** 46-46.

O'FLANAGAN, C. H., O'SHEA, S., LYONS, A., FOGARTY, F. M., MCCABE, N., KENNEDY, R. D. & O'CONNOR, R. 2016. IGF-1R inhibition sensitizes breast cancer cells to ATM-related kinase (ATR) inhibitor and cisplatin. *Oncotarget,* 7**,** 56826-56841.

O'SULLIVAN, TIMOTHY E., JOHNSON, LEXUS R., KANG, HELEN H. & SUN, JOSEPH C. 2015. BNIP3- and BNIP3L-Mediated Mitophagy Promotes the Generation of Natural Killer Cell Memory. *Immunity,* 43**,** 331-342.

OGAWA, F., MURPHY, L. C., MALAVASI, E. L. V., O'SULLIVAN, S. T., TORRANCE, H. S., PORTEOUS, D. J. & MILLAR, J. K. 2016. NDE1 and GSK3β Associate with TRAK1 and Regulate Axonal Mitochondrial Motility: Identification of Cyclic AMP as a Novel Modulator of Axonal Mitochondrial Trafficking. *ACS chemical neuroscience,* 7**,** 553-564.

OGURA, M., YAMAKI, J., HOMMA, M. K. & HOMMA, Y. 2012. Mitochondrial c-Src regulates cell survival through phosphorylation of respiratory chain components. *Biochem J,* 447.

OKATSU, K., OKA, T., IGUCHI, M., IMAMURA, K., KOSAKO, H., TANI, N., KIMURA, M., GO, E., KOYANO, F., FUNAYAMA, M., SHIBA-FUKUSHIMA, K., SATO, S., SHIMIZU, H., FUKUNAGA, Y., TANIGUCHI, H., KOMATSU, M., HATTORI, N., MIHARA, K., TANAKA, K. & MATSUDA, N. 2012. PINK1 autophosphorylation upon membrane potential dissipation is essential for Parkin recruitment to damaged mitochondria. *Nature Communications,* 3**,** 1016.

OLLEROS SANTOS-RUIZ, M., SÁDABA, M. C., MARTÍN-ESTAL, I., MUÑOZ, U., SEBAL NEIRA, C. & CASTILLA-CORTÁZAR, I. 2017. The single IGF-1 partial deficiency is responsible for mitochondrial dysfunction and is restored by IGF-1 replacement therapy. *Growth Hormone & IGF Research,* 35**,** 21-32.

OSHER, E. & MACAULAY, V. M. 2019. Therapeutic Targeting of the IGF Axis. *Cells,* 8.

OSUKA, S., SAMPETREAN, O., SHIMIZU, T., SAGA, I., ONISHI, N., SUGIHARA, E., OKUBO, J., FUJITA, S., TAKANO, S., MATSUMURA, A. & SAYA, H. 2013. IGF1 Receptor Signaling Regulates Adaptive Radioprotection in Glioma Stem Cells. 31**,** 627-640.

OUYANG, D. Y., XU, L. H., HE, X. H., ZHANG, Y. T., ZENG, L. H., CAI, J. Y. & REN, S. 2013. Autophagy is differentially induced in prostate cancer LNCaP, DU145 and PC-3 cells via distinct splicing profiles of ATG5. *Autophagy,* 9**,** 20-32.

PAL, K., CAO, Y., GAISINA, I. N., BHATTACHARYA, S., DUTTA, S. K., WANG, E., GUNOSEWOYO, H., KOZIKOWSKI, A. P., BILLADEAU, D. D. & MUKHOPADHYAY, D. 2014. Inhibition of GSK-3 induces differentiation and impaired glucose metabolism in renal cancer. *Molecular cancer therapeutics,* 13**,** 285-296.

PALADE, G. E. 1952. The fine structure of mitochondria. 114**,** 427-451.

PALIKARAS, K., LIONAKI, E. & TAVERNARAKIS, N. 2015a. Balancing mitochondrial biogenesis and mitophagy to maintain energy metabolism homeostasis. *Cell Death & Differentiation,* 22**,** 1399-1401.

PALIKARAS, K., LIONAKI, E. & TAVERNARAKIS, N. 2015b. Coordination of mitophagy and mitochondrial biogenesis during ageing in C. elegans. *Nature,* 521**,** 525-528.

PALIKARAS, K., LIONAKI, E. & TAVERNARAKIS, N. 2015c. Coupling mitogenesis and mitophagy for longevity. *Autophagy,* 11**,** 1428-30.

PALIKARAS, K., LIONAKI, E. & TAVERNARAKIS, N. 2018. Mechanisms of mitophagy in cellular homeostasis, physiology and pathology. *Nat Cell Biol,* 20**,** 1013-1022.

PANG, Y., ZHENG, B., FAN, L.-W., RHODES, P. G. & CAI, Z. 2007. IGF-1 protects oligodendrocyte progenitors against TNFα-induced damage by activation of PI3K/Akt and interruption of the mitochondrial apoptotic pathway. 55**,** 1099-1107.

PARK, J.-Y., KIM, S., SOHN, H. Y., KOH, Y. H. & JO, C. 2019. TFEB activates Nrf2 by repressing its E3 ubiquitin ligase DCAF11 and promoting phosphorylation of p62. *Scientific Reports,* 9**,** 14354.

PARRIZAS, M., SALTIEL, A. R. & LEROITH, D. 1997. Insulin-like growth factor 1 inhibits apoptosis using the phosphatidylinositol 3'-kinase and mitogen-activated protein kinase pathways. *J Biol Chem,* 272**,** 154-61.

PARZYCH, K. R. & KLIONSKY, D. J. 2014. An overview of autophagy: morphology, mechanism, and regulation. *Antioxidants & redox signaling,* 20**,** 460-473.

PAUTSCH, A., ZOEPHEL, A., AHORN, H., SPEVAK, W., HAUPTMANN, R. & NAR, H. 2001. Crystal Structure of Bisphosphorylated IGF-1 Receptor Kinase: Insight into Domain Movements upon Kinase Activation. *Structure,* 9**,** 955-965.

PEDERSEN, S. B., KRISTENSEN, K., FISKER, S., JØRGENSEN, J. O. L., CHRISTIANSEN, J. S. & RICHELSEN, B. 1999. Regulation of Uncoupling Protein-2 and -3 by Growth

Hormone in Skeletal Muscle and Adipose Tissue in Growth Hormone-Deficient Adults1. *The Journal of Clinical Endocrinology & Metabolism,* 84**,** 4073-4078.
PENG, Y., FANG, Z., LIU, M., WANG, Z., LI, L., MING, S., LU, C., DONG, H., ZHANG, W., WANG, Q., SHEN, R., XIE, F., ZHANG, W., YANG, C., GAO, X. & SUN, Y. J. J. O. T. M. 2019. Testosterone induces renal tubular epithelial cell death through the HIF-1α/BNIP3 pathway. 17**,** 62.
PEYRAT, J. P., LOUCHEZ, M. M., LEFEBVRE, J., BONNETERRE, J., VENNIN, P., DEMAILLE, A., HELQUET, B. & FOURNIER, C. 1993. Plasma insulin-like growth factor-1 (IGF-1) concentrations in human breast cancer. *European Journal of Cancer,* 29**,** 492-497.
PHANIENDRA, A., JESTADI, D. B. & PERIYASAMY, L. 2015. Free radicals: properties, sources, targets, and their implication in various diseases. *Indian journal of clinical biochemistry : IJCB,* 30**,** 11-26.
PIANTADOSI, C. A., CARRAWAY, M. S., BABIKER, A. & SULIMAN, H. B. 2008. Heme oxygenase-1 regulates cardiac mitochondrial biogenesis via Nrf2-mediated transcriptional control of nuclear respiratory factor-1. *Circulation research,* 103**,** 1232-1240.
PICH, S., BACH, D., BRIONES, P., LIESA, M., CAMPS, M., TESTAR, X., PALACÍN, M. & ZORZANO, A. 2005. The Charcot-Marie-Tooth type 2A gene product, Mfn2, up-regulates fuel oxidation through expression of OXPHOS system. *Human molecular genetics,* 14**,** 1405-1415.
PICKLES, S., VIGIE, P. & YOULE, R. J. 2018. Mitophagy and Quality Control Mechanisms in Mitochondrial Maintenance. *Curr Biol,* 28**,** R170-R185.
PUIGSERVER, P., WU, Z., PARK, C. W., GRAVES, R., WRIGHT, M. & SPIEGELMAN, B. M. 1998. A Cold-Inducible Coactivator of Nuclear Receptors Linked to Adaptive Thermogenesis. *Cell,* 92**,** 829-839.
QI, Y., YAN, L., YU, C., GUO, X., ZHOU, X., HU, X., HUANG, X., RAO, Z., LOU, Z. & HU, J. 2016. Structures of human mitofusin 1 provide insight into mitochondrial tethering. *The Journal of cell biology,* 215**,** 621-629.
QU, X., WU, Z., DONG, W., ZHANG, T., WANG, L., PANG, Z., MA, W. & DU, J. 2017. Update of IGF-1 receptor inhibitor (ganitumab, dalotuzumab, cixutumumab, teprotumumab and figitumumab) effects on cancer therapy. 8.
QUEK, R., WANG, Q., MORGAN, J. A., SHAPIRO, G. I., BUTRYNSKI, J. E., RAMAIYA, N., HUFTALEN, T., JEDERLINIC, N., MANOLA, J., WAGNER, A. J., DEMETRI, G. D. & GEORGE, S. 2011. Combination mTOR and IGF-1R inhibition: phase I trial of everolimus and figitumumab in patients with advanced sarcomas and other solid tumors. *Clin Cancer Res,* 17**,** 871-9.
RADA, P., ROJO, A. I., CHOWDHRY, S., MCMAHON, M., HAYES, J. D. & CUADRADO, A. 2011. SCF/{beta}-TrCP promotes glycogen synthase kinase 3-dependent degradation of the Nrf2 transcription factor in a Keap1-independent manner. *Mol Cell Biol,* 31**,** 1121-33.
RAMCHARAN, R., ALEKSIC, T., KAMDOUM, W. P., GAO, S., PFISTER, S. X., TANNER, J., BRIDGES, E., ASHER, R., WATSON, A. J., MARGISON, G. P., WOODCOCK, M., REPAPI, E., LI, J. L., MIDDLETON, M. R. & MACAULAY, V. M. 2015. IGF-1R inhibition induces schedule-dependent sensitization of human melanoma to temozolomide. *Oncotarget,* 6**,** 39877-90.
RASOLA, A. & CHIARA, F. 2013. GSK-3 and mitochondria in cancer cells. 3.
RAY, P. D., HUANG, B.-W. & TSUJI, Y. 2012. Reactive oxygen species (ROS) homeostasis and redox regulation in cellular signaling. *Cellular Signalling,* 24**,** 981-990.
REYA, T., MORRISON, S. J., CLARKE, M. F. & WEISSMAN, I. L. 2001. Stem cells, cancer, and cancer stem cells. *Nature,* 414**,** 105-111.

RIBEIRO, M., ROSENSTOCK, T. R., OLIVEIRA, A. M., OLIVEIRA, C. R. & REGO, A. C. 2014. Insulin and IGF-1 improve mitochondrial function in a PI-3K/Akt-dependent manner and reduce mitochondrial generation of reactive oxygen species in Huntington's disease knock-in striatal cells. *Free Radic Biol Med,* 74**,** 129-44.

RICHARDSON, A. E., HAMILTON, N., DAVIS, W., BRITO, C. & DE LEÓN, D. 2011. Insulin-like growth factor-2 (IGF-2) activates estrogen receptor-α and -β via the IGF-1 and the insulin receptors in breast cancer cells. *Growth Factors,* 29**,** 82-93.

RIIS, S., MURRAY, J. B. & O'CONNOR, R. 2020. IGF-1 Signalling Regulates Mitochondria Dynamics and Turnover through a Conserved GSK-3beta-Nrf2-BNIP3 Pathway. *Cells,* 9.

RIKKA, S., QUINSAY, M. N., THOMAS, R. L., KUBLI, D. A., ZHANG, X., MURPHY, A. N. & GUSTAFSSON Å, B. 2011. Bnip3 impairs mitochondrial bioenergetics and stimulates mitochondrial turnover. *Cell Death Differ,* 18**,** 721-31.

ROGOV, V. V., SUZUKI, H., MARINKOVIĆ, M., LANG, V., KATO, R., KAWASAKI, M., BULJUBAŠIĆ, M., ŠPRUNG, M., ROGOVA, N., WAKATSUKI, S., HAMACHER-BRADY, A., DÖTSCH, V., DIKIC, I., BRADY, N. R. & NOVAK, I. 2017. Phosphorylation of the mitochondrial autophagy receptor Nix enhances its interaction with LC3 proteins. *Scientific reports,* 7**,** 1131-1131.

ROJO DE LA VEGA, M., CHAPMAN, E. & ZHANG, D. D. 2018. NRF2 and the Hallmarks of Cancer. *Cancer Cell,* 34**,** 21-43.

SÁDABA, M. C., MARTÍN-ESTAL, I., PUCHE, J. E. & CASTILLA-CORTÁZAR, I. 2016. Insulin-like growth factor 1 (IGF-1) therapy: Mitochondrial dysfunction and diseases. *Biochimica et Biophysica Acta (BBA) - Molecular Basis of Disease,* 1862**,** 1267-1278.

SALAZAR, M., ROJO, A. I., VELASCO, D., DE SAGARRA, R. M. & CUADRADO, A. 2006. Glycogen Synthase Kinase-3β Inhibits the Xenobiotic and Antioxidant Cell Response by Direct Phosphorylation and Nuclear Exclusion of the Transcription Factor Nrf2. 281**,** 14841-14851.

SAMANI, A. A., YAKAR, S., LEROITH, D. & BRODT, P. 2007. The Role of the IGF System in Cancer Growth and Metastasis: Overview and Recent Insights. *Endocrine Reviews,* 28**,** 20-47.

SAMUDIO, I., FIEGL, M., MCQUEEN, T., CLISE-DWYER, K. & ANDREEFF, M. 2008. The warburg effect in leukemia-stroma cocultures is mediated by mitochondrial uncoupling associated with uncoupling protein 2 activation. *Cancer research,* 68**,** 5198-5205.

SARASTE, M. 1999. Oxidative phosphorylation at the fin de siecle. *Science,* 283**,** 1488-93.

SCHLUETER, P. J., PENG, G., WESTERFIELD, M. & DUAN, C. 2007. Insulin-like growth factor signaling regulates zebrafish embryonic growth and development by promoting cell survival and cell cycle progression. *Cell death and differentiation,* 14**,** 1095-1105.

SCHWARTZ, G. K., TAP, W. D., QIN, L. X., LIVINGSTON, M. B., UNDEVIA, S. D., CHMIELOWSKI, B., AGULNIK, M., SCHUETZE, S. M., REED, D. R., OKUNO, S. H., LUDWIG, J. A., KEEDY, V., RIETSCHEL, P., KRAFT, A. S., ADKINS, D., VAN TINE, B. A., BROCKSTEIN, B., YIM, V., BITAS, C., ABDULLAH, A., ANTONESCU, C. R., CONDY, M., DICKSON, M. A., VASUDEVA, S. D., HO, A. L., DOYLE, L. A., CHEN, H. X. & MAKI, R. G. 2013. Cixutumumab and temsirolimus for patients with bone and soft-tissue sarcoma: a multicentre, open-label, phase 2 trial. *Lancet Oncol,* 14**,** 371-82.

SCHWEERS, R. L., ZHANG, J., RANDALL, M. S., LOYD, M. R., LI, W., DORSEY, F. C., KUNDU, M., OPFERMAN, J. T., CLEVELAND, J. L., MILLER, J. L. & NEY, P. A. 2007. NIX is required for programmed mitochondrial clearance during reticulocyte maturation. *Proceedings of the National Academy of Sciences of the United States of America,* 104**,** 19500-19505.

SEBASTIÁN, D. & ZORZANO, A. 2018. Mitochondrial dynamics and metabolic homeostasis. *Current Opinion in Physiology,* 3**,** 34-40.
SELL, C., DUMENIL, G., DEVEAUD, C., MIURA, M., COPPOLA, D., DEANGELIS, T., RUBIN, R., EFSTRATIADIS, A. & BASERGA, R. 1994. Effect of a null mutation of the insulin-like growth factor I receptor gene on growth and transformation of mouse embryo fibroblasts. 14**,** 3604-3612.
SHAO, D., LIU, Y., LIU, X., ZHU, L., CUI, Y., CUI, A., QIAO, A., KONG, X., LIU, Y., CHEN, Q., GUPTA, N., FANG, F. & CHANG, Y. 2010. PGC-1β-Regulated mitochondrial biogenesis and function in myotubes is mediated by NRF-1 and ERRα. *Mitochondrion,* 10**,** 516-527.
SHEN, Q., LANTVIT, D. D., LIN, Q., LI, Y., CHRISTOV, K., WANG, Z., UNTERMAN, T. G., MEHTA, R. G. & SWANSON, S. M. 2007. Advanced Rat Mammary Cancers Are Growth Hormone Dependent. *Endocrinology,* 148**,** 4536-4544.
SHEVAH, O., KORNREICH, L., GALATZER, A. & LARON, Z. 2005. The intellectual capacity of patients with Laron syndrome (LS) differs with various molecular defects of the growth hormone receptor gene. Correlation with CNS abnormalities. *Horm Metab Res,* 37**,** 757-60.
SHEVAH, O. & LARON, Z. 2007. Patients with congenital deficiency of IGF-I seem protected from the development of malignancies: A preliminary report. *Growth Hormone & IGF Research,* 17**,** 54-57.
SHI, R. Y., ZHU, S. H., LI, V., GIBSON, S. B., XU, X. S. & KONG, J. M. 2014. BNIP3 interacting with LC3 triggers excessive mitophagy in delayed neuronal death in stroke. *CNS Neurosci Ther,* 20**,** 1045-55.
SHIMURA, H., HATTORI, N., KUBO, S.-I., MIZUNO, Y., ASAKAWA, S., MINOSHIMA, S., SHIMIZU, N., IWAI, K., CHIBA, T., TANAKA, K. & SUZUKI, T. 2000. Familial Parkinson disease gene product, parkin, is a ubiquitin-protein ligase. *Nature Genetics,* 25**,** 302-305.
SHINODA, H., SHANNON, M. & NAGAI, T. 2018. Fluorescent Proteins for Investigating Biological Events in Acidic Environments. *Int J Mol Sci,* 19.
SHPILKA, T., WEIDBERG, H., PIETROKOVSKI, S. & ELAZAR, Z. 2011. Atg8: an autophagy-related ubiquitin-like protein family. *Genome biology,* 12**,** 226-226.
SHUBIN, A. V., DEMIDYUK, I. V., KOMISSAROV, A. A., RAFIEVA, L. M. & KOSTROV, S. V. 2016. Cytoplasmic vacuolization in cell death and survival. *Oncotarget,* 7**,** 55863-55889.
SINGH, A., AZAD, M., SHYMKO, M. D., HENSON, E. S., KATYAL, S., EISENSTAT, D. D. & GIBSON, S. B. 2018. The BH3 only Bcl-2 family member BNIP3 regulates cellular proliferation. *PLOS ONE,* 13**,** e0204792.
SJÖGREN, K., LIU, J.-L., BLAD, K., SKRTIC, S., VIDAL, O., WALLENIUS, V., LEROITH, D., TÖRNELL, J., ISAKSSON, O. G. P., JANSSON, J.-O. & OHLSSON, C. 1999. Liver-derived insulin-like growth factor I (IGF-I) is the principal source of IGF-I in blood but is not required for postnatal body growth in mice. 96**,** 7088-7092.
SJOSTRAND, F. S. 1953. Electron microscopy of mitochondria and cytoplasmic double membranes. *Nature,* 171**,** 30-2.
SMIRNOVA, E., GRIPARIC, L., SHURLAND, D.-L. & VAN DER BLIEK, A. M. 2001. Dynamin-related Protein Drp1 Is Required for Mitochondrial Division in Mammalian Cells. *Molecular Biology of the Cell,* 12**,** 2245-2256.
SONG, R. X. D., FAN, P., YUE, W., CHEN, Y. & SANTEN, R. J. 2006. Role of receptor complexes in the extranuclear actions of estrogen receptor alpha in breast cancer. *Endocrine-related cancer,* 13 Suppl 1**,** S3-S13.
SONG, Z., GHOCHANI, M., MCCAFFERY, J. M., FREY, T. G. & CHAN, D. C. 2009. Mitofusins and OPA1 Mediate Sequential Steps in Mitochondrial Membrane Fusion. 20**,** 3525-3532.

SOWTER, H. M., RATCLIFFE, P. J., WATSON, P., GREENBERG, A. H. & HARRIS, A. L. 2001. HIF-1-dependent regulation of hypoxic induction of the cell death factors BNIP3 and NIX in human tumors. *Cancer research,* 61**,** 6669-6673.

SRINIVAS, U. S., TAN, B. W. Q., VELLAYAPPAN, B. A. & JEYASEKHARAN, A. D. 2019. ROS and the DNA damage response in cancer. *Redox Biology,* 25**,** 101084.

STAMBOLIC, V., RUEL, L. & WOODGETT, J. R. 1996. Lithium inhibits glycogen synthase kinase-3 activity and mimics Wingless signalling in intact cells. *Current Biology,* 6**,** 1664-1669.

STANICKA, J., RIEGER, L., O'SHEA, S., COX, O., COLEMAN, M., O'FLANAGAN, C., ADDARIO, B., MCCABE, N., KENNEDY, R. & O'CONNOR, R. 2018. FES-related tyrosine kinase activates the insulin-like growth factor-1 receptor at sites of cell adhesion. *Oncogene,* 37**,** 3131-3150.

STRAPPAZZON, F., NAZIO, F., CORRADO, M., CIANFANELLI, V., ROMAGNOLI, A., FIMIA, G. M., CAMPELLO, S., NARDACCI, R., PIACENTINI, M., CAMPANELLA, M. & CECCONI, F. 2015. AMBRA1 is able to induce mitophagy via LC3 binding, regardless of PARKIN and p62/SQSTM1. *Cell death and differentiation,* 22**,** 419-432.

SUN, N., MALIDE, D., LIU, J., ROVIRA, II, COMBS, C. A. & FINKEL, T. 2017. A fluorescence-based imaging method to measure in vitro and in vivo mitophagy using mt-Keima. *Nat Protoc,* 12**,** 1576-1587.

SUN, Y., LIU, W.-Z., LIU, T., FENG, X., YANG, N. & ZHOU, H.-F. 2015. Signaling pathway of MAPK/ERK in cell proliferation, differentiation, migration, senescence and apoptosis. *Journal of Receptors and Signal Transduction,* 35**,** 600-604.

SUSIN, S. A., LORENZO, H. K., ZAMZAMI, N., MARZO, I., SNOW, B. E., BROTHERS, G. M., MANGION, J., JACOTOT, E., COSTANTINI, P., LOEFFLER, M., LAROCHETTE, N., GOODLETT, D. R., AEBERSOLD, R., SIDEROVSKI, D. P., PENNINGER, J. M. & KROEMER, G. 1999. Molecular characterization of mitochondrial apoptosis-inducing factor. *Nature,* 397**,** 441-446.

SUTHERLAND, C., LEIGHTON, I. A. & COHEN, P. 1993. Inactivation of glycogen synthase kinase-3 beta by phosphorylation: new kinase connections in insulin and growth-factor signalling. *The Biochemical journal,* 296 (Pt 1)**,** 15-19.

SUZUKI, T. & YAMAMOTO, M. 2015. Molecular basis of the Keap1–Nrf2 system. *Free Radical Biology and Medicine,* 88, Part B**,** 93-100.

SWANSON, S. M. & UNTERMAN, T. G. 2002. The growth hormone-deficient Spontaneous Dwarf rat is resistant to chemically induced mammary carcinogenesis. *Carcinogenesis,* 23**,** 977-982.

SYKIOTIS, G. P. & BOHMANN, D. 2010. Stress-activated cap'n'collar transcription factors in aging and human disease. *Science signaling,* 3**,** re3-re3.

TAGUCHI, K., MOTOHASHI, H. & YAMAMOTO, M. 2011. Molecular mechanisms of the Keap1–Nrf2 pathway in stress response and cancer evolution. 16**,** 123-140.

TANG, C., HAN, H., LIU, Z., LIU, Y., YIN, L., CAI, J., HE, L., LIU, Y., CHEN, G., ZHANG, Z., YIN, X.-M. & DONG, Z. 2019. Activation of BNIP3-mediated mitophagy protects against renal ischemia–reperfusion injury. *Cell Death & Disease,* 10**,** 677.

TANNO, M., KUNO, A., ISHIKAWA, S., MIKI, T., KOUZU, H., YANO, T., MURASE, H., TOBISAWA, T., OGASAWARA, M., HORIO, Y. & MIURA, T. 2014. Translocation of glycogen synthase kinase-3β (GSK-3β), a trigger of permeability transition, is kinase activity-dependent and mediated by interaction with voltage-dependent anion channel 2 (VDAC2). *The Journal of biological chemistry,* 289**,** 29285-29296.

TATAR, M., KOPELMAN, A., EPSTEIN, D., TU, M. P., YIN, C. M. & GAROFALO, R. S. 2001. A mutant Drosophila insulin receptor homolog that extends life-span and impairs neuroendocrine function. *Science,* 292**,** 107-10.

TATSUTA, T., MODEL, K. & LANGER, T. 2005. Formation of membrane-bound ring complexes by prohibitins in mitochondria. *Mol Biol Cell,* 16**,** 248-59.

TEBAY, L. E., ROBERTSON, H., DURANT, S. T., VITALE, S. R., PENNING, T. M., DINKOVA-KOSTOVA, A. T. & HAYES, J. D. 2015. Mechanisms of activation of the transcription factor Nrf2 by redox stressors, nutrient cues, and energy status and the pathways through which it attenuates degenerative disease. *Free Radic Biol Med,* 88**,** 108-46.

TENG, C.-F., JENG, L.-B. & SHYU, W.-C. 2018. Role of Insulin-like Growth Factor 1 Receptor Signaling in Stem Cell Stemness and Therapeutic Efficacy. *Cell transplantation,* 27**,** 1313-1319.

THEEUWES, W. F., GOSKER, H. R., LANGEN, R. C. J., PANSTERS, N. A. M., SCHOLS, A. M. W. J. & REMELS, A. H. V. 2018. Inactivation of glycogen synthase kinase 3β (GSK-3β) enhances mitochondrial biogenesis during myogenesis. *Biochimica et biophysica acta. Molecular basis of disease,* 1864**,** 2913-2926.

THEEUWES, W. F., GOSKER, H. R., SCHOLS, A. M. W. J., LANGEN, R. C. J. & REMELS, A. H. V. 2020. Regulation of PGC-1α expression by a GSK-3β-TFEB signaling axis in skeletal muscle. *Biochimica et biophysica acta. Molecular cell research,* 1867**,** 118610-118610.

TIAN, X., HAO, K., QIN, C., XIE, K., XIE, X. & YANG, Y. 2013. Insulin-like growth factor 1 receptor promotes the growth and chemoresistance of pancreatic cancer. *Dig Dis Sci,* 58**,** 2705-12.

TORRES ALEMAN, I. 2012. Insulin-like growth factor-1 and central neurodegenerative diseases. *Endocrinol Metab Clin North Am,* 41**,** 395-408, vii.

TSAI, J. J., DUDAKOV, J. A., TAKAHASHI, K., SHIEH, J.-H., VELARDI, E., HOLLAND, A. M., SINGER, N. V., WEST, M. L., SMITH, O. M., YOUNG, L. F., SHONO, Y., GHOSH, A., HANASH, A. M., TRAN, H. T., MOORE, M. A. S. & VAN DEN BRINK, M. R. M. 2013. Nrf2 regulates haematopoietic stem cell function. *Nature Cell Biology,* 15**,** 309.

TWIG, G., ELORZA, A., MOLINA, A. J. A., MOHAMED, H., WIKSTROM, J. D., WALZER, G., STILES, L., HAIGH, S. E., KATZ, S., LAS, G., ALROY, J., WU, M., PY, B. F., YUAN, J., DEENEY, J. T., CORKEY, B. E. & SHIRIHAI, O. S. 2008. Fission and selective fusion govern mitochondrial segregation and elimination by autophagy. *The EMBO journal,* 27**,** 433-446.

UM, J.-H. & YUN, J. 2017. Emerging role of mitophagy in human diseases and physiology. *BMB reports,* 50**,** 299-307.

URSINI, F., MAIORINO, M. & FORMAN, H. J. 2016. Redox homeostasis: The Golden Mean of healthy living. *Redox Biology,* 8**,** 205-215.

VAN BUNDEREN, C. C., DEIJEN, J. B. & DRENT, M. L. 2018. Effect of low-normal and high-normal IGF-1 levels on memory and wellbeing during growth hormone replacement therapy: a randomized clinical trial in adult growth hormone deficiency. *Health and quality of life outcomes,* 16**,** 135-135.

VAN BUNDEREN, C. C., LIPS, P., KRAMER, M. H. & DRENT, M. L. 2016. Comparison of low-normal and high-normal IGF-1 target levels during growth hormone replacement therapy: A randomized clinical trial in adult growth hormone deficiency. *European journal of internal medicine,* 31**,** 88-93.

VAN HEEMST, D. 2010. Insulin, IGF-1 and longevity. *Aging and disease,* 1**,** 147-157.

VANDE VELDE, C., CIZEAU, J., DUBIK, D., ALIMONTI, J., BROWN, T., ISRAELS, S., HAKEM, R. & GREENBERG, A. H. 2000. BNIP3 and genetic control of necrosis-like cell death through the mitochondrial permeability transition pore. *Molecular and cellular biology,* 20**,** 5454-5468.

VANDER HEIDEN, M. G., CANTLEY, L. C. & THOMPSON, C. B. 2009. Understanding the Warburg effect: the metabolic requirements of cell proliferation. *Science (New York, N.Y.),* 324**,** 1029-1033.

VASAGIRI, N. & KUTALA, V. K. 2014. Structure, function, and epigenetic regulation of BNIP3: a pathophysiological relevance. *Molecular Biology Reports,* 41**,** 7705-7714.
VELDHUIS, J. D., ROELFSEMA, F., KEENAN, D. M. & PINCUS, S. 2011. Gender, Age, Body Mass Index, and IGF-I Individually and Jointly Determine Distinct GH Dynamics: Analyses in One Hundred Healthy Adults. *The Journal of Clinical Endocrinology & Metabolism,* 96**,** 115-121.
VELLA, V., NICOLOSI, M. L., GIULIANO, M., MORRIONE, A., MALAGUARNERA, R. & BELFIORE, A. 2019. Insulin Receptor Isoform A Modulates Metabolic Reprogramming of Breast Cancer Cells in Response to IGF2 and Insulin Stimulation. *Cells,* 8**,** 1017.
VINCIGUERRA, M., SANTINI, M. P., CLAYCOMB, W. C., LADURNER, A. G. & ROSENTHAL, N. 2009. Local IGF-1 isoform protects cardiomyocytes from hypertrophic and oxidative stresses via SirT1 activity. *Aging,* 2**,** 43-62.
VISSER, W., VAN SPRONSEN, E. A., NANNINGA, N., PRONK, J. T., KUENEN, J. G. & VAN DIJKEN, J. P. J. A. V. L. 1995. Effects of growth conditions on mitochondrial morphology inSaccharomyces cerevisiae. 67**,** 243-253.
VITALE, G., PELLEGRINO, G., VOLLERY, M. & HOFLAND, L. J. 2019. ROLE of IGF-1 System in the Modulation of Longevity: Controversies and New Insights From a Centenarians' Perspective. *Frontiers in endocrinology,* 10**,** 27-27.
VLAHOVIC, G., MEADOWS, K. L., HATCH, A. J., JIA, J., NIXON, A. B., URONIS, H. E., MORSE, M. A., SELIM, M. A., CRAWFORD, J., RIEDEL, R. F., ZAFAR, S. Y., HOWARD, L. A., O'NEILL, M., MEADOWS, J. J., HALEY, S. T., ARROWOOD, C. C., RUSHING, C., PANG, H. & HURWITZ, H. I. 2018. A Phase I Trial of the IGF-1R Antibody Ganitumab (AMG 479) in Combination with Everolimus (RAD001) and Panitumumab in Patients with Advanced Cancer. *Oncologist,* 23**,** 782-790.
VOZZA, A., PARISI, G., DE LEONARDIS, F., LASORSA, F. M., CASTEGNA, A., AMORESE, D., MARMO, R., CALCAGNILE, V. M., PALMIERI, L., RICQUIER, D., PARADIES, E., SCARCIA, P., PALMIERI, F., BOUILLAUD, F. & FIERMONTE, G. 2014. UCP2 transports C4 metabolites out of mitochondria, regulating glucose and glutamine oxidation. 111**,** 960-965.
VYAS, S., ZAGANJOR, E. & HAIGIS, M. C. 2016. Mitochondria and Cancer. *Cell,* 166**,** 555-566.
WALLACE, D. C. 2012. Mitochondria and cancer. *Nature Reviews Cancer,* 12**,** 685-698.
WANG, H.-B., ZHOU, C.-J., SONG, S.-Z., CHEN, P., XU, W.-H., LIU, B., ZHU, K.-X., YU, W.-H., WU, H.-L., WANG, H.-J., LIN, S., GUO, J.-Q. & QIN, C.-Y. 2011. Evaluation of Nrf2 and IGF-1 expression in benign, premalignant and malignant gastric lesions. *Pathology - Research and Practice,* 207**,** 169-173.
WANG, S. Q., YANG, X. Y., CUI, S. X., GAO, Z. H. & QU, X. J. 2019. Heterozygous knockout insulin-like growth factor-1 receptor (IGF-1R) regulates mitochondrial functions and prevents colitis and colorectal cancer. *Free Radical Biology and Medicine,* 134**,** 87-98.
WANG, X.-J., SUN, Z., VILLENEUVE, N. F., ZHANG, S., ZHAO, F., LI, Y., CHEN, W., YI, X., ZHENG, W., WONDRAK, G. T., WONG, P. K. & ZHANG, D. D. 2008. Nrf2 enhances resistance of cancer cells to chemotherapeutic drugs, the dark side of Nrf2. *Carcinogenesis,* 29**,** 1235-1243.
WANG, Y.-Y., CHEN, J., LIU, X.-M., ZHAO, R. & ZHE, H. 2018. Nrf2-Mediated Metabolic Reprogramming in Cancer. *Oxidative medicine and cellular longevity,* 2018**,** 9304091-9304091.
WARBURG, O., WIND, F. & NEGELEIN, E. 1927. The Metabolism of Tumors in the Body. *J Gen Physiol,* 8**,** 519-30.
WEI, Y., CHIANG, W. C., SUMPTER, R., JR., MISHRA, P. & LEVINE, B. 2017. Prohibitin 2 Is an Inner Mitochondrial Membrane Mitophagy Receptor. *Cell,* 168**,** 224-238 e10.

WERNER, H., SARFSTEIN, R. & BRUCHIM, I. 2019. Investigational IGF1R inhibitors in early stage clinical trials for cancer therapy. *Expert Opinion on Investigational Drugs,* 28**,** 1101-1112.

WEST, A. P., BRODSKY, I. E., RAHNER, C., WOO, D. K., ERDJUMENT-BROMAGE, H., TEMPST, P., WALSH, M. C., CHOI, Y., SHADEL, G. S. & GHOSH, S. 2011. TLR signalling augments macrophage bactericidal activity through mitochondrial ROS. *Nature,* 472**,** 476-480.

WIEDEMANN, N. & PFANNER, N. 2017. Mitochondrial Machineries for Protein Import and Assembly. *Annual review of biochemistry,* 86**,** 685-714.

WILKY, B. A., RUDEK, M. A., AHMED, S., LAHERU, D. A., COSGROVE, D., DONEHOWER, R. C., NELKIN, B., BALL, D., DOYLE, L. A., CHEN, H., YE, X., BIGLEY, G., WOMACK, C. & AZAD, N. S. 2015. A phase I trial of vertical inhibition of IGF signalling using cixutumumab, an anti-IGF-1R antibody, and selumetinib, an MEK 1/2 inhibitor, in advanced solid tumours. *Br J Cancer,* 112**,** 24-31.

WOLK, A., MANTZOROS, C. S., ANDERSSON, S.-O., BERGSTRÖM, R., SIGNORELLO, L. B., LAGIOU, P., ADAMI, H.-O. & TRICHOPOULOS, D. 1998. Insulin-Like Growth Factor 1 and Prostate Cancer Risk: A Population-Based, Case-Control Study. *JNCI: Journal of the National Cancer Institute,* 90**,** 911-915.

WU, H., HUANG, S., CHEN, Z., LIU, W., ZHOU, X. & ZHANG, D. 2015. Hypoxia-induced autophagy contributes to the invasion of salivary adenoid cystic carcinoma through the HIF-1alpha/BNIP3 signaling pathway. *Mol Med Rep,* 12**,** 6467-74.

WU, H., KANATOUS, S. B., THURMOND, F. A., GALLARDO, T., ISOTANI, E., BASSEL-DUBY, R. & WILLIAMS, R. S. 2002. Regulation of mitochondrial biogenesis in skeletal muscle by CaMK. *Science,* 296**,** 349-52.

WU, T., ZHAO, F., GAO, B., TAN, C., YAGISHITA, N., NAKAJIMA, T., WONG, P. K., CHAPMAN, E., FANG, D. & ZHANG, D. D. 2014. Hrd1 suppresses Nrf2-mediated cellular protection during liver cirrhosis. *Genes & development,* 28**,** 708-722.

WU, Z., PUIGSERVER, P., ANDERSSON, U., ZHANG, C., ADELMANT, G., MOOTHA, V., TROY, A., CINTI, S., LOWELL, B., SCARPULLA, R. C. & SPIEGELMAN, B. M. 1999. Mechanisms Controlling Mitochondrial Biogenesis and Respiration through the Thermogenic Coactivator PGC-1. *Cell,* 98**,** 115-124.

XIAO, L., XU, X., ZHANG, F., WANG, M., XU, Y., TANG, D., WANG, J., QIN, Y., LIU, Y., TANG, C., HE, L., GREKA, A., ZHOU, Z., LIU, F., DONG, Z. & SUN, L. 2017. The mitochondria-targeted antioxidant MitoQ ameliorated tubular injury mediated by mitophagy in diabetic kidney disease via Nrf2/PINK1. *Redox Biology,* 11**,** 297-311.

XIAO, Y., ZHOU, Y., LU, Y., ZHOU, K. & CAI, W. 2018. PHB2 interacts with LC3 and SQSTM1 is required for bile acids-induced mitophagy in cholestatic liver. *Cell Death Dis,* 9**,** 160.

YAN, C., GONG, L., CHEN, L., XU, M., ABOU-HAMDAN, H., TANG, M., DESAUBRY, L. & SONG, Z. 2020. PHB2 (prohibitin 2) promotes PINK1-PRKN/Parkin-dependent mitophagy by the PARL-PGAM5-PINK1 axis. *Autophagy,* 16**,** 419-434.

YAN, F., LIAO, R., FARHAN, M., WANG, T., CHEN, J., WANG, Z., LITTLE, P. J. & ZHENG, W. 2016. Elucidating the role of the FoxO3a transcription factor in the IGF-1-induced migration and invasion of uveal melanoma cancer cells. *Biomedicine & pharmacotherapy = Biomedecine & pharmacotherapie,* 84**,** 1538-1550.

YANG, Z. & KLIONSKY, D. J. 2010. Eaten alive: a history of macroautophagy. *Nat Cell Biol,* 12**,** 814-22.

YASUDA, M., THEODORAKIS, P., SUBRAMANIAN, T. & CHINNADURAI, G. 1998. Adenovirus E1B-19K/BCL-2 Interacting Protein BNIP3 Contains a BH3 Domain and a Mitochondrial Targeting Sequence. 273**,** 12415-12421.

YU, H., SPITZ, M. R., MISTRY, J., GU, J., HONG, W. K. & WU, X. 1999. Plasma Levels of Insulin-Like Growth Factor-I and Lung Cancer Risk: a Case-Control Analysis. *JNCI: Journal of the National Cancer Institute,* 91**,** 151-156.

YU, J., SHI, L., SHEN, X. & ZHAO, Y. 2019. UCP2 regulates cholangiocarcinoma cell plasticity via mitochondria-to-AMPK signals. *Biochemical pharmacology,* 166**,** 174-184.

ZHANG, H.-S., DU, G.-Y., ZHANG, Z.-G., ZHOU, Z., SUN, H.-L., YU, X.-Y., SHI, Y.-T., XIONG, D.-N., LI, H. & HUANG, Y.-H. 2018. NRF2 facilitates breast cancer cell growth via HIF1α-mediated metabolic reprogramming. *The International Journal of Biochemistry & Cell Biology,* 95**,** 85-92.

ZHANG, H., BOSCH-MARCE, M., SHIMODA, L. A., TAN, Y. S., BAEK, J. H., WESLEY, J. B., GONZALEZ, F. J. & SEMENZA, G. L. 2008. Mitochondrial autophagy is an HIF-1-dependent adaptive metabolic response to hypoxia. *J Biol Chem,* 283**,** 10892-903.

ZHANG, J. & NEY, P. A. 2009. Role of BNIP3 and NIX in cell death, autophagy, and mitophagy. *Cell Death Differ,* 16**,** 939-946.

ZHANG, J., ZHANG, D., YAN, T., JIANG, X., ZHANG, C., ZHAO, L., LI, L., TANG, D., ZHANG, Q., JIA, J. & HUANG, Y. 2017. BNIP3 promotes the motility and migration of keratinocyte under hypoxia. *Exp Dermatol,* 26**,** 416-422.

ZHANG, T., XUE, L., LI, L., TANG, C., WAN, Z., WANG, R., TAN, J., TAN, Y., HAN, H., TIAN, R., BILLIAR, T. R., TAO, W. A. & ZHANG, Z. 2016. BNIP3 Protein Suppresses PINK1 Kinase Proteolytic Cleavage to Promote Mitophagy. *J Biol Chem,* 291**,** 21616-21629.

ZHANG, Y., LIU, D., HU, H., ZHANG, P., XIE, R. & CUI, W. 2019. HIF-1alpha/BNIP3 signaling pathway-induced-autophagy plays protective role during myocardial ischemia-reperfusion injury. *Biomed Pharmacother,* 120**,** 109464.

ZHANG, Y., WANG, Q., CHEN, L. & YANG, H. S. 2015. Inhibition of p70S6K1 Activation by Pdcd4 Overcomes the Resistance to an IGF-1R/IR Inhibitor in Colon Carcinoma Cells. *Mol Cancer Ther,* 14**,** 799-809.

ZHAO, H., GROSSMAN, H. B., SPITZ, M. R., LERNER, S. P., ZHANG, K. & WU, X. 2003. Plasma levels of insulin-like growth factor-1 and binding protein-3, and their association with bladder cancer risk. *J Urol,* 169**,** 714-7.

ZHOU, L., AON, M. A., ALMAS, T., CORTASSA, S., WINSLOW, R. L. & O'ROURKE, B. 2010. A Reaction-Diffusion Model of ROS-Induced ROS Release in a Mitochondrial Network. *PLOS Computational Biology,* 6**,** e1000657.

ZHU, Y., MASSEN, S., TERENZIO, M., LANG, V., CHEN-LINDNER, S., EILS, R., NOVAK, I., DIKIC, I., HAMACHER-BRADY, A. & BRADY, N. R. 2013. Modulation of serines 17 and 24 in the LC3-interacting region of Bnip3 determines pro-survival mitophagy versus apoptosis. *J Biol Chem,* 288**,** 1099-113.

ZUO, W., ZHANG, S., XIA, C. Y., GUO, X. F., HE, W. B. & CHEN, N. H. 2014. Mitochondria autophagy is induced after hypoxic/ischemic stress in a Drp1 dependent manner: the role of inhibition of Drp1 in ischemic brain damage. *Neuropharmacology,* 86**,** 103-15.